A Sheffield Hallam University thesis

A STATIC MODEL OF A SENDZIMIR MILL
FOR USE IN SHAPE CONTROL

BY

G W D M GUNAWARDENE MSc

A STATIC MODEL OF A SENDZIMIR MILL

FOR USE IN SHAPE CONTROL

by

G W D M GUNAWARDENE MSc

ABSTRACT

The design of shape control systems is an area of current interest in the steel industry. Shape is defined as the internal stress distribution resulting from a transverse variation in the reduction of the strip thickness. The object of shape control is to adjust the mill so that the rolled strip is free from internal stresses. Both static and dynamic models of the mill are required for the control system design.

The subject of this thesis is the static model of the Sendzimir cold rolling mill, which is a 1-2-3-4 type cluster mill. The static model derived enables shape profiles to be calculated for a given set of actuator positions, and is used to generate the steady state mill gains. The method of calculation of these shape profiles is discussed. The shape profiles obtained for different mill schedules are plotted against the distance across the strip. The corresponding mill gains are calculated and these relate the shape changes to the actuator changes. These mill gains are presented in the form of a square matrix, obtained by measuring shape at eight points across the strip.

DECLARATION

I hereby declare that this thesis is a record of work undertaken by myself, that it has not been the subject of any previous application for a degree and that all sources of information have been duly referenced.

ACKNOWLEDGEMENTS

FOR USE IN SHAPE CONTROL
by
G W D M GUNAWARDENE MSc

ABSTRACT

The design of shape control systems is an area of current interest in the steel industry. Shape is defined as the internal stress distribution resulting from a transverse variation in the reduction of the strip thickness. The object of shape control is to adjust the mill so that the rolled strip is free from internal stresses. Both static and dynamic models of the mill are required for the control system design.

The subject of this thesis is the static model of the Sendzimir cold rolling mill, which is a 1-2-3-4 type cluster mill. The static model derived enables shape profiles to be calculated for a given set of actuator positions, and is used to generate the steady state mill gains. The method of calculation of these shape profiles is discussed. The shape profiles obtained for different mill schedules are plotted against the distance across the strip. The corresponding mill gains are calculated and these relate the shape changes to the actuator changes. These mill gains are presented in the form of a square matrix, obtained by measuring shape at eight points across the strip.

CONTENTS.

Chapter 1.

INTRODUCTION.

1.1. Review of the history of rolling mills.

First evidence of a possible attempt to design a cold rolling mill appears in a sketch by Leonardo da Vinchi[1]. The machine was built later to stretch and roll copper strips of sufficient evenness and thinness, for the making of mirrors. The history of rolling records the construction of a hand mill for lead rolling in 1615. Nearly a century later there were various plate mills powered by water wheels or horses for rolling lead and copper[2]. By around 1700, reasonably large mills were in operation for rolling hot ferrous metals. The idea of the three - high mill for rolling metal was more than a century old before it was first introduced into iron works in Sweden in 1856 and in England in 1862. Its inventor, Christopher Polheim had realised the value of being able to pass the metal back and forth without having to reverse the rolls.

Another idea from the previous century, the continuous mill, had been patented by William Hazeldine in 1798, but was not used until it was reinvented by George Bedson in 1862. Here the metal was fed successively into a series of roller stands placed in line so that its size was reduced[3].

The development of rolling mills has continued at a high increasing rate from 1920's onwards. Today there are a wide range of mill configurations and associated equipment to suit all applications. The period of greatest evolutionary change, which spans the last fifty five years, can be divided into three distinct periods: first generation mills from 1927 to 1960, second generation from 1961 to 1969 and third generation from 1970 to present day.[4]

Up to 1960, strip mills operated at low speeds (with exit speeds not more than 12 m/s) and handled small coils weighing up to about 10,000 kg. From 1960 the progress was rapid and the second generation mills were designed to deal with heavier coils and at faster speeds. By the end of the decade automatic gauge control was introduced to meet the more demanding market. The third generation mills emerged in response to the need to roll much larger coils. These mills were capable of handling 45,000 kg coils at speeds up to about 29 m/s.

Major requirements of rolling may be outlined as increasing coil sizes, gauge and shape performance, and led to many new developments. These include the introduction of more stands per tandem mill, improved automatic gauge control systems, hydraulically loaded mills, automatic roll changing, strip threading and coil stripping facilities and continuous rolling.[5]

The development of computers helped the automation of tandem mills. The first computer controlled mill was commissioned at British Steel Corporation, Port Talbot, England in 1964. This was followed by a chain of developments of computer controlled mills, with the objective of obtaining good shape and accurate gauge. The subject of automatic gauge control and shape control became more important in computer control development with the application of shape measuring devices.[6]

1.2. The purpose of rolling mill research.

Rolling first started with hot materials, with the knowledge of how to obtain a desired result. In many cases the reasons were unknown and the practical knowledge was more advanced than the theory. Weaknesses and defects of rolling were discovered through failures, and succesful designs were produced by improving the faulty parts. This experience of success through failure stimulated the understanding of rolling, such as what happened to a material when it passed between rolls, what forces were required to deform it, etc. The knowledge was needed by the designer to estimate, for example, the stresses in his machine, and by the operator to produce his product as cheaply and efficiently as possible.

Later, when cold rolling was introduced, a new set of problems had to be faced, since the requirements of the rolling process was to produce materials reasonably flat and

of uniform thickness across the width and length of the material. This required that the screwdown mechanism was carefully adjusted for each pass and that the rolls were maintained in good condition with the right shape. When rolling at high speeds, the rolls became heated and lost their shape, so that temperature control of the rolls became necessary. The lubricant to use on the strip demanded further investigation, and the best type to use for a given case is still a matter for experiment.

Materials also began to be rolled in the form of very long strip, so that it had to be wound on drums driven from the mill. Front and back tensions were introduced to obtain a better product. These tensions affected the performance of the mill and suitable values had to be found by experience.

The friction forces between two rolls, and between work rolls and material cannot be directly measured. It was found, by experience, that the pressure required to deform the material between the rolls is much greater than that needed for a similar reduction between flat frictionless plates, owing to the friction effects. It was also found that the pressure varies with the thickness of the material. Vertical plane sections of the material became distorted in an almost unpredictable manner and the material was found to spread laterally in addition to the longitudinal spread. The amount of spread was found to be

dependent not only on the dimensions and type of material used, but also on the diameter and surface conditions of the rolls, rolling speed, etc. To understand these it was necessary to develop the mathematics of rolling.

In addition to these, new materials, higher outputs, lower rolling costs, better products with uniform gauge, etc., demand more knowledge of the principles underlying rolling. The functions of rolling mill research are to provide this knowledge and to show the ways of improvement[7].

1.3. The Sendzimir cold rolling mill.

The Sendzimir cold rolling mill has achieved recognition throughout industry in rolling ferrous and non-ferrous metals[8]. Sendzimir mills are cluster mills and they differ fundamentally from conventional mills. This fundamental difference is the way in which the roll separating forces are transmitted from the work rolls, through the intermediate rolls to the back-up assemblies, and finally to the rigid housing. As this design permits the support of the work rolls throughout their length, deflection is minimised and extremely close gauge tolerances can be acheived across the full width of the material being rolled. In comparison to Sendzimir mills, the rigidity of conventional mills is governed by the size of the work rolls and the back-up rolls, which are supported by their

necks in two separate housings. Under rolling pressures
this results in roll deflection and therefore thickness
variation, especially near the centre of the strip.

The housing of Sendzimir mills is designed to
deflect uniformly across the entire width of the mill. It
provides continuous backing to the roll cluster and has
the heaviest cross section at the centre of the mill
where the forces are greatest. It also has short heavy
columns to carry the roll separating forces which makes
the mill very rigid. This makes it possible to produce
strips with extremely close tolerances across and throughout
the length.

All bearing shafts (see fig.1.1) of Sendzimir
mills have concentrically mounted roller bearings and are
located eccentrically in saddles. A cross section of one
is shown in fig.1.2. By rotating the bearing shafts, the
position of the backing bearings can be changed with
respect to the housing, to closely control the distance
between the work rolls. This is the basic control movement
of the mill that permits accurate positioning of its rolls.
A detailed description is given in section 2.7.2.

On Sendzimir mills crown control adjustment
operates on the top backing bearings. It is known as
"As-U-Roll" crown adjustment and is actuated hydraulically
from the operator's desk while the mill is running.
As-U-Roll operation is described in detail in section
2.7.3.

Another feature of Sendzimir mills is the capability of using small work rolls. Small work rolls are subject to less flattening and can continue to reduce metal even after it has become work hardened and very thin. This means that the mill is capable of rolling harder metals without intermediate annealing. Another advantage of the small rolls is that tungsten carbide rolls can be used economically. Rolls of this material produce high standard surface finish and maintain it over long production runs. Small rolls can be changed very easily and quickly so that strip of various widths and finishes can be rolled without stopping the mill for long periods of time.

On Sendzimir mills, lateral adjustment of the first intermediate rolls provide a means for rolling strip of various widths with a minimum of set up time, (see section 2.7.4). These intermediate rolls are furnished with tapered ends and this exclusive feature adds greatly to the flexibility of the mill.

When rolling materials like stainless steel the rolls and the strip get extremely hot due to friction effects. Recirculating coolant is used to lubricate and cool the roll gap, rolls and backing bearings of the mill. The main cooling of the mill is done at the roll gap by using high pressure sprays. In general, the flow of the lubricant is directed from the centre to the outside edges

of the strip so that the lubricant would wash away any loose particles of the metal being rolled. One of the requirements for good operation of the mill is good filtration of the lubricant and good maintenance of the filters. Normally the coolant system consists of a dirty lubricant tank, pumps to send the lubricant to filters, a clean oil tank and pumps to send the lubricant to the mill.[9]

There are several different types of Sendzimir mill[10] and the four basic types are shown in fig. 1.1. The subject of this study is the type 1-2-3-4 Sendzimir mill which is the most powerful and most flexible. The roll cluster contains twelve rolls and eight backing bearing assemblies as shown in fig. 2.4. The type 1-2-3-4 mill also varies with size, and are used to roll different dimension strips. In particular this study is concerned with a 1.7 m wide type 1-2-3-4 mill which is situated at British Steel Corporation Stainless, Shepcote Lane, Sheffield, England.

1.4. Shape control problem.[11-18]

Shape describes a deviation from flatness in sheet or strip of metal. The change in demand from sheet to coil experienced by wide strip produced over the past fifteen years has brought about the need for good shape to be acheived during continuous strip processing. The demands on shape for domestic products such as washing machines,

- 8 -

fridges, freezers, etc., are most severe.

Shape is the second largest single cause for the rejection of cold rolled steel strip. Bad shape is often caused by the mismatch between the roll gap profile and the incoming strip thickness profile. This can produce transverse variations in thickness (or variations in reduction of thickness across the width) which result in differential elongations across the width of the rolled strip. These differences can be accommodated only by large internal stresses within the strip which may cause local elastic buckling. Shape is related to internal stresses of the strip and shape is defined as the internal stress distribution due to a transverse variation in thickness reduction. The strip is said to have good shape when the internal stress distribution is uniform (see sections 2.1 and 2.2). Hence shape control refers to control of internal stress distribution across strip width when undergoing a thickness reduction.

The assessment of shape during rolling was simple when waves and the profile of ends could be seen in strips. The changing pattern of reflections on the surface may allow the deviation of flatness to be detected and the effect of corrective actions to be judged. However, with increases in strip tension, speed, coolant supply and enclosure of rolling mills, the observation is often unreliable. An instrumental method of detecting shape has

thus became desirable and essential for closed loop control. It was only in the last fifteen years that reliable shape measuring devices have become commercially available and the situation with shape control is now rapidly changing.

It has been well known that transverse variations in thickness are associated with bad shape and cambered rolls were used to counteract the mismatch between roll gap profile and the incoming thickness profile. It has been suggested that roll deflections should be minimised, to correct shape defects, by reducing roll force with smaller work rolls and backing them with stiff support rolls. It has also been suggested that roll force should be maintained constant at the correct value to match camber and that thermal camber should be minimised by efficient cooling. Strips may have localised bad shape due to uneven coolant application causing hot bands on the rolls and this may be remedied using efficient coolant distribution.

Tension can correct bad shape during rolling, but its effectiveness is not prominent, and it must be kept well below the yield stress to avoid fracture. By regulating screw-down settings, tension or speed it is possible to adjust roll force and deflection, but this action may affect the mean gauge as well as the transverse gauge variation. The resultant effect on shape is judged by the operator and he will attempt to choose a suitable

corrective action for improving flatness as well as gauge uniformity.

One of the main obstacles for automatic closed loop control of shape was the commercial availability of reliable shape measuring devices. In the last fifteen years this has been overcome and reliable shape meters are available as shape monitoring element. The design of closed loop shape control systems became the current interest in the metal rolling industry.

1.5. Objectives and summary of presentation.

The first requirement in the design of a shape control system for a rolling mill is a model of the mill. Both static and dynamic models are required for this purpose. The static model is used to calculate the steady state gains which will then be used in the dynamic simulation. The main objective of this study is the development of the mill model which represents the roll cluster and the conditions within the roll gap.[19]

The shape problem is discussed in chapter two. The definition and units of shape are given and shape measuring devices are discussed briefly. A detailed discription of the Sendzimir type 1-2-3-4 mill is also given.

Chapter three describes the basic foundations of the static model and in chapter four the complete

static model algorithm is discussed. A discussion of the state space representation of the whole shape control system is also given in chapter five. The static model results are presented and discussed in chapter six and some suggestions for improvement of the model are also given.

Backing bearing

Bearing shaft

(a) 1-1 mill (4 high)

(b) 1-1-2 mill (8 high)

Backing bearing
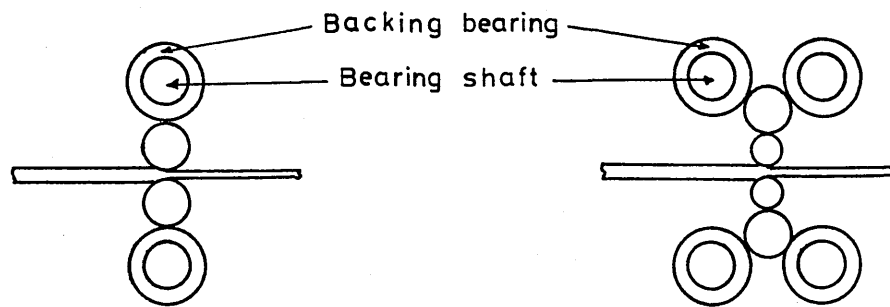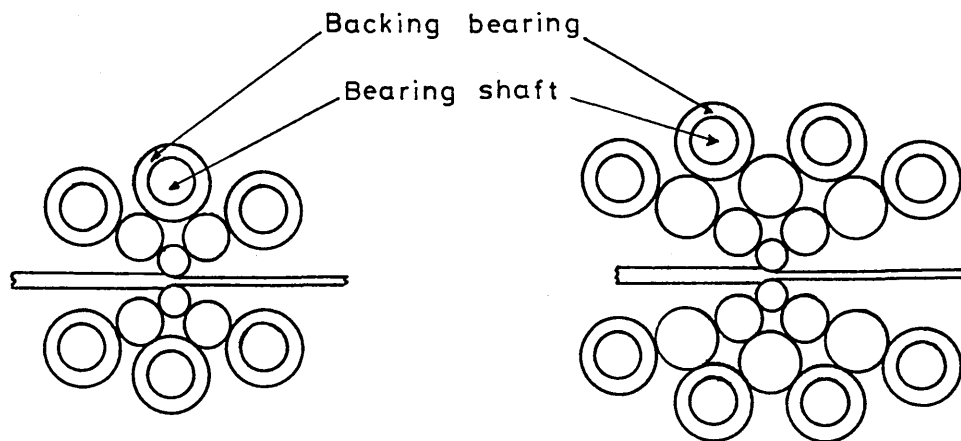
Bearing shaft

(c) 1-2-3 mill (12 high)

(d) 1-2-3-4 mill (20 high)

Fig. 1.1. Types of Sendzimir mill.

Eccentric ring

Backing bearing

Bearing shaft

Foot of the saddle
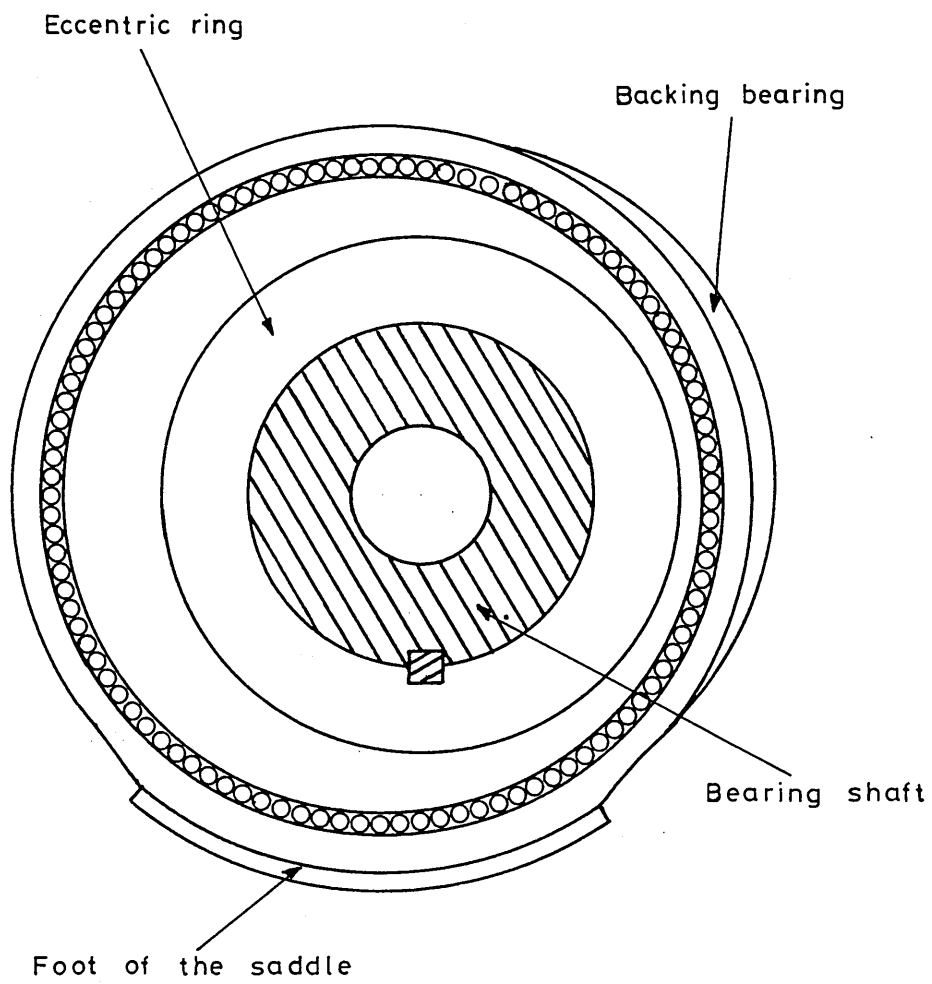
Fig. 1.2. Cross section of a bearing shaft

showing eccentric rings.

Chapter 2.

THE SHAPE CONTROL PROBLEM.

2.1. Introduction.

In recent years, the problem of the control
of the gauge of steel strip leaving a rolling mill, has
largely been solved[20]. The major problem of current interest
in cold rolling mills involves the control of internal
stresses in the rolled strip[21-27]. This is referred to as
shape control, a term which often causes confusion. Strip
with good shape does not have internal stresses rolled into
it. When such a strip is cut into sections, they should
remain flat when laid on a flat surface. Shape measurement
is generally a difficult problem, since the strip is
normally rolled under very high tensions which makes the
shape defects not visible to the naked eye. It is only
in the last fifteen years that reliable shape measuring
devices have become available and this has enabled recent
work on shape control to progress to the closed loop
control stage.

To illustrate how bad shape might arise
consider a strip having an entry gauge profile of uniform
thickness. Assume also that the work roll has a profile
such that the diameter of the work roll at the centre is
larger than at the edges (barrel shape). When a strip
having uniform thickness is rolled using the work roll

described above the reduction of thickness at the centre of strip will be greater than at the edges, assuming that there is no lateral spread. Since strip is one homogeneous mass such differential elongations cannot occur and internal stresses result. Clearly if the strip is to be flat after rolling, the reduction of thickness as it passes through the roll gap must be a constant across the strip width.

Shape may be defined as the internal stress distribution due to a transverse variation of reduction of the strip thickness. There are two types of bad shape. If a section of strip is sufficiently stiff to resist deformation the strip may appear to have good shape, but latent forces will be released causing deformations during slitting operations. This type of bad shape is referred to as latent shape. The second type of bad shape is called manifest shape, where thin strip having insufficient strength to resist forces imposed, exhibits bad shape in the form of waves or ripples extending along the length of the strip and covering the whole or part of the width.[12] These two types of bad shape are illustrated in fig. 2.1.

The stress distribution patterns giving rise to bad shape may be tensile or compressive in nature. The actual appearance of buckling will depend upon the distribution of stresses and some examples[28] of manifest shape known generally as long edge, long middle, herring bone and quarter buckle are illustrated in fig. 2.2. Long

edge and long middle arise from fairly elementary stress configurations. As the strip thickness decreases the latent stress capacity decreases and hence manifest shape defects are more often observed. Frequently these appear in complex forms such as herring bone and quarter buckle.

Deformations such as long edge and long middle are caused by the mismatch between the strip and roll gap profiles under rolling. The factors which affect strip shape may be listed as:[29]

1. Incoming hot band strip profile,

2. Roll separating force and its effect on roll camber,

3. Strip entry and exit tensions,

4. Slip in the roll gap.

2.2. Definition and units of shape.

Shape may be defined as the internal stress distribution due to transverse variations of reduction of the strip thickness. The transverse variation in the longitudinal stresses is caused by the transverse variations in the slip and hence the strip velocity at the exit of the stand (or at the entry to the next stand in a multistand mill).

Pearson[14] has defined a unit of shape called the 'mon' in terms of the classical long edge or long middle defects. Pearson relates shape to the amount of

bowing present in narrow bands slit from the strip. The mon defines the shape of strip which if slit into bands of 1 cm wide, would produce a lateral curvature corresponding to a radius of 10^4 cm. If this definition is applied to a long edge or long middle defect, the shape in mons is the fractional difference in elongation between the centre and edge of the strip multiplied by a factor of 10^4. That is, let $\Delta\ell$ represent the difference in length between the longest and shortest line segments of the strip, then

$$\text{mons} = \frac{\Delta\ell}{\ell} \cdot 10^4 \qquad\qquad (2.1)$$

For example, for 0.01 % elongation $\Delta\ell/\ell = 0.0001$ and this equals one mon unit. The strip shape may be defined as the relative length difference per unit width expressed in mon/cm. That is

$$\text{Shape} = \frac{\Delta\ell}{\ell} \cdot \frac{1}{w_s} \cdot 10^4 \quad \text{mon/cm} \qquad\qquad (2.2)$$

where w_s is the width of the strip in cm. For most applications a shape of 0.05 mon/cm is considered very good and a shape of 1 mon/cm is considered very bad in rolling strip.

Sivilotti et al[30] define another unit for shape called I units. It is defined as

$$\text{I unit} = \frac{\Delta\ell}{\ell} \cdot 10^5 \qquad\qquad (2.3)$$

2.3. Shape measuring devices.

The lack of a good shape measuring device for many years frustrated the proper control of flatness of strip. As compared to gauge measurement, shape is rather difficult to measure. The strip tension between the last stand and the coiler is usually high and therefore the strip appears perfectly flat (latent shape). Here the visual inspection is no use and is little help to the operator who has to decide whether the shape is acceptable or not. Therefore a reliable measuring device which indicates the shape was required. It was only in the last fifteen years that reliable shape measuring devices have become commercially available and have been applied in the steel industry. Due to this fact the situation with shape control is now rapidly changing.

There are various types of shape measuring devices. The most successful and reliable devices seem to be the Leowy Robertson Vidimon shapemeter[31] and the ASEA Stressometer shapemeter.[32-34] The Japanese have already applied the former to open loop control on a Sendzimir mill.[35,36] However the latter device will be considered here since this is the instrument employed on the steel mill of interest.

2.3.1. Principles for shape measurement.[12,21,22]

Only two practical basic methods are available for shape measurement. The first method which can be

- 19 -

applied to magnetic materials, uses the fact that magnetic permeability of ferromagnetic materials changes with stress. This system consists of two U-shaped iron cores, where one core is magnetised with alternating current which induces a magnetic field in the strip. The other core is used for sensing the magnetic potential difference between two points in the field, which will produce an output voltage proportional to the local stress without touching the strip. A set of devices spaced across the strip or one single device moving across the strip will produce a measurement of strip stress distribution.

The second method uses a device which deflects the strip a certain angle by means of a roll and measures the deflecting forces on a number of measuring zones.

2.3.2. ASEA Stressometer.

The ASEA Stressometer shapemeter uses the second method mentioned above. The stressometer measuring equipment consists of a measuring roll, a slip ring device, an electronic unit and a display unit. A schematic diagram is shown in fig.2.3. The measuring roll is divided into a number of measuring zones (for the Sendzimir mill 31 zones) across the roll, and the display unit has the same number of indicating panels. Stress in each section of strip is measured in the zone independent of adjacent zones. A condition for this independence is that the whole roll assembly and the individual measuring zones are very much

stiffer than the curved part of strip. The sensors are a form of magnetoelastic force transducer and these are placed in four slots equally spaced around the roll periphery. The periodic signals from each zone are filtered and the stress in each zone is calculated. The average stress is also calculated and the deviation of actual stress from the mean is displayed on corresponding display units. To obtain the best possible representation of the actual stress distribution, it is required to arrange the measuring roll and coiler parallel to the roll gap. Any deviation from this will introduce false stress profiles superimposed on the true profile.

2.4. Shape control mechanisms.

The main task of any shape control scheme is to produce a strip with low transverse variation of stress at the mill exit. The shape can be affected either by changing the roll deformation,[37] by changing the roll profile, or by changing the thickness profile of the ingoing strip. Roll deformation can be changed either by varying the reduction or by applying bending forces to roll bending mechanisms. It is usual to maintain the correct exit gauge and thence the reduction must be kept constant. Thus roll bending mechanisms are used to affect the shape. Another factor affecting the shape is the strip tension. By altering the strip tension, the roll force can be changed which in turn changes the roll gap profile.

Another method sometimes used is to change the thermal camber of the rolls. The thermal profiles developed on the rolls during rolling are due to friction and the heat input across the strip width in the roll gap. By varying the amount and/or distribution of the coolant on different parts of the rolls, the thermal expansion and hence the strip shape can be modified. Coolant spray control has the advantage that it can produce a wide range of roll profiles. This type of control has a long time constant, sometimes several minutes, which can be a disadvantage.[38] Regulation by tension and roll bending can clearly be faster than the action of the thermal camber control. Regulation by tension, though it is faster, is limited by what additional tensile stress the strip can sustain. The comparative efficiency of these methods still remains to be investigated.

2.5. Disturbances to shape.

Changes in mill entry gauge profile can be considered as one type of disturbance to shape. Another disturbance would be due to changes in roll force following from changes in the mean entry thickness of strip, hardness or friction. Changes in friction or the properties of the coolant may cause a change in thermal camber which also can be considered as a disturbance to shape. Changes in the thermal profile will always be slow. Roll wear, which

is very gradual, is also a problem in shape control.

2.6. Interaction between shape and gauge.

If a gauge error is corrected by the screwdown then the total rolling force changes the resulting shape. If a shape is corrected by adjusting tension then again roll force changes affect the gauge. On the other hand if shape is corrected by roll bending, then in addition to a change in the distribution of rolling pressures, the overall pressure between work roll and back-up roll will change altering their mutual flattenning. This will produce a change in the roll gap, thus affecting the gauge.

The gauge and shape control therefore always interact and a combined gauge and shape control system is required to be effective. However, since shape control systems are often added to existing steel mills, this is not always possible. In this study the effect of the gauge control loop will be neglected.

2.7. Description of the mill.

2.7.1. General description of the mill.

There are various types of Sendzimir mill. The mill considered here is 1.7 m wide and is a cluster mill where the work rolls rest between supporting rolls. The mill has eight backing shafts labelled A to H, six second intermediate rolls (I to N), four first intermediate

rolls (O to R) and two work rolls (S to T) as shown in fig. 2.4. This type of mill is used for rolling hard materials such as stainless steel.

The motor drive is applied to the outer second intermediate rolls (I, K, L and N) and the transmission of the drive to the work rolls via the first intermediate rolls is due to inter roll friction. Rolls labelled I to T have free ends and are free to float. The outer rolls (A to H) are split into seven roll segments as shown in fig. 2.5. The shafts in which these rotate are supported by eight saddles per shaft, positioned between each pair of roll segments and at the shaft ends. The saddles are rigidly fixed to the mill housing. The saddles contain eccentric rings. The outer circumferences of these rings are free to rotate in the circular saddle bores, while the inner circumferences are keyed to the shafts.

2.7.2. Upper and lower screwdown operation.

The upper screwdown racks act on assembles B and C, while assemblies F and G are responsible for the lower screwup system. Each saddle of the assemblies B and C is constructed as shown in fig. 2.6. The saddles on the F and G assemblies are also constructed in the same way but without the As-U-Roll eccentric rings. When the shaft is rotated, the eccentric screwdown ring also rotates in the saddle bore, since it is keyed to the shaft. This allows the centre c_2 of the shaft to rotate about the centre c_1

of the saddle bore, thus causing a nett movement of the shaft towards or away from the mill housing. Since the shaft is keyed to the screwdown eccentric rings in all eight saddles, the same motion will occur at each end and the shaft will remain parallel to the mill housing. Essentially, the screwdowns cause the movement of rolls I, J, K, O, P and S up or down which enables the distance between the two work rolls to be adjusted finely during rolling. A similar operation takes place at the lower assemblies F and G, which is used principally for roll changing and mill threading.

2.7.3. As-U-Roll operation.

In addition to the screwdown system, the upper shaft assemblies B and C contain further eccentrics, which allow roll bending to take place during rolling to adjust strip shape. Such a facility is referred to as the 'As-U-Roll'.

Each of the saddles supporting these two shafts is fitted with an extra eccentric ring (fig. 2.6) situated between the saddle and the screwdown eccentric ring. This eccentric ring can be rotated independently to the shaft and screwdown eccentric ring, by moving a rack which operates on two annular cheeks fitted on each side of this extra ring, as shown in fig. 2.7. Such a rotation will cause the centre c_3 of the inner bore of this ring to move in a circular path about the centre c_1. There

are eight such As-U-Roll racks on saddles between the
segments. These racks are capable of individual adjustment,
producing a different displacement between the shafts and
the housing at each saddle position. This allows a profile
to be forced on to the shaft as shown in fig. 2.8, which
will propagate to the work roll through the cluster.
Although the As-U-Rolls and upper screwdowns act on the
same common shaft they are essentially non-interactive.

2.7.4. First intermediate roll tapers.

In addition to As-U-Roll control of strip
shape there is another type of control on the Sendzimir
mill. The first intermediate rolls O, P, Q and R are
furnished with tapered off ends. This is illustrated in
fig. 2.9. These rolls can be moved laterally in and out
of the cluster. The top and the bottom rolls may be
moved independently and it is thus possible to control the
pressure at the edges of the strip within certain limits.
These rolls are therefore used to control the stresses
at the edge of the strip.

2.8. Elementary shape control scheme (fig. 2.10).

The major part of the shape control scheme
is the Sendzimir mill (section 2.7) which is a reversible
mill, i.e. the mill can be operated in both directions.
There are two ASEA Stressometer shapemeters (section 2.3.1)

- 26 -

on either side of the mill to measure the shape of the outgoing strip from the mill. Only one shapemeter is in operation at any particular pass. There is a decoiler which feeds the strip to be rolled into the mill. The purpose of the coiler is to roll the outgoing strip into a coil. When the mill is operating in the reverse direction the actions of decoiler and coiler are interchanged.

Between the coiler and the shapemeter, there is a third roll called the deflector roll. As the strip is rolled the coiler diameter is increased which changes the shapemeter deflector angle. The purpose of the deflector roll is to keep the deflector angle constant so that the shape is measured relative to this constant deflector angle.

There are two X-ray measurement devices on either side of the mill which measure the input and output mean gauge of the strip. In addition there is a control computer and an operator desk with the shape display unit. The basic scheme is illustrated in fig. 2.10.

2.9. Purpose of the study.

The first requirement in the design of a shape control system for a cold rolling mill is a model of the mill. Both static and dynamic models are required for this purpose. The static model must provide steady

state gains of the mill which relates the shape to a

given set of actuator positions. Therefore the static model

will calculate the shape profiles for a given set of

actuator positions, from which the mill gain can be

obtained. These gains are used in the dynamic model which

is a simulation of the state equations for the complete

system, including the shapemeter and strip dynamics.

The main objective of the present study is

the static model of the mill representing the roll

cluster and conditions within the roll gap. The strip

width is split into eight zones for modelling purposes and

it is assumed that there are eight shape measurements. The

design method, however, is applicable in the actual

situation where the number of shape measurement zones (≤ 31)

depends upon the strip width being rolled. The static model

enables an 8×8 mill gain matrix to be calculated, which

can then be used within a state space dynamic model for

the complete system.

Latent shape on subsequent

slitting along edge or middle

Manifest shape

with long edges

Fig. 2.1. Various forms of shape defect.

Stress distributions

Quarter buckle

Herringbone

Long middle

Long edge
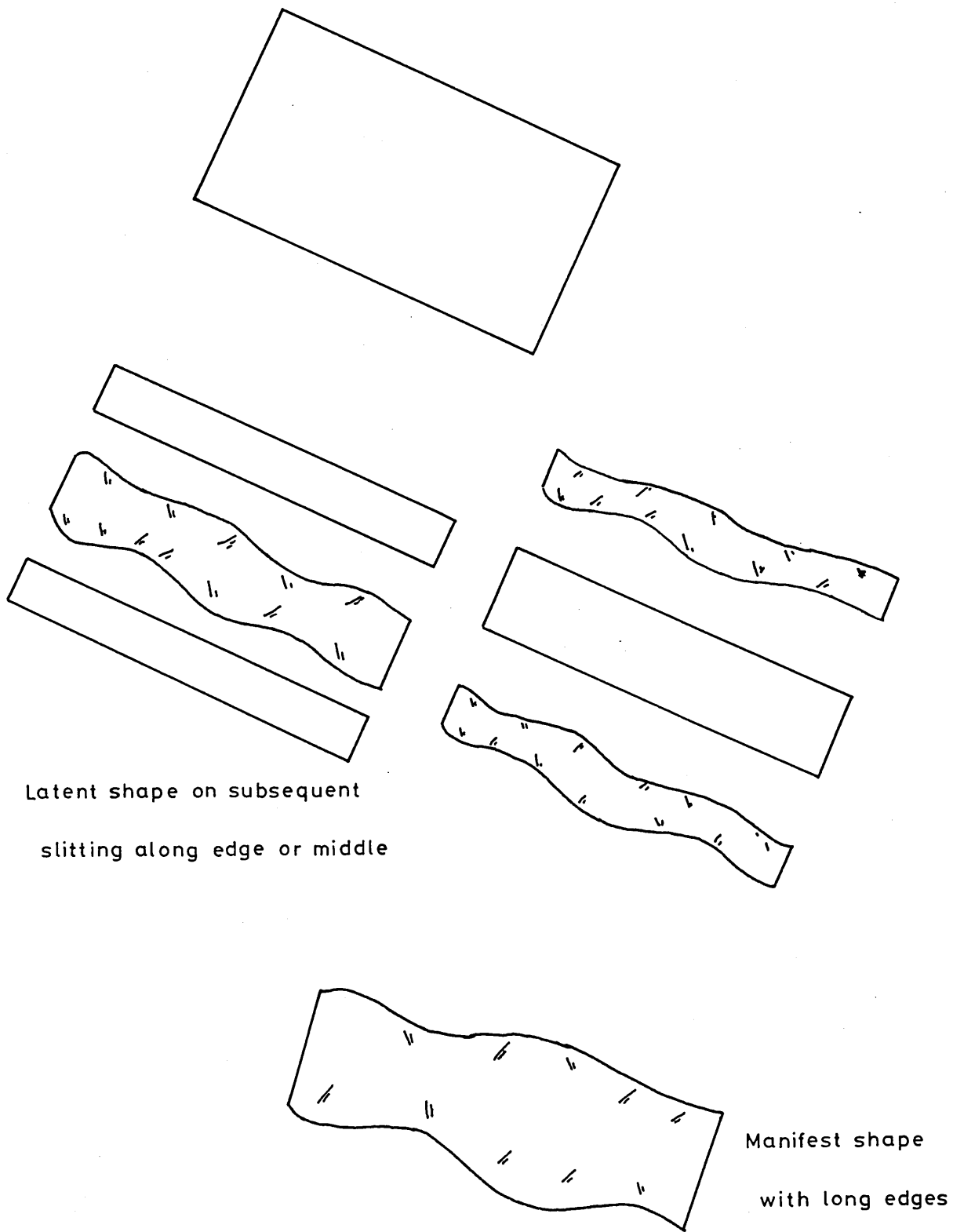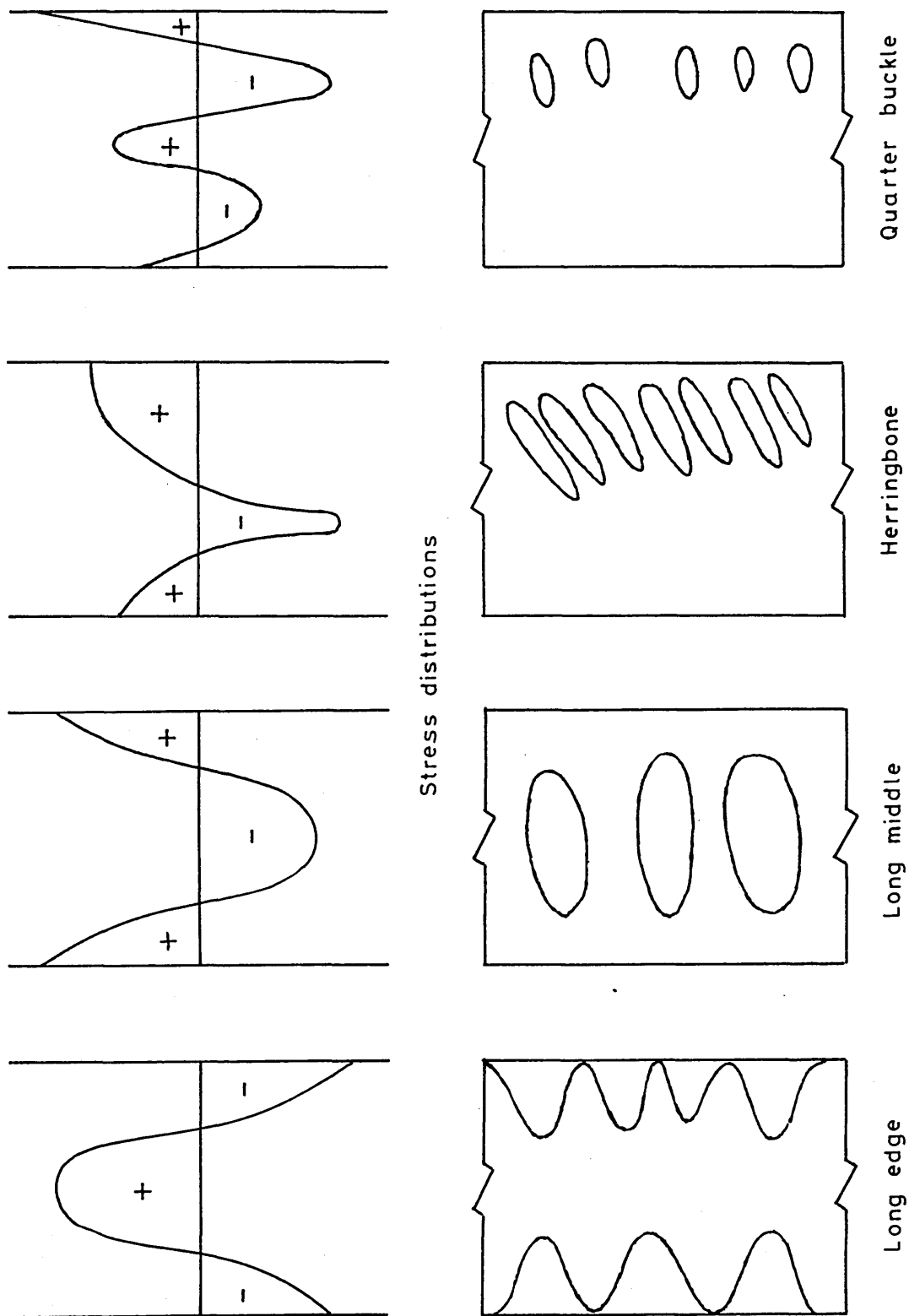
Fig. 2.2. Manifest buckling forms.
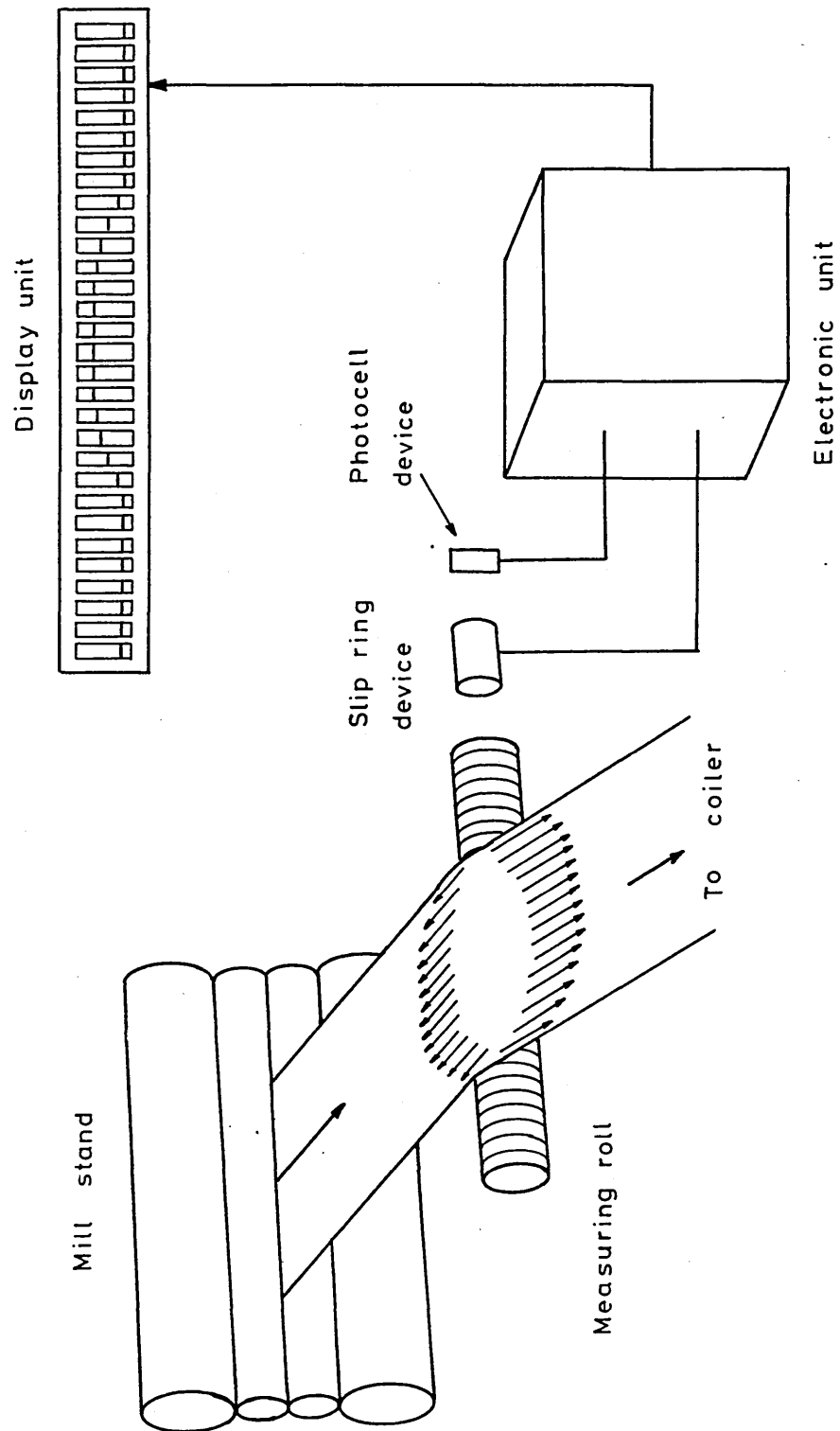
Fig. 2.3. Schematic diagram of Stressometer shapemeter.

Display unit

Photocell device

Slip ring device

Electronic unit

Mill stand

Measuring roll

To coiler
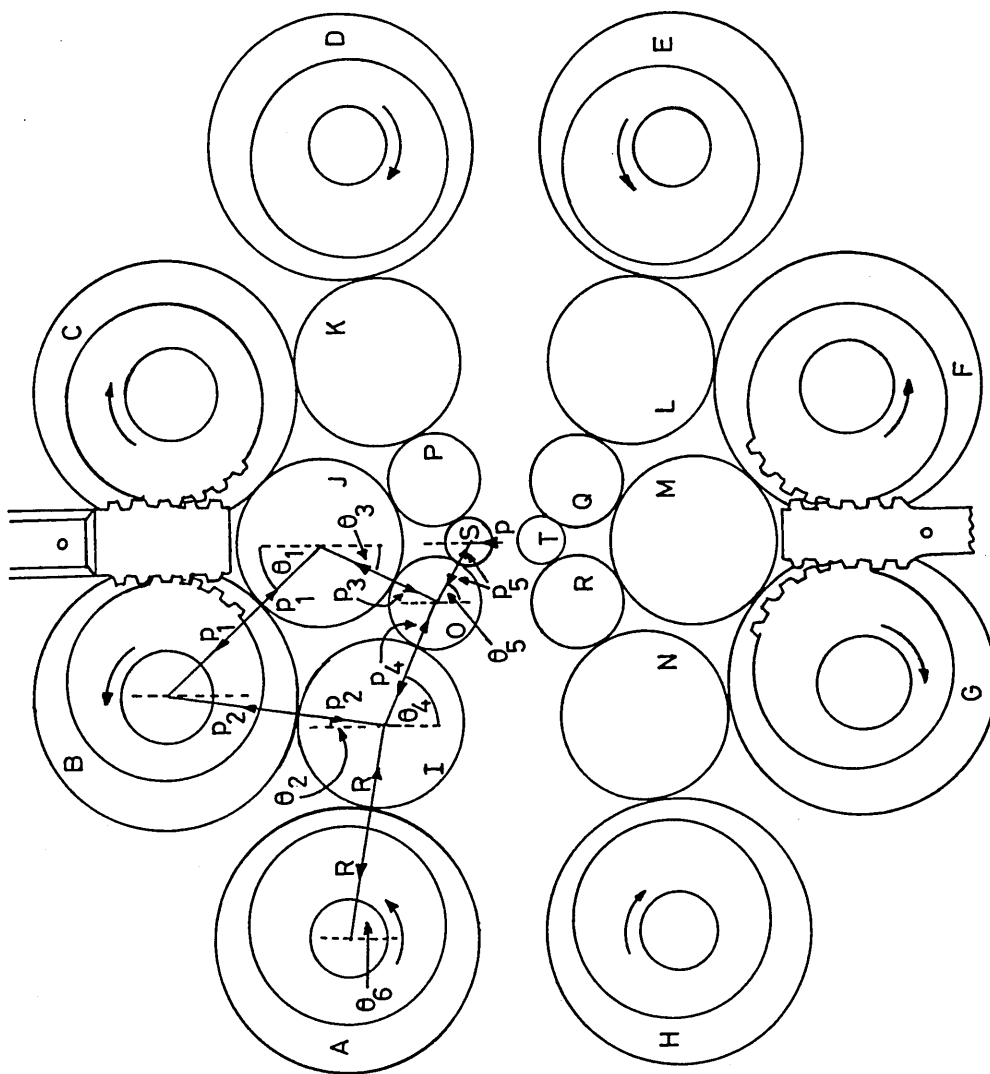
Fig.2.4. Zendzimir mill roll cluster.

Saddles bolted to mill housing

Roll segments (backing bearings) are free to rotate on shaft

Saddles

Eccentric ring in each saddle (keyed to shaft)
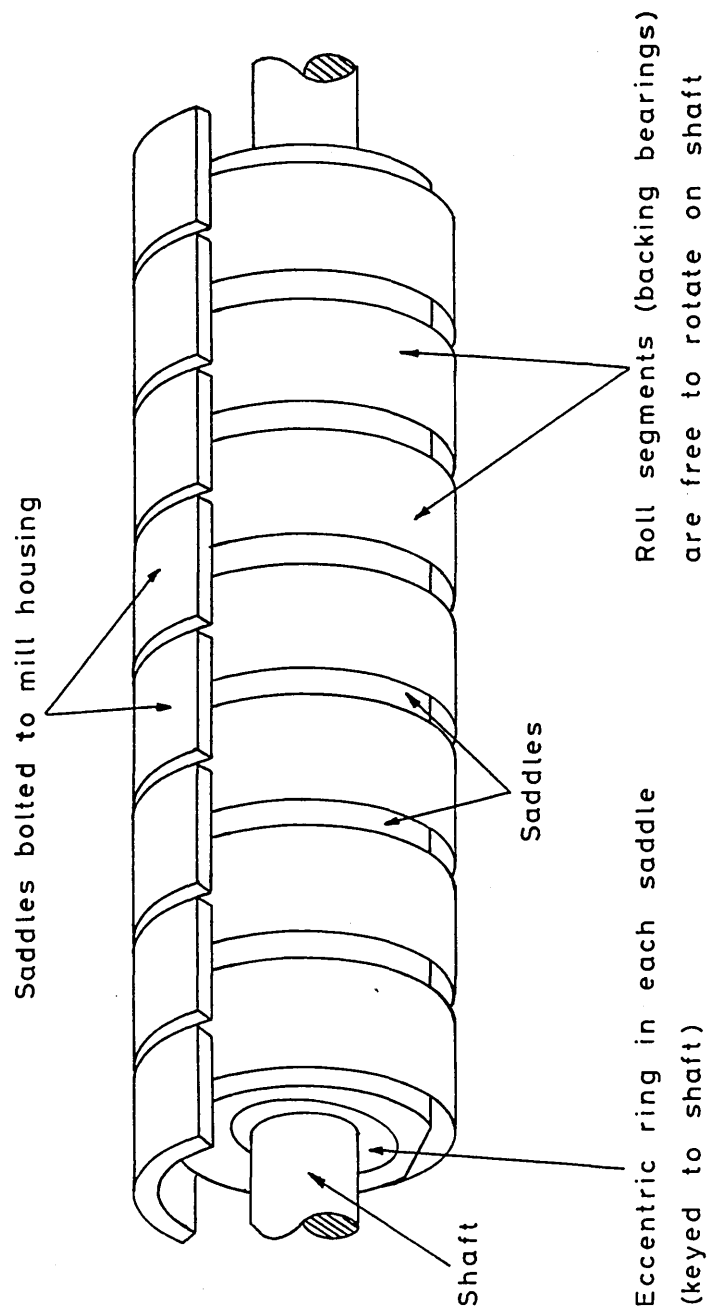
Shaft

Fig.2.5. Backing shaft assembly.
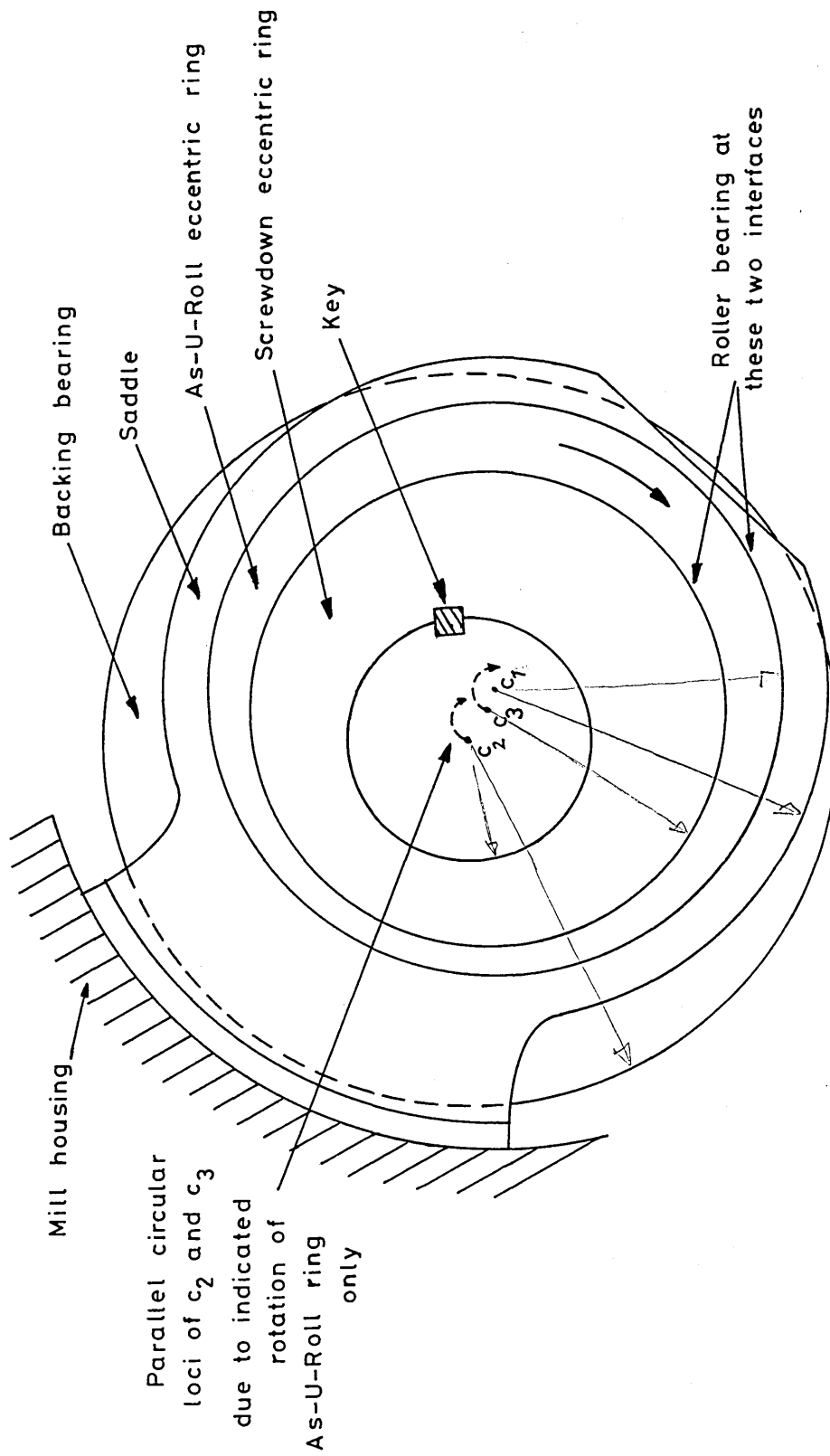
Fig. 2.6. Saddle detail shafts B and C (not to scale).

Backing bearing

Saddle

As-U-Roll eccentric ring

Screwdown eccentric ring

Key

Roller bearing at these two interfaces

Mill housing

Parallel circular loci of c_2 and c_3 due to indicated rotation of As-U-Roll ring only

c_2 c_3 c_1
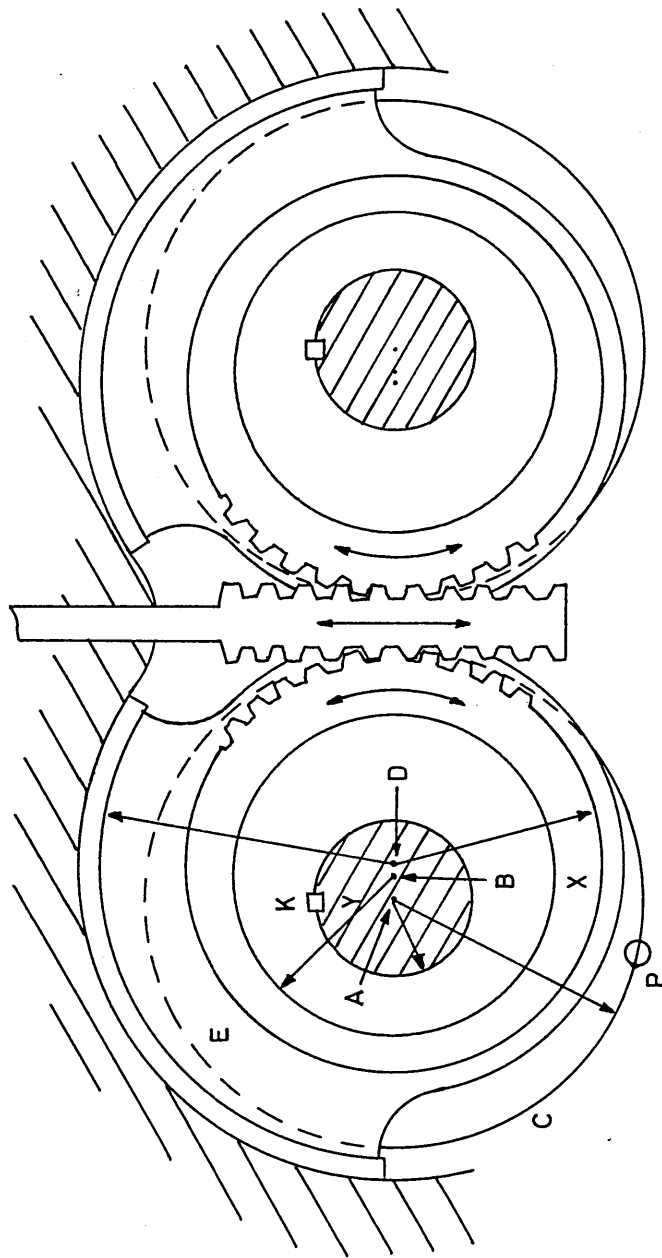
Fig.2.7. As-U-Roll assembly.
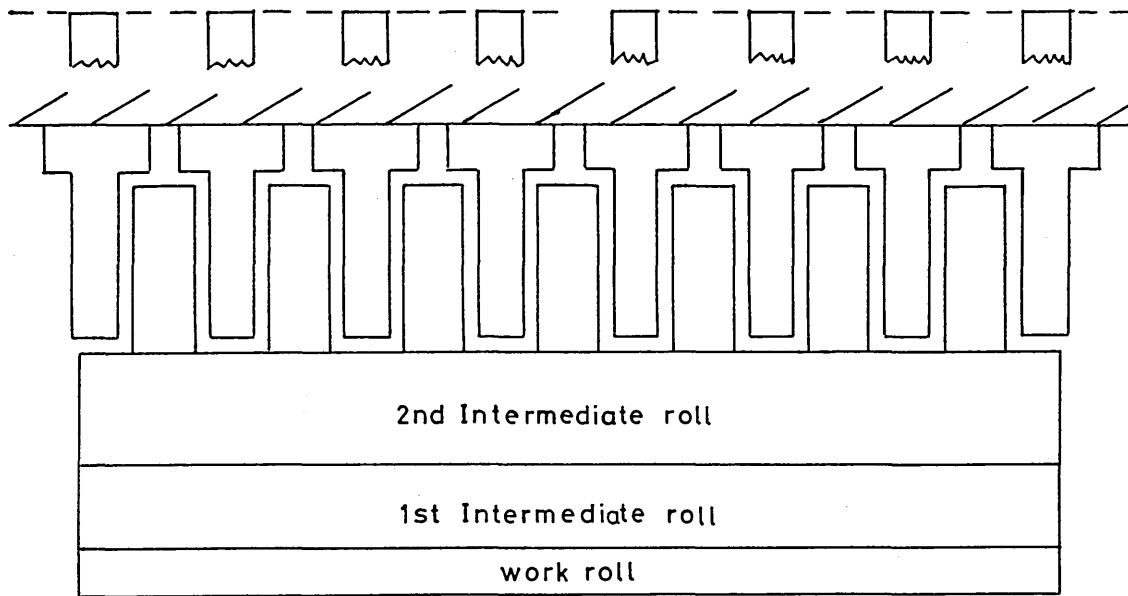
(a) As-U-Roll racks before motion
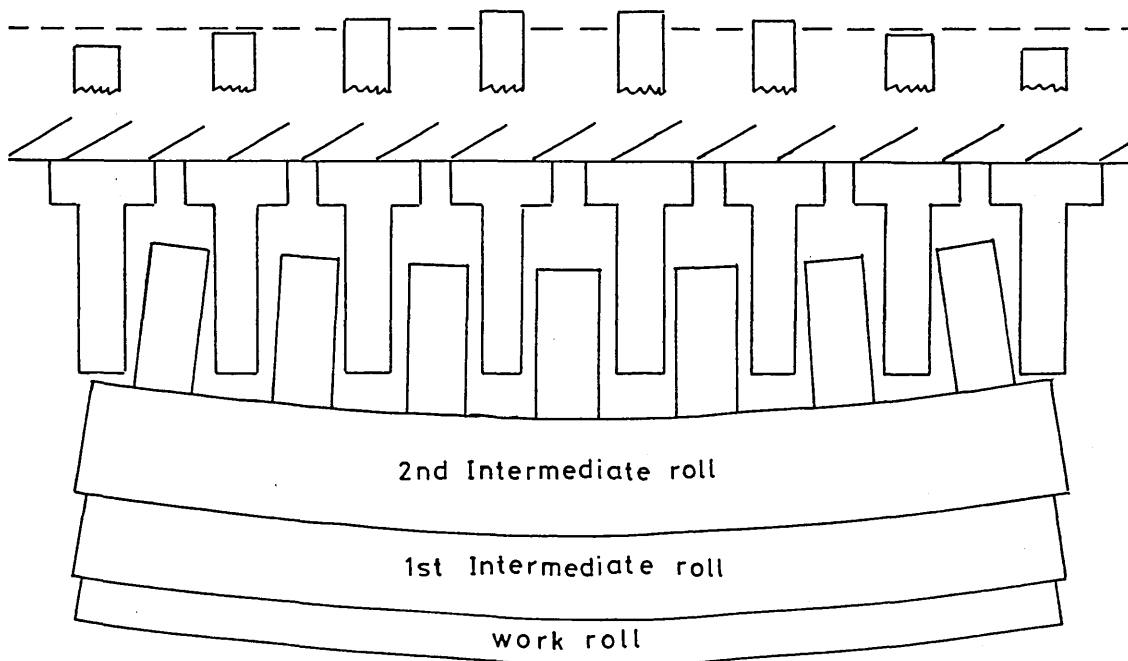
(b) As-U-Roll racks after motion

Fig. 2.8. Example of As-U-Roll action.

Fig.2.9. Tapered first intermediate rolls.

1st Intermediate roll with tapered end

work roll

strip

work roll

1st Intermediate roll with tapered end

Front of the mill
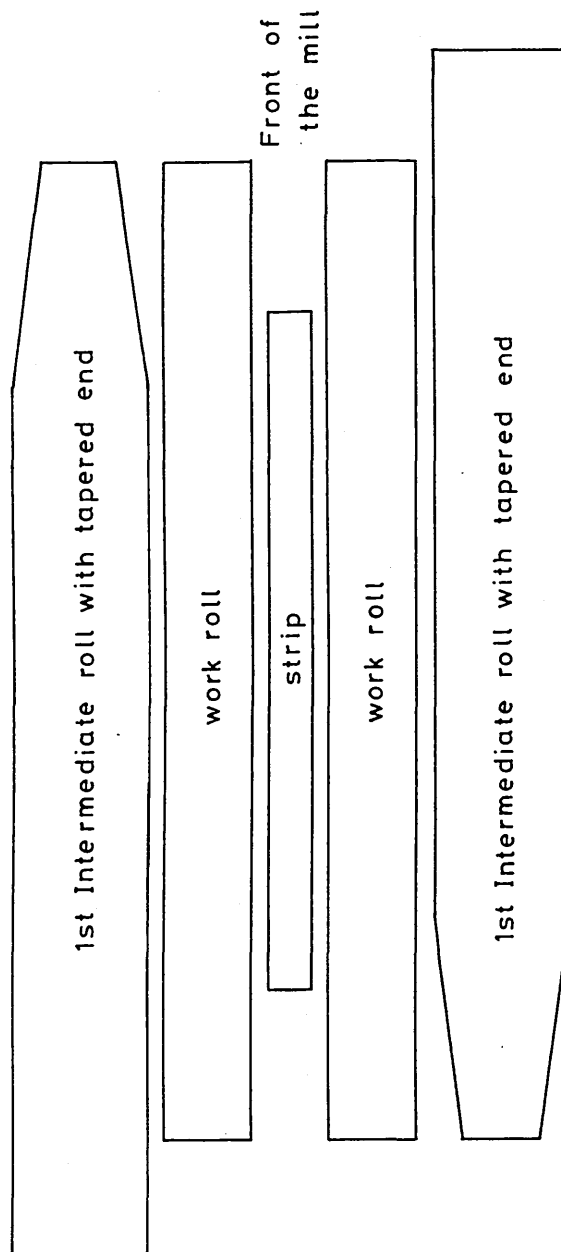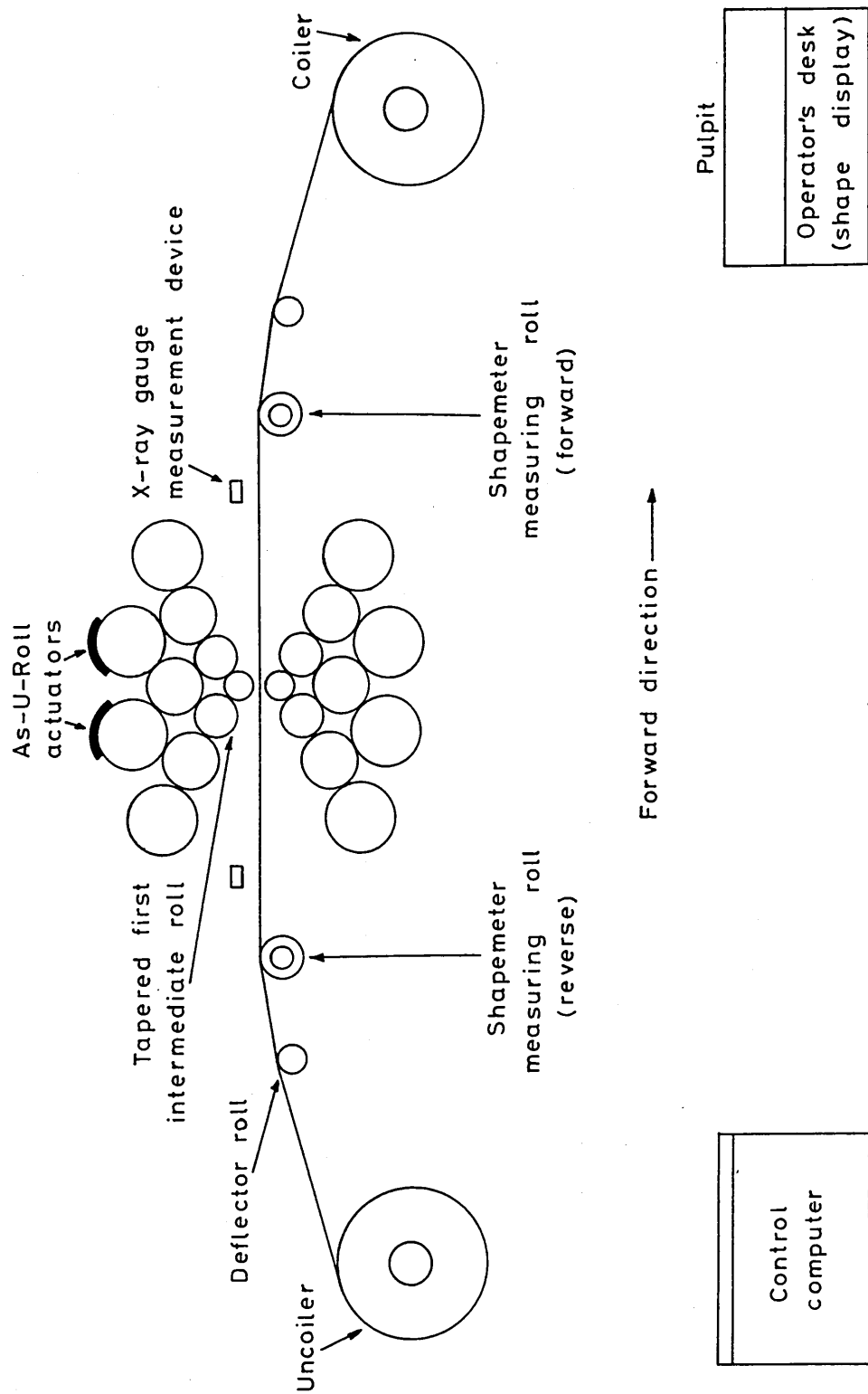
Fig.2.10. Schematic diagram showing the basic components in the system.

Chapter 3.

THE STATIC MODEL.

3.1. Introduction.

The study of any scheme for control of strip shape must be preceded by an accurate analysis of the formation of the loaded roll gap in the rolling stand. A static model[39] for the single stand Sendzimir cold rolling mill is described in this chapter, which provides a complete analysis of strip shape. The static model is a mechanical model for the mill which represents all force deformation relationships in the roll cluster and in the roll gap. It is important for control purposes to note that these relationships are both non-linear and schedule dependent.

The static model must allow for the bending and flattening of the rolls in the mill cluster and for the plastic deformation of the strip in the roll gap. The model should provide

(a) mill gains between actuator movements and strip shape changes based upon a small perturbation analysis,

(b) details of the degree of control which may be achieved with a given shape actuator or the first intermediate roll tapers and

(c) an understanding of the mechanisms involved in the

roll cluster and the roll gap which affect strip shape.

The model was developed in the form of a Fortran computer program. The model enables the output shape profile to be calculated corresponding to a given set of shape actuator (As-U-Roll rack) positions and hence the change in shape for a given change in actuator positions; the model also enables the shape change due to a change in the roll cambers to be calculated. Such a change can result from movement of the first intermediate rolls.

There are four main sets of calculations involved in the model which may be listed as follows:

1. Roll bending calculation: This is based on the theory of beams on elastic foundations[40]. This is justified, as in the mill cluster, Since rolls rest on each other and will be deflected due to elastic properties under loading conditions.

2. Roll flattening and inter roll pressure calculations: This enables the roll flattening between two rolls to be found for a given pressure distribution. The pressure distribution itself depends on roll flattening and hence this calculation is iterative.

3. Roll force calculation: This enables the roll force to be calculated for given strip dimensions and properties.

4. Output gauge and shape profiles calculation: This determines output gauge and shape profiles corresponding to inter roll pressure and deflection profiles.

The assumptions made in deriving the static model described may be listed as:

1. Elastic recovery of the strip may be neglected.

2. Horizontal deflections of rolls may be neglected.

3. The centre line strip thickness is assumed to be specified.

4. The mill is symmetrical about a line passing through the work roll centres (this need not be the case if the side eccentrics are set differently).

5. Strip edge effects may be neglected.

6. Deflections due to shear stresses may be neglected.

The first assumption is justified as small work rolls are used in the Sendzimir mill, which limit the arc contact and give small roll gap angles. The work rolls are laterally supported by the roll cluster and therefore there are no appreciable deflections of rolls in the horizontal direction, hence the second assumption follows. Because shape control depends on the profile of the loaded roll gap, it is assumed that the stand is operating under automatic gauge control and assumption three follows.

The strip is normally placed at the centre of the mill so that the strip width is symmetrical about the line passing through the work roll centres. The side eccentrics are used to adjust the roll gap and for normal operation both side eccentrics are moved by the same amount and hence the fourth assumption follows. The fifth assumption is made to simplify the calculations and this is one of the areas where improvements have to be made. The sixth assumption is justified as the deflection of a beam due to shear forces is very small compared to that due to bending forces.

3.2. Roll bending calculation.

It is well known that if a force is applied to a beam supported at two ends, the reactions at the ends and the deflection of the beam can be calculated using simple beam theory. If the beam is resting upon an elastic foundation, where the whole length of the beam is in contact with the foundation, the deflection of the beam may be calculated by assuming that the deflection is proportional to the reaction at that point. All the rolls in the middle of the mill cluster are resting upon one another and since these rolls are elastic bodies it can be assumed that each roll is resting on an elastic foundation. Thus the actual bending deflection y can be calculated as a function of the applied force F and the

distance x from one end of the beam; i.e. $y = f(F,x)$. To be more specific if ℓ is the length of the roll and the force F is applied at a point $x = a$, then

$$y(x) = \frac{F + K \cdot \Delta y(x)}{K} \cdot \lambda \cdot \beta(\lambda, \ell, a) \qquad (0 \leqslant x \leqslant a) \qquad (3.1)$$

where K is the foundation constant for a given roll and λ is a constant given by,

$$\lambda \triangleq \left[K/(4 \cdot EI) \right]^{\frac{1}{4}} \qquad (3.2)$$

Here $\beta(\lambda, \ell, a)$ is a function of λ and the length ℓ and a. The gap between the unloaded roll and the foundation is denoted by $\Delta y(x)$. Eq. (3.1) is the solution to the differential equation,

$$EI \cdot \frac{d^4 y}{dx^4} = F - K(y - \Delta y) \qquad (3.3)$$

which follows from the theory of elastic foundations.[40] Eq. (3.1) is true only when x is less than or equal to a. Deflections of points on the beam at distances greater than a may be calculated using the eq. (3.1) but with a replaced by $(\ell - a)$ and with x replaced by $(\ell - x)$.

3.3. Roll flattening calculation.

The calculation of the deformation which occurs between two touching rolls in the cluster, or between the work rolls and the strip, is discussed in this section. The roll surfaces may be assumed to be

cylindrical, neglecting minor bending distortions. Now when two infinitely long elastic cylinders are in contact the total interference $y_{12}(x)$ can be written as a function of the load per unit length $q'(x)$. That is,

$$y_{12}(x) = q'(x) \cdot (C_1 + C_2) \cdot \log_e \left[\frac{e^{2/3} (d_1 + d_2)}{2q'(x) \cdot (C_1 + C_2)} \right] \qquad (3.4)$$

where d_1 and d_2 are the diameters of the cylinders and C_1 and C_2 are two elastic constants for respective cylinders.[41-43] The loading along a roll is of course non-uniform and the roll is also of finite length. However, the influence of a point load does not extend far along the roll and, neglecting second order errors, $q'(x)$ may be replaced by the inter roll specific force $q(x)$ to calculate the interference $y_{12}(x)$. That is,

$$y_{12}(x) = f_1(q(x)). \qquad (3.5)$$

The interference $y_{12}(x)$ can also be calculated using the roll contours due to bending. If $y_1(x)$ and $y_2(x)$ are the deflections of the two rolls respectively, then the interference $y_{12}(x)$ is a function of these two deflections. Also the interference depends upon the thermal and ground camber $y_c(x)$. Thus,

$$y_{12}(x) = f_2(y_1(x), y_2(x), y_c(x)). \qquad (3.6)$$

Now deflections $y_1(x)$ and $y_2(x)$ will clearly depend upon the pressure $q(x)$ between the rolls and hence on $y_{12}(x)$. Therefore a third equation can be written for $q(x)$ given by,

$$q(x) = f_3(y_{12}(x)). \tag{3.7}$$

From eqs. (3.5) and (3.7) it is seen that $y_{12}(x)$ depends on $q(x)$ and $q(x)$ depends on $y_{12}(x)$ and hence $q(x)$ and $y_{12}(x)$ must be solved iteratively. The total pressure across the roll width w must be equal to the applied force F for the system to be in equilibrium, i.e.,

$$F = \int_0^W q(x)dx. \tag{3.8}$$

The method of calculating $q(x)$ and $y_{12}(x)$ is to substitute for $y_{12}(x)$ in eq. (3.7) from eq. (3.6) and to solve eq. (3.5) and eq. (3.6) iteratively by changing the distance between the roll centres until eq. (3.8) is satisfied to within a specified tolerance.

Orowan[44] has previously noted that extensive work roll flattening can occur. He also suggested a relatively complex method for calculating work roll flattening. However, for the present model, approximate results are used based upon the work of Edwards and Spooner.[24] They noted that the work roll flattening was

- 45 -

slightly dependent upon specific roll force and related to the Hertzian flattening which occurs between two elastic cylinders of the same diameter. The model proposed by them for the work roll flattening $y_{ws}(x)$ is given by,

$$y_{ws}(x) = \left[b_1 + b_2 p(x)\right] y_h(x) \tag{3.9}$$

where

$$y_H(x) = 2p(x) \cdot C \cdot \log_e\left[\frac{e^{2/3} d}{2p(x) \cdot C}\right]. \tag{3.10}$$

Eq. (3.10) is obtained from eq. (3.4) by setting $C_1 = C_2 = C$ and $d_1 = d_2 = d$. The constants b_1 and b_2 are estimated using plant test results and $C \triangleq (1 - v^2)/(\pi E)$, where v is the Poison's ratio and E is the Young's modulus of elasticity.

3.4. Roll force calculation.

The roll force calculations are an important part of the static model. The amount of reduction in thickness of the strip is related to the total load in the mill or roll force. An extensive literature exists on the calculation of specific rolling force $p(x)$ as a function of input output thicknesses, input output tensions and work roll radius[45] i.e.,

$$p(x) = f(h_1(x), h_2(x), \sigma_1(x), \sigma_2(x), R). \tag{3.11}$$

- 46 -

When rolling hard materials, like stainless steel, very high forces must be applied. Since work rolls are elastic bodies they will be deformed and flattened at the roll gap.[46] In order to calculate the roll force, including the flattening effects, an iterative procedure must be adopted because the deformed roll radius is a function of the roll force. The deformed roll radius R' can be calculated using Hitchcock's formula[43,47] given as

$$\frac{R'}{R} = 1 + \frac{c\ p(x)}{\delta} \qquad (3.12)$$

where c is a constant,

δ is the amount of reduction equal to $\left[h_1(x) - h_2(x)\right]$,

R is the initial roll radius.

The roll force may be calculated by solving eqs. (3.11) and (3.12) iteratively.

The disadvantage of the above approach for roll force calculation is the time the algorithm takes to converge. For modelling purposes the width of the strip is split into 25 mm sections (this is to match the physical dimensions of the back-up-roll) and the roll force must be calculated in each of these sections. Thus for one metre wide strip the roll force model must be made to converge forty times. The shape calculation is also iterative and thus all the roll force calculations must be performed on each of the iterations of the shape algorithm. Thus, although the roll force calculation does not require

a very large computing time this is multiplied by the number of strip sections and the number of shape program iterations.

3.5. Output gauge and shape profile calculations.

The output gauge profile may be calculated once a given set of inter roll pressures and deflections are known. The shape profile then follows from the input and output gauge profiles and the input shape profile.

3.5.1. Output gauge profile calculation.

The output gauge profile is determined by the combined effects of roll bending, thermal and ground roll cambers and differential strip flattening. The change in the gauge profile due to these effects is given by

$$\Delta h_2'(x) = 2\left[y_{ws}(x) - \overline{y}_{ws}\right] + y_s(x) + y_t(x) + 2y_{wc}(x) \tag{3.13}$$

where $y_{ws}(x)$ and $\overline{y}_{ws}$ represent interference and mean interference between the work roll and the strip, $y_s(x)$ and $y_t(x)$ represent the upper and lower cluster work roll deflections and $y_{wc}(x)$ is the total of the thermal and ground work roll cambers. The mean of the change in output gauge is thus given by

$$\overline{\Delta h_2'} = \frac{1}{w_s} \int_0^{w_s} \Delta h_2'(x)dx \tag{3.14}$$

- 48 -

and hence the deviation of the change in gauge from mean is given by

$$\Delta h_2''(x) = \Delta h_2'(x) - \overline{\Delta h_2'} . \qquad (3.15)$$

The new change in output gauge is calculated from the iterative formula

$$\Delta h_2^{k+1}(x) = \Delta h_2^k(x) - \alpha\left[\Delta h_2^k(x) - \Delta h_2''(x)\right] \qquad (3.16)$$

where α is chosen to give a stable solution. The new output gauge profile is therefore given by

$$h_2(x) = h_{2m} + \Delta h_2^{k+1}(x) \qquad (3.17)$$

where h_{2m} is the specified output gauge.

3.5.2. Input and output stress profile calculation.

The new output stress profile can be calculated using the new gauge profile and the following result due to Edwards and Spooner:[24]

$$\Delta \sigma_2(x) = \beta E\left[\frac{h_2(x)}{h_1(x)} \cdot \frac{h_{1m}}{h_{2m}} - 1\right] + \frac{\Delta \sigma_0(x)}{1 + \gamma} . \qquad (3.18)$$

The input stress profile is given by

$$\Delta \sigma_1(x) = \gamma \Delta \sigma_2(x) \qquad (3.19)$$

where

$$\gamma \triangleq \frac{\sigma_1(x) - \overline{\sigma}_1}{\sigma_2(x) - \overline{\sigma}_2} \qquad (3.20)$$

and β is a constant ($\beta \simeq 0.5$); details are described in section 4.10.

3.6. Brief description of the static model computer algorithm.

The static model program uses an iterative procedure as shown in fig. 3.1. The model includes the calculations for the top half of the cluster as well as for the bottom half of the mill. It is assumed that the mill is symmetrical about the line passing through work roll centres. The model can be used for different values of strip width but for the present analysis the roll flattening equations ignore strip edge effects. The input data required by the model may be summarised as follows:

1. Cluster angles (see fig. 2.4)
2. Roll diameters
3. Roll profiles (camber, wedge etc.)
4. As-U-Roll positions
5. First intermediate roll positions
6. Entry gauge profile
7. Mean entry gauge
8. Mean exit gauge
9. Annealed gauge
10. Yield stress curve
11. Entry tension
12. Exit tension

13. Width of strip

The output data may be listed as:

1. Inter roll pressures (12 profiles)

2. Roll force profile

3. Roll deflections (12 profiles)

4. Exit shape (stress distribution) profile

5. Exit gauge profile

The mill width is divided into a number of section multiples of 67 and the following assumptions are made (the number 67 is chosen to match the physical dimensions of the back-up-roll and its segments).

1. The pressure distribution in each section may be calculated using a point load applied at the centre of the section and the width of the section.

2. The mean deflection of a roll over a section is taken to be equal to the deflection at the centre of the section.

These assumptions also apply to the stress distribution, strip profile, rolling pressure profile etc.

The computer algorithm enables a change in the shape profile due to a change in the rack position, and hence the gains of the mill to be calculated. The flow chart for the main program is shown in fig. 3.1.

The program begins by initialising all the variables and the roll force is then calculated using the

roll gap model. Symmetry about a line passing through the work roll centres can be assumed so that calculations are necessary only for the left half of the mill cluster. The subroutine BEND calculates the pressure profiles and roll profiles of one half of either the top or bottom mill cluster. If symmetry is not assumed then the routine BEND has to be called four times to calculate all the pressure and roll profiles. At the end of each calculation of all pressure and roll profiles a convergence test is carried out on the output shape profile. The above calculations are repeated until the error between two successive shape profiles is less than a predetermined value.
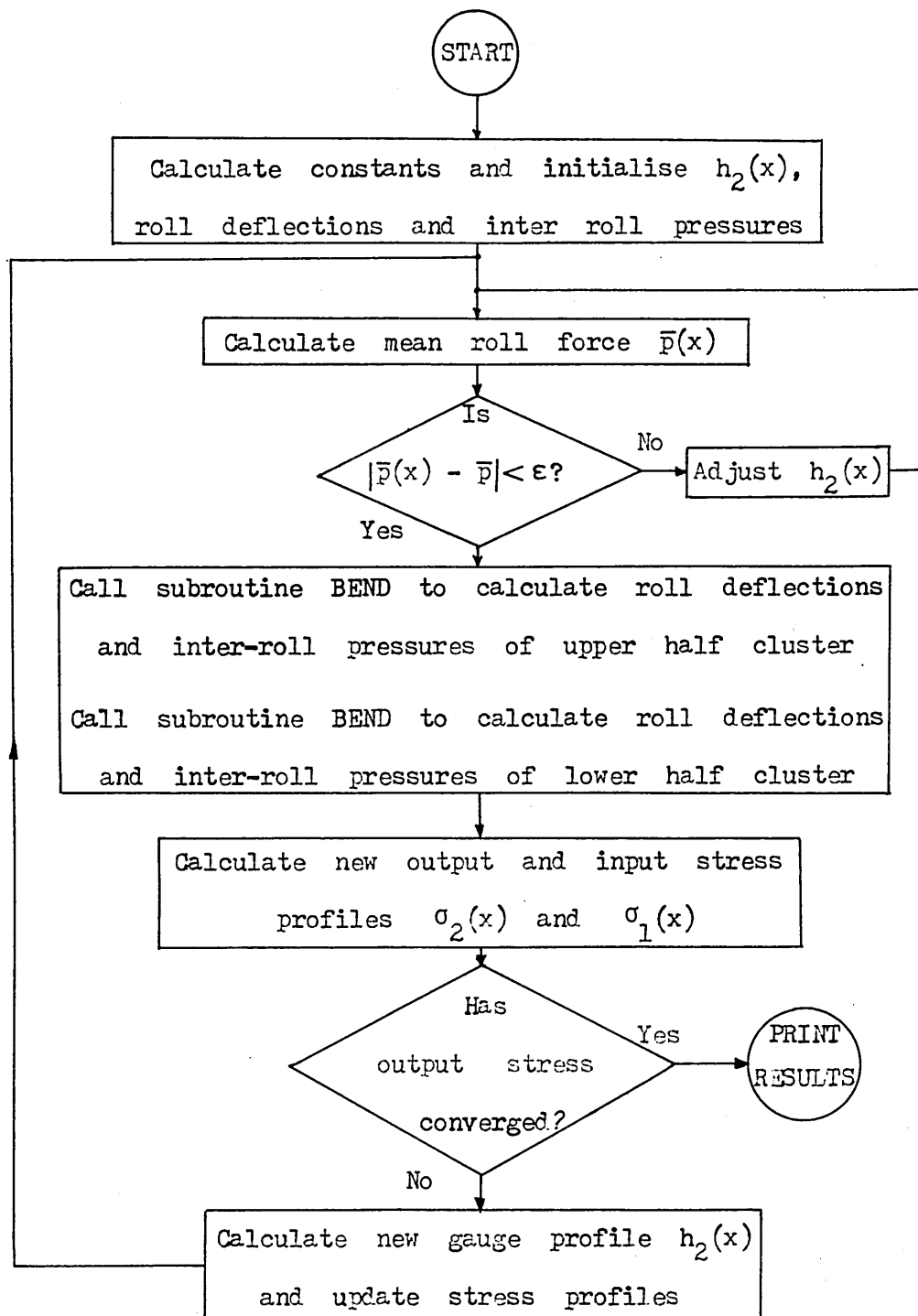
Fig. 3.1. Flow chart for the main program.

Chapter 4.

COMPLETE STATIC MODEL ALGORITHM.

4.1. Introduction.

The complete description of the mill gain calculation is described in this chapter. Sections 4.2 to 4.7 describe the calculation of mill constants. Sections 4.8 to 4.11 describe the roll force model, roll pressure and deflection calculation, thickness and stress profile calculation. The final two sections describe the complete model and the gain matrix calculation.

The mill width is divided into 67 sections or multiples of 67 sections. This odd number 67 is chosen to match the back-up roll dimensions to its segments. To be more precise, for one segment of the back-up roll (see fig. 4.1), the ratio between the portion in contact with the second intermediate roll b to non contact area $(\ell - b)$ is an integer if the mill width is divided into 67 sections. That is lengths b and $(\ell - b)$ can be divided into an integer number of sections. The width of each section is given by

$$dx = \frac{W_m}{N} = \frac{W_m}{67} .$$ (4.1)

4.2. Strip width adjustment.

The width of the strip w_s has also to be adjusted so that the strip width will have an integer number of sections. This is done in the following manner. The strip is placed in the mill so that the centre of the strip width lies on the vertical line passing through the mill centre. If the edge of the strip lies inside a section (see fig. 4.2) the distance between the edge of section and the edge of the strip is calculated. This is denoted by Δw_s.

If $\Delta w_s > \frac{dx}{2}$, then

$$w_s = \left[(N - r - 1) - (r + 1)\right]dx = (N - 2r - 2)dx \qquad (4.2)$$

If $\Delta w_s \leq \frac{dx}{2}$, then

$$w_s = \left[(N - r) - r\right]dx = (N - 2r)dx \qquad (4.3)$$

where $(r + 1)$ is the integer number of the section in which the strip edge lies inside.

4.3. Strip dimensions.

Since most of the input gauge profiles are either rectangular or parabolic the model considers only these two types of profile. If the strip centre line thickness h_m and the amount of strip camber h_c are specified then the strip profile can be obtained as shown

below.

An equation for a parabolic profile as shown in fig. 4.3a can be written as (variables defined in fig. 4.3a)

$$y(x) = h_c \left[1 - (\frac{2x}{w_m} - 1)^2 \right] \qquad (4.4)$$

As shown in fig. 4.3b the thickness at any point distance x from the left hand end of the mill can be written as

$$h(x) = h_w + 2y(x) \qquad (4.5)$$

$$= h_w + 2h_c \left[1 - (\frac{2x}{w_m} - 1)^2 \right]$$

$$= h_w + 2h_c - 2h_c (\frac{2x}{w_m} - 1)^2.$$

But

$$h_m = h_w + 2h_c$$

i.e.

$$h(x) = h_m - 2h_c (\frac{2x}{w_m} - 1)^2. \qquad (4.6)$$

If the strip is rectangular then this profile can be obtained by putting $h_c = 0$ in eq. (4.6).

The input thickness profile is given by

$$h_1(x) = h_{1m} - 2h_c (\frac{2x}{w_m} - 1)^2 \qquad (4.7)$$

where the suffix 1 stands for the input side of the mill. The output thickness $h_2(x)$ can be calculated if the

reduction is known. This can be done by specifying the centreline output strip thickness. Let this be h_{2m}. Assuming that there is constant reduction across strip width, $h_2(x)$ is given by

$$h_2(x) = \frac{h_{2m}}{h_{1m}} \cdot h_1(x). \qquad (4.8)$$

The mean output thickness is given by

$$\overline{h}_{2m} = \frac{1}{w_s} \int_0^{w_s} h_2(x) dx \qquad (4.9)$$

therefore the deviation of output gauge from mean is given by

$$\Delta h_2(x) = h_2(x) - \frac{1}{w_s} \int_0^{w_s} h_2(x) dx. \qquad (4.10)$$

Eq.(4.8) assumes constant reduction which implies that the output strip has perfect shape. This is only an initialization process and the deviation $\Delta h_2(x)$ given by eq.(4.10) will be updated at later stages, since the work roll profile will be deformed when forces are applied.

4.4. Back-up roll profile.

When the As-U-Rolls are moved by a certain distance the back-up roll axis is deflected. The back-up roll profile calculation for a given As-U-Roll movement is

described here. When the As-U-Roll is moved vertically upwards or downwards the mechanics are designed in such a way that the centre c_1 of disc B rotates about a fixed point c_2 (see section 2.7.3) as shown in fig.4.4a. If c is the distance between c_1 and c_2, the centre c_1 describes a circle of radius c with centre at c_2. This means that, since disc B is solid, any point on the disc describes a circular arc with radius c. Let z be the vertical movement made by the As-U-Roll. Since the disc B is geared to racks, any point on the circumference also experiences a net movement of z. This point also rotates about c_2 and therefore the angle of rotation θ about c_2 as shown in fig.4.4b is given by

$$\theta = \frac{z}{R} \qquad\qquad (4.11)$$

where R is the distance between c_2 to the racks. Therefore the net vertical distance y travelled by c_1 or any other point on the circumference is given by

$$y = c \cdot \sin\theta = c \cdot \sin\left(\frac{z}{R}\right). \qquad\qquad (4.12)$$

On either side of each segment there are two such discs which can be moved independently. The profile of the back-up roll between two racks are calculated assuming a linear relationship. Fig.4.5a shows the profile when the first rack is moved by a distance z_1 with zero movement

- 58 -

in all other racks. The profile $y_1(x_1)$ can be calculated from

$$y_1(x_1) = z_1 - \frac{z_1 x_1}{\ell} \qquad (4.13)$$

where ℓ is the distance between two racks. Fig.4.5b shows the profile when only the first and second racks are moved by distances z_1 and z_2. In this case the profiles $y_1(x_1)$ and $y_2(x_2)$ corresponding to first and second segments are given by

$$y_1(x_1) = z_1 - \frac{(z_1 - z_2)x_1}{\ell} \qquad (4.14)$$

and

$$y_2(x_2) = z_2 - \frac{z_2}{\ell} \cdot x_2. \qquad (4.15)$$

The profile for the case when alternative racks are moved by the same amount (say z_1) is shown in fig.4.5c. Fig.4.5d shows the profile when all racks are moved by different amounts (say z_1, z_2, ...z_8). When all racks are moved by the same amount then obviously the whole of the back-up roll will be moved vertically. The same result can be achieved by moving the two screwdowns situated at both ends of the back-up roll, by the same amount.

4.5. First intermediate roll profile calculation.

The first intermediate rolls are furnished with tapered ends (see section 2.7.4). The top and bottom rolls can be moved laterally in and out independently and therefore will have different profiles depending on the position at which they are placed. These rolls can be modelled by defining the position of the tapered edges (vertical planes e_1 and e_2 in fig.4.6) with respect to the mill.

If x_r is the distance from the left hand corner of the mill to the plane e_1 and θ is the angle of inclination of the tapered end, then the tapered profile $y_{t1}(x)$ is given by

$$y_{t1}(x) = \begin{cases} 0 & \text{for } 0 \leqslant x \leqslant x_r \\ (x - x_r)\tan\theta & \text{for } x_r < x < w_m . \end{cases} \tag{4.16}$$

Similarly for the bottom first intermediate roll the tapered profile $y_{t2}(x)$ is given by

$$y_{t2}(x) = \begin{cases} (x_m - x)\tan\theta & \text{for } 0 \leqslant x \leqslant x_m \\ 0 & \text{for } x_m < x < w_m \end{cases} \tag{4.17}$$

where variables x, x_m and w_m are defined in fig.4.6. These profiles must be added to the camber profile (if any) to obtain the total first intermediate roll profiles.

- 60 -

4.6. Static forces in the mill cluster.

When three forces are acting on a cylinder as shown in fig.4.7, the two unknown forces P_1 and P_2 can be calculated in terms of the known force P and the angles of inclination. If forces are resolved in a direction XX (fig.4.7a) perpendicular to P_2, P_1 can be calculated. That is

$$P_1 \cos\left[\theta_1 - (90 - \theta_2)\right] = P\cos\left[\theta - (90 - \theta_2)\right]$$

i.e.

$$P_1 = P \cdot \frac{\sin(\theta + \theta_2)}{\sin(\theta_1 + \theta_2)} \cdot \qquad (4.18)$$

Similarly if forces are resolved in a direction YY (fig.4.7b) perpendicular to P_1

$$P_2 \cos\left[\theta_2 - (90 - \theta_1)\right] = P\cos\left[\theta + 90 - \theta_1\right]$$

i.e.

$$P_2 = P \cdot \frac{\sin(\theta_1 - \theta)}{\sin(\theta_1 + \theta_2)} \cdot \qquad (4.19)$$

The eqs.(4.18) and (4.19) can be applied to obtain the static forces P_1, P_2, P_3, P_4, P_5 and R shown in fig.2.4 in terms of the roll force P. If symmetry is assumed then P_5 can be written as

$$P_5 = \frac{P}{2\cos\theta_5} \qquad (4.20)$$

and

$$P_4 = P_5 \cdot \frac{\sin(\theta_3 + \theta_5)}{\sin(\theta_3 + \theta_4)} \ , \tag{4.21}$$

$$P_3 = P_5 \cdot \frac{\sin(\theta_4 - \theta_5)}{\sin(\theta_3 + \theta_4)} \ , \tag{4.22}$$

$$P_2 = P_4 \cdot \frac{\sin(\theta_6 - \theta_4)}{\sin(\theta_2 + \theta_6)} \ , \tag{4.23}$$

$$R = P_4 \cdot \frac{\sin(\theta_2 + \theta_4)}{\sin(\theta_2 + \theta_6)} \tag{4.24}$$

and finally

$$P_1 = P_3 \cdot \frac{\cos\theta_3}{\cos\theta_1} \ . \tag{4.25}$$

4.7. Elastic foundation constant K.

If two cylinders are in contact the elastic foundation constant K can be found by knowing the force applied. If the mean force per unit length is p_m then the Hertzian flattening equation[41,43] can be written as

$$y = 2Cp_m \log_e \left[\frac{e^{2/3}(d_1 + d_2)}{4Cp_m} \right] \tag{4.26}$$

where the force p_m is proportional to y and the constant of proportionality is the foundation constant K (eq. (4.26) is obtained by putting $C_1 = C_2 = C$ in eq. (3.4)). Therefore

- 62 -

K can be written as

$$K = \frac{1}{2C \cdot \log_e \left[\dfrac{e^{2/3}(d_1 + d_2)}{4Cp_m} \right]} .$$

(4.27)

At various points in the roll cluster two rolls rest on one roll. In order to use bending equations it is convenient to use a single equivalent value for the foundation constant. This is illustrated in fig.4.8.

Let the deflection of roll A in the direction of P be y_A. The deflection y_{AB} in the direction P_1 is given by

$$y_{AB} = y_A \cos(\theta_1 - \theta)$$

(4.28)

and similarly the deflection y_{AC} in the direction P_2 is given by

$$y_{AC} = y_A \cos(\theta + \theta_2).$$

(4.29)

If K_1 and K_2 are the foundation constants between the cylinder A and B, and between A and C, respectively, then

$$P_1 = K_1 y_{AB}$$

(4.30)

and

$$P_2 = K_2 y_{AC} .$$

(4.31)

But

$$P = P_1 \cos(\theta_1 - \theta) + P_2 \cos(\theta + \theta_2).$$

(4.32)

Substituting for P_1 and P_2 from eqs. (4.30) and (4.31) and

- 63 -

eliminating y_{AB} and y_{AC} we have

$$P = K_1 y_A \cos^2(\theta_1 - \theta) + K_2 y_A \cos^2(\theta + \theta_2). \tag{4.33}$$

But

$$K = \frac{P}{y_A} \tag{4.34}$$

and we obtain

$$K = K_1 \cos^2(\theta_1 - \theta) + K_2 \cos^2(\theta + \theta_2). \tag{4.35}$$

By applying eq. (4.35) to the mill cluster (see fig.2.4) the foundation constants for rolls I, J, O and S can be written as

$$K_I = K_{AI} \cos^2(\theta_6 - \theta_4) + K_{BI} \cos^2(\theta_2 + \theta_4), \tag{4.36}$$

$$K_J = K_{BJ} \cos^2\theta_1 + K_{CJ} \cos^2\theta_1, \tag{4.37}$$

$$K_O = K_{IO} \cos^2(\theta_4 - \theta_5) + K_{JO} \cos^2(\theta_3 + \theta_5), \tag{4.38}$$

$$K_S = K_{OS} \cos^2\theta_5 + K_{PS} \cos^2\theta_5 . \tag{4.39}$$

Eq.(4.37) is obtained by resolving forces in a vertical direction and, if symmetry is assumed, $K_{BJ} = K_{CJ}$ and $K_{OS} = K_{PS}$.

- 64 -

4.8. Roll force model.

For the reasons given in section 3.4 iterative roll force algorithms are not used in the present mill model. Bryant and Osborne[48] developed an explicit roll force formula which thus avoids iterative calculations. The formula is not so accurate as the algorithm described in section 3.4 for this type of mill but is efficient in the use of computer time. The error of the roll force using this method was found to be about one per cent.

The roll force is a function of input/output thicknesses, input/output stresses and input/output yield stresses and can be written as

$$p = f(h_1, h_2, \sigma_1, \sigma_2, k_1, k_2). \tag{4.40}$$

The Bryant and Osborne model has equation for roll force given by

$$P = \frac{P_o}{1 - bP_o - 0.4ab_o} \tag{4.41}$$

where

$$P_o = (\bar{k} - \bar{\sigma})\sqrt{R\delta}\,(1 + 0.4a_o) + P_{EO} \ ,$$

$$\bar{k} = \frac{1}{3}{\cdot}k_1 + \frac{2}{3}{\cdot}k_2 \ ,$$

$$\bar{\sigma} = \frac{2}{3}{\cdot}\sigma_1 + \frac{1}{3}{\cdot}\sigma_2 \ ,$$

R = work roll radius,

- 65 -

$$\delta = h_1 - h_2 \, ,$$

$$a_o = \sqrt{\frac{h_2}{h_1}} \, e^{\alpha_o} - 1 \, ,$$

$$\alpha_o = \frac{\mu\sqrt{R\delta}}{\bar{h}} \, ,$$

μ = coefficient of friction,

$$\bar{h} = 0.72 h_2 + 0.28 h_1 \, ,$$

$$P_{EO} = \frac{2}{3}\sqrt{R h_2}\,(k_2 - \sigma_2)^{3/2}\sqrt{\frac{1 - v^2}{E}} \, ,$$

$$a = 1.4\sqrt{\frac{h_2}{h_1}}\cdot\left(\frac{\mu}{\bar{h}}\right)^2 Rc \, ,$$

$$c = \frac{4(1 - v^2)}{\pi E} \, ,$$

$$b = \frac{c}{2\delta} - \frac{P_o}{8}(c/\delta)^2 \, ,$$

$$b_o = (\bar{k} - \bar{\sigma})\sqrt{R\delta}.$$

To calculate the roll force profile eq. (4.41) must be solved at every point across the strip. If $p(x)$ is the roll force profile then to obtain the required reduction the mean of $p(x)$ must be equal to the mean roll force $\bar{p}$ which is the roll force required to obtain the specific reduction. That is,

- 66 -

$$\overline{p} = \frac{1}{w_s} \int_0^{w_s} p(x)dx. \qquad (4.42)$$

Every time the roll force $p(x)$ is calculated it must satisfy eq.(4.42) and if the mean of $p(x)$ deviates from $\overline{p}$, then $p(x)$ must be adjusted until eq.(4.42) is satisfied. This can be done by moving the two work rolls away from or towards each other. If they are moved away from each other then the distance d between their two centres will be increased, thus reducing the roll force $p(x)$ (see fig.4.9). The roll force will be increased if the work rolls are moved towards each other, that is decreasing d. The flowchart for this process is shown in fig.4.10.

4.9. Inter roll pressures.[49]

When two elastic cylinders are in contact the total interference $y_{12}(x)$ can be written as a function of the load per unit length $q(x)$ as

$$y_{12}(x) = (C_1 + C_2)q(x) \cdot \log_e \left[\frac{e^{2/3}(d_1 + d_2)}{2(C_1 + C_2)q(x)} \right]. \qquad (4.43)$$

The loading is of course non-uniform but, neglecting second order errors, is given by

$$q(x) = \frac{y_{12}(x)}{(C_1 + C_2) \cdot \log_e \left[\frac{e^{2/3}(d_1 + d_2)}{2(C_1 + C_2)q(x)} \right]}. \qquad (4.44)$$

- 67 -

Eq. (4.44) contains q(x) on the right hand side and q(x) to be calculated from the knowledge of $y_{12}(x)$; thus the term q(x) must be eliminated from the right hand side. A new variable $q_d(x)$ is defined as

$$q_d(x) = \frac{q(x)}{F/\ell} = \frac{q(x)}{\bar{q}} \qquad (4.45)$$

where F is the rolling force, ℓ is the length of the roll and $\bar{q}$ is the mean specific rolling force. Thus

$$q(x) = \frac{y_{12}(x)}{(C_1 + C_2) \cdot \log_e \left[\dfrac{e^{2/3}(d_1 + d_2)}{2(C_1 + C_2)\bar{q}q_d(x)} \right]}$$

$$= \frac{y_{12}(x)}{(C_1 + C_2) \left\{ \log_e \left[\dfrac{e^{2/3}(d_1 + d_2)}{2(C_1 + C_2)\bar{q}} \right] - \log_e \left[q_d(x) \right] \right\}} \qquad (4.46)$$

Now

$$\log_e \left[\frac{e^{2/3}(d_1 + d_2)}{2(C_1 + C_2)\bar{q}} \right] \gg \log_e \left[q_d(x) \right]$$

as $q(x) \simeq \bar{q}$.

Thus eq. (4.46) becomes

$$q(x) = \frac{y_{12}(x)}{(C_1 + C_2) \left\{ \log_e \left[\dfrac{e^{2/3}}{2(C_1 + C_2)} \right] + \log_e(d_1 + d_2) - \log_e(\bar{q}) \right\}} \qquad (4.47)$$

Eq. (4.47) is only true for positive values of $y_{12}(x)$.

- 68 -

Therefore it is assumed that when $y_{12}(x) \leqslant 0$, $q(x) = 0$.

The interference $y_{12}(x)$ can also be calculated from roll bending using roll contours. If two perfectly flat cylinders (i.e. without any ground camber), one resting on the other, are considered and if there are no forces acting on these cylinders, then $y_{12}(x)$ must be equal to zero. That is $y_{12}(x)$ can be written as

$$y_{12}(x) = \tfrac{1}{2}(d_1 + d_2) - d_{12} = 0 \qquad (4.48)$$

where d_1 and d_2 are the diameters of the two cylinders and d_{12} is the distance between the two centres. Now let an external force be applied to the roll 1 which is the top roll, so that only roll 1 is deflected downwards. If it is assumed that roll 2 has zero deflection then the distance between the two centres must increase and, to keep $d_{12} = \tfrac{1}{2}(d_1 + d_2)$, the roll surface must be flattened by $y_1(x)$ the actual deflection of roll 1. Therefore the interference $y_{12}(x)$ can be written as

$$y_{12}(x) = \tfrac{1}{2}(d_1 + d_2) - d_{12} + y_1(x). \qquad (4.49)$$

Similarly if forces are applied so that only roll 2 is deflected upwards the interference $y_{12}(x)$, to keep the distance between two centres the same as before, can be

written as

$$y_{12}(x) = \tfrac{1}{2}(d_1 + d_2) - d_{12} - y_2(x). \qquad (4.50)$$

If both cylinders are allowed to deflect then $y_{12}(x)$
becomes

$$y_{12}(x) = \tfrac{1}{2}(d_1 + d_2) - d_{12} + y_1(x) - y_2(x). \qquad (4.51)$$

If both cylinders are grounded with camber (e.g. barrel
shape) then the camber profiles must be added to the
interference term $y_{12}(x)$ to keep $d_{12} = \tfrac{1}{2}(d_1 + d_2)$. That is

$$y_{12}(x) = \tfrac{1}{2}(d_1 + d_2) - d_{12} + y_1(x) - y_2(x)$$
$$+ y_{1c}(x) + y_{2c}(x). \qquad (4.52)$$

If the cylinders have concave camber profiles then $y_{1c}(x)$
and $y_{2c}(x)$ will be negative in eq. (4.52).

When a roll pressure $q(x)$ between any two
rolls in the mill cluster is to be calculated the mean
of $q(x)$ must be equal to the mean $\bar{q}$, to keep the force
balance in the mill. The pressure $q(x)$ can be adjusted by
moving the two rolls either away or towards each other.
This is done by adjusting mathematically the term d_{12} in
eq. (4.52). The pressure $q(x)$ can be increased by decreasing
d_{12}, that is moving the rolls towards each other. The
force balance equation is given by

- 70 -

$$\bar{q} = \frac{1}{w} \int_0^w q(x)dx = \bar{q}(x). \qquad (4.53)$$

The method of calculation of $p(x)$ is to change d_{12} in eq.(4.52) to change $y_{12}(x)$, and hence $q(x)$ iteratively until eq.(4.53) is satisfied. A flowchart for this process is shown in fig.4.11 and the subroutine used in the computer program is called INPRESS.

4.10. Roll deflections.

An expression for the roll deflection caused by a point load, applied to a roll resting upon an elastic foundation is given in this section. From bending theory the deflection y is given by the differential equation

$$EI \cdot \frac{d^4y}{dx^4} = F - Ky \qquad (4.54)$$

where F is the applied force and K is the elastic foundation constant. This equation is only true if the roll is in complete contact with its foundation under no load conditions. However in the mill cluster, this is not always true as one particular roll may be resting on an already deflected roll, as shown in fig.4.12. In a case like this there will be a gap between the roll and its foundation under no load conditions; let this gap be Δy.

Then eq. (4.52) becomes

$$EI \cdot \frac{d^4 y}{dx^4} = F - K(y - \Delta y)$$

$$= F - Ky + K\Delta y. \tag{4.55}$$

But

$$K\Delta y = \Delta F.$$

Eq. (4.55) becomes

$$EI \cdot \frac{d^4 y}{dx^4} = (F + \Delta F) - Ky \tag{4.56}$$

where $F + \Delta F$ is the equivalent total force.

The solution to the differential equation (4.56) is given by

$$y(x) = \frac{(F + \Delta F)}{K} \cdot \frac{1}{A} \left[B(C - D) + H(J + G) \right] \tag{4.57}$$

where

$$A = \sinh^2(\lambda \ell) - \sin^2(\lambda \ell),$$

$$B = 2\cosh(\lambda x)\cos(\lambda x),$$

$$C = \sinh(\lambda \ell)\cos(\lambda a)\cosh(\lambda b),$$

$$D = \sin(\lambda \ell)\cosh(\lambda a)\cos(\lambda b),$$

$$H = \cosh(\lambda x)\sin(\lambda x) + \sinh(\lambda x)\cos(\lambda x),$$

$$J = \sinh(\lambda \ell)\left[\sin(\lambda a)\cosh(\lambda b) - \cos(\lambda a)\sinh(\lambda b)\right],$$

$$G = \sin(\lambda \ell)\left[\sinh(\lambda a)\cos(\lambda b) - \cosh(\lambda a)\sin(\lambda b)\right]$$

and

$$\lambda = \left(\frac{K}{4EI}\right)^{\frac{1}{4}}.$$

All variables not defined are shown in fig.4.13. The eq.(4.57) is only true for values of $x < a$. The deflection for distances $a < x < \ell$ can be calculated using eq.(4.57) but with a and b interchanged while measuring the distance from right hand end.

At various points in the roll cluster three rolls are in contact with a fourth roll as shown in fig.4.8. If the deflection of roll A is required the net force acting on A must be calculated. In direction P the net force per unit length is given by

$$F(x) = P(x) - P_1(x)\cos(\theta_1 - \theta) - P_2(x)\cos(\theta + \theta_2). \qquad (4.58)$$

If an elemental length dx across the roll length is considered, then the total net force acting on dx is given by

$$F_t(x) = F(x)dx$$
$$= \left[P(x) - P_1(x)\cos(\theta_1 - \theta) - P_2(x)\cos(\theta + \theta_2)\right]dx. \qquad (4.59)$$

If the roll length is divided into N such small segments of length dx then the distributed load can be treated as a series of point loads acting on each segment. The deflection due to one such force at the jth element, given by eq.(4.59), can be written as

$$y_{aj}(x) + y_{bj}(x) = f(F_j(x)dx, \ a, \ b) \qquad (4.60)$$

- 73 -

where $y_{aj}(x)$ is the deflection for $x \leqslant a$, $y_{bj}(x)$ is the deflection for $a < x < \ell$ and $x = a$ defines the point of application of the force $F_j(x)dx$ (see fig.4.13). The total roll deflection, from the theorem of superposition is given by

$$y(x) = \sum_{j=1}^{N} \left[y_{aj}(x) + y_{bj}(x) \right] . \tag{4.61}$$

Subroutine MUMMY in the computer program calculates the total deflection and a simple flowchart is shown in fig. 4.14.

4.11. Strip thickness and stress profiles.

The procedure adopted by Edwards and Spooner[24] to find the interference $y_{ws}(x)$ between work roll and strip was to compute the roll flattening for numerous rolling schedules, roll diameters and Young's modulus. From the results they found a strong correlation between the total roll flattening $y_{ws}(x)$ and Hertzian flattening $y_H(x)$ occurring between two infinitely long elastic cylinders having the same diameters. They computed the ratio $y_{ws}(x)/y_H(x)$ and a model was proposed to match these results. The proposed model is given by eqs.(3.9) and (3.10). The constants b_1 and b_2 are estimated using least square methods to be 0.5 and 0.325 mm/tonne respectively.

First, the mean interference $\bar{y}_{ws}$ between strip
and work rolls is calculated using mean roll force $\bar{p}$
which corresponds to the required reduction. If $h_2(x)$ is
the actual output thickness, then the change in interference
corresponding to a deviation in strip thickness from h_{2m} is
$(y_{ws}(x) - \bar{y}_{ws})$, where $y_{ws}(x)$ is the true interference between
strip and work rolls. That is the change in gauge is
higher if the change in interference is high. The change
in gauge also increases with the increase of work roll
deflection. If work roll camber is included, then the
change in gauge can be written as

$$\Delta h_2(x) = y_w(x) + y_{wc}(x) + \left[y_{ws}(x) - \bar{y}_{ws} \right] \qquad (4.62)$$

where $y_{wc}(x)$ is the work roll camber.

Since there are two work rolls the effect
will be doubled and $\Delta h_2(x)$ becomes

$$\Delta h_2(x) = y_{wu}(x) + y_{w\ell}(x) + 2y_{wc}(x) + 2\left[y_{ws}(x) - \bar{y}_{ws} \right] \qquad (4.63)$$

where $y_{wu}(x)$ and $y_{w\ell}(x)$ refer to upper and lower work
roll deflections.

The output thickness profile is calculated as
explained in section 3.5.1 and is given by eq. (3.17), i.e.

$$h_2(x) = h_{2m} + \Delta h_2^{k+1} . \qquad (4.64)$$

The change in output stress is calculated by the model proposed by Edwards and Spooner[24] given by eqs. (3.18) and (3.19), using the output thickness calculated. Edwards and Spooner found β to be 0.5 and that the shape distribution was insensitive to β. The constant γ is calculated as described below.

From the geometry of fig. 4.15 it can be easily shown that

$$h_n \simeq h_{n_2} + R\theta_n^2 . \tag{4.65}$$

From continuity of mass flow

$$v_2 h_2 = v_n h_n . \tag{4.66}$$

By substituting h_n from eq. (4.65) in eq. (4.66) we have

$$v_2 = v_n (1 + \frac{R\theta_n^2}{h_2}). \tag{4.67}$$

The per unit slip is defined as

$$s = \frac{v_2 - v_n}{v_n} . \tag{4.68}$$

From eqs. (4.67) and (4.68) the value of s is found to be

$$s = \frac{R\theta_n^2}{h_2} \tag{4.69}$$

where

$$\theta_n = \sqrt{\frac{h_2}{R}} \cdot \tan\left[\sqrt{\frac{h_2}{R}} \cdot \frac{H_n}{2}\right] , \qquad (4.70)$$

$$H_n = \frac{H_1}{2} + \frac{1}{2\mu} \cdot \log_e\left[\frac{h_2}{h_1} \cdot \frac{1 - \sigma_1/k_1}{1 - \sigma_2/k_2}\right] , \qquad (4.71)$$

$$H_1 = 2\sqrt{\frac{R}{h_2}} \cdot \tan^{-1}\left[\sqrt{\frac{R}{h_2}}\,\theta\right] . \qquad (4.72)$$

Eqs. (4.70), (4.71) and (4.72) can be derived by considering roll gap variables and are given in Appendix 1.

By differentiating s with respect to σ_1 we have

$$\frac{ds}{d\sigma_1} = \frac{2R}{h_2} \cdot \theta_n \cdot \frac{d\theta_n}{d\sigma_1}$$

$$= \frac{2R}{h_2} \cdot \theta_n \cdot \frac{d\theta_n}{dH_n} \cdot \frac{dH_n}{d\sigma_1} . \qquad (4.73)$$

But

$$\frac{d\theta_n}{dH_n} = \frac{1}{2} \cdot \frac{h_2}{R}\left[1 + \tan^2\left(\sqrt{\frac{h_2}{R}} \cdot \frac{H_n}{2}\right)\right] \qquad (4.74)$$

and

$$\frac{dH_n}{d\sigma_1} = \frac{-1}{2\mu} \cdot \frac{1}{k_1 - \sigma_1} . \qquad (4.75)$$

By substituting these values in eq. (4.73) and simplifying we obtain

$$\frac{ds}{d\sigma_1} = \frac{-a}{k_1 - \sigma_1} \qquad (4.76)$$

- 77 -

where

$$a = \frac{\theta_n}{2\mu}\left[1 + \tan^2\left(\sqrt{\frac{h_2}{R}} \cdot \frac{H_n}{2}\right)\right].$$ (4.77)

Similarly

$$\frac{ds}{d\sigma_1} = \frac{a}{k_2 - \sigma_2}.$$ (4.78)

In order that the slip variations are to remain very small we must have

$$\Delta s = \Delta\sigma_1 \cdot \frac{ds}{d\sigma_1} + \Delta\sigma_2 \cdot \frac{ds}{d\sigma_2} = 0.$$ (4.79)

By substituting for $\frac{ds}{d\sigma_1}$ and $\frac{ds}{d\sigma_2}$ in eq. (4.79) we have

$$\Delta\sigma_1 = \gamma\Delta\sigma_2$$ (4.80)

where

$$\gamma = \frac{k_1 - \sigma_1}{k_2 - \sigma_2}.$$ (4.81)

4.12. Pressure and deflection profiles for one quarter of the mill cluster.

Pressure and deflection profiles for one quarter of the mill are calculated by using the subroutine called BEND. This routine has to be called four times to calculate the profiles of all twenty rolls. If symmetry is assumed it is only necessary to calculate only one half of the mill and therefore routine BEND is used only twice.

Since the pressure between two rolls depends on the interference between them, and the interference is a function of the roll deflections which directly depend on pressure, the process is iterative. Whenever two rolls are in contact this iterative procedure must be adopted to calculate the pressure profiles. In the mill cluster every roll is in contact with more than one roll. Suppose that the first profile is obtained after satisfying a convergence criterion. In the process of convergence the roll deflections and pressures, other than those of the one in question, change at every iteration. On the other hand, if convergence is obtained on the second profile then the first profile may have deviated from the true value. The procedure adopted is therefore to converge the first profile and then the second profile initially, and then return to first and then the second until convergence is obtained on both profiles. If other pressures are included then the process becomes a nested convergence procedure.

For one such pressure (e.g. q_{BJ} between rolls B and J in cluster) the convergence procedure can be explained. First the vertical deflection $y_J(x)$ of roll J (see fig. 4.16) is calculated using existing pressure profiles $q_{BJ}(x)$ and $q_{JO}(x)$. The deflection $y_J(x)$ is resolved into q_{BJ} and q_{JO} directions and these together with $y_B(x)$ and $y_O(x)$ are used to calculate new $q_{BJ}(x)$ and $q_{JO}(x)$. That

is

$$q_{BJ}(x) = f_q(y_B \cos\theta_1, \; y_J \cos\theta_1) \tag{4.82}$$

and

$$q_{JO}(x) = f_q(y_J \cos\theta_2, \; y_0) \tag{4.83}$$

since y_B and y_0 are calculated in vertical and q_{JO} directions respectively. At this point a convergence test is carried out on q_{BJ} using a root mean square error criteria. If this criteria is satisfied, the present profiles $q_{BJ}(x)$ and $y_J(x)$ are taken as the corrected pressure profile between B and J and the deflection of J. If a convergence has not been reached the nett force F acting on J in the vertical direction is calculated, i.e.

$$F = q_{JO} \cos\theta_2 - q_{BJ} \cos\theta_1. \tag{4.84}$$

Using this value F a new vertical deflection $y_J'(x)$ is calculated. This is done using the subroutine MUMMY and can be written as

$$y_J'(x) = f_y(F). \tag{4.85}$$

The new deflection $y_J(x)$ is calculated using the iterative formula

$$y_J^{k+1}(x) = y_J^k(x) - \alpha \left[y_J^k(x) - y_J'(x) \right] \tag{4.86}$$

where α is a convergence parameter chosen to give a stable solution. The above procedure is repeated until a

- 80 -

convergence is obtained on q_{BJ}. The flowchart for this procedure is shown in fig.4.17.

There are four main convergence loops in the subroutine BEND which calculates the pressure and roll profiles. Referring to fig.2.4, the first iteration loop is concerned with the convergence of p_1. The next loop is for the convergence of the combined effects of p_2 and R in the direction p_4 and can be written as

$$q_D = R\cos(\theta_6 - \theta_4) + p_2\cos(\theta_2 + \theta_4). \tag{4.87}$$

The third loop is for the calculation of the combined effect of p_4 and p_3 and the fourth loop is for p_5. A flowchart is shown in fig.4.18 and the procedure is illustrated in fig.4.19. Only the top half cluster is shown in this figure and thick lines are drawn to show the path of calculation. Each of the small circles denoted by c_1, c_2, c_3 and c_4 represents an iterative procedure described above. A satisfactory convergence in pressure is shown by the letter Y and non-convergence is represented by N.

To calculate the pressure profiles and deflections of the bottom half cluster the same procedure described above is repeated using the corresponding variables. Once the calculations from subroutine BEND are completed the two work rolls will have new profiles. These new work roll profiles are used to calculate the new output thickness

profile and hence the new stress profile. A final convergence test is applied on the stress deviation profile as shown in the flowchart of fig.3.1 and described in section 3.5. The convergence test carried out here is also based on the root mean square error criterion.

4.13. Mill gain matrix.[39]

The model calculates output gauge and shape profiles and roll deflection and pressure profiles for a given set of rack movements. The static gain of the mill is the ratio of the change in stress due to a change in rack position. There are eight racks and the gains must show the effect of shape at each point on the strip due to each rack. Therefore, the gains are calculated by changing each rack at a time by the same amount. First the stress profile is calculated by setting all the racks at a common position. Then eight new stress profiles are calculated by changing one rack at a time by the same amount. The difference between any one of these stress profiles and the previous profile is taken as the stress change due to that particular rack change. For computing purposes the mill width and the strip width are divided into a number of sections as explained in section 4.1. Therefore the gain can be represented as an $N \times 8$ matrix, where N is the number of sections. Any element of this

matrix is therefore given by

$$g_{ij} = \frac{\Delta\sigma_{ij}}{\Delta z_j} \qquad i = 1,2,\ldots N \text{ and } j = 1,2,\ldots 8 \qquad (4.88)$$

where $\Delta\sigma$ and Δz are the changes in stress and rack position respectively.

The above matrix is not a square matrix and for the use in the dynamic model it is convenient to have a square matrix. The non-square matrix can be converted into a square matrix by considering eight zones in the strip. This is done by dividing the strip into eight zones and calculating the average gain in each zone. If M is the number of sections in each zone, then each element G_{ij} in the square matrix is given by

$$G_{ij} = \sum_{k = 1 + M \times (i-1)}^{M + M \times (i-1)} \frac{g_{kj}}{M} \qquad \begin{array}{l} i = 1,2,\ldots 8 \\ j = 1,2,\ldots 8 \end{array} \qquad (4.89)$$

so the gain matrix G_m can be written as

$$G_m = G_{ij} \qquad i = 1,2,\ldots 8 \text{ and } j = 1,2,\ldots 8. \qquad (4.90)$$

Therefore each column of G_m contains the shape change at each zone due to a change in the corresponding rack.
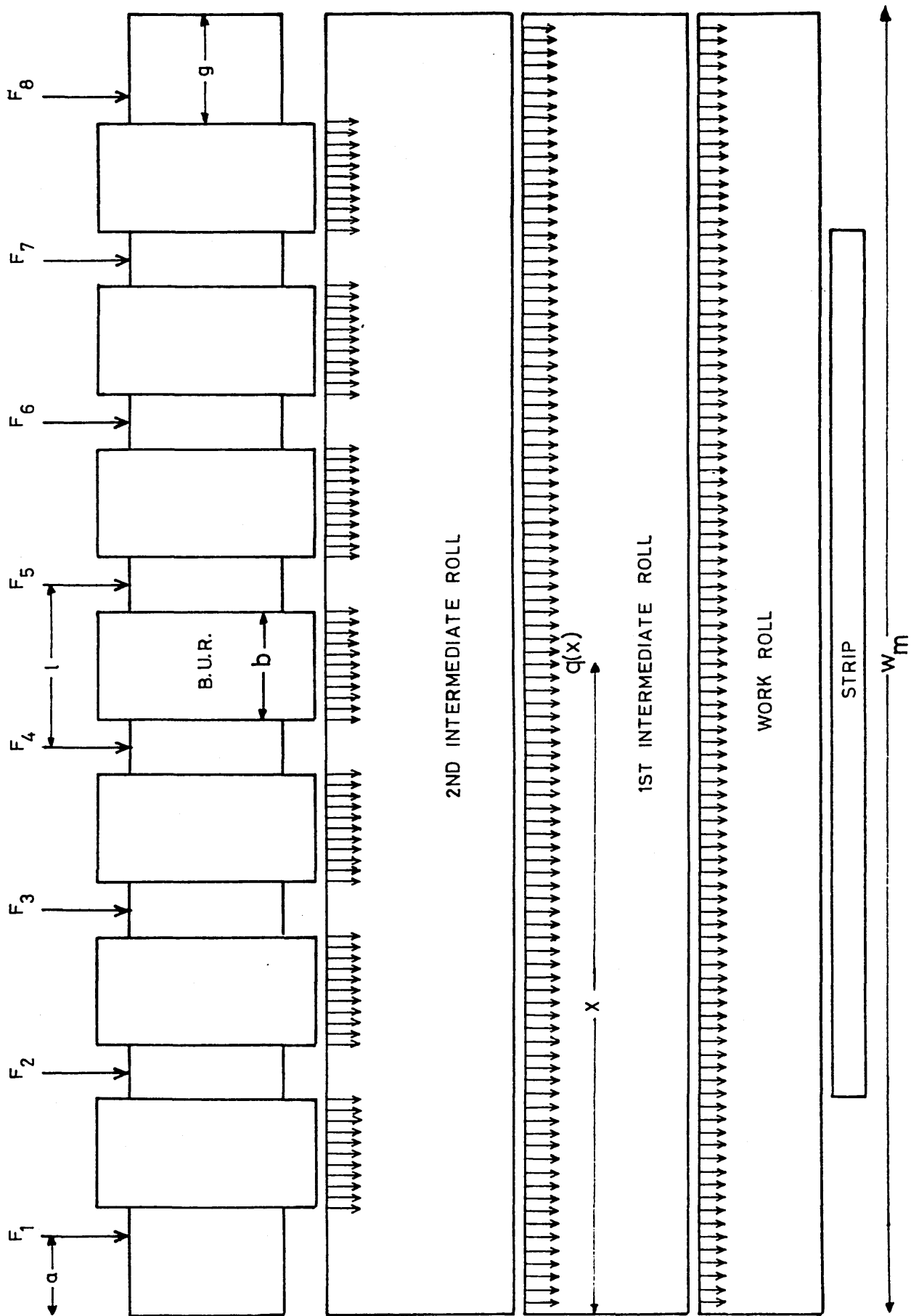
Fig. 4.1. Mill constants.
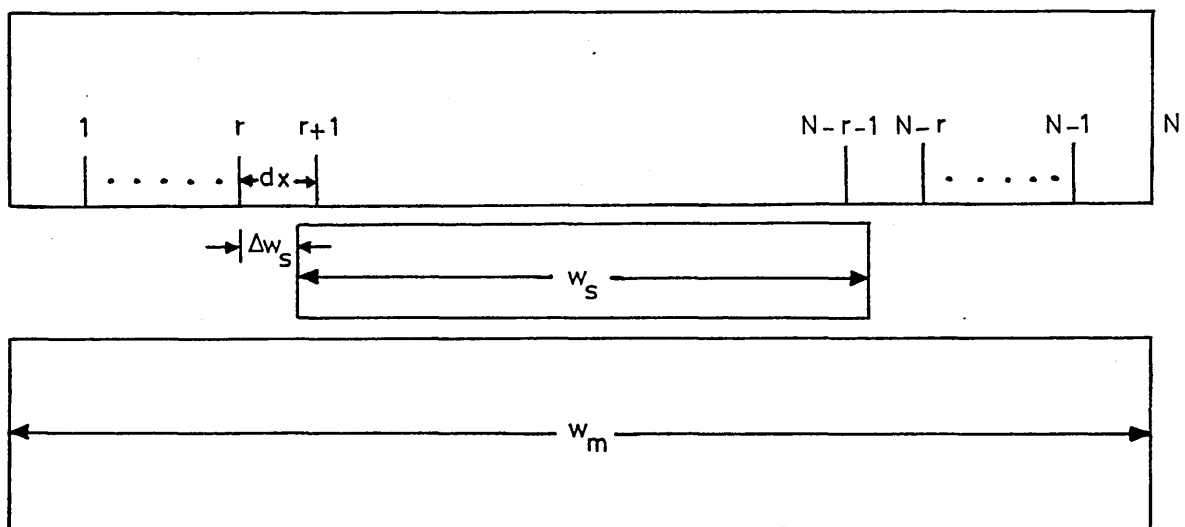
Fig. 4.2 Strip   with   adjustment
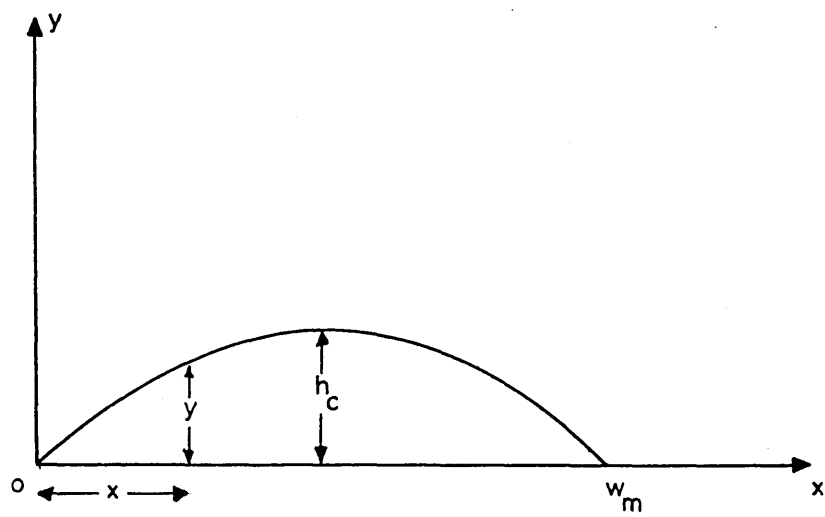
(a)
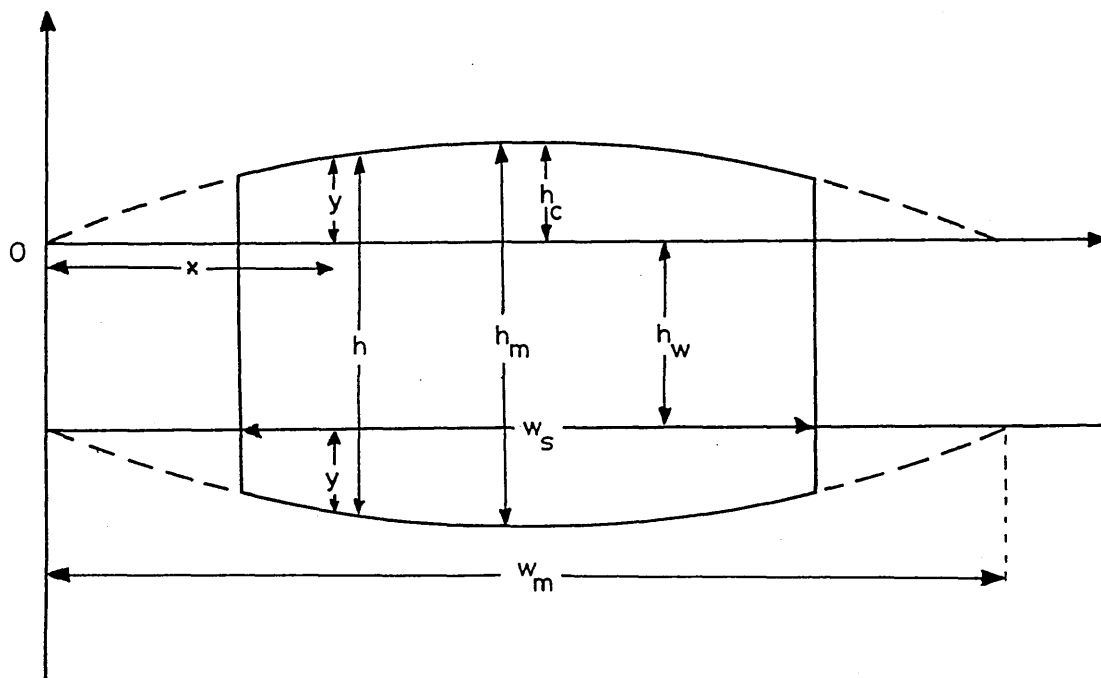
(b)

Fig. 4.3. Strip profile dimensions.

(a)

(b)
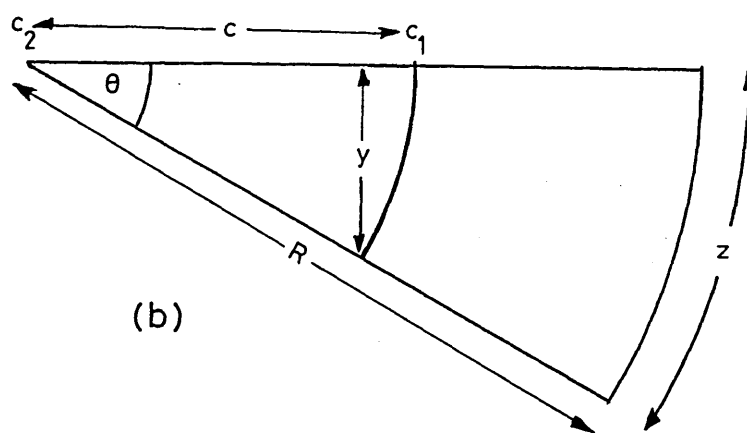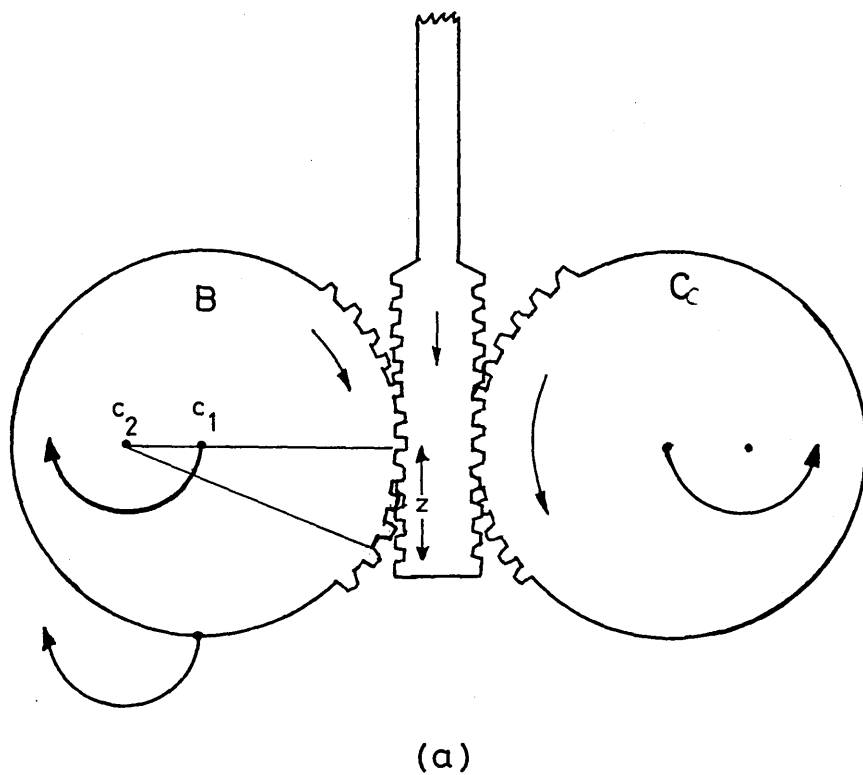
Fig. 4.4. Back up roll As-U-Roll movement.
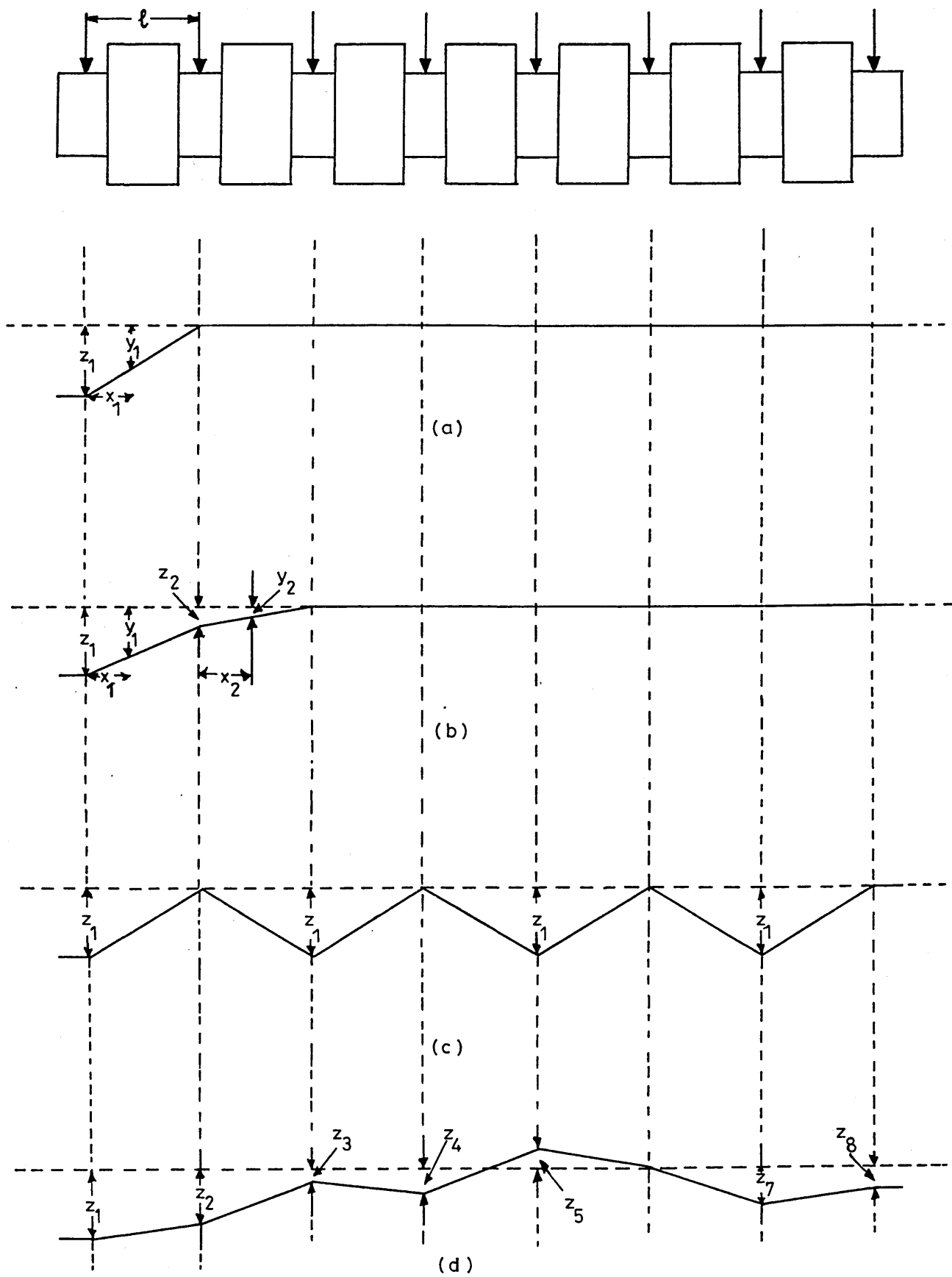
Fig. 4.5. Back up roll profiles.
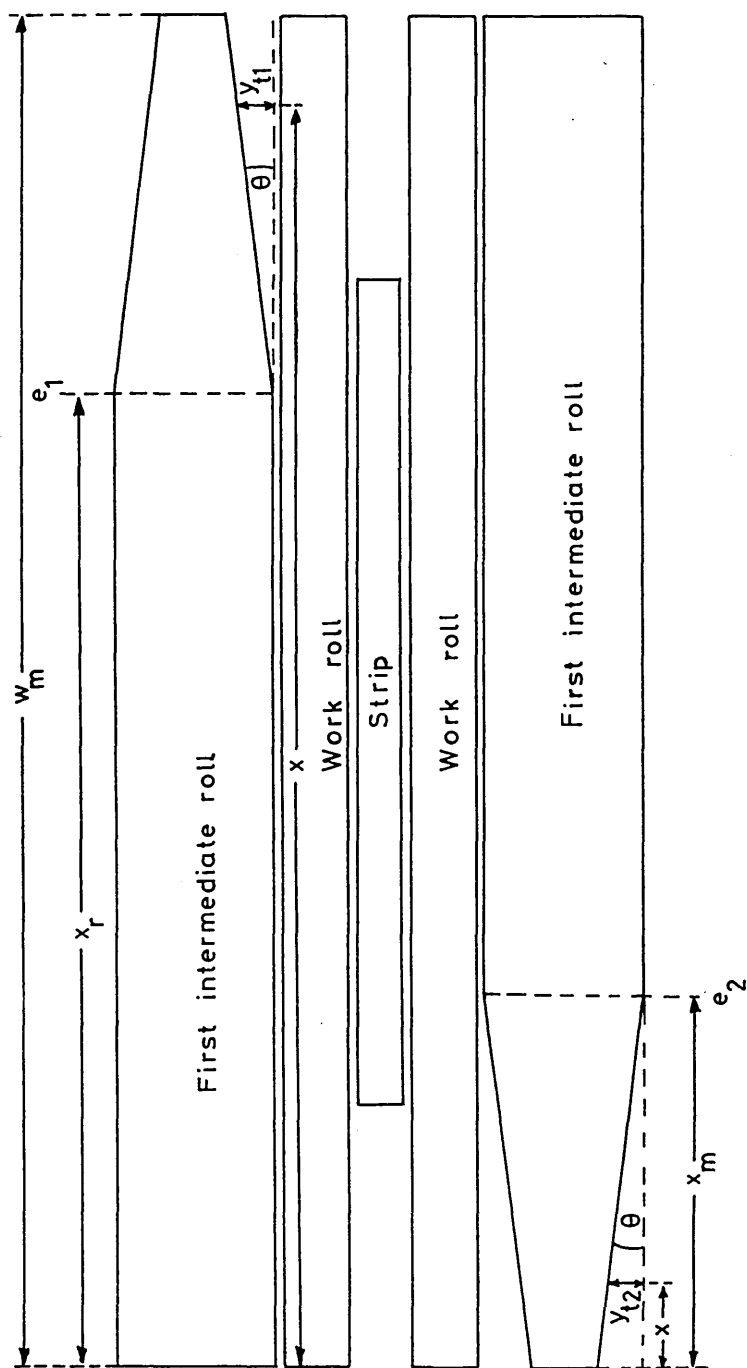
Fig.4.6. First intermediate roll profile.
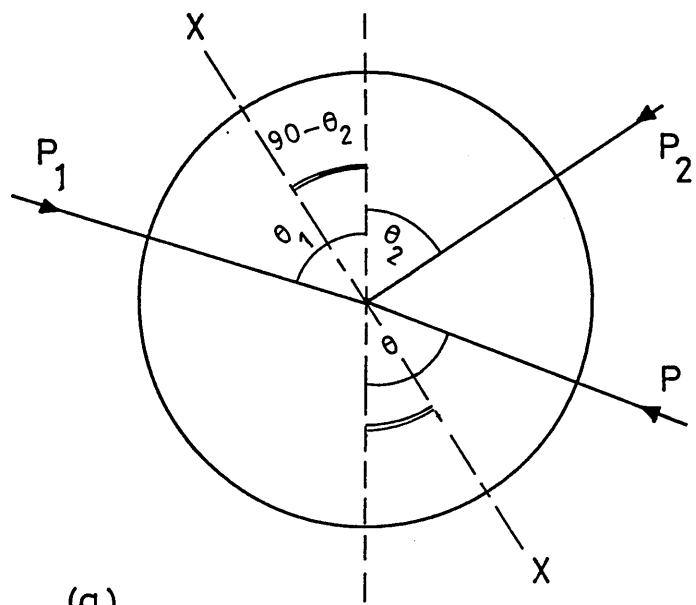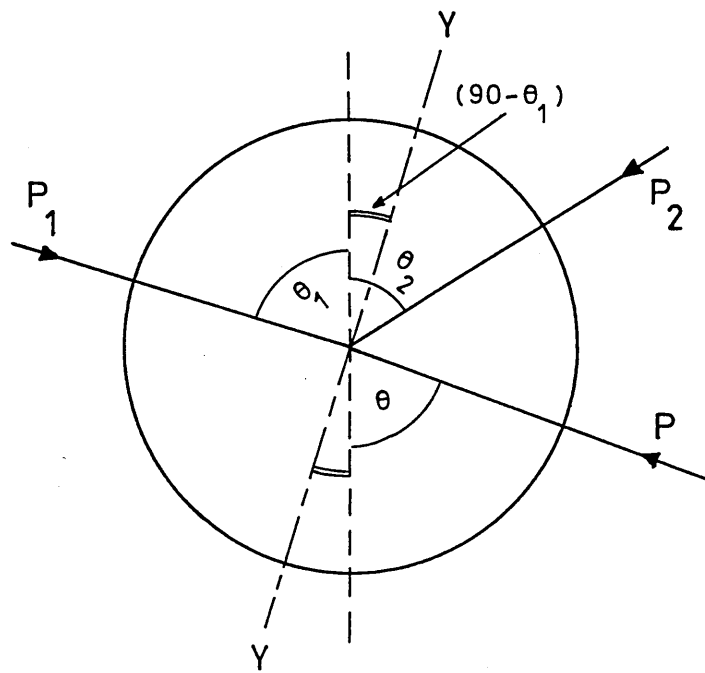
Fig. 4.7. Forces acting on one roll in cluster.

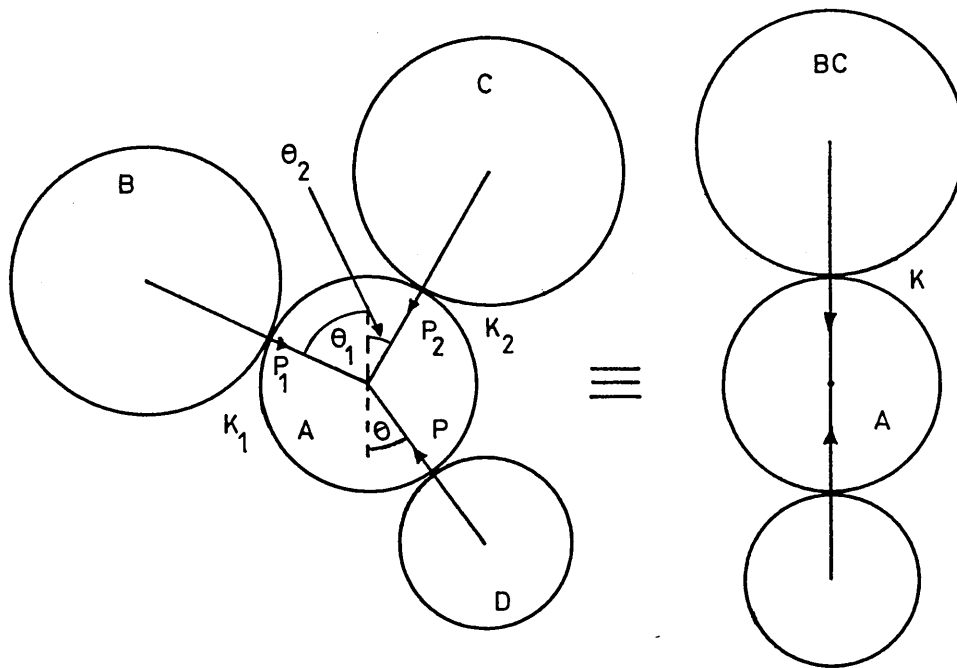Fig. 4.8. Equivalent elastic foundation constant.

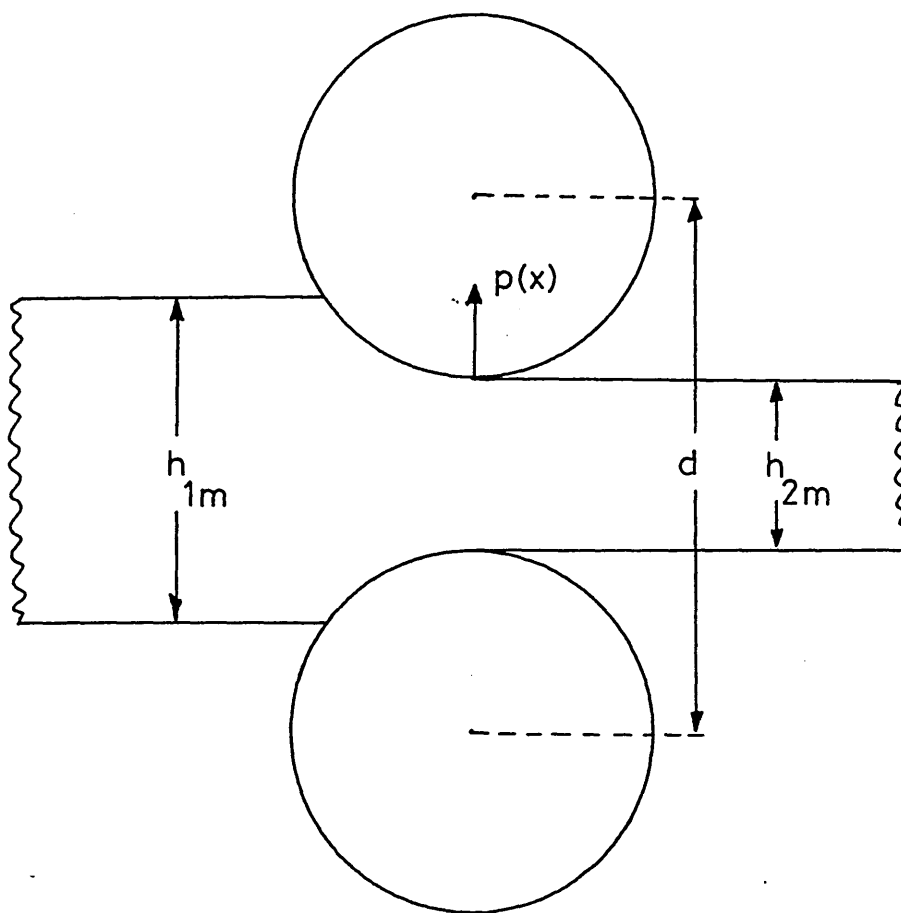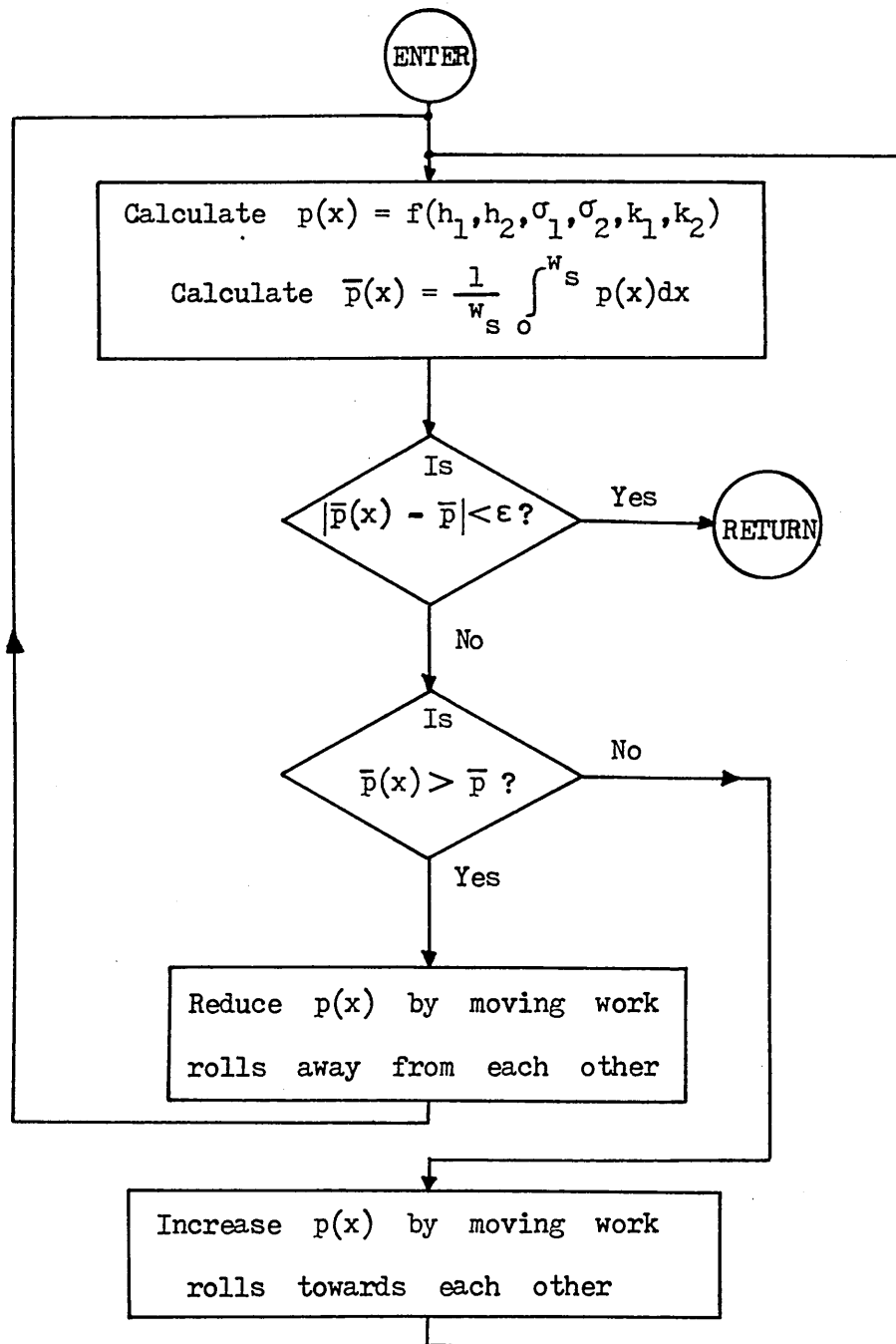Fig. 4.9. Roll force adjustment.

ENTER

Calculate $p(x) = f(h_1, h_2, \sigma_1, \sigma_2, k_1, k_2)$

Calculate $\bar{p}(x) = \dfrac{1}{W_s} \displaystyle\int_0^{W_s} p(x)\,dx$

Is $|\bar{p}(x) - \bar{p}| < \varepsilon$?

Yes → RETURN

No

Is $\bar{p}(x) > \bar{p}$?

No

Yes

Reduce $p(x)$ by moving work rolls away from each other

Increase $p(x)$ by moving work rolls towards each other

Fig. 4.10. Roll force adjustment.

ENTER

Calculate $y_{12}(x)$

Calculate $q(x) = f(y_{12}(x))$

Calculate $\bar{q}(x) = \dfrac{1}{w} \displaystyle\int_0^W q(x)dx$

Is $|\bar{q}(x) - \bar{q}| < \varepsilon$?

Yes → RETURN

No

Is $\bar{q}(x) > \bar{q}$?

No

Yes

Reduce $q(x)$ by moving the two rolls away from each other

Increase $q(x)$ by moving the two rolls towards each other
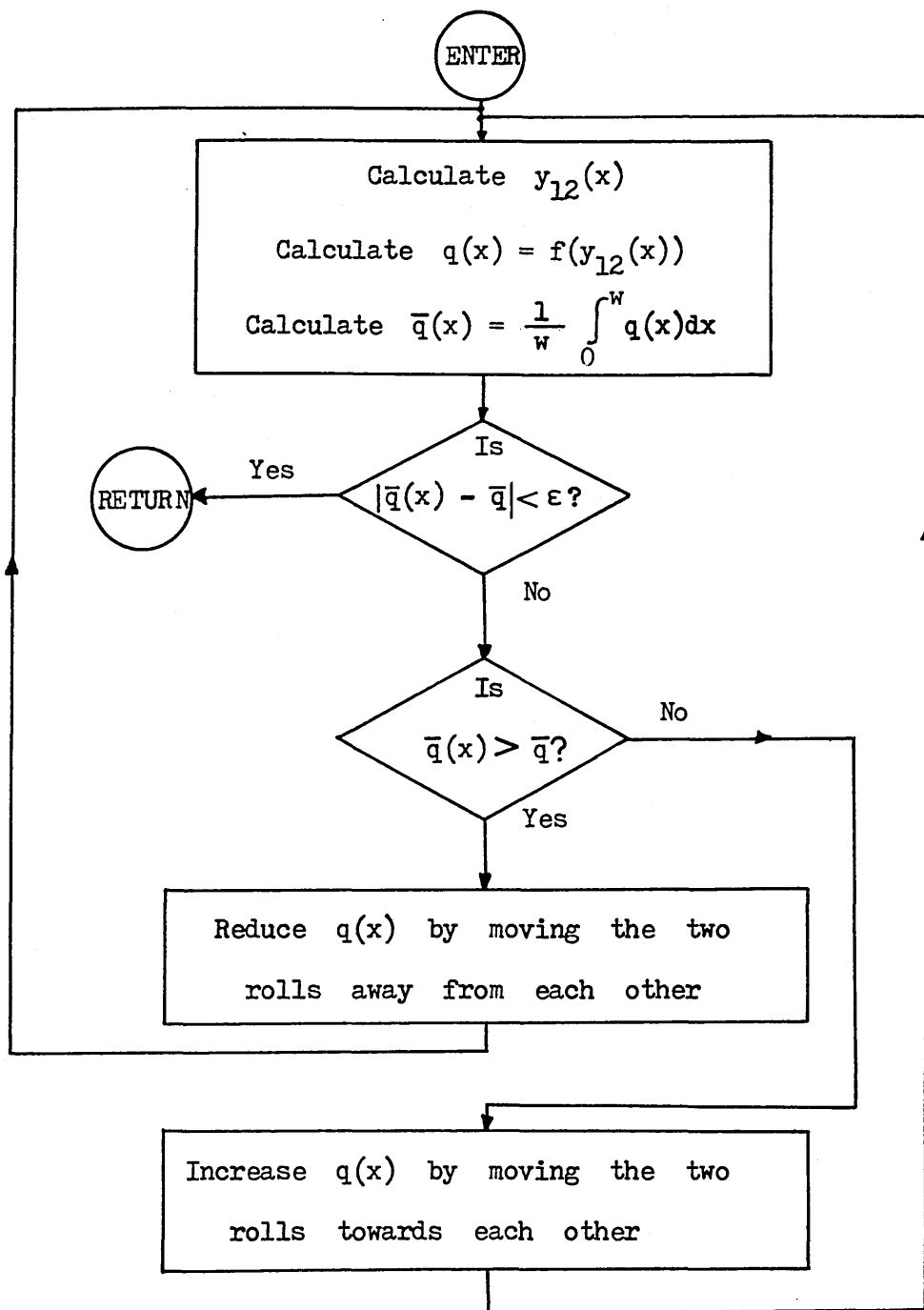
Fig. 4.11. Flow chart for roll pressure calculation (Subroutine INPRESS).

No load case   Loaded case
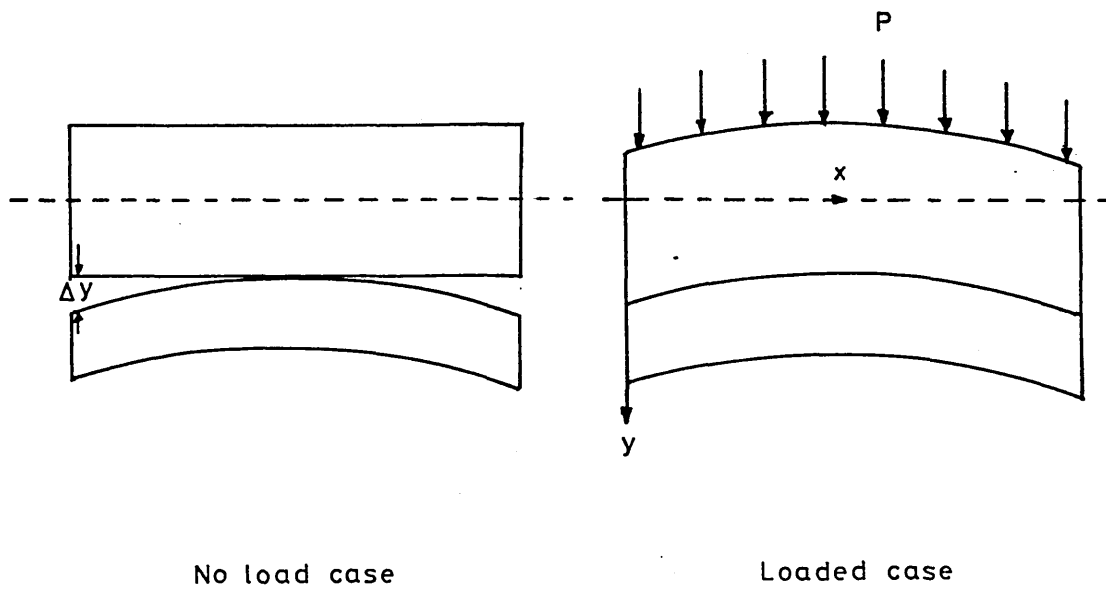
Fig. 4.12. Roll deflection.
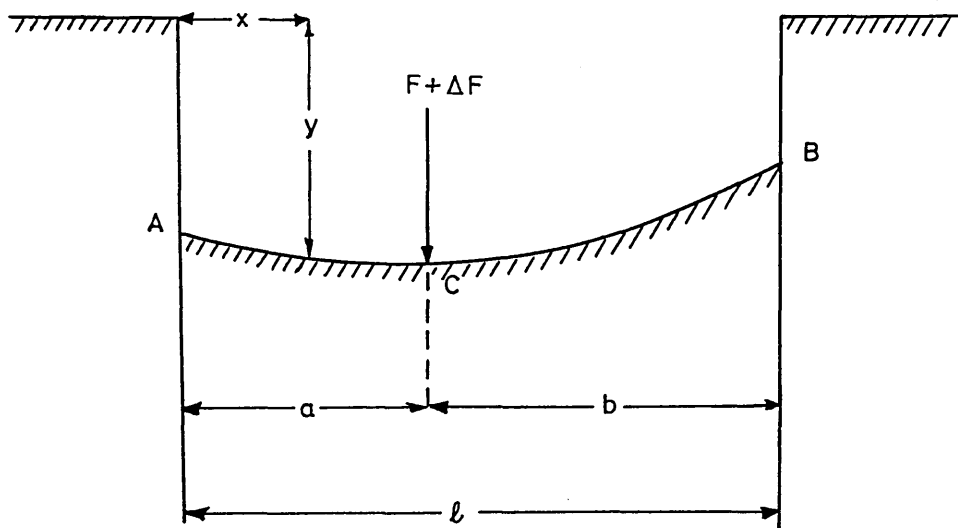
Fig. 4.13. Roll resting on an elastic foundation.
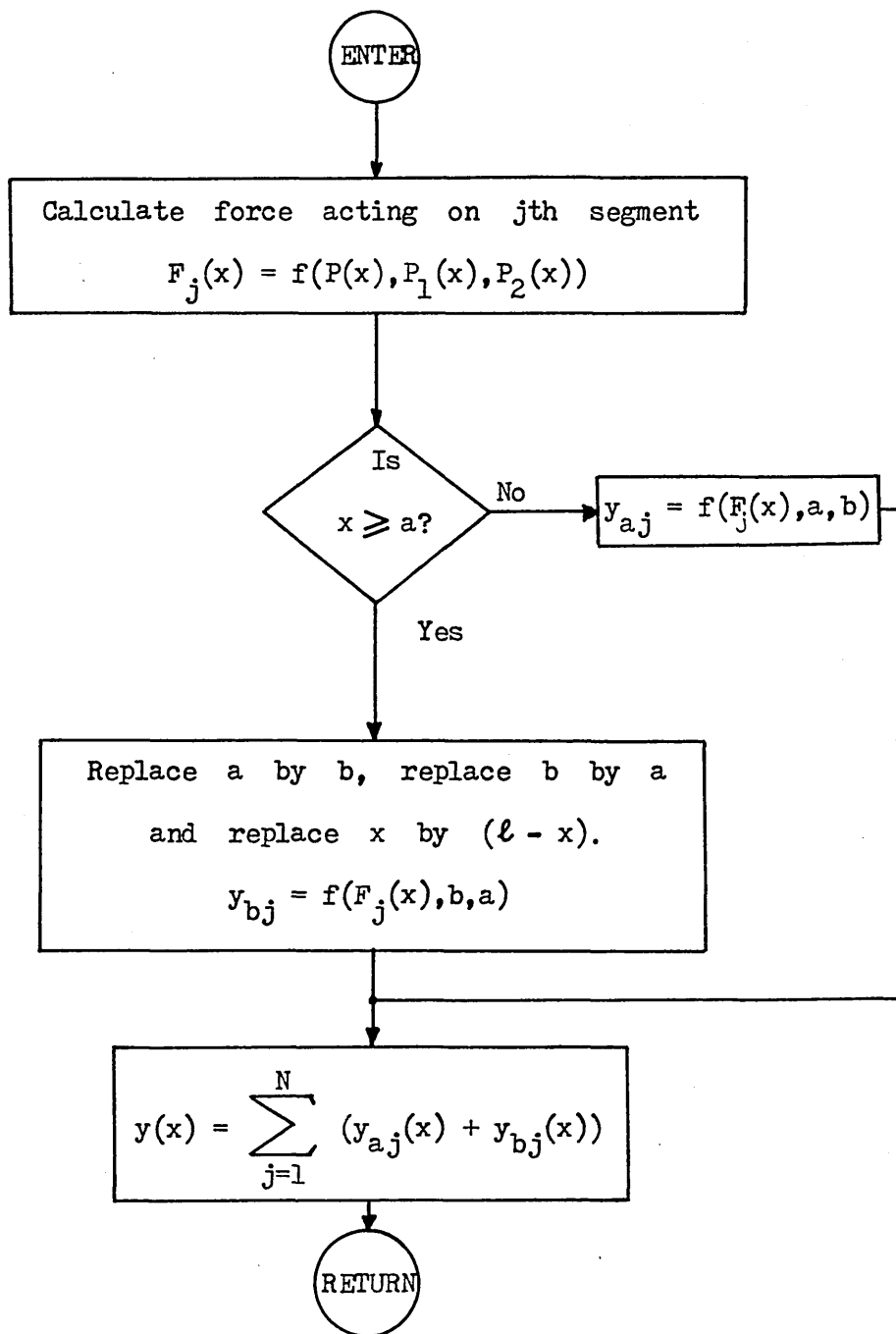
Fig. 4.14. Flow chart for deflection calculation (Subroutine MUMMY).

Fig. 4.15. Roll gap variables.
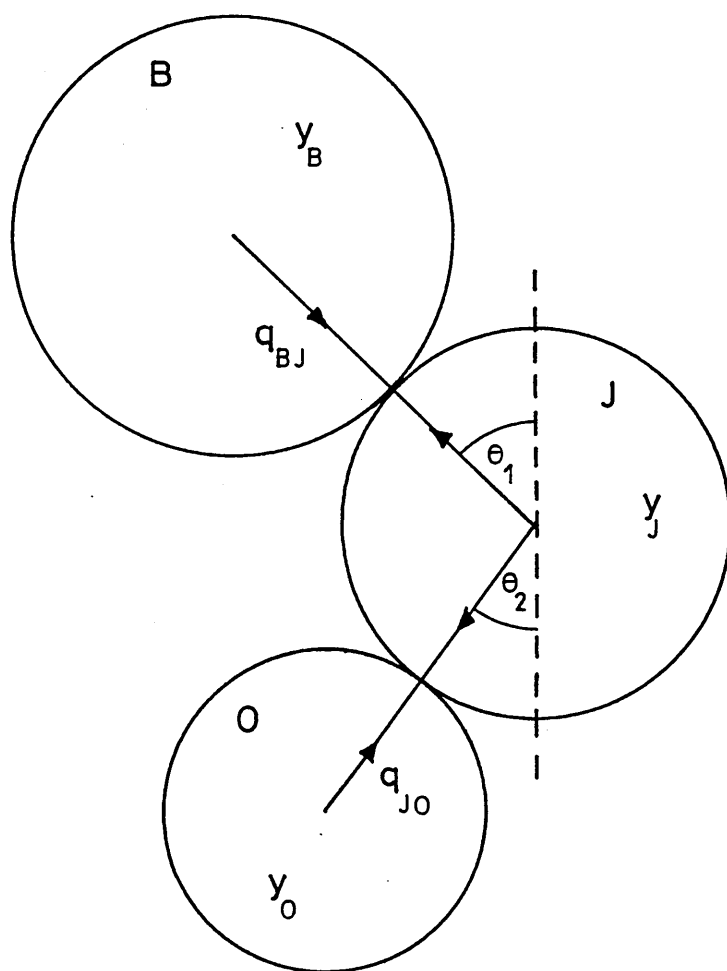
Fig. 4.16. Inter roll pressure and deflection.
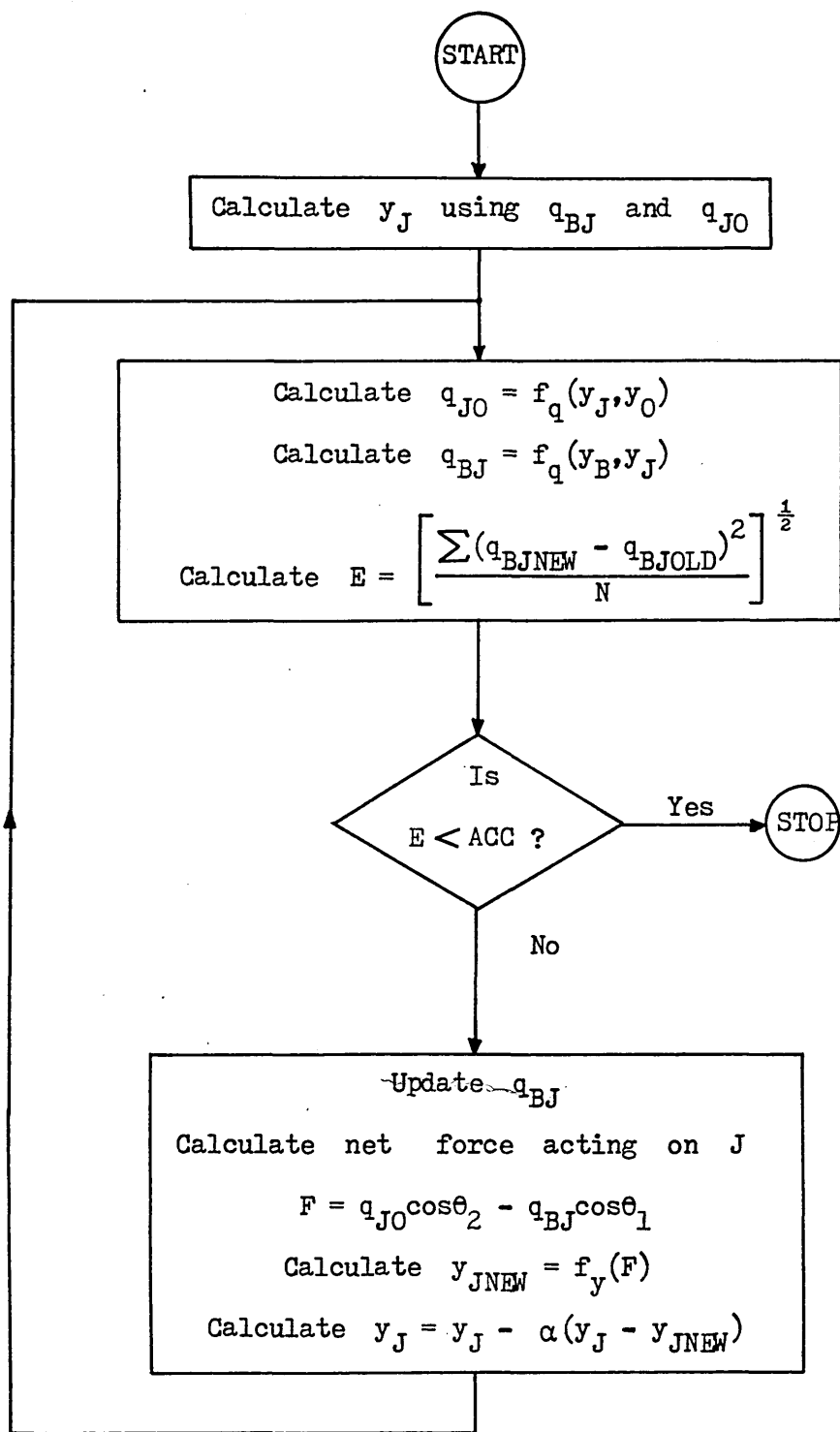
Fig. 4.17. Flow chart for q_{BJ} calculation.
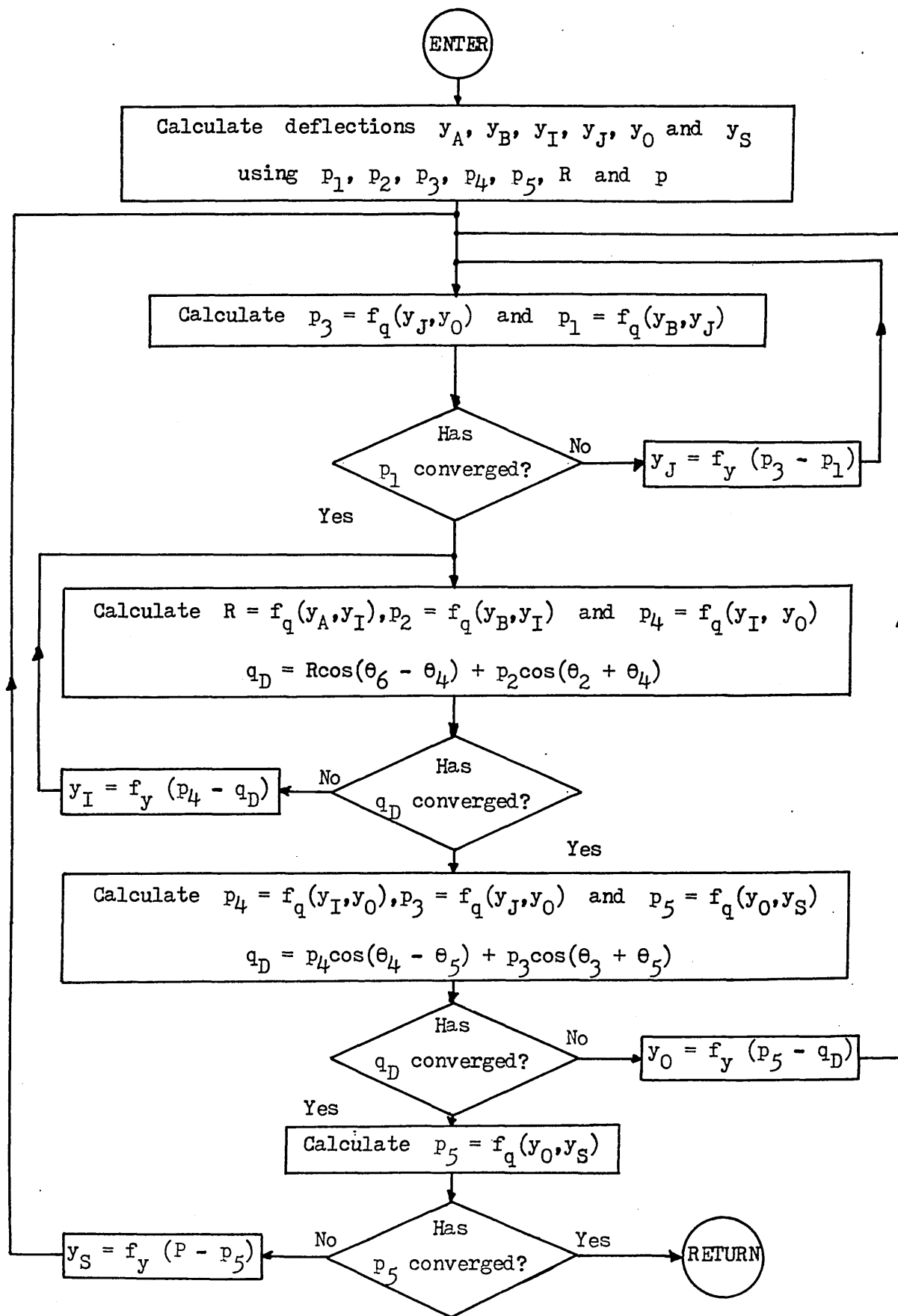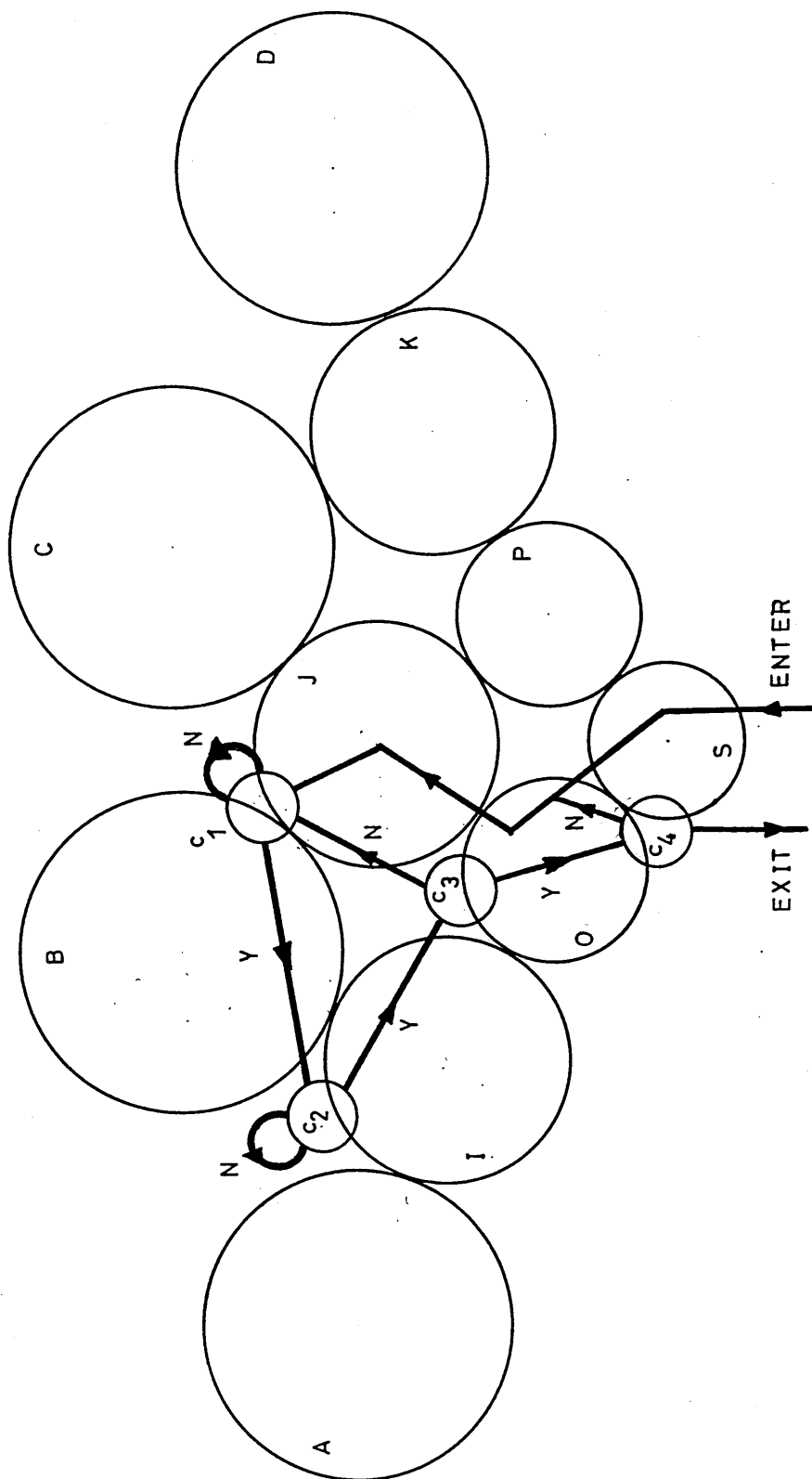
Fig. 4.18.   Flow chart for subroutine BEND.

Fig. 4.19. Path of calculation for subroutine BEND.

Chapter 5.

STATE SPACE REPRESENTATION OF THE MILL.

5.1. Introduction.

The analysis and design of linear systems can be achieved by using one of two major approaches. One method uses Laplace and z-transforms, transfer functions, and block diagrams. The other approach, in which modern control system design techniques are based, is the state variable technique.

The state variable method has at least the following advantages over the transfer function method:

1. It is convenient for computer solutions.

2. It allows a unified representation of digital systems with various types of sampling schemes.

3. It allows a unified representation of single and multivariable systems.

4. It can be applied to certain types of nonlinear and time varying systems.

In the state variable method a continuous data system is represented by a set of first order differential equations called state equations. For a discrete system the state equations become first order difference equations.[50,51]

- 103 -

5.1.1. State equations for continuous systems.

The multivariable continuous system with m inputs and r outputs shown in fig. 5.1 can be characterised by the following set of n first order differential equations:

$$\frac{dx_i(t)}{dt} = f_i\left[x_1(t),\ldots x_n(t), u_1(t),\ldots u_m(t)\right] \quad (i = 1,\ldots n) \quad (5.1)$$

where $x_1(t),\ldots x_n(t)$ are called state variables. The r outputs $y_k(t)$ (k = 1,2,...r), can be related to the state variables and the inputs in the following manner:

$$y_k(t) = g_k\left[x_1(t),\ldots x_n(t), u_1(t),\ldots u_m(t)\right] \quad (k = 1,\ldots r). \quad (5.2)$$

Eqs. (5.1) and (5.2) can be written in compact form using vector terminology as

$$\dot{\underline{x}}(t) = A\underline{x}(t) + B\underline{u}(t) \quad (5.3)$$

and

$$\underline{y}(t) = C\underline{x}(t) + D\underline{u}(t) \quad (5.4)$$

where A, B, C and D are constant matrices for linear time invariant systems.

The solution to eq. (5.3) can be obtained using the Laplace transform method and is given by

$$x(t) = \underline{\phi}(t)x(0) + \int_0^t \underline{\phi}(t - \tau)Bu(\tau)d\tau \quad t \geqslant 0 \quad (5.5)$$

where

$$\Phi(t) = \mathcal{L}^{-1}\left[(sI - A)^{-1}\right] = e^{At} = \sum_{k=0}^{\infty} A^k \frac{t^k}{\underline{|k}} \qquad (5.6)$$

and $\Phi(t)$ is called the state transition matrix. Eq.(5.5) is true only when the initial time is taken at $t = 0$. If the initial time is taken to be t_o then eq.(5.5) can be modified to include t_o and is written as

$$x(t) = \Phi(t - t_o)x(t_o) + \int_{t_o}^{t} \Phi(t - \tau)Bu(\tau)d\tau \qquad t \geq t_o. \qquad (5.7)$$

5.1.2. State equations for discrete systems.

A discrete system is shown in fig.5.2. The inputs to the linear system are discretised and they are described by

$$u_i(t) = u_i(kT) = e_i(kT). \qquad (5.8)$$

Now letting $t_o = kT$ and since $u(\tau) = u(kT) =$ constant vector, eq.(5.5) for discrete system can be written as

$$x(t) = \Phi(t - kT)x(kT) + \left[\int_{kT}^{t} \Phi(t - \tau)Bd\tau\right]u(kT). \qquad (5.9)$$

Eq.(5.9) is only valid for one sampling period. If we are interested only in the response at the sampling instants by setting $t = (k + 1)T$ we obtain the discrete version of

eq. (5.5) as

$$x\big[(k + 1)T\big] = \rho(T)x(kT) + \Lambda(T)u(kT) \qquad (5.10)$$

where

$$\rho(T) = e^{AT} \qquad (5.11)$$

and

$$\Lambda(T) = \int_0^T \rho\big[(k + 1)T - \tau\big] B d\tau. \qquad (5.12)$$

5.2. Mill representation in state space form.

5.2.1. Introduction.

The overall block diagram of the shape control scheme is shown in fig. 5.3. The control scheme is divided into several subsystems. The system has 8 + 2 inputs and a number of shapemeter measurements ($\leqslant 31$) as outputs. The 8 + 2 inputs represent eight As-U-Roll actuators plus the two first intermediate roll positions. For the present analysis it is not proposed to control the first intermediate roll positions. Therefore only the eight actuators are considered as inputs. The investigation becomes easier when the number of inputs are equal to the number of outputs, hence for the initial design it is assumed that there are eight shapemeter outputs. This is done by dividing the strip into eight zones and treating shape at each zone as constant.

The set point actuators are assumed to control
their positions by means of a servo type control system.
Variations in the actuator positions are assumed to have an
instantaneous additive effect to incoming shape. This is
justified, as the dynamics of the mill cluster are much
faster than the overall system dynamics and can be ignored.
A movement in any one actuator affects the shape across
the entire strip width. Any corrective effect of the shape
at the roll gap due to actuator movement is calculated
from the static mill gains[39]. These effects are added to
the incoming strip shape disturbance. The shapemeter is
situated at a fair distance from the roll gap and therefore
the stress distribution of the strip, as it moves
downstream to the shapemeter, is affected by a combination
of pure transport delay and a lag effect. The shapemeter
transducer is effectively a discrete system, as explained in
section 2.3.2, the output from it being electronically
smoothed by filters.

A cascade controller[52] is proposed to correct
shape changes and the control is obtained by comparing the
shapemeter measurements with the actuator signals which
produces zero shape.

5.2.2. The actuator subsystem.

The eight actuators are assumed to be
noninteracting and are modelled as second order systems. In
practice actuators are simple integrators accompanied by a

- 107 -

dead space arising from the solenoid valve spool, and from friction in the hydraulic motor. The open loop transfer function for the actuators can be written as[52]

$$G_a(s) = \frac{k_a}{s(1 + sT_a)}.$$

(5.13)

The output position can be fed back via a position tranducer to control the actuator positions accurately. The forward path has a variable gain k and the closed loop system for one actuator is shown in fig.5.4. The closed loop transfer function of the actuator can be written as

$$g_a(s) = \frac{kk_a}{s(1 + sT_a) + kk_a k_f}.$$

(5.14)

If the roots of the characteristic equation of eq.(5.14) are complex then the actuator positions will have overshoots. Since the mill dynamics are much faster than the overall system dynamics, these overshoots have instantaneous effect on shape which will cause a problem on control. Therefore it is proposed to choose k to give equal roots for the characteristic equation so that the actuators will have the fastest response without any overshoot. Hence the closed loop transfer function of each actuator can be written as

$$g_a(s) = \frac{K_A}{(1 + sT_A)^2}.$$

(5.15)

The state space form of each actuator is therefore given by

$$\dot{\underline{x}}_a(t) = A_a \underline{x}_a(t) + B_a u_a(t)$$
$$y_a(t) = C_a \underline{x}_a(t) \qquad\qquad\qquad\qquad (5.16)$$

where

$$A_a = \begin{bmatrix} 0 & 1 \\ -\dfrac{1}{T_A^2} & -\dfrac{2}{T_A} \end{bmatrix}, \quad B_a = \begin{bmatrix} 0 \\ \dfrac{K_A}{T_A^2} \end{bmatrix} \quad \text{and} \quad C_a = \begin{bmatrix} 1 & 0 \end{bmatrix} \qquad (5.17)$$

(See Appendix 3 for numerical values of K_A and T_A). Since there are eight actuators with eight inputs and eight outputs, and they have the same transfer function, the state space form of the multivariable nature actuator subsystem can be written as

$$\begin{bmatrix} \dot{\underline{x}}_{a1}(t) \\ \vdots \\ \dot{\underline{x}}_{a8}(t) \end{bmatrix} = \begin{bmatrix} A_{a1} & & 0 \\ & \ddots & \\ 0 & & A_{a8} \end{bmatrix} \begin{bmatrix} \underline{x}_{a1}(t) \\ \vdots \\ \underline{x}_{a8}(t) \end{bmatrix} + \begin{bmatrix} B_{a1} & & 0 \\ & \ddots & \\ 0 & & B_{a8} \end{bmatrix} \begin{bmatrix} u_{a1}(t) \\ \vdots \\ u_{a8}(t) \end{bmatrix}$$

and

$$\begin{bmatrix} y_{a1}(t) \\ \vdots \\ y_{a8}(t) \end{bmatrix} = \begin{bmatrix} C_{a1} & & 0 \\ & \ddots & \\ 0 & & C_{a8} \end{bmatrix} \begin{bmatrix} \underline{x}_{a1}(t) \\ \vdots \\ \underline{x}_{a8}(t) \end{bmatrix} = \begin{bmatrix} 1 & 0 & & 0 \\ & \ddots & \\ 0 & & 1 & 0 \end{bmatrix} \begin{bmatrix} \underline{x}_{a1}(t) \\ \vdots \\ \underline{x}_{a8}(t) \end{bmatrix}$$

$$\qquad\qquad\qquad\qquad (5.18)$$

- 109 -

i.e. in compact form we can write the actuator state equations as

$$\dot{\underline{X}}_A(t) = A_A\underline{X}_A(t) + B_A\underline{U}_A(t)$$

$$\underline{Y}_A(t) = C_A\underline{X}_A(t)$$

(5.19)

where

$\underline{X}_A(t)$ is a 16×1 column vector,

$\underline{U}_A(t)$ is a 8×1 column vector,

$\underline{Y}_A(t)$ is a 8×1 column vector,

A_A is a 16×16 square matrix,

B_A is a 16×8 matrix

and

C_A is a 8×16 matrix.

5.2.3. Mill cluster subsystem.

Among mill plant subsystems, the mill cluster model is the most complicated due to its sophiticated mechanical design. The mill cluster is assumed to be non-dynamic so that the relationship between an actuator change $\delta x_a(t)$ and a shape profile change $\delta y'_m(t)$, at the roll gap, is simply a gain which may be calculated using the static model. The mill equation therefore can be

written as

$$\underline{Y}_m(t) = G_m \underline{Y}_A(t) + \underline{v}_m(t). \qquad (5.20)$$

The gain matrix G_m depends upon the material being rolled and is also schedule dependent. The matrix is a constant matrix for a given pass and can be calculated off-line using the static model or on-line using measurement techniques. The vector $\underline{v}_m(t)$ in eq.(5.20) represents shape disturbances which may result from changes in the input shape profile or indirectly via changes in the input gauge profile, material hardness or thermal camber.

5.2.4. Strip dynamics subsystem.

At any instant the stress distribution measured by the shapemeter differs from that at the roll gap since the shapemeter is located at some distance downstream from the roll gap. The representation of the relation between these two stress profiles is a subject of current interest. However it was suggested that this be represented as either a pure time delay or a simple lag.

The strip between the roll gap and the shapemeter is unsupported and in general will have a catenary profile. For such a strip processing line Grimble[53-55] derived a transfer function relating tension changes to speed changes of the strip. He also showed that if the tension in the strip is such that the sag can be neglected, then

the transfer function can be represented by a simple lag term. Since the stress at the roll gap depends on the input/output strip velocities it can easily be shown that the relationship between the shape at the roll gap and the shape at the shapemeter is also a simple lag term.[52] The shapemeter is situated at a certain distance from the roll gap, and therefore the shape measured at the shapemeter is not the true shape, but delayed by time τ. Thus for the present analysis the transfer function of the strip includes a time delay term and a simple lag term in cascade. Therefore the transfer function of the strip is written as

$$g_d(s) = \frac{e^{-s\tau}}{1 + sT_d} \cdot \qquad (5.21)$$

For simulation purposes the delay term $e^{-s\tau}$ is replaced by first order Pade approximation and hence the strip transfer function is given by

$$g_d(s) = \frac{(1 - s\tau/2)}{(1 + s\tau/2)(1 + sT_d)} \cdot \qquad (5.22)$$

The state space form of one of the strip zones is given by

$$\left. \begin{array}{l} \dot{\underline{x}}_d(t) = A_d \underline{x}_d(t) + B_d y_m(t) \\[2mm] y_d(t) = C_d \underline{x}_d(t) \end{array} \right\} \qquad (5.23)$$

where

$$A_d = \begin{bmatrix} 0 & 1 \\ \\ -\dfrac{2}{\tau T_d} & -\dfrac{\tau + 2T_d}{\tau T} \end{bmatrix}, \quad B_d = \begin{bmatrix} -\dfrac{1}{T_d} \\ \\ \dfrac{4T_d + \tau}{\tau T^2} \end{bmatrix} \quad \text{and}$$

$$C_d = \begin{bmatrix} 1 & 0 \end{bmatrix}$$

(See Appendix 4 for derivation of A_d and B_d). The strip width is divided into eight zones and each zone has the state equations described by eq.(5.23). Hence the strip dynamics subsystem becomes:

$$\begin{bmatrix} \dot{\underline{x}}_{d1}(t) \\ \vdots \\ \dot{\underline{x}}_{d8}(t) \end{bmatrix} = \begin{bmatrix} A_{d1} & & 0 \\ & \ddots & \\ 0 & & A_{d8} \end{bmatrix} \begin{bmatrix} \underline{x}_{d1}(t) \\ \vdots \\ \underline{x}_{d8}(t) \end{bmatrix} + \begin{bmatrix} B_{d1} & & 0 \\ & \ddots & \\ 0 & & B_{d8} \end{bmatrix} \begin{bmatrix} y_{m1}(t) \\ \vdots \\ y_{m8}(t) \end{bmatrix}$$

and

$$\begin{bmatrix} y_{d1}(t) \\ \vdots \\ y_{d8}(t) \end{bmatrix} = \begin{bmatrix} C_{d1} & & 0 \\ & \ddots & \\ 0 & & C_{d8} \end{bmatrix} \begin{bmatrix} \underline{x}_{d1}(t) \\ \vdots \\ \underline{x}_{d8}(t) \end{bmatrix} = \begin{bmatrix} 1 & 0 & & & 0 \\ & \ddots & \ddots & & \\ 0 & & 1 & 0 \end{bmatrix} \begin{bmatrix} \underline{x}_{d1}(t) \\ \vdots \\ \underline{x}_{d8}(t) \end{bmatrix}.$$

$$(5.24)$$

In compact form the strip subsystem becomes

$$\left. \begin{array}{l} \dot{\underline{X}}_D(t) = A_D \underline{X}_D(t) + B_D \underline{Y}_m(t) \\ \\ \underline{Y}_D(t) = C_D \underline{X}_D(t) \end{array} \right\} \qquad (5.25)$$

- 113 -

Each strip zone is second order and therefore eq. (5.25) has the dimensions as eq. (5.19).

5.2.5. The shapemeter dynamics subsystem.

The shapemeter forms an output subsystem and is represented by a second order system with a dominant shapemeter filter time constant which varies as the strip speed (see Appendix 5). A series of filters is switched on at preset mill speeds to smooth the discretised shapemeter signals. The shapemeter signals from the thirty one measuring zones are assumed to be non-interactive and are reduced to eight signals to avoid dimensionality problems. The shapemeter transfer function approximates to a unity gain second order system and is given by

$$g_s(s) = \frac{1}{(1 + sT_{s1})(1 + sT_{s2})} \qquad (5.26)$$

where T_{s1} is the speed dependent dominant time constant. In state space form the shapemeter is represented as

$$\left. \begin{aligned} \dot{\underline{x}}_s(t) &= A_s \underline{x}_s(t) + B_s y_d(t) \\ y_s(t) &= C_s \underline{x}_s(t) \end{aligned} \right\} \qquad (5.27)$$

where

$$A_s = \begin{bmatrix} 0 & 1 \\ -\dfrac{1}{T_{s1}T_{s2}} & -\dfrac{T_{s1} + T_{s2}}{T_{s1}T_{s2}} \end{bmatrix}, \quad B_s = \begin{bmatrix} 0 \\ \dfrac{1}{T_{s1}T_{s2}} \end{bmatrix} \text{ and } C_s = \begin{bmatrix} 1 & 0 \end{bmatrix}.$$

The complete shapemeter subsystem consists of eight zones and hence this subsystem is represented in state space form as

$$
\begin{bmatrix} \dot{\underline{x}}_{s1}(t) \\ \vdots \\ \vdots \\ \dot{\underline{x}}_{s8}(t) \end{bmatrix} = \begin{bmatrix} A_{s1} & & & 0 \\ & \ddots & & \\ 0 & & & A_{s8} \end{bmatrix} \begin{bmatrix} \underline{x}_{s1}(t) \\ \vdots \\ \vdots \\ \underline{x}_{s8}(t) \end{bmatrix} + \begin{bmatrix} B_{s1} & & & 0 \\ & \ddots & & \\ 0 & & & B_{s8} \end{bmatrix} \begin{bmatrix} \underline{y}_{d1}(t) \\ \vdots \\ \vdots \\ \underline{y}_{d8}(t) \end{bmatrix}
$$

and

$$
\begin{bmatrix} \underline{y}_{s1}(t) \\ \vdots \\ \vdots \\ \underline{y}_{s8}(t) \end{bmatrix} = \begin{bmatrix} C_{s1} & & & 0 \\ & \ddots & & \\ 0 & & & C_{s8} \end{bmatrix} \begin{bmatrix} \underline{x}_{s1}(t) \\ \vdots \\ \vdots \\ \underline{x}_{s8}(t) \end{bmatrix} = \begin{bmatrix} 1 & 0 & & & 0 \\ & \ddots & \ddots & & \\ 0 & & & 1 & 0 \end{bmatrix} \begin{bmatrix} \underline{x}_{s1}(t) \\ \vdots \\ \vdots \\ \underline{x}_{s8}(t) \end{bmatrix} .
$$

$$(5.28)$$

In vector form the shapemeter subsystem becomes

$$
\left. \begin{aligned} \dot{\underline{X}}_S(t) &= A_S \underline{X}_S(t) + B_S \underline{Y}_D(t) \\ \underline{Y}_S(t) &= C_S \underline{X}_S(t). \end{aligned} \right\}
$$

$$(5.29)$$

Since each zone is second order eq. (5.29) has the same dimensions as eq. (5.19).

5.3. State equation of the complete system.

Eqs. (5.19), (5.20), (5.25) and (5.29) can be combined, to represent the complete multivariable system in state space form, as follows:

$\underline{Y}_A(t)$ is substituted from eq. (5.19) in eq. (5.20) to give

$$
\underline{Y}_m(t) = G_m C_A \underline{X}_A(t) + \underline{v}_m(t).
$$

$$(5.30)$$

Eq.(5.30) is substituted in eq.(5.25) to give

$$\dot{\underline{X}}_D(t) = A_D\underline{X}_D(t) + B_D\left[G_mC_A\underline{X}_A(t) + \underline{v}_m(t)\right]$$

$$= B_DG_mC_A\underline{X}_A(t) + A_D\underline{X}_D(t) + B_D\underline{v}_m(t). \qquad (5.31)$$

From eq.(5.29) $\underline{Y}_D(t)$ is eliminated using eq.(5.25) to give

$$\dot{\underline{X}}_S(t) = B_SC_D\underline{X}_D(t) + A_S\underline{X}_S(t). \qquad (5.32)$$

The state equations of the complete system in terms of subsystems can be written as

$$\dot{\underline{X}}_A(t) = A_A\underline{X}_A(t) + B_A\underline{U}_A(t),$$

$$\dot{\underline{X}}_D(t) = B_DG_mC_A\underline{X}_A(t) + A_D\underline{X}_D(t) + B_D\underline{v}_m(t),$$

$$\dot{\underline{X}}_S(t) = B_SC_D\underline{X}_D(t) + A_S\underline{X}_S(t), \qquad (5.33)$$

$$\underline{Y}_S(t) = C_S\underline{X}_S(t).$$

The set of eq.(5.33) can be put in the matrix form as

$$\dot{\underline{X}}(t) = A\underline{X}(t) + B\underline{U}(t) + D\underline{v}_m(t),$$

$$\underline{Y}(t) = C\underline{X}(t) \qquad (5.34)$$

where

$$A = \begin{bmatrix} A_A & 0 & 0 \\ B_DG_mC_A & A_D & 0 \\ 0 & B_SC_D & A_S \end{bmatrix}, \qquad (48 \times 48) \qquad (5.35)$$

- 116 -

$$B = \begin{bmatrix} B_A \\ 0 \\ 0 \end{bmatrix}, \qquad (48 \times 8) \qquad\qquad (5.36)$$

$$D = \begin{bmatrix} 0 \\ B_D \\ 0 \end{bmatrix}, \qquad (48 \times 8) \qquad\qquad (5.37)$$

$$C = \begin{bmatrix} 0 & 0 & C_S \end{bmatrix}, \qquad (8 \times 48) \qquad\qquad (5.38)$$

$$\underline{X}^T(t) = \begin{bmatrix} \underline{X}_A^T(t) & \underline{X}_D^T(t) & \underline{X}_S^T(t) \end{bmatrix}, \qquad\qquad (5.39)$$

$$\underline{U}^T(t) = \begin{bmatrix} u_{a1}(t) & u_{a2}(t) \ldots \ldots u_{a8}(t) \end{bmatrix}, \qquad\qquad (5.40)$$

$$\underline{Y}^T(t) = \begin{bmatrix} y_{s1}(t) & y_{s2}(t) \ldots \ldots y_{s8}(t) \end{bmatrix}. \qquad\qquad (5.41)$$

This state space description of the mill forms the basis of the dynamic model simulation. In the above description the A matrix being lower triangular allows some simplifications in the computation. For control design the transfer function form of the system is more convenient. Also the plant structure is indicated far more clearly than in the time domain equations. As explained in section 5.2 all the dynamic elements are non-interactive. Therefore the actuator, strip and shapemeter subsystems can be written respectively in matrix form as

$$G_a(s) = \frac{K_A}{(1 + sT_A)^2} \cdot I_8 , \qquad\qquad (5.42)$$

$$G_d(s) = \frac{(1 - s\tau/2)}{(1 + s\tau/2)(1 + sT_d)} \cdot I_8 \qquad (5.43)$$

and

$$G_s(s) = \frac{1}{(1 + sT_{s1})(1 + sT_{s2})} \cdot I_8 \qquad (5.44)$$

where I_8 is the 8×8 identity matrix.

Therefore the open loop transfer function matrix $G(s)$ of the system can be obtained as

$$G(s) = G_s(s)G_d(s)G_m G_a(s)$$

$$= \frac{K_A(1 - s\tau/2)}{(1 + sT_A)^2(1 + s\tau/2)(1 + sT_d)(1 + sT_{s1})(1 + sT_{s2})} \cdot G_m$$

$$= \frac{N(s)}{D(s)} \cdot G_m \qquad (5.45)$$

where $N(s)$ and $D(s)$ are numerator and denominator polynomials respectively. (See Appendix 6 for polynomials $N(s)$ and $D(s)$ obtained for low, medium and high speeds).

5.4. Shape profile parameterisation.

The use of parameterisation of the shape profile presents several advantages and is often used. In the present system the maximum number of shapemeter outputs to be controlled are thirty one. The number of shape outputs also varies with the strip width. It is convenient if the number of outputs to be controlled is fixed for design purposes. Since the shape profile is a smooth curve

this can be represented by a polynomial of given order. If the parameters of this polynomial are taken as outputs then the number of outputs to be controlled become fixed rather than controlling the shape outputs directly. If the shape profile is represented by a third order polynomial (say $ax^3 + bx^2 + cx + d$) then the number of parameters to be controlled become four namely a, b, c and d. This means that parameterisation reduces the number of outputs to be controlled.

Let $y_s(x)$ be the shape measured or observed at the shapemeter and x be the distance across the strip width. The measured shape can be expressed in matrix form as

$$\underline{Y}(x) = X\underline{\beta} + \underline{\varepsilon} \tag{5.46}$$

where $\underline{\beta}$ is a vector containing the parameters to be controlled, $\underline{\varepsilon}$ is a vector of errors and X is a known constant matrix. If the polynomial which describes shape is third order then

$$\underline{\beta}^T = \begin{bmatrix} a & b & c & d \end{bmatrix}. \tag{5.47}$$

The error sum of squares is

$$\underline{\varepsilon}^T\underline{\varepsilon} = (\underline{Y} - X\underline{\beta})^T(\underline{Y} - X\underline{\beta})$$

$$= \underline{Y}^T\underline{Y} - 2\underline{\beta}^TX^T\underline{Y} + \underline{\beta}^TX^TX\underline{\beta}. \tag{5.48}$$

Let $\hat{\underline{\beta}}$ be the least square estimates of $\underline{\beta}$ which when

substituted in eq.(5.48) minimises $\underline{\varepsilon}^T\underline{\varepsilon}$. This can be obtained by differentiating eq.(5.48) with respect to β and equating the result to zero. This will give a solution to $\hat{\underline{\beta}}$ as[56]

$$\hat{\underline{\beta}} = (X^TX)^{-1}X^T\underline{Y}. \qquad (5.49)$$

Thus the estimated values of the parameters representing the shape are taken as the outputs of the control system. A modified block diagram of the shape control system is shown in fig.5.5. In this figure $G(s)$ represents the transfer function matrix of the plant and is given by eq.(5.45). There are eight actuator input signals to this block and the outputs are the eight shapemeter measurements. These eight signals are transformed into four estimated parameter outputs using eq.(5.49). These four estimated parameters are compared with four reference parameters $(r_1$ to $r_4)$ which will produce the desired shape. The controller is a 4×4 matrix which transforms these error signals to control signals $u(t)$. These four control inputs must be transformed via a matrix to act on the plant matrix $G(s)$. This transformation matrix may be chosen freely. However, if same matrix X is selected, as shown in fig.5.5, the open loop transfer function becomes

$$G_X(s) = (X^TX)^{-1}X^TG(s)X$$

$$= \frac{N(s)}{D(s)}(X^TX)^{-1}X^TG_mX$$

$$= \frac{N(s)}{D(s)} \cdot G_{mx} \qquad (5.50)$$

- 120 -

where $G_{mx} = (X^TX)^{-1}X^TG_mX$ and $G_X(s)$ will be a 4×4 matrix.

5.5. Shape control system design.

An acceptable control scheme must provide:

1. Transient response with small overshoot and rise time in the region of say 5 seconds (experience of mill operators).

2. Relative insensitivity to errors of calculation and variations of static gain matrix G_m.

3. Relative insensitivity to line speed.

Furthermore there are certain shape profiles which must never be reached, even in transients, for the safe operation of the mill. These aspects are still under discussion with the mill engineers.

As discussed in section 5.2 the mill is a multivariable plant with eight inputs and eight outputs. Straight forward application of either of the two modern multivariable design methods, i.e. the Characteristic Locus[57] or the Inverse Nyquist Array,[58] will produce compensators highly dependent on G_m^{-1} as all the interactions in the plant comes from G_m. From the properties of G_m described by eqs.(6.1) and (6.2) in section 6.1, the matrix G_m is not of full rank and therefore the inverse does not exist. But the matrix G_m, calculated from the static model described

- 121 -

in chapters 2 and 3, is often full rank and this may be due to numerical errors. Consequently a control system cannot be based on G_m^{-1}.

The use of input-output transformation of the plant discussed in section 5.4 produces a smaller dimension system. This yields a four by four multivariable system with $G_x(s)$ as the forward path transfer function (eq.(5.50)). The gain matrix G_{mx} in eq.(5.50) is not diagonal. Suitable pre and post compensators can be found to diagonalise G_{mx} using singular value decomposition to reduce interactions.

5.5.1. Singular value decomposition.

The singular value decomposition was developed for real square matrices in the 1870's by Beltrami and Jordan.[59] The singular value decomposition theorem[60] can be stated as, 'If A is a real $n \times n$ square matrix then there exists orthogonal real square matrices U and V such that

$$A = USV^T \tag{5.51}$$

where

$$S = \text{diag}(\sigma_1, \sigma_2, \ldots \ldots \sigma_n) \tag{5.52}$$

with

$$\sigma_1 \geqslant \sigma_2 \geqslant \ldots \ldots \geqslant \sigma_n \geqslant 0'.$$

Proof:-

Since $A^T A$ is symmetric and positive definite the characteristic roots or eigenvalues of $A^T A$ are real and positive. Denoting these characteristic roots by

$$\sigma_i^2 , \qquad i = 1, 2, \ldots \ldots n$$

we can arrange that

$$\sigma_1 \geqslant \sigma_2 \geqslant \ldots \ldots \geqslant \sigma_n \geqslant 0. \qquad (5.53)$$

Let $v_1, v_2, \ldots \ldots v_n$ be the corresponding orthogonal characteristic vectors. i.e. $V = (v_1, v_2, \ldots \ldots v_n)$ is orthogonal. If

$$S = \text{diag}(\sigma_1, \sigma_2, \ldots \ldots \sigma_n) \qquad (5.54)$$

and

$$S^2 = \text{diag}(\sigma_1^2, \sigma_2^2, \ldots \ldots \sigma_n^2) \qquad (5.55)$$

then we have

$$A^T A V = V S^2. \qquad (5.56)$$

Since V is orthogonal $V^T V = I$ and eq. (5.56) can be written as

$$S^{-1} V^T A^T A V S^{-1} = S^{-1} V^T V S S S^{-1} = I. \qquad (5.57)$$

Let

$$U = A V S^{-1}. \qquad (5.58)$$

Therefore

$$U^T = S^{-1}V^TA^T. \qquad (5.59)$$

Then from eq. (5.57) we have

$$U^TU = I \qquad (5.60)$$

which means that U is orthogonal. Then from eq. (5.57) we have

$$U^TAVS^{-1} = I \qquad (5.61)$$

from which

$$A = USV^T. \qquad (5.62)$$

From the above theorem, the transformed gain matrix G_{mx} can be written as

$$G_{mx} = U \Sigma V^T \qquad (5.63)$$

where Σ is a diagonal matrix, and U and V are orthogonal matrices. From eq. (5.63)

$$U^TG_{mx}V = \Sigma. \qquad (5.64)$$

If V and U^T are chosen[61] to be the pre and post compensators, the forward transfer function of the plant can be written as

$$P_1G_xP_2 = \frac{N(s)}{D(s)} . U^TG_{mx}V$$

$$= \frac{N(s)}{D(s)} \Sigma \qquad (5.65)$$

and the closed loop transfer function matrix becomes

$$G_{CL}(s) = \frac{N(s)}{D(s)} \cdot \Sigma \cdot \left[I + \frac{N(s)}{D(s)} \Sigma \right]^{-1}.$$ (5.66)

The present study is only concerned with the static model and therefore the actual control system design is not discussed any further. The results for singular value decomposition are given in chapter 6 and the complete block diagram for the plant is shown in fig. 5.5.
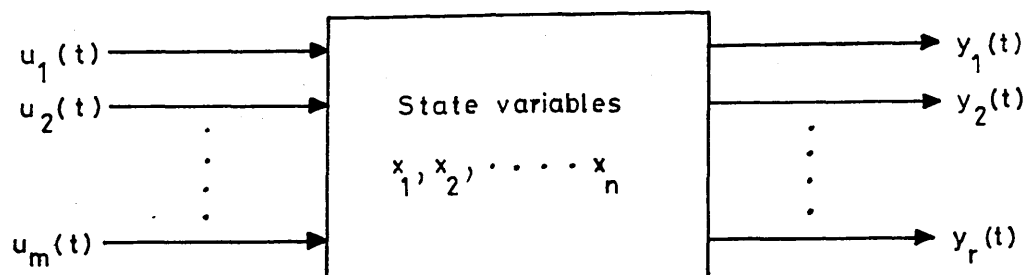
Fig. 5.1. Multivariable linear continous system.
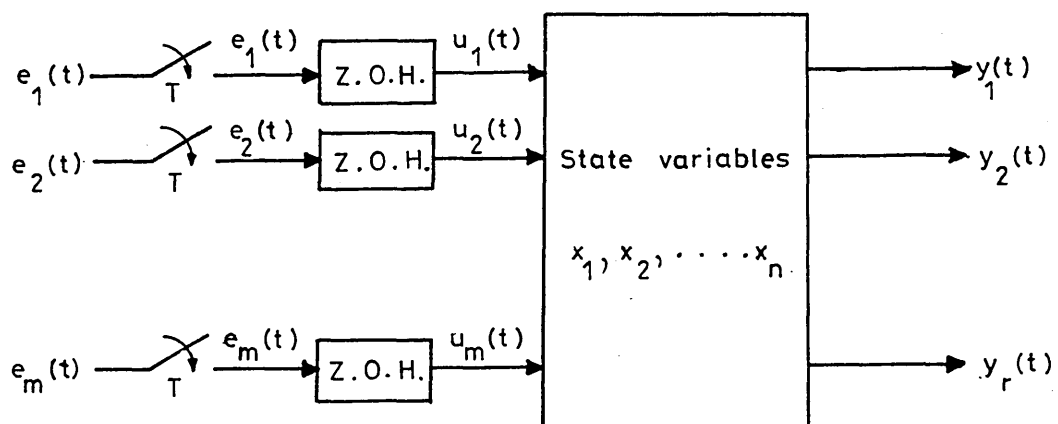
Fig. 5.2. Multivariable linear discrete system.
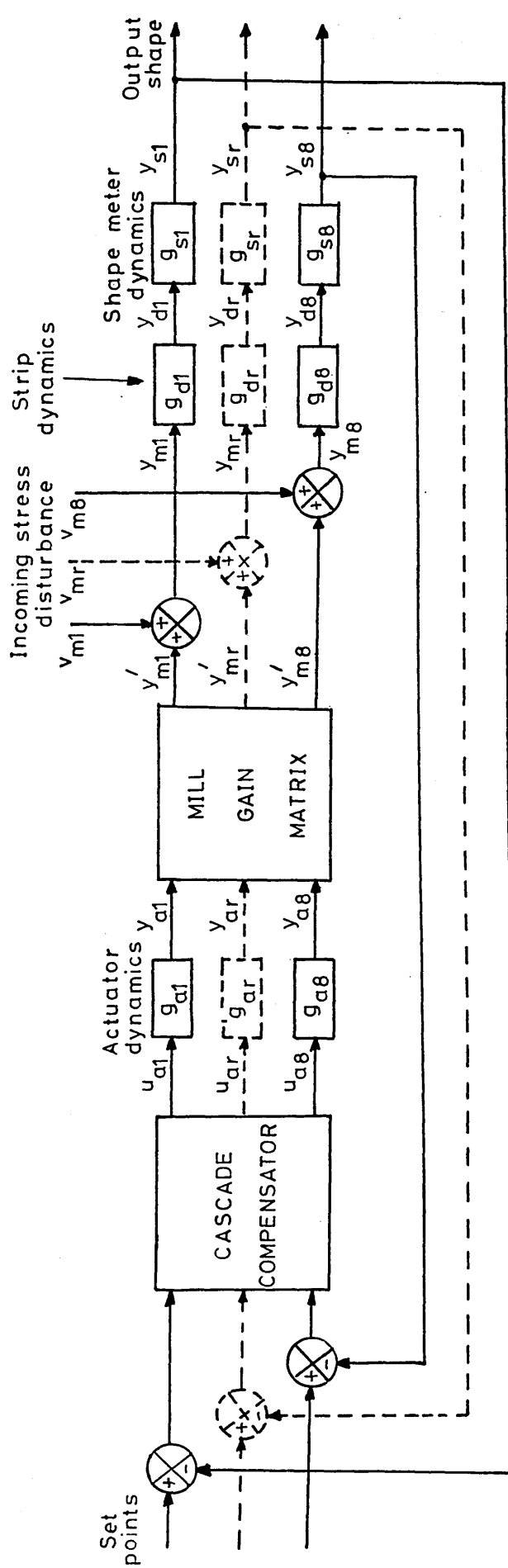
Fig. 5.3. Overall mill block diagram.
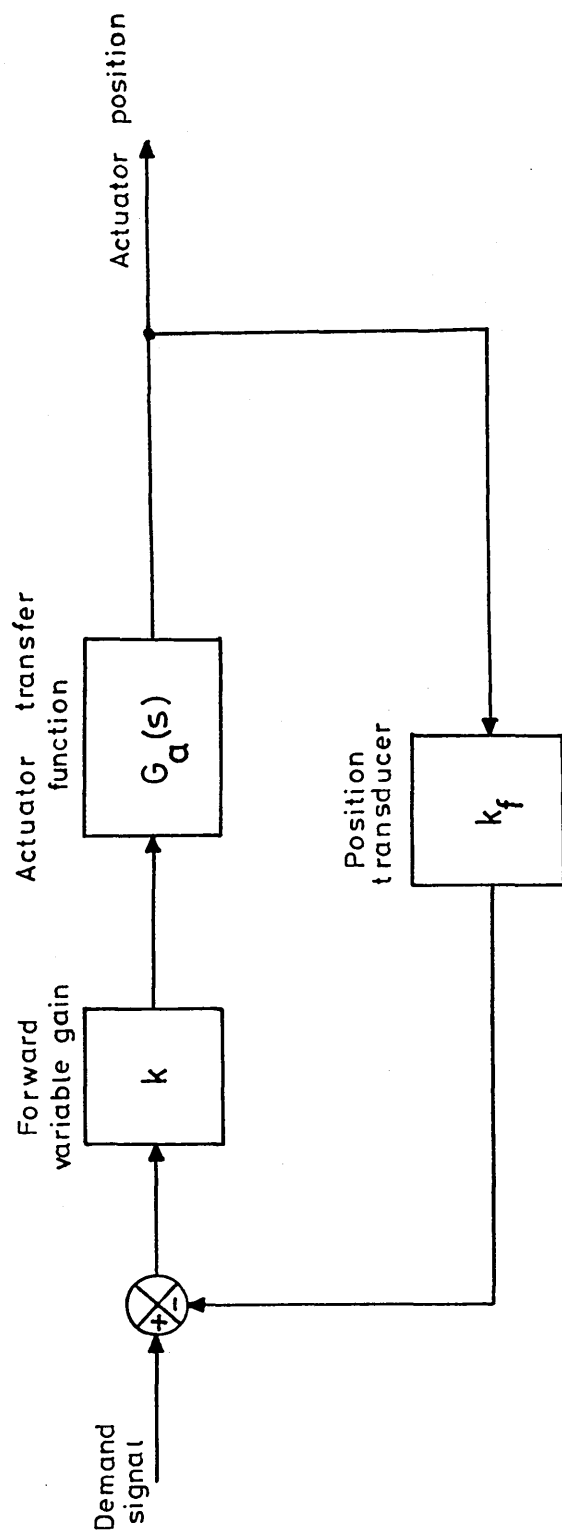
Fig. 5.4. Block diagram of actuator position control system.
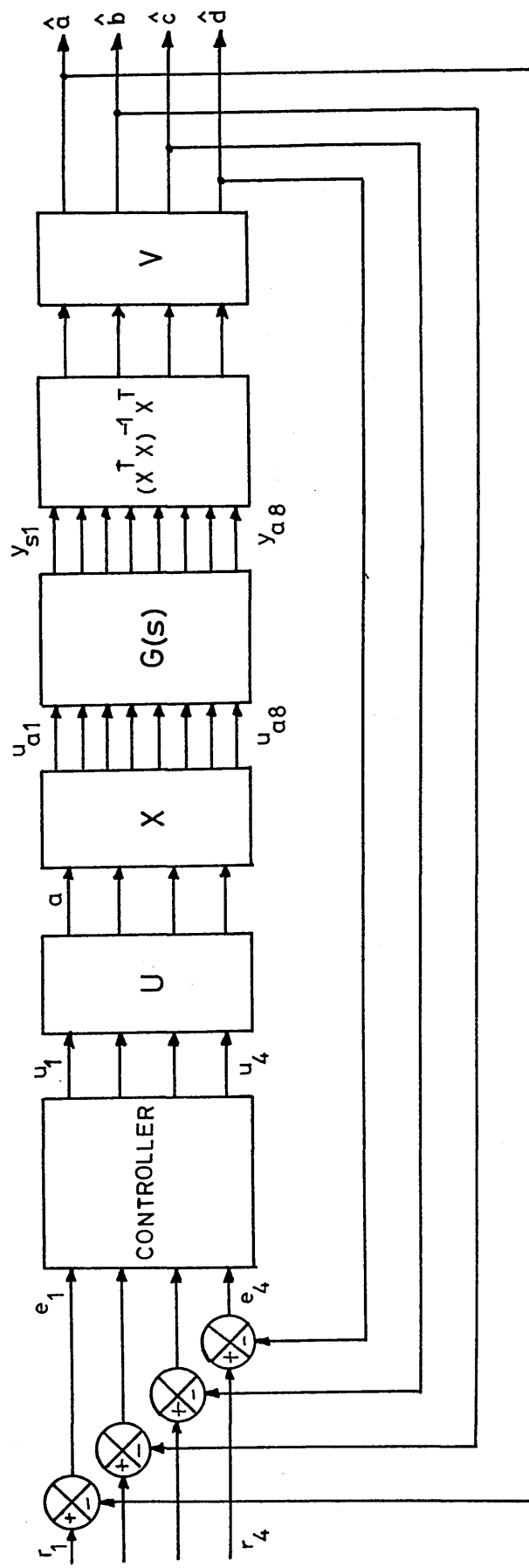
Fig. 5.5. Block diagram of shape control system.

Chapter 6.

RESULTS AND DISCUSSION OF RESULTS.

6.1. Properties of shape profiles.

The static model provides two main types of
result for a given rolling schedule. The first category
is concerned with the physical processes and is the
calculated shape, gauge and pressure profiles. These are
important when the degree of control of a particular
profile is of interest. The shape profiles for eight
actuator changes (RUN 0) are shown in fig.6.1 (e.g. in
fig.6.1a the curve marked with a cross is the
shape profile due to a change of 6 mm in rack 8,
keeping
all other racks at zero position etc.). Inspection of
figs.6.1 to 6.22 shows the property of symmetry when the
strip is placed at the centre of the mill. Units used in
these figures are N/m^2 for shape and the distance x is
given in terms of number of sections. The actual distance
can be obtained by multiplying the number of sections by
dx the width of one section. Inter roll pressure
distributions and the corresponding roll deflections for a
change in rack 1 are shown in fig.6.24 and fig.6.25
respectively. These profiles are obtained for the mill
schedule given in table 6.1. The corresponding gain matrix
is denoted by G_m^0.

If the shape profiles shown in fig.6.1 are inspected closely it is seen that the largest shape change is found in the vicinity of a point, which is directly under the particular shape actuator which has been moved from the null point, across the strip width. It is also clear that a rack change appears to affect widely separated sections of the strip. This can be explained by considering a localised change in the back-up rolls. This change in the back-up rolls will modify the inter roll forces between the back-up and second intermediate rolls. Similarly, this change in the inter roll force will change the effective profiles of both the back-up and second intermediate rolls. From the study of a point force acting on a roll, it can be seen that the roll profile is changed, not just below the point of action of the force but over a region surrounding the point. The change is significant in the vicinity of the point of application of the force. Thus, a localised change in the back-up roll profile is converted to a distributed change in the profile of the second intermediate roll. Further interaction between the second intermediate rolls and the first intermediate rolls and between the first intermediate rolls and work rolls spread the effect. Thus in general the largest shape change occurs under the actuator which is moved.

In fig.6.1 the negative shape corresponds to compressive stresses and the positive shape to tensile

stresses. When rack 1 is moved downwards for example, the left hand side of all the rolls will be deflected downwards with respect to the other end. This results in an increase in reduction of the thickness at the left hand edge of the strip which will produce a longer edge. To keep the applied tension constant, the left hand edge of the strip must be compressed and at the same time the right hand end will have tensile forces. This corresponds to the compressive and tensile nature of the stress and is shown in fig.6.1a.

~ The static model developed ignores the strip edge effects. When the strip width is less than the mill width (or the length of the work rolls) there will be two portions from either end of the upper work roll with no support. The model is based on the assumption of zero shape directly under these two portions and therefore the shape changes from zero to a high value at the edge of the strip. This is shown in fig.6.1 (and in all other shape profiles where the strip width is less than the mill width) by the rapid change at the edges. The calculated shape near the edge of the strip is therefore not the true shape.

6.2. Properties of the mill gain matrix.

The mill gains represent the second major source of information available from the static model.

Linearised mill gains are calculated about a given shape operating point and these relate the shape changes to the As-U-Roll changes. If the shape is measured at eight zones across the strip, the gain matrix has the form G_m^0 given in section 6.6 (units = N/mm^3). The eight rows of the gain matrix represent the eight zones across the strip and the eight columns correspond to eight As-U-Rolls, e.g. the elements in the second column give the shape at each zone across the strip width when the second As-U-Roll is moved. Thus, $g_{46} = -0.377$ in G_m^0 is the shape at zone 4 when As-U-Roll 6 is moved. The negative gains result from the assumption that the average tension is maintained constant. The gains include small errors due to numerical problems and due to the fact that the mill is non-linear. The gains are dependent upon the operating point and are very dependent upon the strip width. The way the gain matrices vary with different schedule settings are shown in table 6.3.

If the strip is centred across the mill then the gain matrix has a special type of symmetry. The first four columns of the matrix are repeated as the last four columns but in reverse order and vice versa. Another property of the gain matrix is that the elements of each column and row sum to zero. That is, it must satisfy

$$\sum_{j=1}^{8} g_{ij} = 0 \quad, \tag{6.1}$$

and

$$\sum_{i=1}^{8} g_{ij} = 0 \quad. \tag{6.2}$$

Eq.(6.1) describes the condition that the row elements sum to zero. This can be explained by considering a situation where all actuators are moved together by the same amount. This would result in a movement of the work rolls vertically downwards without introducing any bending effects, which is equivalent to a screwdown movement situated at the sides of the mill. The resulting major effect will be on the strip thickness and there will be no appreciable shape change. This is the case for RUN 22 and fig.6.23 shows the corresponding shape profile which illustrates this point clearly.

Eq.(6.2) is the condition that the column elements sum to zero. This is so since by the definition of shape (the deviation in the tensile stress from the mean), the average value across the strip should be zero.

Table 6.3 is obtained by comparing matrices G_m^1 to G_m^{21} with G_m^0. The diagonal elements are compared and the changes are expressed as a percentage change. The

- 134 -

negative sign indicates a reduction in gain compared to G_m^0 and the overall, change is the average percentage change when all actuators are considered.

6.3. Shape changes for strip width variation.

The gain matrices G_m^1 to G_m^7 given in section 6.6 are obtained by varying the strip width from 1.7m to 1.0m and keeping all other variables constant. The corresponding shape profiles are shown in figs.6.1 to 6.7. All these shape profiles and gain matrices have the properties discussed in sections 6.1 and 6.2 if minor numerical errors are ignored.

The maximum shape occurs in the vicinity of the particular actuator which has been moved. In figs.6.1 to 6.8 this is shown as the minimum or the trough of the shape profiles. A graphical representation of the variation of these maximum values is shown in fig.6.26. As seen from the figure the maximum shape hardly changes with the strip width if actuators 3, 4, 5 and 6 are used. This is because all actuators are situated well within the strip considered. The distance between racks 3 and 6 is about 0.68m and the minimum width considered is 1.0m. Therefore racks 3, 4, 5 and 6 lie well within the strip widths considered. When there is any change occurring in these four racks, there is a portion of the strip directly under the particular rack moved to support the work roll. For these widths the

conditions of the strip in the vicinity of racks 3, 4, 5 and 6 do not change considerably, and hence the shape change due to the same movement in any of these four racks will be roughly the same (see figs.6.1 to 6.8).

The maximum shape for strip widths 1.7m and 1.6m remain approximately the same when racks 2 and 7 are used. This is similar to the above case as racks 2 and 7 are situated well within these two strip widths. If the strip width w_s is reduced further then the work rolls have no strip to support and they act as cantilevers. This cantilever bending action will attempt to reduce the thickness of the strip at the edges more than at the middle and therefore will produce higher compressive stresses near the edge. The length of this cantilever portion increases when w_s is reduced, and hence the bending action which produces the variation in the maximum shape. As seen from fig.6.26, the variation of maximum shape for racks 1 and 8 has a maximum (in the negative sense) when $w_s = 1.5m$, and for racks 2 and 7 this occurs at $w_s = 1.4m$. When w_s is further reduced than these two limiting values, the two work rolls will touch each other. This reduces the cantilever bending effects on the strip edge and therefore results in a reduction of the magnitude of the maximum shape.

The corresponding gain matrices for the seven different widths are denoted by G_m^1 to G_m^7 in section 6.6. It is seen from these matrices that the gain elements reduce in magnitude as w_s decreases. In table 6.3 the first seven rows represent the percentage change in diagonal elements of G_m^1 to G_m^7 compared with G_m^0 which is the gain matrix when $w_s = 1.4m$. The details of RUN numbers are given in table 6.2. The overall percent change is the average change in diagonal elements. This overall percent change is just an indication showing how the gain matrices vary compared to G_m^0. RUNS 1 to 3 have widths wider than for RUN 0 ($w_s = 1.4m$) while RUNS 4 to 7 have narrower widths. It is seen from table 6.3 that the overall percent change decreases with w_s.

When using narrower widths the region of work roll which is in contact with the strip is less and therefore the roll force $p(x)$ must be larger to keep the force balance in the mill cluster. The interference between strip and work roll must be higher for larger roll force and hence the output thickness becomes smaller. From eq.(3.18) it is seen that the output stress is smaller for smaller output thicknesses and hence the gains must decrease with the strip width.

6.4. The effect on gains of changing other variables.

In the previous section the effect of the variation of strip width was discussed. The matrices G_m^8 to G_m^{22} are the gains of the mill for the cases in which the strip width is fixed at $w_s = 1.4m$. All these cases have the mill schedule used for RUN 0 (see table 6.1) with one change in at least one of the input data. These cases will be discussed here.

The test for RUN 8 is to see the effect on yield stress of the material being rolled. The yield stress curve (see Appendix 7) is increased by a factor of 0.5 so that the material rolled is stiffer. It is seen from table 6.3 that the overall gain is reduced by 7% for this case. When rolling harder materials the rolling force must be greater to obtain the same reduction. Higher rolling forces produce more interference between strip and work roll, and hence the change in output thickness will be more. This results in a smaller output stress profile and therefore this case will have smaller gains.

The RUNS 9 and 10 are carried out to see the effect of changing the mean reduction. For RUN 9 the input mean thickness is increased by 2.5 times to 6mm with a reduction of 20% compared to 15% for RUN 0. For RUN 10 the mean input thickness is adjusted to 1.5m with a reduction of 13%. That is, for the first case the reduction

is increased by 5% and for the second case this is reduced by about 2% which is roughly half the value of the previous case. When the overall gain change figures are inspected it is seen that for case one it is -40% and for the second case it is about +21%, which is roughly half of the previous figure. From these two results it is seen that the gains of the mill obey approximately a linear relationship with the percentage reduction.

The RUNS 11 to 16 correspond to changes in roll diameters. RUNS 11 to 12 show the effect of work roll diameters, RUNS 13 to 14 the effect of first intermediate roll diameters and finally RUNS 15 to 16 the effect of second intermediate roll diameters. In each case the diameters are changed by $\pm$ 15% and the changes of the overall gain are given in table 6.3. When the work roll diameter is reduced the overall change in gain is + 7.9% and this figure is -6.7% for the bigger work roll. For the first and second intermediate rolls these figures are + 2.3% and - 2.8%, and + 8.8% and - 8.0% respectively. When the diameter of a roll is increased the deflection caused by a given mill loading will decrease, that is, the roll will become stiffer. In other words, the bending effects will decrease. When the roll diameters are changed by the same amount ($\pm$ 15%) the figures show that the corresponding changes in gain also have the same order of magnitude, except for the case of the first intermediate roll. This may

be due to the fact that the first intermediate rolls are furnished with tapered ends, which will produce a less bending effect than a roll without tapered ends. The function of first and second intermediate rolls and back-up rolls is to prevent excessive bending of the work rolls which assist the elimination of shape and gauge defects. Also the roll separating force for a given reduction increases with roll radius. The effect of increasing roll diameters is therefore to increase the roll force which in turn reduces the gains of the mill. Conversely if smaller rolls are used the corresponding gains will decrease. increase

For RUN 17 the mill cluster angles θ_1 to θ_6 are changed as given in table 6.2. For this RUN the overall gain is increased by 9.8%. The change in cluster angles will disturb the mill cluster configuration and the vertical and horizontal components of roll separating forces will therefore differ. This will change the roll force and hence the change in gain follows.

The RUNS 18 and 19 show the effect of changing the output tensile force. In RUN 18 the tension is decreased by 50% to 95294N and for RUN 19 it is increased to 285882N again by 50%. The overall gain change figure for these two cases are + 2.4% and - 3.1% respectively. When rolling metal strips higher reductions or smaller output thicknesses can be obtained for higher output tensions, assuming that the roll force remains the same.

Smaller output thicknesses mean smaller stress profiles and hence mill gains will be smaller for higher tensions.

The first intermediate rolls are moved by 100mm for RUN 20, and there is an increase of 6.2% in the overall gains of the mill. The edges of the tapered wedge positions (vertical planes e_1 and e_2 in fig.4.6) of the first intermediate rolls are set at the vertical plane passing through the strip edges for RUN 0. That is, along the strip width, first intermediate rolls have a flat surface. This is not the case for RUN 20, where these rolls are pushed in by 100mm, so that the roll surface is no longer flat. That is, near the strip edge area first intermediate rolls have a smaller diameter. This increases the bending effect of this roll thus increasing the gain.

RUN 21 is carried out to see the effect of increase in the roll rack movement. Here all racks are moved, individually one at a time, by twice the distance as for RUN 0. If each element of gain matrices G_m^0 and G_m^{21} is compared it is seen that the change is quite small. The overall gain changes by + 0.3% and theoretically these two matrices must be the same. The variation is due to numerical errors.

RUN 22 is a special case where no comparison is made with matrix G_m^0. This is to see the effect of

moving all racks at the same time by 6mm. As seen from the gain matrix G_m^{22} all elements are very small compared to other cases considered. The shape profile for this case is shown in fig.6.23 and the variation is hardly noticable. The effect of moving all racks by the same amount is to move the whole of the back-up roll vertically. This will not produce an appreciable change in the shape profile as the incoming strip profile is rectangular, and there will be no transverse variations in the reduction. The same effect can be produced by moving the two side screwdowns by the same amount and hence the very small gain matrix results.

6.5. Shape control system diagonalisation using singular value decomposition.

One of the most important results obtained from the static model is the mill gain matrix which is a square 8 X 8 matrix. Each column of this matrix represents the shape at eight zones of the strip due to each rack movement. The overall mill block diagram is shown in fig.5.3 and is an eighth order multivariable system and the only interaction comes from the mill gain matrix. It is convenient to represent the shape profile by a third order polynomial and to control the polynomial coefficients, rather than controlling the shape at eight zones directly (see section 5.4). By using a transformation matrix (see Appendix 8) it is possible to transform the eighth order

system into a fourth order system as explained in section 5.4. The block diagram of the transformed system is shown in fig.5.5. Here $G(s)$ is the transfer function matrix of the plant and is given by eq.(5.45). As seen from this equation $G(s)$ contains the static mill gain matrix G_m and therefore will be interactive. The transformed 4×4 plant transfer function $G_X(s)$ is given by eq.(5.50), which contains $G_{mX} = (X^T X)^{-1} X^T G_m X$.

Each transfer matrix for all twenty one RUNS considered are computed and presented in section 6.6 as 'Transformed gain matrix G_{mX}'. A quick glance at these reduced order matrices show that they are non-diagonal matrices. To design controls it is convenient if the system can be made diagonal by removing interactions. The singular value decomposition is used for this purpose and the orthogonal matrices U and V together with the diagonal matrix are computed. The diagonal form is obtained by computing $\Sigma = U^T G_{mX} V$ for each case. In section 6.6 the diagonal elements of Σ are presented under the heading 'Transpose of W vector is', and matrices U and V directly under these elements. The pre and post compensators can be chosen as V and U^T which are pure gain terms and can be implemented easily.

If these sets of U and V (for different schedules considered) are compared, it is seen that the

variation is quite small and they are remarkably similar. This is encouraging as it is possible to use one set of U and V instead of one set for each schedule. This set of U and V can be derived, for example, by taking the average of each element. This has to be investigated further. By doing this of course the interactions cannot be removed completely, but can be made small so that they can be ignored. Again this area has to be investigated further by considering more mill schedules.

MILL DATA.

Back-up-roll diameter	= 0.405 m
Second intermediate roll diameter	= 0.235 m
First intermediate roll diameter	= 0.137 m
Work roll diameter	= 0.09 m
Work roll crown(camber)	= 0.0508 mm
Second intermediate roll crown(camber)	= 0.0762 mm
First intermediate roll tapered end gradient	= 1 mm/m
Length of tapered end	= 0.355 m

Mill cluster angles (see fig. 2.4)

$\theta_1 = 41.69°$

$\theta_2 = 3.72°$

$\theta_3 = 22.56°$

$\theta_4 = 60.54°$

$\theta_5 = 41.04°$

$\theta_6 = 79.59°$

STRIP DATA.

Strip width	= 1.4 m
Input mean thickness	= 2.4 mm
Output mean thickness	= 2.05 mm
Percentage reduction	= 15 %
Input mean tension	= 134352.0 N
Output mean tension	= 190588.0 N
Input mean stress	= 55.98 MN/m^2
Output mean stress	= 92.9699 MN/m^2

Coefficient of friction between strip and work roll = 0.06

Incoming strip is rectangular. The tapered first intermediate roll is set up so that the end of wedge is in line with the edge of strip.

Table 6.1. Mill schedule for gain matrix G_m^0 (RUN 0).

- 145 -

RUN 1 to RUN 7 :- Effect of changing the strip width.

RUN 1 :- Strip width = 1.7 m

RUN 2 :- Strip width = 1.6 m

RUN 3 :- Strip width = 1.5 m

RUN 4 :- Strip width = 1.3 m

RUN 5 :- Strip width = 1.2 m

RUN 6 :- Strip width = 1.1 m

RUN 7 :- Strip width = 1.0 m

RUN 8 to RUN 22 :- Effect of changing other variables.

RUN 8 :- Yield stress increased by 50 %.

RUN 9 :- Input mean thickness = 6 mm, output mean
thickness = 4.8mm, mean reduction = 20 %.

RUN 10 :- Input mean thickness = 1.5 mm, output mean
thicknes = 1.3 mm, mean reduction = 13 %.

RUN 11 :- Work roll diameter reduced by 15 % to 0.076 m.

RUN 12 :- Work roll diameter increased by 15 % to 0.104 m.

RUN 13 :- First intermediate roll diameter reduced by 15 %
to 0.116 m.

RUN 14 :- First intermediate roll diameter increased by 15 %
to 0.158 m.

RUN 15 :- Second intermediate roll diameter reduced by 15 %
to 0.198 m.

RUN 16 :- Second intermediate roll diameter increased by 15 %
to 0,272 m.

Table 6.2 cond.

RUN 17 :- Mill cluster angle changes and new angles are

$$\theta_1 = 40.99^\circ$$
$$\theta_2 = 2.69^\circ$$
$$\theta_3 = 23.63^\circ$$
$$\theta_4 = 59.43^\circ$$
$$\theta_5 = 37.89^\circ$$
$$\theta_6 = 79.05^\circ$$

RUN 18 :- Output tension reduced by 50 % to 95294.0 N.

RUN 19 :- Output tension increased by 50 % to 285882.0 N.

RUN 20 :- Wedge position moved in by 100 mm.

RUN 21 :- Each actuator moved individually by 12 mm.

Run 22 :- All actuators moved together by 6 mm.

All RUNS given above have the mill schedule used for RUN 0 (Table 6.1), and the changes in input data in each particular RUN are given against that RUN number.

Table 6.2. Input data for different cases considered.

	% Change in Shape Gain								Overall
	Rack 1	Rack 2	Rack 3	Rack 4	Rack 5	Rack 6	Rack 7	Rack 8	% change
RUN 1	7.7	23.9	10.6	7.4	5.4	10.1	20.4	-29.8	7.0
RUN 2	13.0	18.6	7.2	5.5	4.5	6.5	17.5	-17.5	6.9
RUN 3	8.5	6.7	4.9	3.0	2.7	4.9	7.2	-7.0	3.9
RUN 4	-15.3	-9.5	-6.1	-3.4	-3.0	-5.8	-8.2	-1.2	-6.6
RUN 5	-29.0	-13.8	-16.2	-8.7	-8.6	-14.9	-7.5	-7.1	-13.2
RUN 6	-41.4	-25.0	-28.5	-16.7	-16.0	-24.9	-10.5	-15.1	-22.3
RUN 7	-47.2	-31.1	-38.9	-24.1	-24.3	-32.3	-5.5	-24.8	-28.5
RUN 8	2.2	-14.7	-4.1	-6.0	-6.2	-4.5	-6.0	-16.4	-7.0
RUN 9	-29.9	-50.6	-42.6	-40.5	-40.5	-37.7	-30.7	-50.9	-40.4
RUN 10	7.9	33.9	23.6	22.1	21.7	19.1	27.4	17.1	21.6
RUN 11	3.0	11.4	6.8	8.2	7.8	8.7	9.8	7.2	7.9
RUN 12	-4.0	-9.1	-6.0	-6.7	-6.8	-7.7	-6.9	-6.5	-6.7
RUN 13	0.6	2.2	2.8	3.6	3.6	3.4	2.0	-0.3	2.3
RUN 14	-0.9	-2.5	-3.7	-4.2	-4.3	-4.4	-1.6	-0.3	-2.8
RUN 15	1.2	2.6	15.7	14.9	15.1	14.5	3.1	3.2	8.8
RUN 16	-3.7	-1.3	-14.5	-12.5	-13.0	-13.6	-1.6	-4.2	-8.0
RUN 17	10.0	9.1	9.7	10.2	9.5	10.0	9.1	10.6	9.8
RUN 18	2.6	1.8	3.0	2.3	2.4	2.9	2.1	1.8	2.4
RUN 19	-4.7	-3.4	-2.6	-2.7	-2.8	-3.2	-3.0	-2.5	-3.1
RUN 20	-0.7	9.6	3.0	6.5	7.1	7.2	9.8	7.2	6.3
RUN 21	4.4	2.0	0.9	1.5	0.9	-1.5	-5.0	-1.1	0.3

Table 6.3. Percent changes in gain for RUNS 1 to 21.

6.6. Gain matrices for different scedules.

GAIN MATRIX G_m^0 FOR RUN 0

2.423	3.262	0.453	-1.211	-1.645	-1.414	-1.095	-1.171
0.405	1.520	1.631	0.321	-0.915	-1.279	-1.057	-1.110
-0.447	0.145	1.588	1.324	-0.104	-1.119	-1.178	-1.221
-0.616	-0.710	0.633	1.587	1.024	-0.377	-1.122	-1.169
-0.515	-1.025	-0.437	0.863	1.618	0.734	-0.758	-0.816
-0.423	-1.082	-1.091	-0.234	1.182	1.603	0.180	0.143
-0.341	-1.003	-1.255	-0.969	0.147	1.578	1.630	1.661
-0.485	-1.109	-1.523	-1.680	-1.308	0.275	3.399	3.679

SUM OF COLUMN ELEMENTS

-0.000	-0.002	-0.003	0.001	-0.001	0.001	-0.001	-0.005

TRANSFORMED GAIN MATRIX G_{mx}^0

7.493	-1.353	-3.038	-0.997
-0.367	4.848	-0.369	-2.212
0.365	0.234	2.004	0.112
0.135	0.165	0.193	0.407

TRANSPOSE OF W VECTOR IS

8.325	5.271	2.014	0.422

MATRIX U IS

-0.988	0.145	-0.060	-0.004
0.146	0.989	-0.015	0.007
0.057	-0.022	-0.989	-0.131
0.003	-0.009	-0.131	0.991

MATRIX V IS

-0.893	0.135	-0.409	0.131
0.247	0.871	-0.121	0.406
0.368	-0.161	-0.903	-0.149
0.080	-0.443	-0.035	0.892

GAIN MATRIX G_m^1 FOR RUN 1

2.610	2.596	-0.315	-1.135	-0.981	-0.779	-0.809	-0.849
0.847	1.883	1.243	-0.180	-1.089	-1.268	-1.234	-1.254
-0.429	0.447	1.756	1.189	-0.243	-1.085	-1.256	-1.260
-0.750	-0.663	0.831	1.704	1.031	-0.343	-1.194	-1.220
-0.673	-1.108	-0.412	0.861	1.706	0.969	-0.630	-0.712
-0.606	-1.183	-1.045	-0.352	0.998	1.765	0.654	0.604
-0.616	-1.177	-1.208	-1.083	-0.354	1.046	1.961	2.070
-0.447	-0.841	-0.812	-0.960	-1.026	-0.266	2.464	2.581

SUM OF COLUMN ELEMENTS

| -0.064 | -0.046 | 0.039 | 0.044 | 0.043 | 0.038 | -0.042 | -0.041 |

TRANSFORMED GAIN MATRIX G_{mx}^1

6.856	-0.795	-1.774	-0.683
0.032	4.572	-0.054	-1.695
-0.937	0.666	2.443	0.340
0.246	-0.755	0.383	0.862

TRANSPOSE OF W VECTOR IS

| 7.373 | 4.968 | 2.171 | 0.459 |

MATRIX U IS

-0.964	0.109	-0.226	-0.063
0.091	0.972	0.023	0.215
0.241	0.051	-0.940	-0.234
-0.025	-0.201	-0.253	0.946

MATRIX V IS

-0.929	0.137	-0.337	0.064
0.185	0.914	-0.070	0.353
0.310	-0.040	-0.918	-0.241
0.077	-0.378	-0.194	0.902

GAIN MATRIX G^2_m FOR RUN 2

2.739	2.951	-0.121	-1.216	-1.172	-0.968	-0.924	-0.989
0.726	1.802	1.394	-0.002	-1.036	-1.269	-1.178	-1.208
-0.471	0.318	1.702	1.235	-0.228	-1.113	-1.259	-1.274
-0.731	-0.701	0.765	1.673	1.028	-0.343	-1.190	-1.220
-0.638	-1.095	-0.420	0.869	1.690	0.896	-0.701	-0.771
-0.567	-1.176	-1.081	-0.329	1.063	1.706	0.478	0.432
-0.536	-1.123	-1.217	-1.045	-0.194	1.225	1.914	1.990
-0.524	-0.977	-1.023	-1.187	-1.155	-0.138	2.860	3.036

SUM OF COLUMN ELEMENTS

-0.002	-0.002	-0.003	-0.002	-0.006	-0.002	-0.001	-0.004

TRANSFORMED GAIN MATRIX G^2_{mx}

7.274	-0.961	-2.072	-0.793
-0.082	4.768	-0.142	-1.848
-0.445	0.564	2.395	0.296
0.228	-0.432	0.354	0.733

TRANSPOSE OF W VECTOR IS

7.789	5.128	2.237	0.463

MATRIX U IS

-0.980	0.116	-0.156	-0.036
0.108	0.984	0.023	0.140
0.165	0.034	-0.963	-0.209
-0.017	-0.130	-0.217	0.967

MATRIX V IS

-0.926	0.140	-0.340	0.080
0.200	0.908	-0.085	0.358
0.303	-0.067	-0.922	-0.221
0.079	-0.389	-0.161	0.903

GAIN MATRIX G_m^3 FOR RUN 3

2.629	3.175	0.163	-1.242	-1.433	-1.206	-1.040	-1.113
0.515	1.622	1.536	0.208	-0.957	-1.271	-1.128	-1.176
-0.477	0.210	1.665	1.317	-0.148	-1.111	-1.218	-1.255
-0.683	-0.712	0.713	1.635	1.025	-0.366	-1.164	-1.209
-0.582	-1.069	-0.433	0.858	1.661	0.826	-0.740	-0.804
-0.496	-1.133	-1.084	-0.271	1.150	1.681	0.308	0.269
-0.442	-1.076	-1.242	-1.000	0.001	1.436	1.747	1.798
-0.525	-1.082	-1.279	-1.435	-1.234	0.052	3.176	3.421

SUM OF COLUMN ELEMENTS

-0.062	-0.065	0.039	0.069	0.065	0.037	-0.058	-0.067

TRANSFORMED GAIN MATRIX G_{mx}^3

7.446	-1.169	-2.581	-0.919
-0.229	4.856	-0.268	-2.043
0.034	0.411	2.232	0.173
0.190	-0.075	0.259	0.549

TRANSPOSE OF W VECTOR IS

8.099	5.229	2.158	0.449

MATRIX U IS

-0.986	0.130	-0.099	-0.016
0.129	0.989	0.012	0.060
0.102	0.008	-0.981	-0.161
-0.007	-0.057	-0.162	0.985

MATRIX V IS

-0.910	0.140	-0.374	0.109
0.225	0.891	-0.101	0.380
0.338	-0.114	-0.918	-0.174
0.081	-0.415	-0.089	0.901

GAIN MATRIX G_m^4 FOR RUN 4

```
 2.051   3.129   0.801  -1.123  -1.834  -1.640  -1.144  -1.223
 0.292   1.376   1.747   0.502  -0.815  -1.256  -0.946  -1.008
-0.412   0.087   1.490   1.340  -0.046  -1.117  -1.116  -1.170
-0.533  -0.665   0.560   1.532   1.003  -0.393  -1.055  -1.111
-0.436  -0.956  -0.449   0.851   1.570   0.659  -0.734  -0.789
-0.345  -1.010  -1.081  -0.174   1.228   1.510   0.067   0.041
-0.222  -0.898  -1.231  -0.870   0.370   1.741   1.496   1.538
-0.455  -1.138  -1.809  -1.971  -1.388   0.522   3.348   3.634
```

SUM OF COLUMN ELEMENTS

```
-0.060  -0.075   0.027   0.087   0.089   0.026  -0.084  -0.086
```

TRANSFORMED GAIN MATRIX G_{mx}^4

```
 7.304  -1.551  -3.551  -1.039
-0.479   4.700  -0.457  -2.346
 0.575   0.039   1.700   0.081
 0.098   0.391   0.133   0.207
```

TRANSPOSE OF W VECTOR IS

```
 8.400   5.205   1.774   0.354
```

MATRIX U IS

```
-0.987   0.154  -0.035   0.0002
 0.155   0.985  -0.045  -0.048
 0.026  -0.056  -0.991  -0.116
 0.011   0.041  -0.119   0.991
```

MATRIX V IS

```
-0.865   0.121  -0.461   0.155
 0.270   0.846  -0.138   0.437
 0.414  -0.209  -0.876  -0.128
 0.079  -0.474   0.022   0.876
```

- 153 -

GAIN MATRIX G_m^5 FOR RUN 5

```
 1.721    3.005    1.301   -1.006   -1.963   -1.819   -1.138   -1.206
 0.251    1.310    1.784    0.562   -0.771   -1.246   -0.810   -0.869
-0.357    0.073    1.330    1.298   -0.024   -1.134   -1.051   -1.103
-0.458   -0.635    0.408    1.448    0.957   -0.434   -0.988   -1.045
-0.375   -0.909   -0.503    0.831    1.479    0.525   -0.690   -0.750
-0.282   -0.955   -1.100   -0.137    1.214    1.364    0.049    0.014
-0.143   -0.818   -1.245   -0.810    0.519    1.858    1.507    1.540
-0.357   -1.071   -1.976   -2.186   -1.411    0.887    3.118    3.415
```

SUM OF COLUMN ELEMENTS

```
-0.002   -0.002    0.000    0.000    0.000    0.000   -0.002   -0.004
```

TRANSFORMED GAIN MATRIX G_{mx}^5

```
 7.075   -1.630   -4.053   -1.062
-0.451    4.387   -0.537   -2.425
 0.639   -0.097    1.334    0.067
 0.180    0.472    0.072    0.074
```

TRANSPOSE OF W VECTOR IS

```
 8.424    5.018    1.456    0.310
```

MATRIX U IS

```
-0.992    0.120   -0.016   -0.009
 0.122    0.987   -0.059   -0.079
 0.008   -0.072   -0.986   -0.143
 0.002    0.070   -0.149    0.986
```

MATRIX V IS

```
-0.839    0.075   -0.511    0.166
 0.255    0.832   -0.144    0.470
 0.471   -0.221   -0.844   -0.122
 0.090   -0.502    0.058    0.857
```

GAIN MATRIX G_m^6 FOR RUN 6

1.420	2.848	1.839	-0.731	-1.974	-1.909	-1.092	-1.156
0.158	1.140	1.742	0.637	-0.744	-1.251	-0.698	-0.762
-0.327	0.021	1.135	1.243	-0.037	-1.166	-1.000	-1.064
-0.398	-0.599	0.261	1.321	0.847	-0.525	-0.944	-1.013
-0.328	-0.864	-0.579	0.750	1.359	0.374	-0.651	-0.717
-0.240	-0.907	-1.125	-0.114	1.200	1.203	0.017	-0.016
-0.091	-0.758	-1.280	-0.755	0.688	1.955	1.458	1.510
-0.244	-0.957	-1.994	-2.249	-1.232	1.323	2.823	3.122

SUM OF COLUMN ELEMENTS

-0.051	-0.076	0.000	0.102	0.105	0.003	-0.089	-0.098

TRANSFORMED GAIN MATRIX G_{mx}^6

6.728	-1.640	-4.498	-1.069
-0.425	3.857	-0.604	-2.366
0.650	-0.199	0.968	0.061
0.290	0.456	-0.005	-0.042

TRANSPOSE OF W VECTOR IS

8.348	4.585	1.138	0.254

MATRIX U IS

-0.996	0.078	0.003	-0.023
0.080	0.989	-0.069	-0.101
-0.006	-0.088	-0.976	-0.195
-0.016	0.087	-0.203	0.975

MATRIX V IS

-0.808	0.016	-0.561	0.176
0.232	0.816	-0.150	0.506
0.530	-0.226	-0.808	-0.118
0.104	-0.530	0.095	0.835

GAIN MATRIX G_m^7 FOR RUN 7

1.278	2.837	2.283	-0.531	-2.026	-2.018	-1.119	-1.162
0.119	1.047	1.664	0.629	-0.755	-1.252	-0.591	-0.638
-0.302	-0.013	0.969	1.185	-0.019	-1.159	-0.913	-0.971
-0.367	-0.593	0.129	1.204	0.761	-0.605	-0.893	-0.963
-0.301	-0.828	-0.618	0.693	1.225	0.205	-0.599	-0.674
-0.195	-0.839	-1.107	-0.073	1.171	1.085	0.097	0.051
-0.060	-0.703	-1.307	-0.741	0.775	2.060	1.540	1.592
-0.168	-0.906	-2.013	-2.367	-1.132	1.684	2.479	2.766

SUM OF COLUMN ELEMENTS

0.003	-0.000	-0.000	-0.000	-0.000	-0.001	0.001	0.000

TRANSFORMED GAIN MATRIX G_{mx}^7

6.538	-1.595	-4.862	-1.050
-0.274	3.427	-0.617	-2.338
0.667	-0.248	0.616	0.045
0.481	0.404	-0.082	-0.126

TRANSPOSE OF W VECTOR IS

8.383	4.231	0.893	0.217

MATRIX U IS

-0.998	-0.031	0.036	0.035
0.033	-0.991	-0.050	0.116
-0.025	0.084	-0.942	0.321
-0.042	-0.095	-0.327	-0.938

MATRIX V IS

-0.784	0.018	-0.598	-0.162
0.202	-0.805	-0.143	-0.538
0.575	0.195	-0.783	0.132
0.116	0.559	0.086	-0.816

GAIN MATRIX G_m^8 FOR RUN 8

2.475	3.068	0.286	-1.269	-1.685	-1.461	-1.118	-1.191
0.287	1.295	1.496	0.318	-0.797	-1.113	-0.886	-0.936
-0.467	0.126	1.522	1.275	-0.041	-0.973	-0.998	-1.030
-0.577	-0.613	0.625	1.492	0.971	-0.317	-0.962	-0.994
-0.480	-0.907	-0.379	0.817	1.518	0.710	-0.630	-0.671
-0.400	-0.966	-0.966	-0.174	1.134	1.530	0.229	0.201
-0.319	-0.899	-1.101	-0.831	0.197	1.515	1.531	1.548
-0.519	-1.105	-1.484	-1.625	-1.299	0.108	2.832	3.075

SUM OF COLUMN ELEMENTS

-0.000	-0.001	-0.001	0.002	-0.002	-0.002	-0.003	0.001

TRANSFORMED GAIN MATRIX G_{mx}^8

6.851	-1.040	-2.740	-0.902
-0.078	4.605	-0.249	-2.066
0.415	0.350	1.886	0.107
0.307	0.290	0.185	0.331

TRANSPOSE OF W VECTOR IS

7.534	5.033	1.951	0.414

MATRIX U IS

-0.994	0.091	-0.046	-0.027
0.089	0.995	0.039	-0.019
0.053	0.030	-0.981	-0.179
-0.016	0.027	-0.180	0.983

MATRIX V IS

-0.902	0.112	-0.402	0.101
0.194	0.895	-0.086	0.391
0.371	-0.086	-0.905	-0.185
0.094	-0.422	-0.104	0.895

- 157 -

GAIN MATRIX G_m^9 FOR RUN 9

```
 1.698    2.032    0.449   -0.695   -1.139   -1.083   -0.814   -0.858
 0.228    0.750    0.958    0.288   -0.427   -0.701   -0.560   -0.604
-0.344   -0.023    0.910    0.860    0.095   -0.572   -0.687   -0.735
-0.409   -0.417    0.361    0.944    0.710   -0.082   -0.616   -0.671
-0.337   -0.564   -0.272    0.466    0.962    0.567   -0.323   -0.379
-0.282   -0.591   -0.663   -0.185    0.640    0.998    0.267    0.249
-0.202   -0.517   -0.726   -0.561    0.078    0.951    1.128    1.193
-0.350   -0.665   -1.014   -1.116   -0.919   -0.079    1.603    1.805
```

SUM OF COLUMN ELEMENTS

```
-0.000   -0.000    0.002    0.000    0.000   -0.002   -0.002    0.000
```

TRANSFORMED GAIN MATRIX G_{mx}^9

```
 4.512   -0.900   -1.742   -0.408
 0.226    2.990   -0.357   -1.288
 0.224    0.363    1.069   -0.017
 0.346    0.122    0.098    0.144
```

TRANSPOSE OF W VECTOR IS

```
 4.951    3.290    1.126    0.195
```

MATRIX U IS

```
-0.996    0.042   -0.035   -0.059
 0.039    0.995    0.082   -0.007
 0.051    0.077   -0.971   -0.219
-0.049    0.027   -0.220    0.973
```

MATRIX V IS

```
-0.907    0.135   -0.387    0.087
 0.207    0.902   -0.089    0.365
 0.357   -0.104   -0.912   -0.168
 0.070   -0.394   -0.094    0.911
```

GAIN MATRIX G_m^{10} FOR RUN 10

2.615	3.789	0.687	-1.334	-1.654	-1.389	-1.041	-1.110
0.470	2.034	2.231	0.258	-1.349	-1.819	-1.407	-1.426
-0.439	0.294	1.962	1.499	-0.378	-1.656	-1.532	-1.538
-0.711	-0.932	0.623	1.937	1.135	-0.746	-1.468	-1.484
-0.617	-1.372	-0.739	1.050	1.969	0.669	-1.007	-1.052
-0.503	-1.437	-1.568	-0.413	1.405	1.908	0.258	0.215
-0.447	-1.334	-1.745	-1.374	0.050	2.043	2.075	2.092
-0.362	-1.035	-1.447	-1.613	-1.174	0.995	4.126	4.308

SUM OF COLUMN ELEMENTS

0.004	0.006	0.004	0.010	0.004	0.004	0.002	0.004

TRANSFORMED GAIN MATRIX G_{mx}^{10}

8.953	-1.470	-4.142	-1.335
-0.652	5.243	-0.367	-2.686
-0.132	0.381	2.654	0.223
0.087	-0.191	0.350	0.766

TRANSPOSE OF W VECTOR IS

10.202	5.882	2.360	0.537

MATRIX U IS

-0.983	0.115	-0.138	0.002
0.121	0.987	-0.037	0.094
0.133	-0.040	-0.979	-0.145
0.010	-0.100	-0.140	0.984

MATRIX V IS

-0.872	0.065	-0.466	0.129
0.208	0.852	-0.144	0.457
0.430	-0.166	-0.872	-0.161
0.100	-0.491	-0.016	0.864

GAIN MATRIX G_m^{11} FOR RUN 11

```
2.496    3.443    0.612   -1.201   -1.675   -1.451   -1.093   -1.178
0.475    1.693    1.767    0.270   -1.065   -1.460   -1.199   -1.270
-0.459    0.161    1.695    1.413   -0.124   -1.223   -1.282   -1.347
-0.660   -0.785    0.641    1.717    1.101   -0.425   -1.230   -1.299
-0.554   -1.123   -0.518    0.922    1.744    0.781   -0.834   -0.903
-0.448   -1.174   -1.217   -0.285    1.256    1.741    0.216    0.188
-0.390   -1.119   -1.443   -1.146    0.053    1.655    1.789    1.867
-0.458   -1.095   -1.537   -1.688   -1.289    0.384    3.639    3.943
```

SUM OF COLUMN ELEMENTS

```
-0.001   -0.001   -0.001    0.002    0.001    0.001   -0.001   -0.001
```

TRANSFORMED GAIN MATRIX G_{mx}^{11}

```
8.056   -1.525   -3.323   -1.113
-0.424    5.090   -0.478   -2.351
0.225    0.281    2.144    0.114
0.123   -0.016    0.209    0.522
```

TRANSPOSE OF W VECTOR IS

```
8.997    5.563    2.081    0.449
```

MATRIX U IS

```
-0.987    0.138   -0.079   -0.001
0.140    0.988   -0.025    0.045
0.076   -0.030   -0.989   -0.118
0.001   -0.049   -0.117    0.991
```

MATRIX V IS

```
-0.888    0.122   -0.418    0.142
0.249    0.865   -0.135    0.412
0.375   -0.181   -0.897   -0.141
0.086   -0.450   -0.012    0.888
```

GAIN MATRIX G_m^{12} FOR RUN 12

2.325	3.065	0.353	-1.214	-1.602	-1.368	-1.073	-1.148
0.366	1.381	1.522	0.347	-0.793	-1.137	-0.937	-0.983
-0.436	0.130	1.492	1.247	-0.076	-1.038	-1.099	-1.132
-0.572	-0.634	0.619	1.481	0.962	-0.335	-1.035	-1.072
-0.477	-0.933	-0.376	0.820	1.507	0.695	-0.695	-0.744
-0.395	-0.995	-0.991	-0.188	1.109	1.479	0.140	0.108
-0.292	-0.894	-1.103	-0.820	0.223	1.517	1.516	1.532
-0.518	-1.120	-1.512	-1.677	-1.330	0.181	3.181	3.440

SUM OF COLUMN ELEMENTS

-0.000	-0.001	0.002	-0.003	0.001	-0.005	-0.002	0.000

TRANSFORMED GAIN MATRIX G_{mx}^{12}

7.025	-1.248	-2.787	-0.915
-0.352	4.635	-0.295	-2.091
0.455	0.190	1.873	0.111
0.138	0.290	0.171	0.305

TRANSPOSE OF W VECTOR IS

7.778	5.020	1.930	0.385

MATRIX U IS

-0.986	0.157	-0.043	-0.005
0.158	0.987	-0.010	-0.024
0.040	-0.019	-0.989	-0.133
0.004	0.022	-0.134	0.990

MATRIX V IS

-0.895	0.150	-0.398	0.127
0.253	0.872	-0.113	0.401
0.357	-0.152	-0.908	-0.152
0.074	-0.438	-0.047	0.894

GAIN MATRIX G_m^{13} FOR RUN 13

2.438	3.286	0.415	-1.247	-1.634	-1.413	-1.104	-1.180
0.392	1.553	1.688	0.296	-0.950	-1.286	-1.057	-1.110
-0.470	0.117	1.632	1.351	-0.140	-1.133	-1.164	-1.206
-0.612	-0.733	0.621	1.643	1.037	-0.406	-1.117	-1.164
-0.506	-1.030	-0.473	0.876	1.676	0.731	-0.776	-0.834
-0.421	-1.081	-1.112	-0.265	1.208	1.657	0.167	0.130
-0.336	-1.002	-1.261	-1.001	0.110	1.624	1.662	1.697
-0.488	-1.110	-1.510	-1.653	-1.305	0.224	3.388	3.668

SUM OF COLUMN ELEMENTS

-0.005	-0.001	0.001	0.000	0.000	-0.003	-0.002	-0.001

TRANSFORMED GAIN MATRIX G_{mx}^{13}

7.517	-1.351	-3.056	-1.031
-0.353	4.887	-0.389	-2.250
0.357	0.250	2.093	0.103
0.153	0.140	0.208	0.471

TRANSPOSE OF W VECTOR IS

8.356	5.331	2.093	0.472

MATRIX U IS

-0.988	0.138	-0.065	-0.004
0.139	0.989	-0.015	0.016
0.063	-0.022	-0.988	-0.135
0.001	-0.019	-0.134	0.990

MATRIX V IS

-0.892	0.128	-0.411	0.135
0.243	0.870	-0.122	0.409
0.370	-0.161	-0.902	-0.146
0.085	-0.446	-0.029	0.890

GAIN MATRIX G_m^{14} FOR RUN 14

2.400	3.228	0.501	-1.161	-1.647	-1.419	-1.082	-1.155
0.425	1.481	1.560	0.343	-0.871	-1.274	-1.063	-1.114
-0.418	0.171	1.529	1.288	-0.059	-1.091	-1.195	-1.233
-0.618	-0.676	0.643	1.520	1.003	-0.337	-1.123	-1.169
-0.529	-1.012	-0.388	0.845	1.548	0.732	-0.733	-0.790
-0.431	-1.080	-1.054	-0.194	1.147	1.532	0.196	0.160
-0.348	-1.005	-1.247	-0.931	0.175	1.515	1.602	1.633
-0.480	-1.107	-1.545	-1.711	-1.298	0.338	3.398	3.666

SUM OF COLUMN ELEMENTS

-0.001	-0.002	-0.002	-0.001	-0.003	-0.003	-0.001	-0.003

TRANSFORMED GAIN MATRIX G_{mx}^{14}

7.475	-1.367	-3.007	-0.965
-0.384	4.797	-0.342	-2.153
0.377	0.211	1.878	0.111
0.112	0.183	0.170	0.333

TRANSPOSE OF W VECTOR IS

8.299	5.191	1.901	0.364

MATRIX U IS

-0.987	0.151	-0.051	-0.002
0.152	0.988	-0.013	-0.002
0.048	-0.021	-0.990	-0.123
0.003	0.001	-0.123	0.992

MATRIX V IS

-0.893	0.143	-0.404	0.129
0.252	0.872	-0.119	0.401
0.362	-0.160	-0.905	-0.147
0.076	-0.438	-0.037	0.894

GAIN MATRIX G_m^{15} FOR RUN 15

2.452	3.354	0.297	-1.379	-1.601	-1.343	-1.100	-1.173
0.215	1.559	1.894	0.282	-1.068	-1.309	-1.000	-1.049
-0.542	0.081	1.836	1.487	-0.265	-1.276	-1.137	-1.175
-0.565	-0.793	0.605	1.822	1.079	-0.570	-1.166	-1.206
-0.419	-1.056	-0.637	0.915	1.862	0.722	-0.889	-0.944
-0.349	-1.062	-1.234	-0.364	1.343	1.835	0.082	0.044
-0.292	-0.962	-1.268	-1.078	0.114	1.804	1.679	1.711
-0.497	-1.120	-1.490	-1.683	-1.462	0.136	3.532	3.797

SUM OF COLUMN ELEMENTS

0.002	0.000	0.003	0.002	0.003	-0.001	0.002	0.003

TRANSFORMED GAIN MATRIX G_{mx}^{15}

7.526	-1.434	-3.232	-1.084
-0.496	5.056	-0.444	-2.477
0.402	0.228	2.487	0.160
0.212	0.197	0.301	0.624

TRANSPOSE OF W VECTOR IS

8.482	5.573	2.460	0.622

MATRIX U IS

-0.982	0.163	-0.090	-0.006
0.168	0.984	-0.049	0.020
0.081	-0.059	-0.981	-0.163
0.003	-0.029	-0.162	0.986

MATRIX V IS

-0.877	0.127	-0.440	0.139
0.268	0.847	-0.152	0.431
0.389	-0.201	-0.884	-0.159
0.078	-0.474	-0.015	0.876

GAIN MATRIX G_m^{16} FOR RUN 16

```
 2.333   3.096   0.583  -1.032  -1.603  -1.474  -1.116  -1.195
 0.570   1.499   1.408   0.301  -0.775  -1.211  -1.107  -1.175
-0.310   0.225   1.357   1.149   0.014  -0.943  -1.199  -1.259
-0.609  -0.614   0.614   1.388   0.962  -0.204  -1.058  -1.121
-0.587  -0.975  -0.283   0.819   1.408   0.726  -0.627  -0.688
-0.506  -1.085  -0.938  -0.128   1.018   1.384   0.276   0.253
-0.403  -1.035  -1.205  -0.861   0.140   1.367   1.603   1.662
-0.485  -1.108  -1.540  -1.638  -1.165   0.355   3.232   3.525
```

SUM OF COLUMN ELEMENTS

```
 0.002   0.003  -0.004  -0.001   0.001   0.000   0.003   0.000
```

TRANSFORMED GAIN MATRIX G_{mx}^{16}

```
 7.444  -1.323  -2.771  -0.926
-0.266   4.568  -0.332  -1.940
 0.286   0.200   1.533   0.079
 0.077   0.109   0.113   0.269
```

TRANSPOSE OF W VECTOR IS

```
 8.153   4.913   1.552   0.281
```

MATRIX U IS

```
-0.991   0.126  -0.038  -0.001
 0.126   0.991  -0.001   0.003
 0.038  -0.006  -0.994  -0.100
 0.001  -0.004  -0.100   0.994
```

MATRIX V IS

```
-0.907   0.131  -0.374   0.128
 0.232   0.887  -0.107   0.381
 0.338  -0.140  -0.919  -0.139
 0.082  -0.415  -0.042   0.904
```

GAIN MATRIX G_m^{17} FOR RUN 17

```
 2.664   3.589   0.542  -1.298  -1.781  -1.545  -1.198  -1.276
 0.441   1.658   1.779   0.325  -1.019  -1.425  -1.184  -1.246
-0.487   0.154   1.740   1.453  -0.098  -1.214  -1.290  -1.342
-0.675  -0.779   0.690   1.748   1.128  -0.401  -1.229  -1.286
-0.565  -1.121  -0.484   0.954   1.772   0.812  -0.830  -0.896
-0.464  -1.180  -1.197  -0.250   1.294   1.761   0.200   0.161
-0.389  -1.111  -1.399  -1.084   0.138   1.708   1.777   1.821
-0.523  -1.204  -1.668  -1.846  -1.437   0.303   3.755   4.068
```

SUM OF COLUMN ELEMENTS

```
 0.000   0.004   0.003   0.002  -0.003   0.001   0.000   0.003
```

TRANSFORMED GAIN MATRIX G_{mx}^{17}

```
 8.255  -1.533  -3.328  -1.091
-0.405   5.329  -0.430  -2.420
 0.409   0.240   2.182   0.122
 0.138   0.159   0.204   0.462
```

TRANSPOSE OF W VECTOR IS

```
 9.172   5.789   2.195   0.469
```

MATRIX U IS

```
-0.987   0.146  -0.058  -0.002
 0.148   0.988  -0.020   0.010
 0.054  -0.027  -0.990  -0.125
 0.003  -0.014  -0.125   0.992
```

MATRIX V IS

```
-0.892   0.138  -0.407   0.133
 0.252   0.869  -0.126   0.404
 0.364  -0.162  -0.904  -0.146
 0.071  -0.442  -0.030   0.892
```

GAIN MATRIX G_m^{18} FOR RUN 18

2.486	3.325	0.429	-1.246	-1.700	-1.468	-1.139	-1.216
0.424	1.547	1.675	0.348	-0.916	-1.292	-1.071	-1.125
-0.462	0.144	1.635	1.365	-0.086	-1.125	-1.194	-1.237
-0.629	-0.714	0.660	1.622	1.056	-0.366	-1.137	-1.184
-0.523	-1.033	-0.435	0.882	1.657	0.766	-0.769	-0.825
-0.429	-1.092	-1.100	-0.229	1.216	1.648	0.180	0.147
-0.342	-1.011	-1.264	-0.973	0.167	1.619	1.663	1.698
-0.526	-1.165	-1.597	-1.768	-1.391	0.215	3.466	3.744

SUM OF COLUMN ELEMENTS

-0.002	0.001	0.002	0.001	0.002	-0.002	-0.002	0.001

TRANSFORMED GAIN MATRIX G_{mx}^{18}

7.669	-1.409	-3.076	-0.996
-0.370	5.006	-0.376	-2.267
0.401	0.225	2.051	0.119
0.134	0.208	0.193	0.391

TRANSPOSE OF W VECTOR IS

8.512	5.430	2.073	0.425

MATRIX U IS

-0.986	0.151	-0.056	-0.003
0.152	0.988	-0.016	-0.002
0.053	-0.024	-0.989	-0.129
0.003	-0.001	-0.129	0.991

MATRIX V IS

-0.893	0.144	-0.405	0.130
0.254	0.870	-0.121	0.403
0.362	-0.163	-0.905	-0.148
0.075	-0.440	-0.036	0.893

GAIN MATRIX G_m^{19} FOR RUN 19

2.309	3.158	0.448	-1.167	-1.564	-1.346	-1.032	-1.106
0.392	1.468	1.590	0.296	-0.910	-1.260	-1.036	-1.087
-0.420	0.138	1.545	1.278	-0.121	-1.101	-1.154	-1.195
-0.592	-0.695	0.609	1.543	0.985	-0.370	-1.099	-1.145
-0.497	-1.000	-0.436	0.841	1.573	0.712	-0.746	-0.802
-0.408	-1.055	-1.075	-0.234	1.146	1.551	0.170	0.136
-0.332	-0.979	-1.239	-0.959	0.126	1.519	1.581	1.614
-0.449	-1.032	-1.442	-1.596	-1.232	0.297	3.318	3.586

SUM OF COLUMN ELEMENTS

0.000	0.003	0.000	0.002	0.003	0.002	0.001	-0.001

TRANSFORMED GAIN MATRIX G_{mx}^{19}

7.254	-1.321	-2.956	-0.988
-0.388	4.675	-0.377	-2.148
0.318	0.223	1.956	0.102
0.118	0.120	0.185	0.410

TRANSPOSE OF W VECTOR IS

8.074	5.092	1.946	0.407

MATRIX U IS

-0.987	0.146	-0.065	-0.002
0.147	0.988	-0.020	0.015
0.062	-0.027	-0.989	-0.123
0.003	-0.018	-0.123	0.992

MATRIX V IS

-0.891	0.130	-0.411	0.138
0.248	0.868	-0.125	0.410
0.369	-0.169	-0.902	-0.141
0.082	-0.447	-0.022	0.890

GAIN MATRIX G_m^{20} FOR RUN 20

2.440	3.202	0.488	-0.981	-1.254	-0.950	-0.605	-0.653
0.252	1.374	1.475	0.108	-1.181	-1.564	-1.275	-1.298
-0.448	0.136	1.540	1.234	-0.212	-1.215	-1.204	-1.217
-0.658	-0.771	0.553	1.484	0.905	-0.494	-1.163	-1.204
-0.563	-1.087	-0.506	0.769	1.503	0.604	-0.747	-0.827
-0.445	-1.108	-1.120	-0.291	1.096	1.488	0.299	0.248
-0.551	-1.227	-1.506	-1.268	-0.192	1.233	1.470	1.545
-0.024	-0.519	-0.917	-1.053	-0.663	0.899	3.229	3.412

SUM OF COLUMN ELEMENTS

0.002	-0.001	0.007	0.004	0.001	-0.000	0.002	0.005

TRANSFORMED GAIN MATRIX G_{mx}^{20}

7.435	-1.245	-3.060	-1.052
-0.176	4.736	-0.422	-2.160
0.270	0.369	1.954	0.082
0.320	0.047	0.168	0.425

TRANSPOSE OF W VECTOR IS

8.245	5.193	1.949	0.416

MATRIX U IS

-0.993	0.092	-0.065	-0.029
0.090	0.995	0.013	0.031
0.071	0.011	-0.984	-0.159
-0.020	-0.025	-0.161	0.986

MATRIX V IS

-0.895	0.097	-0.415	0.124
0.205	0.885	-0.115	0.400
0.380	-0.131	-0.900	-0.164
0.102	-0.434	-0.056	0.893

GAIN MATRIX G_m^{21} FOR RUN 21

2.529	3.319	0.491	-1.172	-1.509	-1.333	-1.051	-1.095
0.373	1.550	1.699	0.228	-1.006	-1.342	-1.087	-1.106
-0.463	0.167	1.601	1.277	-0.199	-1.178	-1.168	-1.180
-0.628	-0.724	0.590	1.610	0.971	-0.471	-1.119	-1.133
-0.530	-1.057	-0.499	0.894	1.632	0.642	-0.778	-0.799
-0.440	-1.114	-1.146	-0.239	1.213	1.578	0.143	0.128
-0.374	-1.049	-1.315	-1.019	0.120	1.601	1.547	1.551
-0.463	-1.088	-1.422	-1.577	-1.223	0.503	3.513	3.637

SUM OF COLUMN ELEMENTS

0.000	0.002	0.000	0.001	0.000	0.001	0.000	0.001

TRANSFORMED GAIN MATRIX G_{mx}^{21}

7.521	-1.190	-3.175	-0.981
-0.359	4.695	-0.250	-2.219
0.379	0.226	2.068	0.217
0.093	0.104	0.228	0.508

TRANSPOSE OF W VECTOR IS

8.364	5.152	2.079	0.463

MATRIX U IS

-0.990	0.121	-0.067	0.002
0.122	0.991	-0.023	0.026
0.063	-0.027	-0.987	-0.144
0.008	-0.031	-0.143	0.989

MATRIX V IS

-0.892	0.104	-0.426	0.101
0.211	0.874	-0.129	0.417
0.388	-0.135	-0.891	-0.189
0.085	-0.454	-0.081	0.882

GAIN MATRIX G_m^{22} FOR RUN 22

-0.015	-0.021	-0.028	-0.034	-0.040	-0.046	-0.052	-0.057
0.015	0.019	0.023	0.028	0.033	0.037	0.041	0.044
-0.001	-0.001	-0.000	0.000	0.001	0.002	0.002	0.003
0.002	0.003	0.004	0.005	0.007	0.008	0.009	0.010
0.002	0.003	0.004	0.005	0.007	0.008	0.009	0.010
-0.001	-0.001	-0.000	0.000	0.001	0.002	0.002	0.003
0.015	0.019	0.023	0.028	0.033	0.037	0.041	0.044
-0.015	-0.021	-0.028	-0.034	-0.040	-0.046	-0.052	-0.057

R1&8 6MM CHG W=1.4M

Fig. 6.1a.

R2&7 6MM CHG W=1.4M

Fig. 6.1b.

R3&6 6MM CHG W=1.4

Fig. 6.1c.

R4&5 6MM CHG W=1.4M
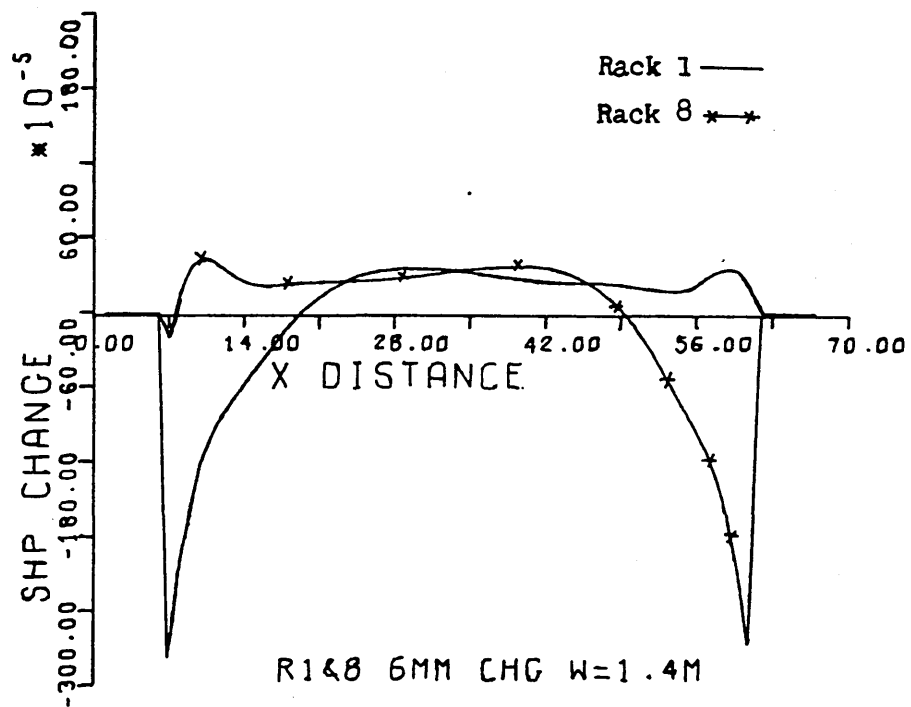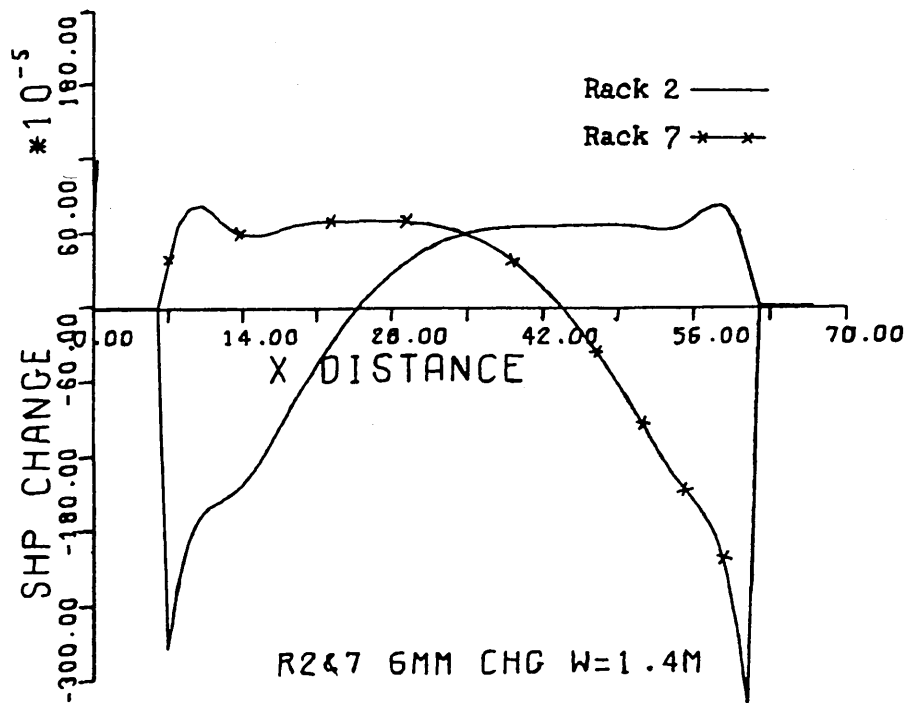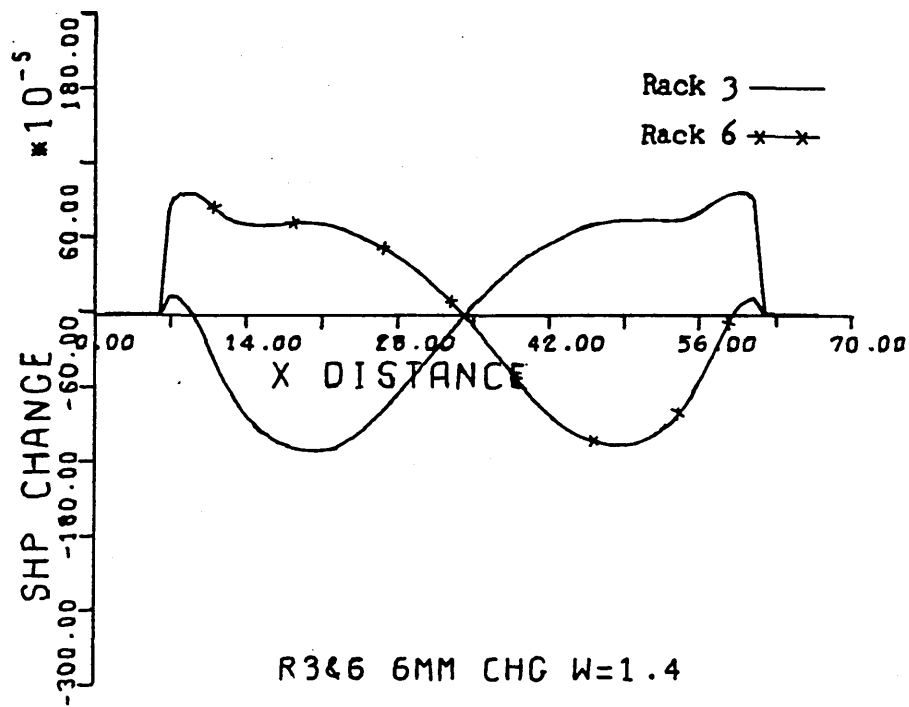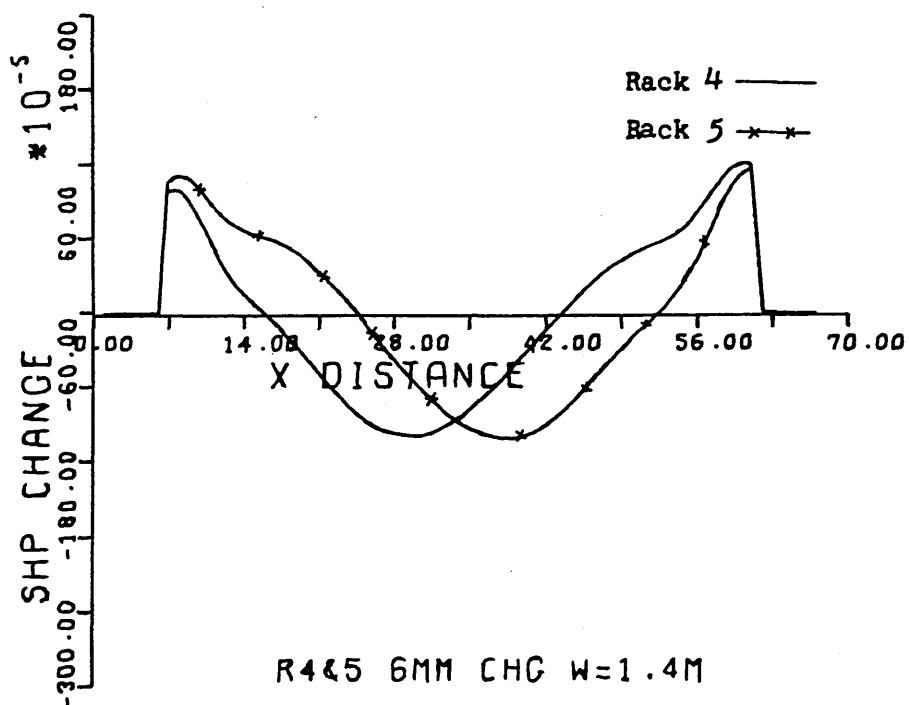
Fig. 6.1d.

Fig. 6.1. Shape profiles for RUN 0.
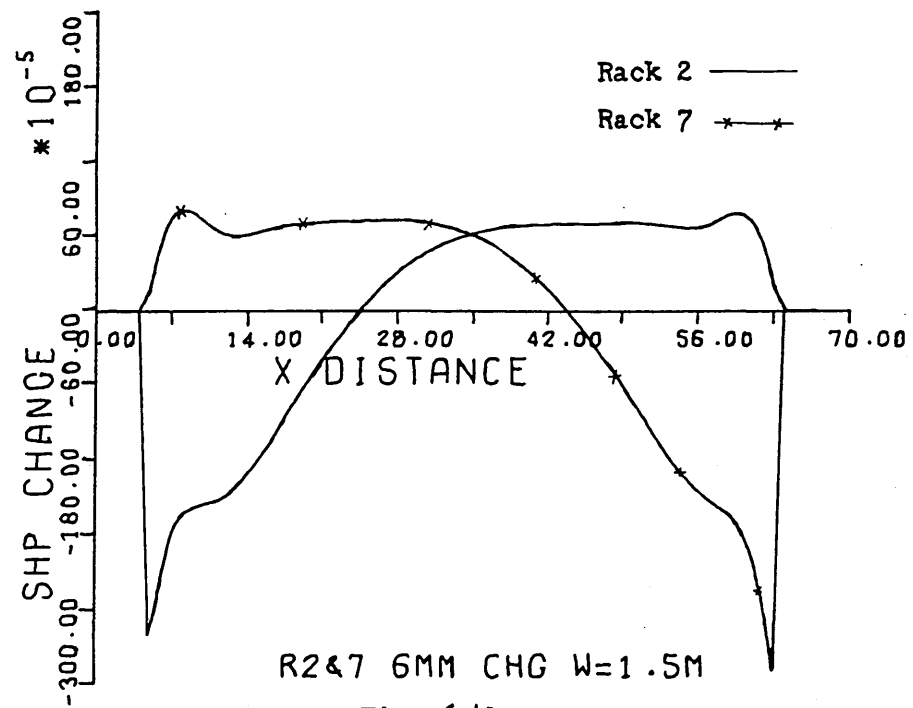
R1&8 6MM CHG W=1.7M

Fig. 6.2a.

R2&7 6MM CHG W=1.7M
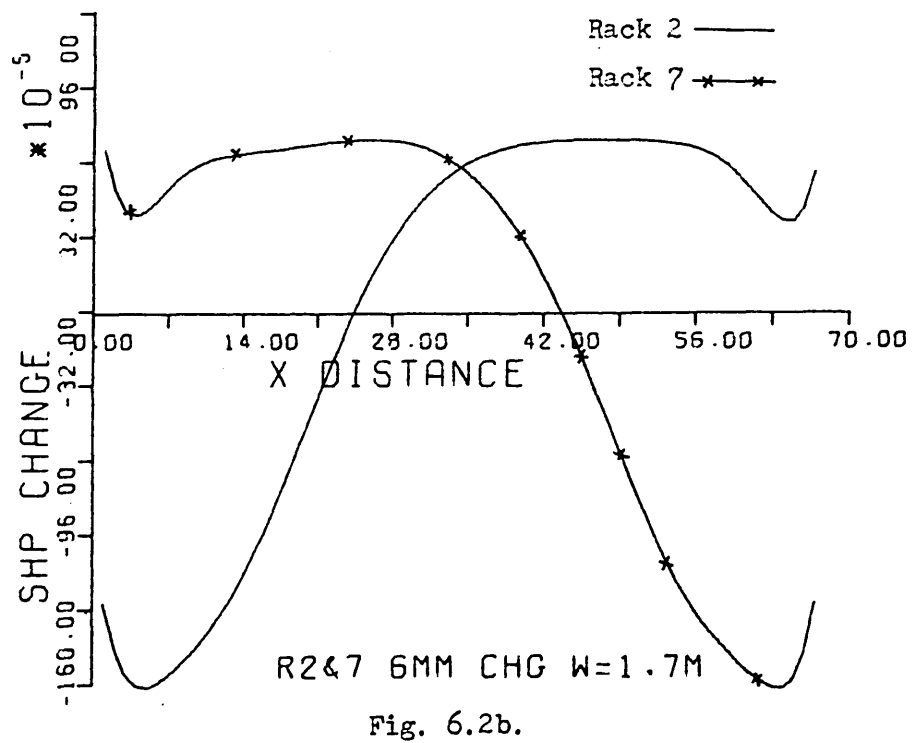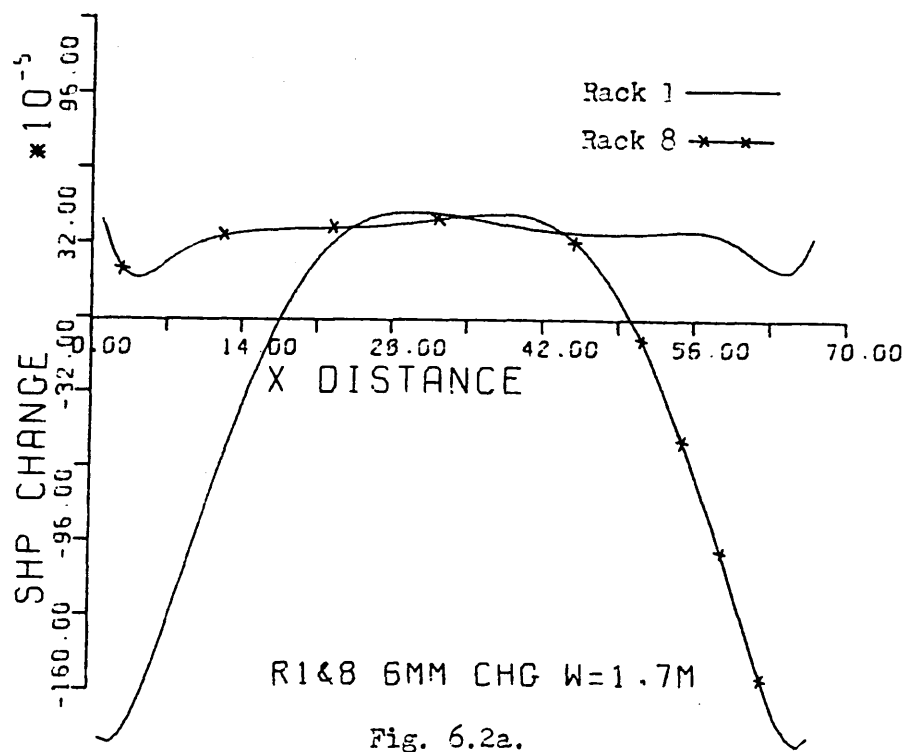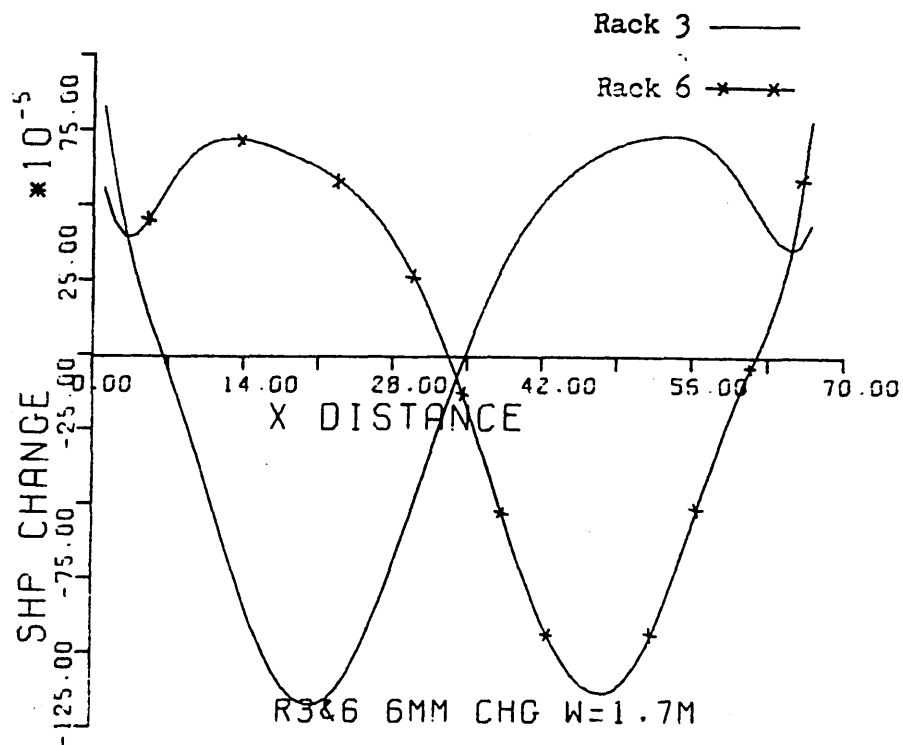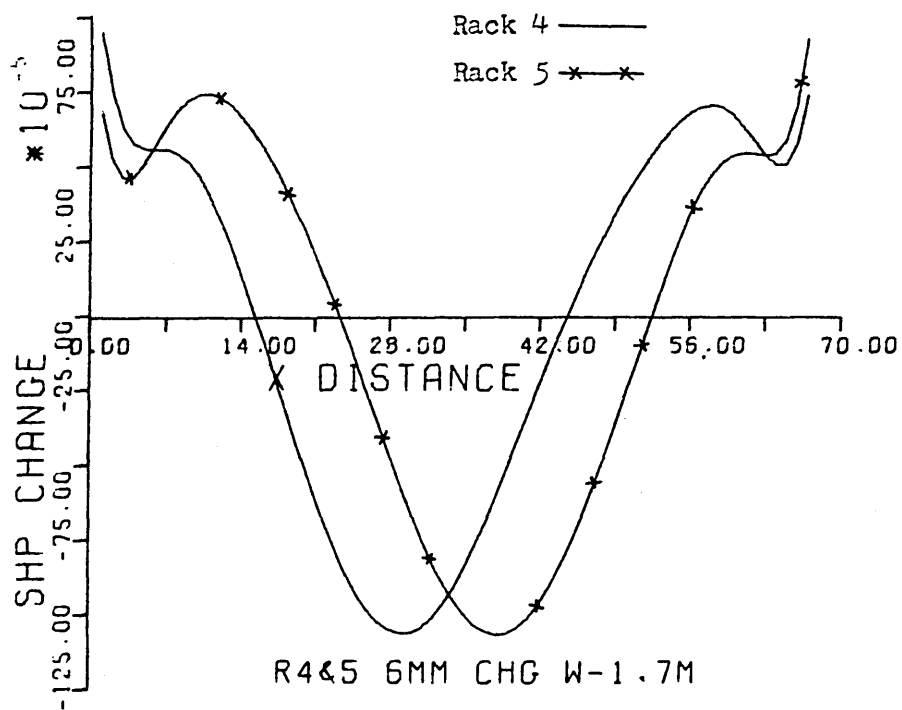
Fig. 6.2b.

Fig. 6.2c.

Fig. 6.2d.

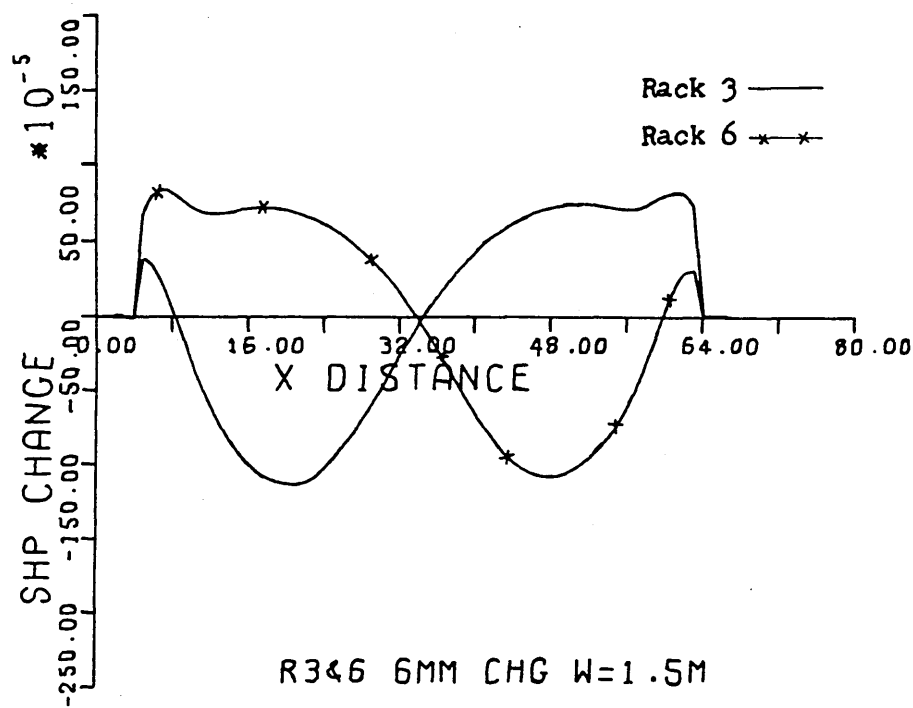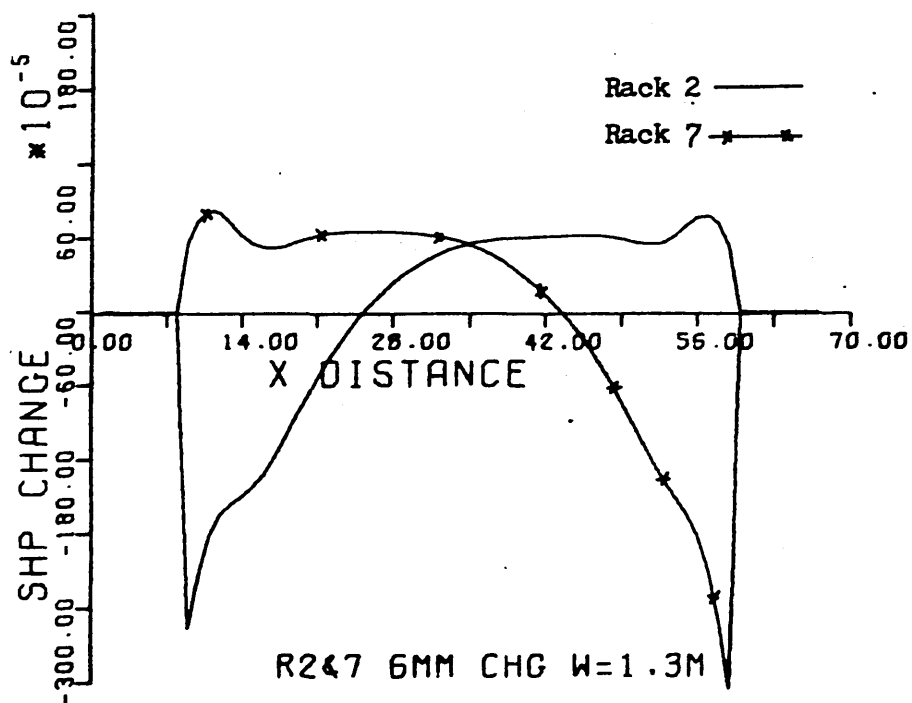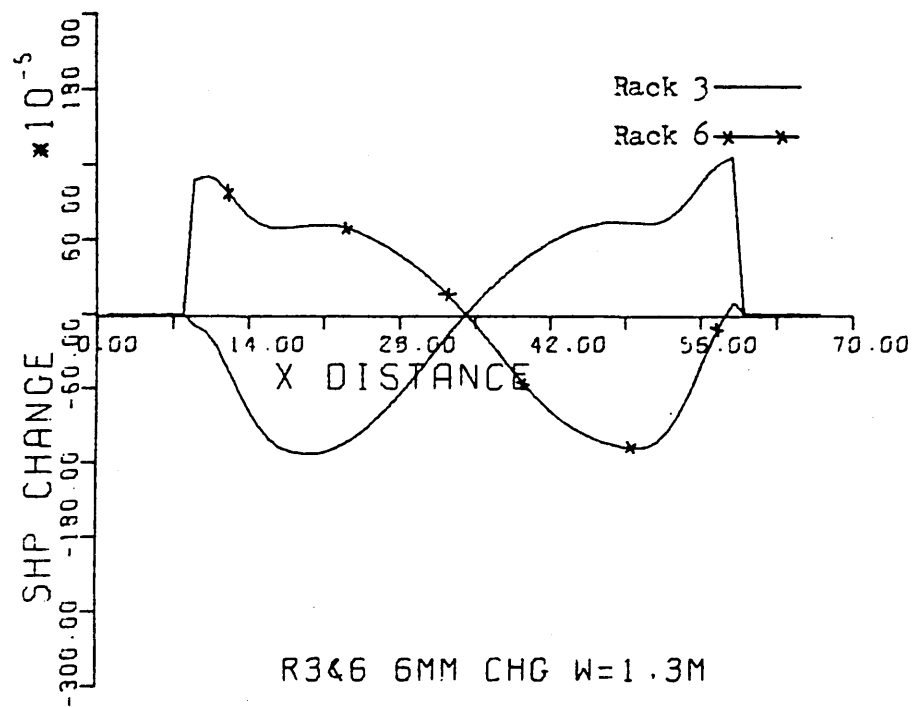Fig. 6.2. Shape profiles for RUN 1.

Fig. 6.3a.

Fig. 6.3b.

R3&6 6MM CHG W=1.6M

Fig. 6.3c.

R4&5 6MM CHG W=1.6M
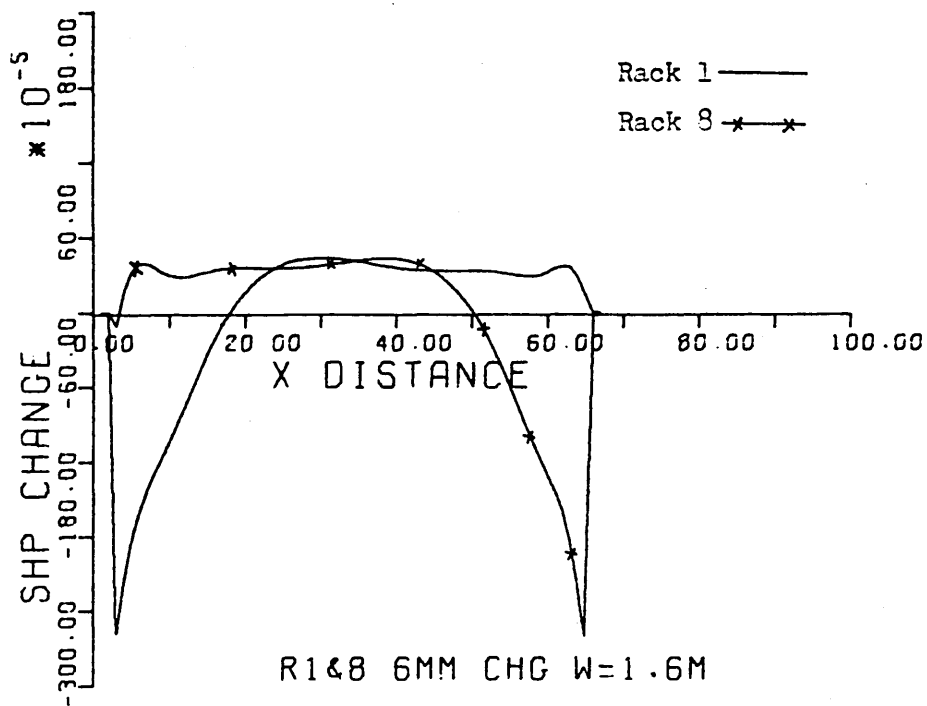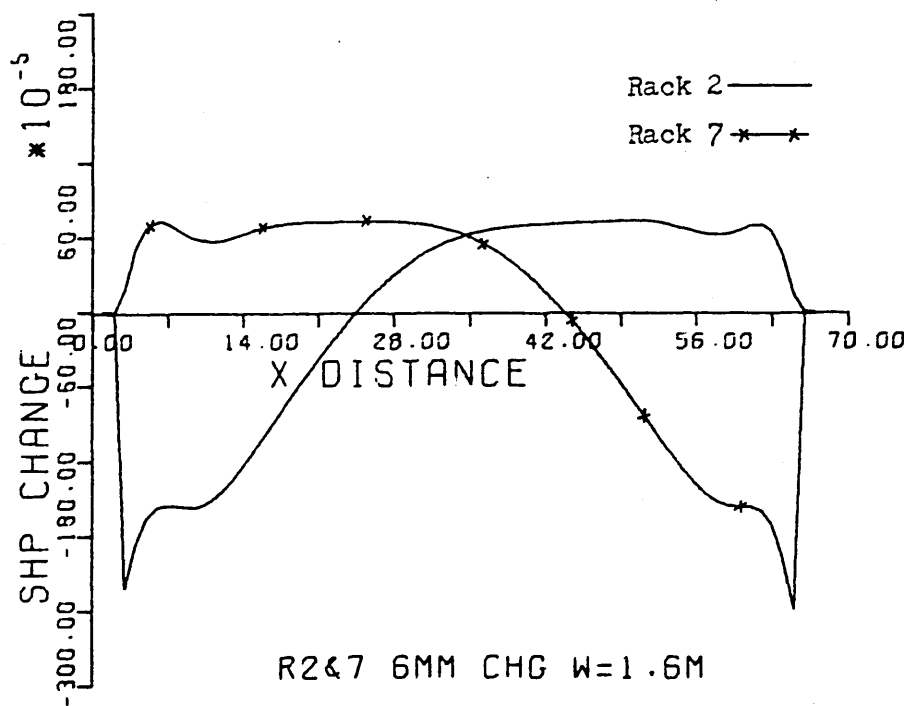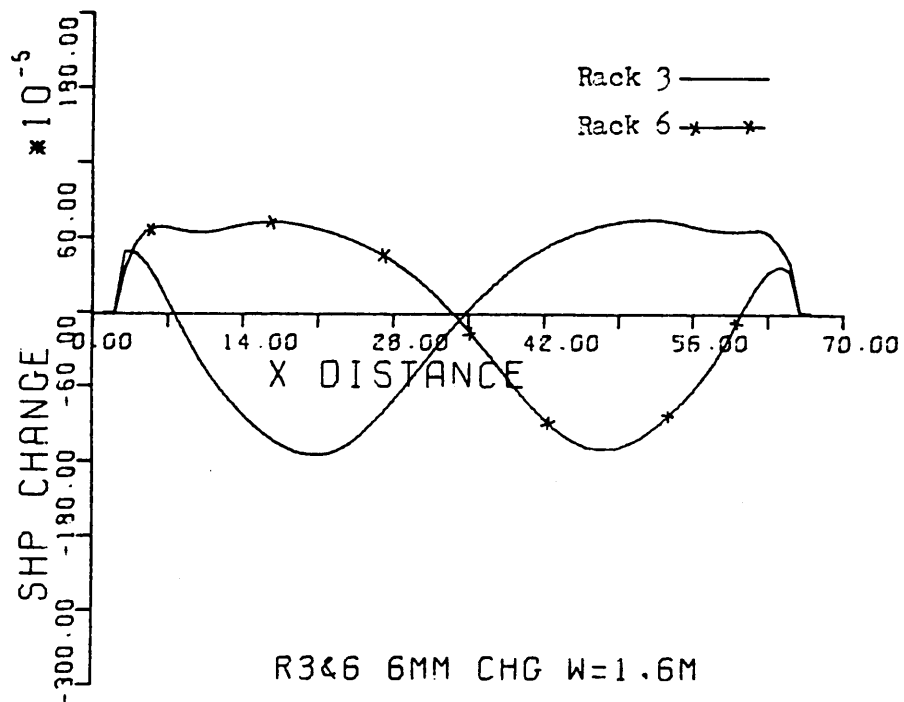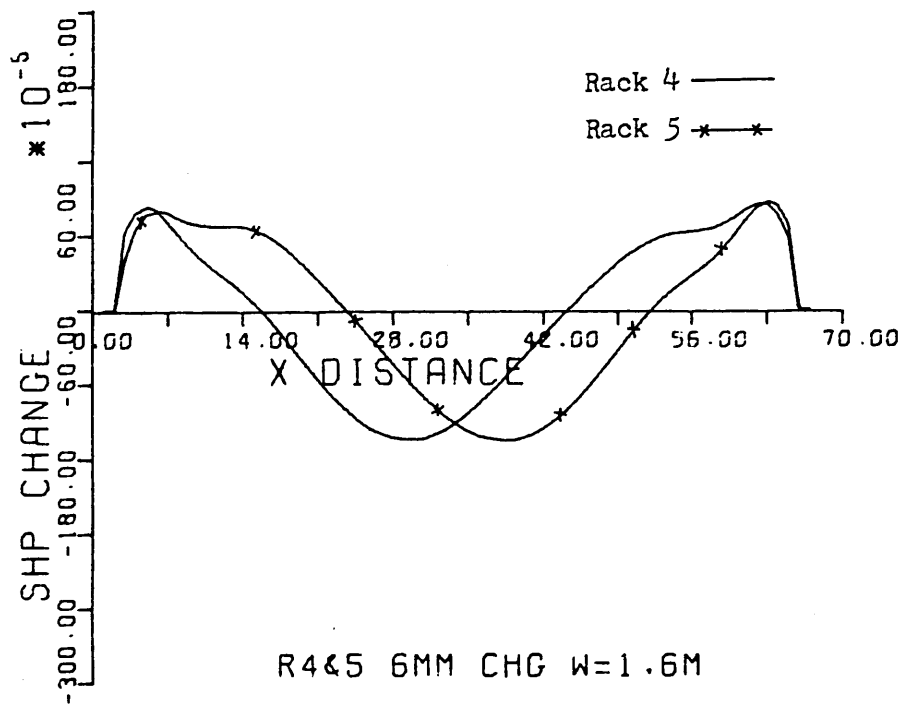
Fig. 6.3d.

Fig. 6.3. Shape profiles for RUN 2.

Rack 1 ——————
Rack 8 ✱—✱—✱

SHP CHANGE   ✱10⁻⁵

180.00
60.00
-60.00
-180.00
-300.00

X DISTANCE

14.00   28.00   42.00   56.00   70.00

R1&8 6MM CHG W=1.5

Fig. 6.4a.

Rack 2 ——————
Rack 7 ✱—✱—✱

SHP CHANGE   ✱10⁻⁵

180.00
60.00
-60.00
-180.00
-300.00

X DISTANCE

14.00   28.00   42.00   56.00   70.00

R2&7 6MM CHG W=1.5M

Fig. 6.4b.

R3&6 6MM CHG W=1.5M

Fig. 6.4c.

R4&5 6MM CHG W=1.5M
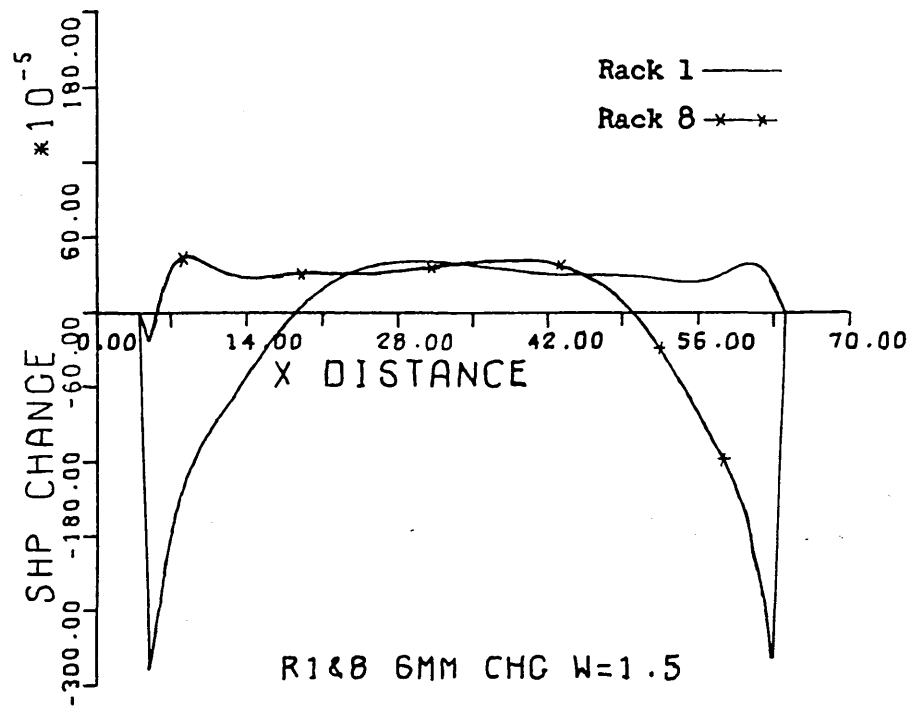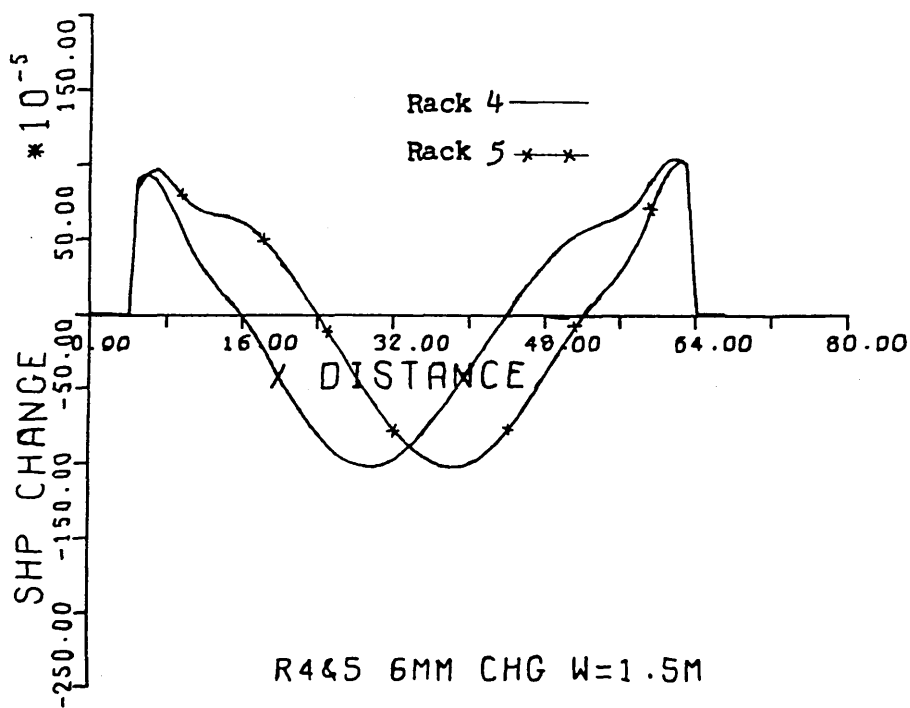
Fig. 6.4d.

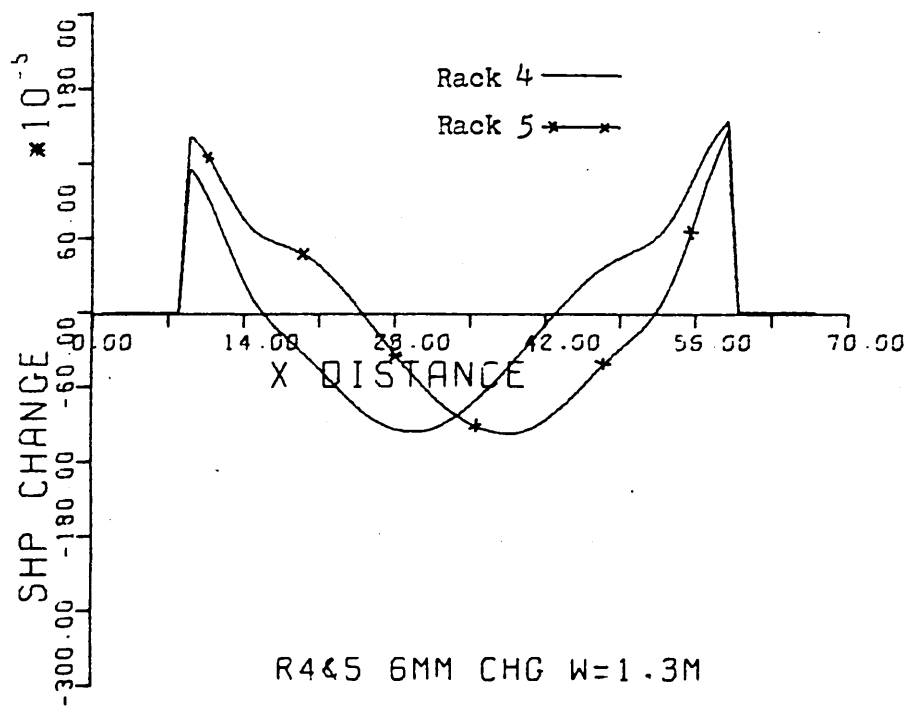Fig. 6.4. Shape profiles for RUN 3.

Fig. 6.5a.

Fig. 6.5b.

R3&6 6MM CHG W=1.3M

Fig. 6.5c.

R4&5 6MM CHG W=1.3M
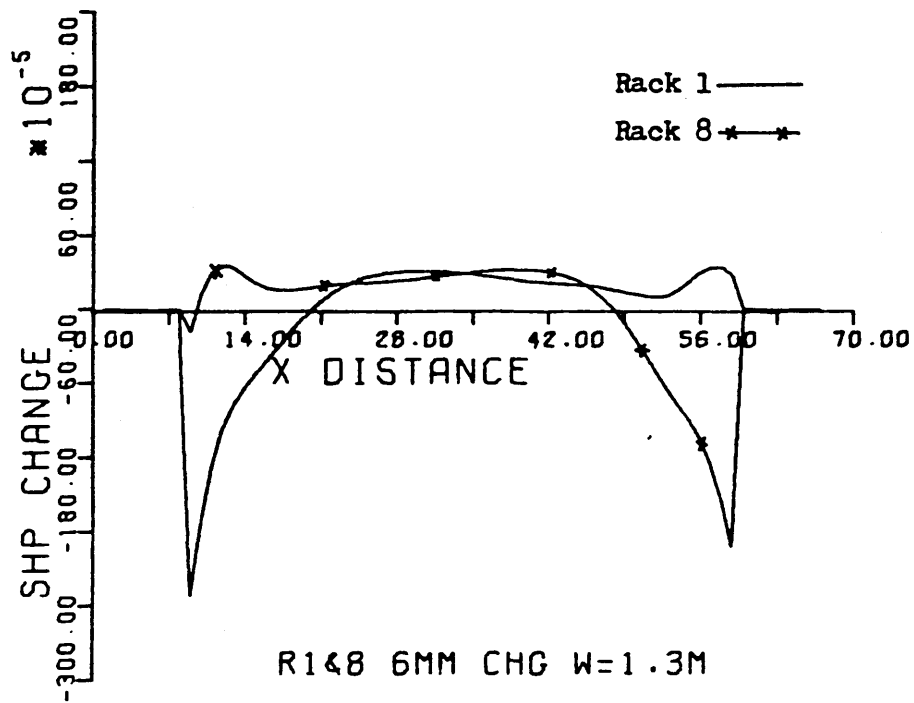
Fig. 6.5d.

Fig. 6.5. Shape profiles for RUN 4.

Fig. 6.6a.

Fig. 6.6b.

R3&6 6MM CHG W=1.2M
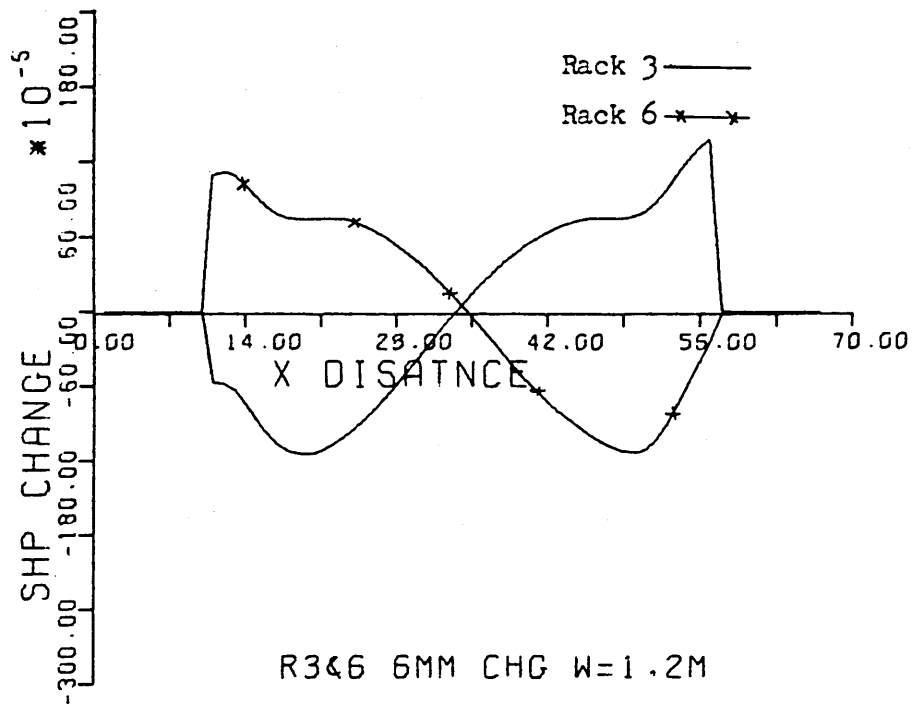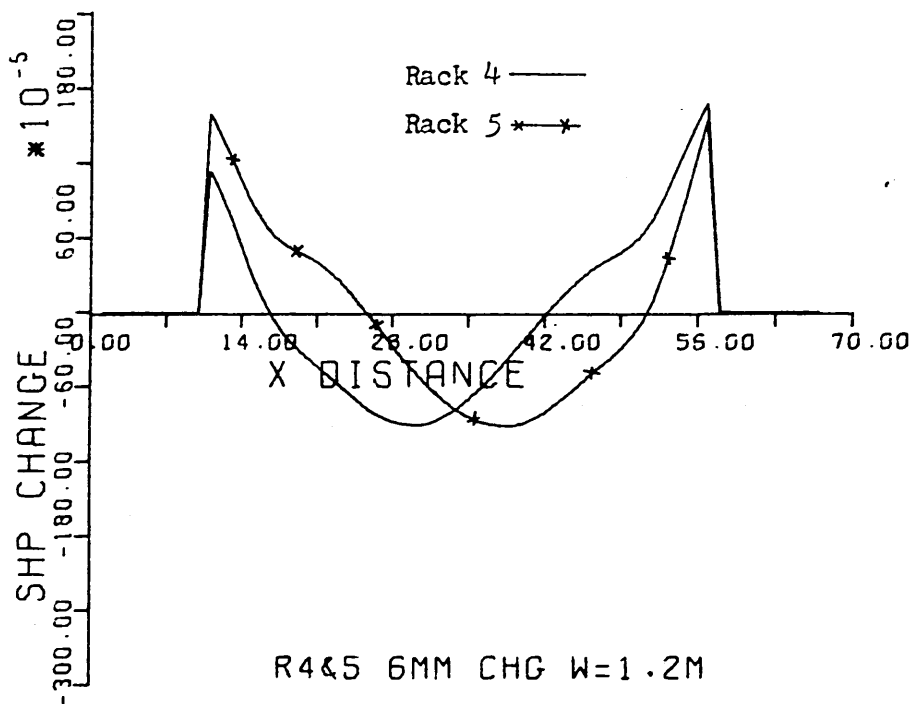
Fig. 6.6c.

R4&5 6MM CHG W=1.2M
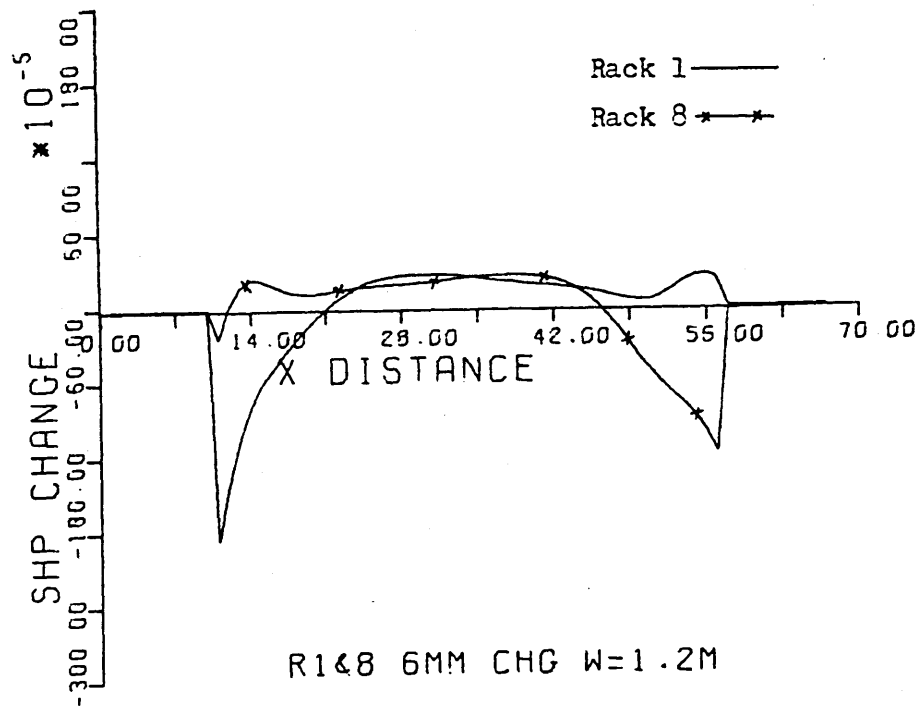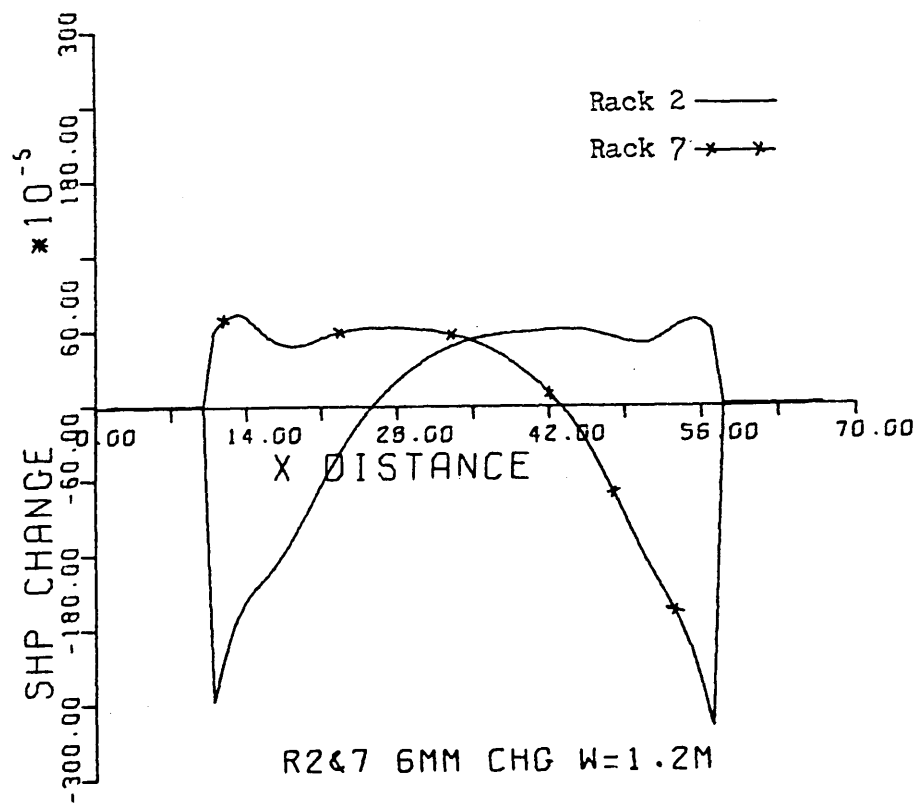
Fig. 6.6d.

Fig. 6.6. Shape profiles for RUN 5.

Fig. 6.7a.

Fig. 6.7b.

R3&6 W=1.1M 6MMCHG

Fig. 6.7c.

R4&5 W=1.1M 6MM CHG
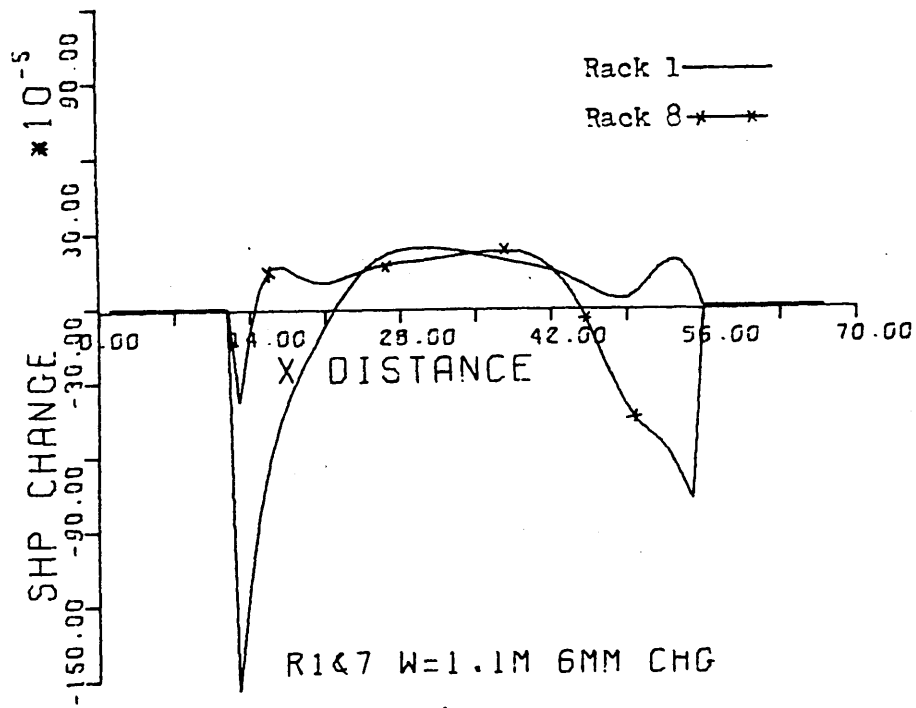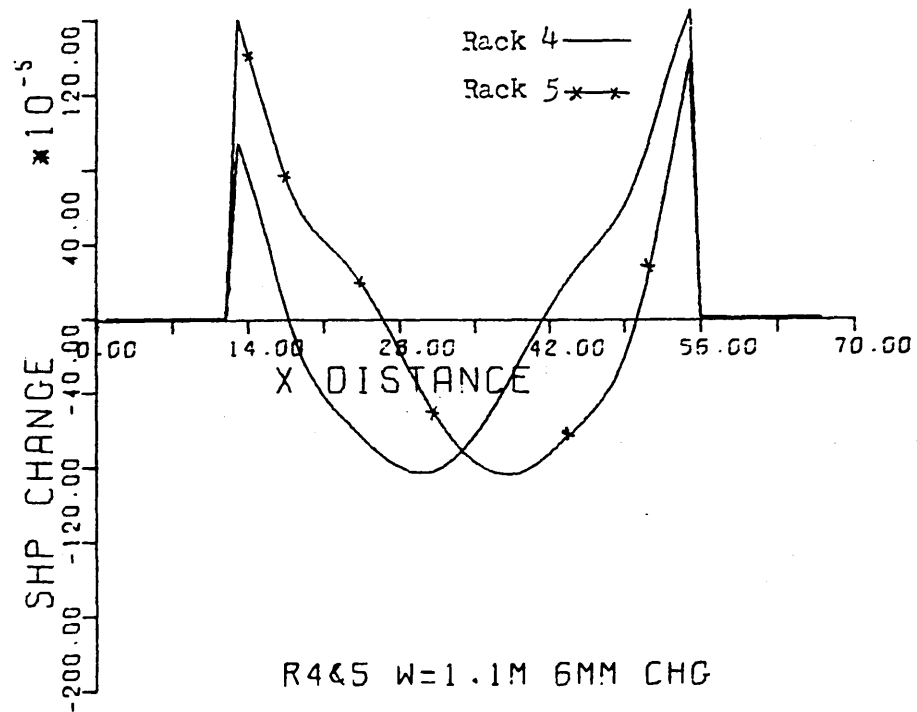
Fig. 6.7d.

Fig. 6.7. Shape profiles for RUN 6.

Rack 1
Rack 8

R1&8 W=1M 6MM CHG

Fig. 6.8a.

Rack 2
Rack 7

R2&7 W=1M 6MM CHG
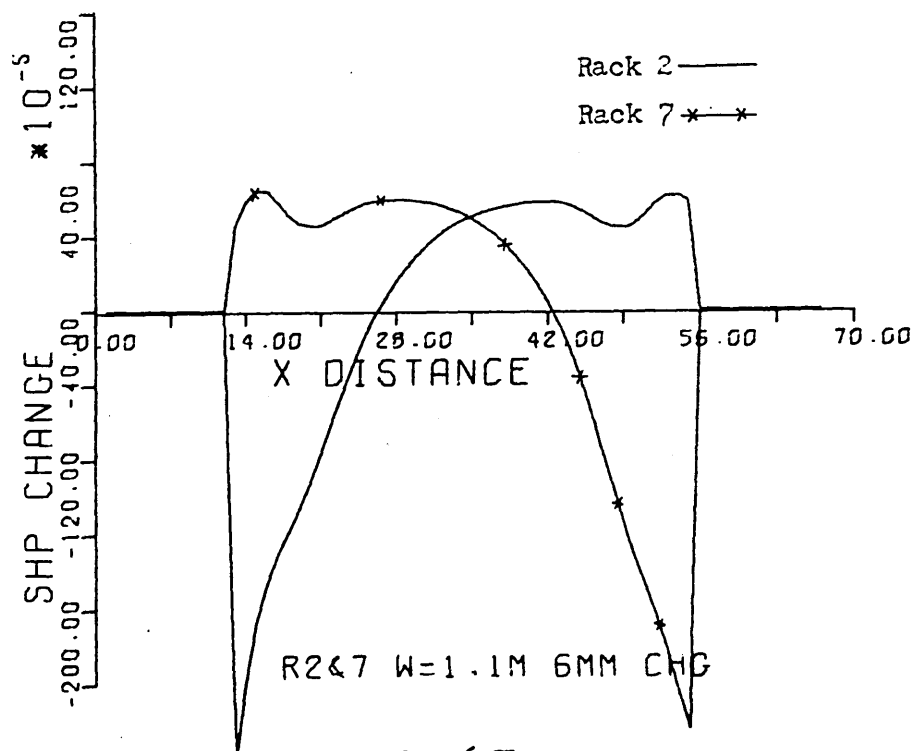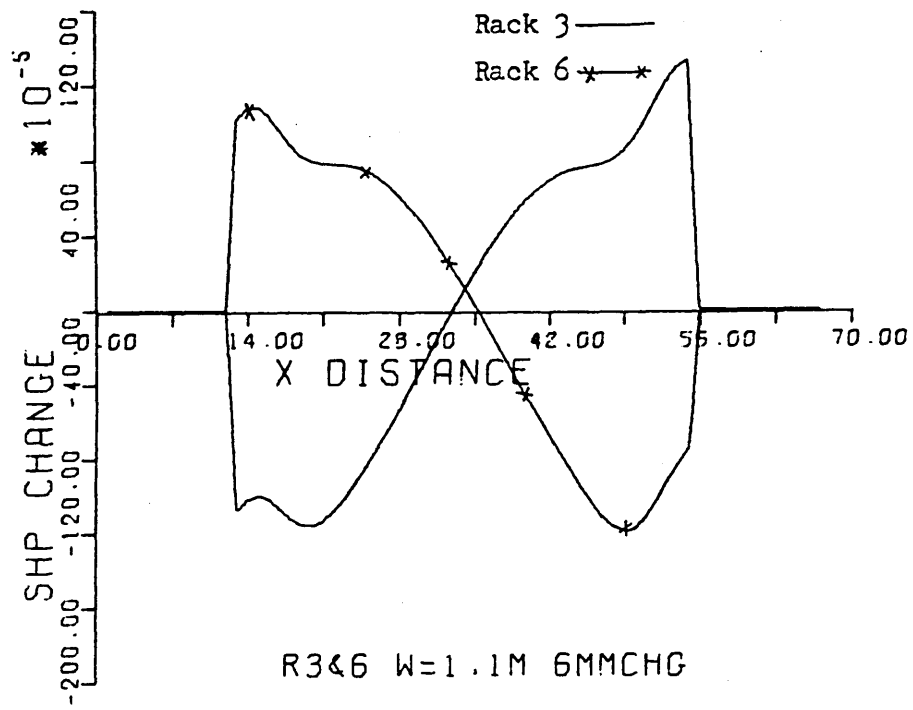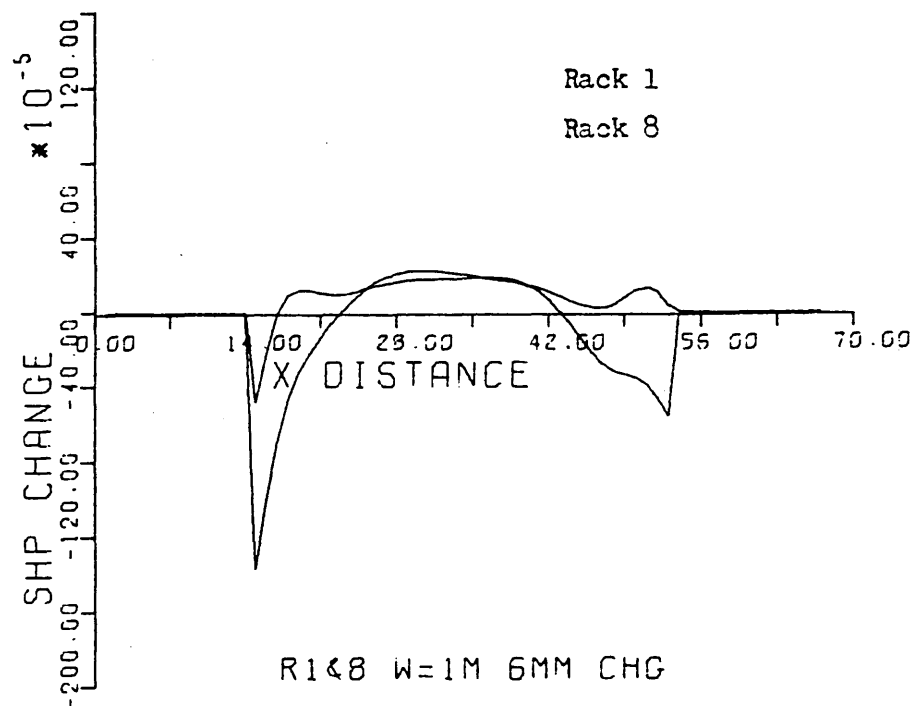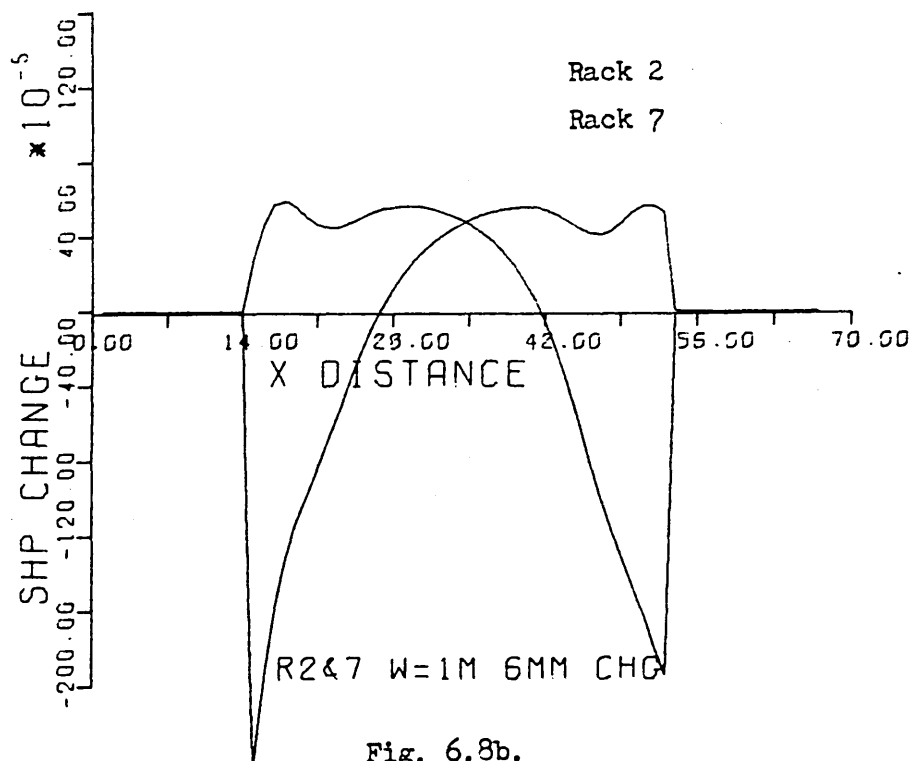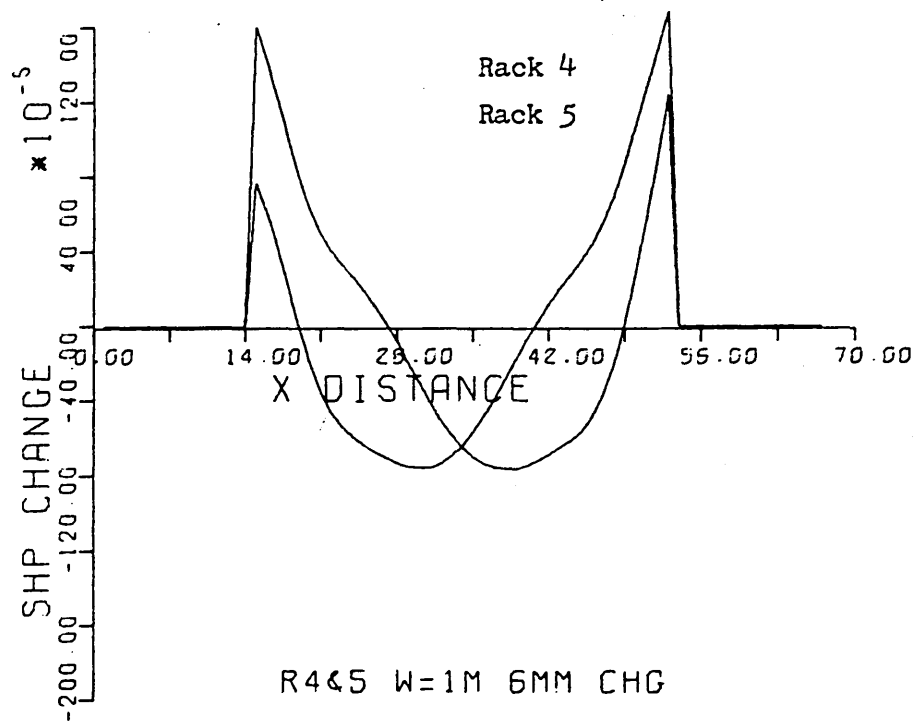
Fig. 6.8b.

Fig. 6.8c.

Fig. 6.8d.

Fig. 6.8. Shape profiles for RUN 7.

Fig. 6.9a.

Fig. 6.9b.

Rack 3
Rack 6

YS 50% MORE R3&6 1.4

Fig. 6.9c.

Rack 4
Rack 5

YS 50% MORE R4&5 1.4
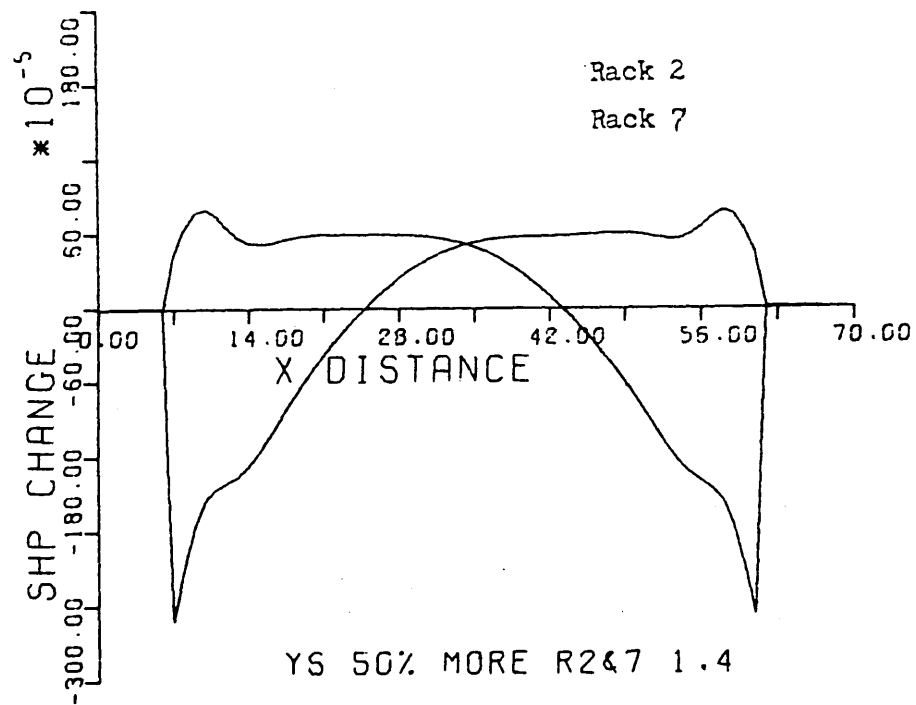
Fig. 6.9d.

Fig. 6.9. Shape profiles for RUN 8.

Rack 1
Rack 2

RACK1&7 W=1.4

Fig. 6.10a.

Rack 2
Rack 7

RACK 2&7 W=1.4

Fig. 6.10b.

RACK 3&6 W-1.4

Fig. 6.10c.

RACK 4&5 W=1.4
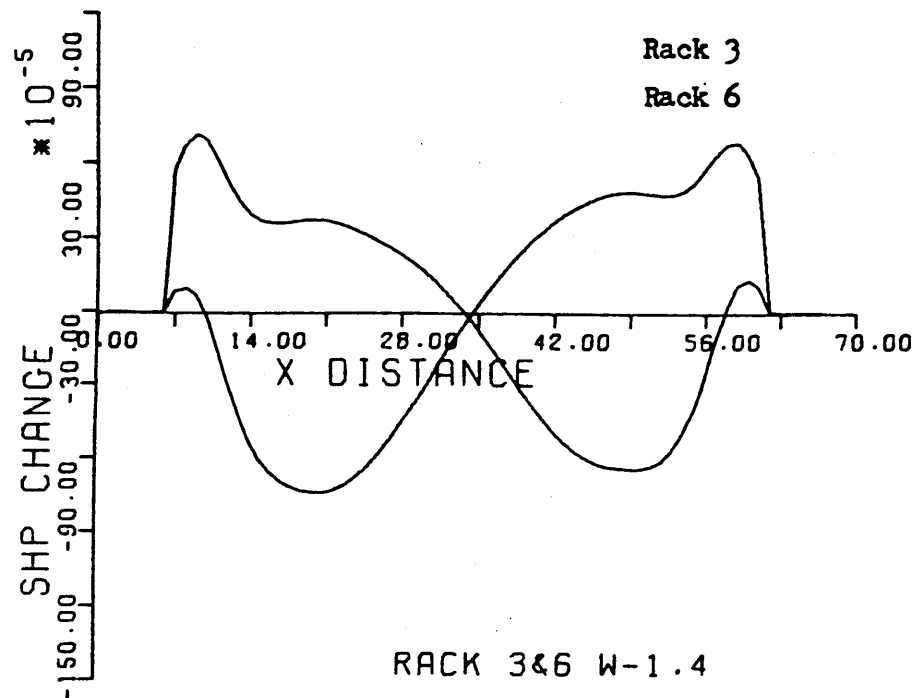
Fig. 6.10d.

Fig. 6.10. Shape profiles for RUN 9.

Rack 1
Rack 8

RACK 1&8 W=1.4

Fig. 6.11a.

Rack 2
Rack 7

RACK 2&7 W=1.4

Fig. 6.11b.

RACK 3&6 W=1.4

Fig. 6.11c.

RACK 4&5 W=1.4
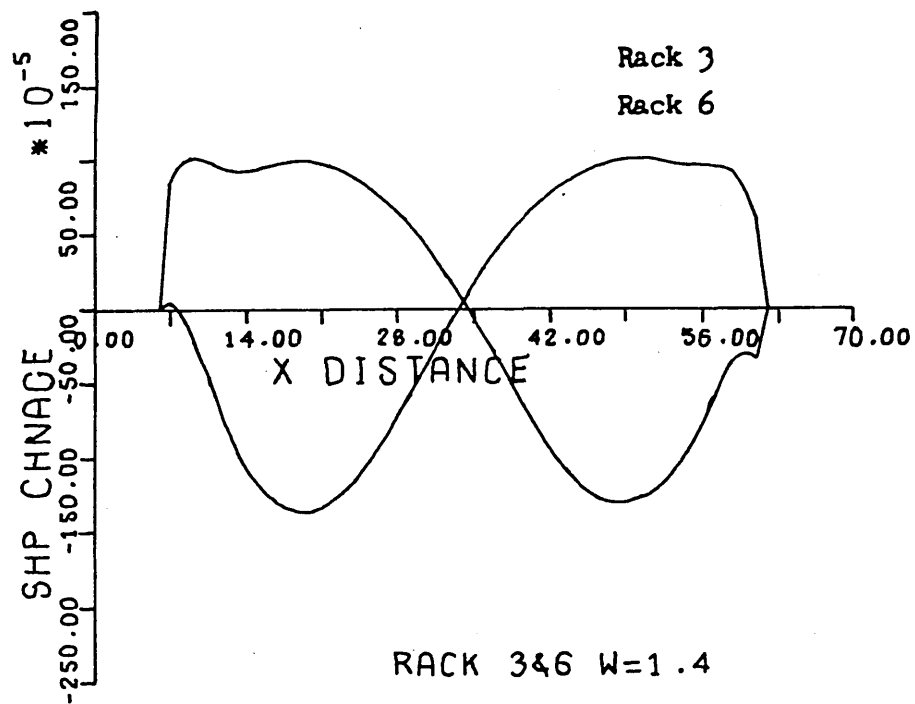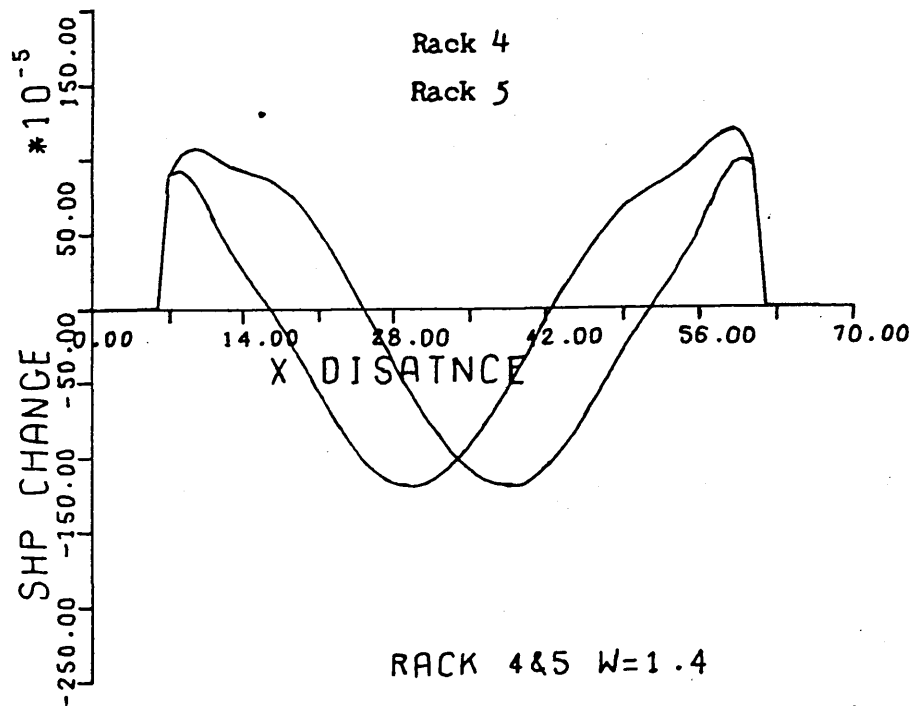
Fig. 6.11d.

Fig. 6.11. Shape profiles for RUN 10.

Fig. 6.12a.

Fig. 6.12b.

RACK 3&6

Fig. 6.12c.

RACK 4&5
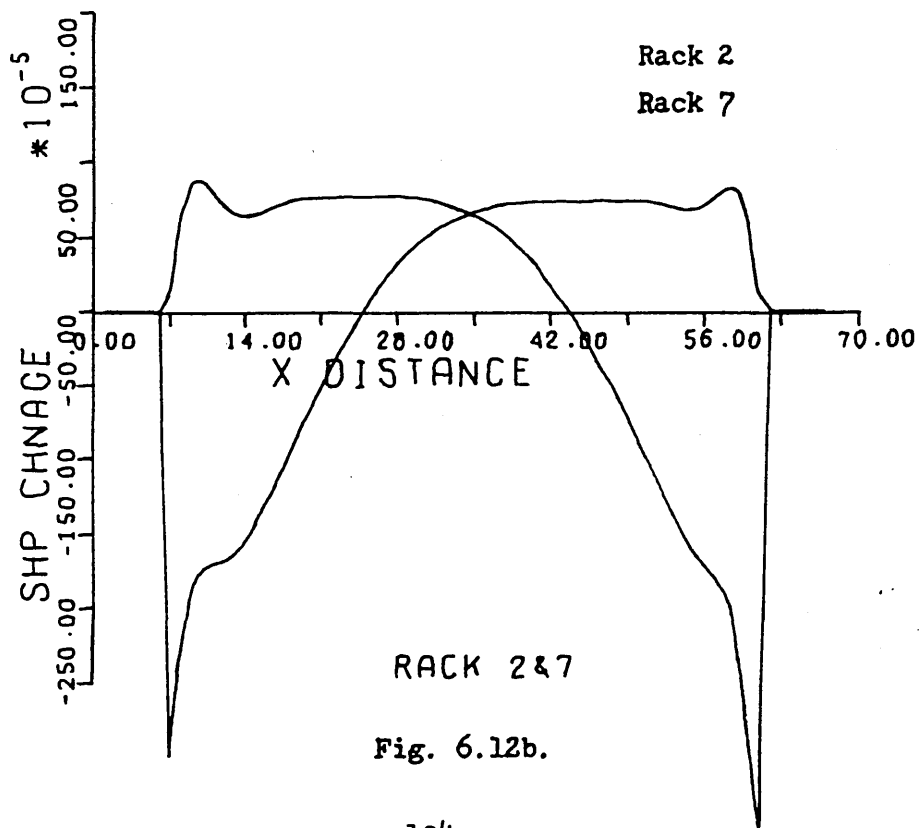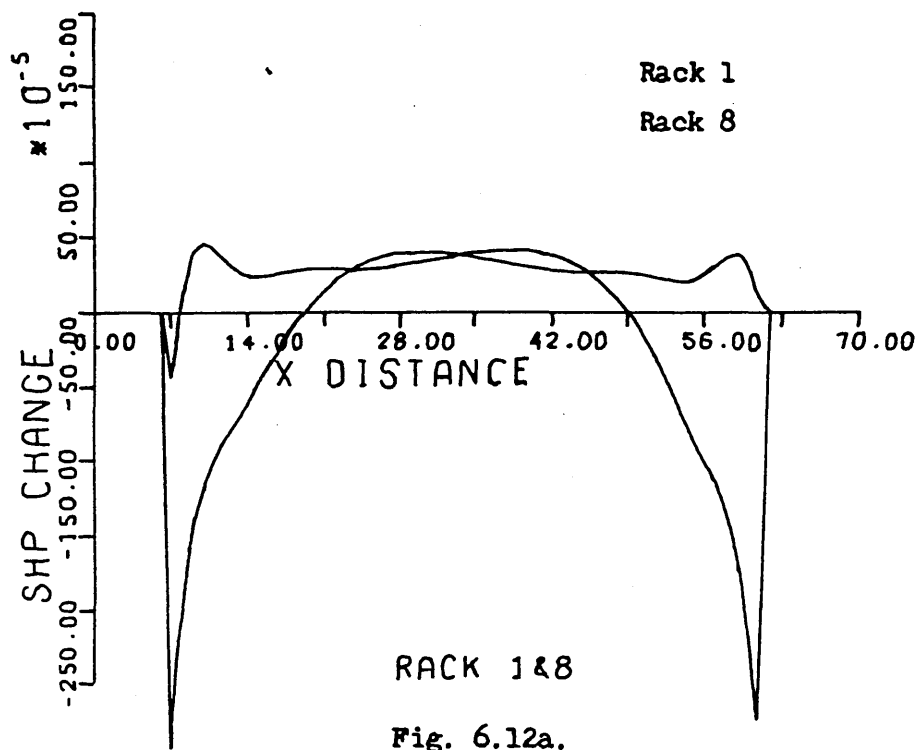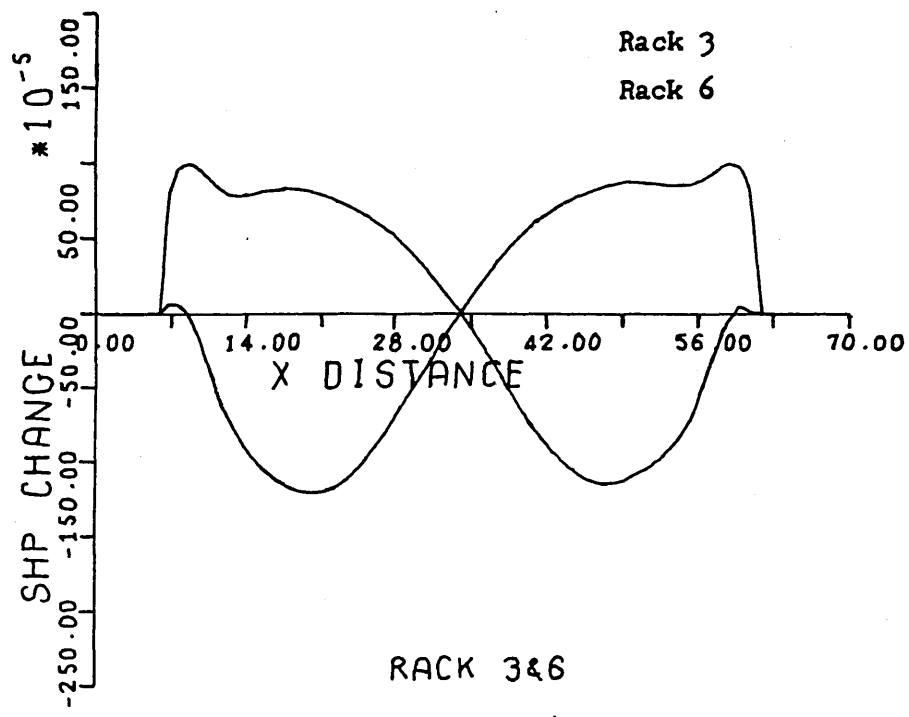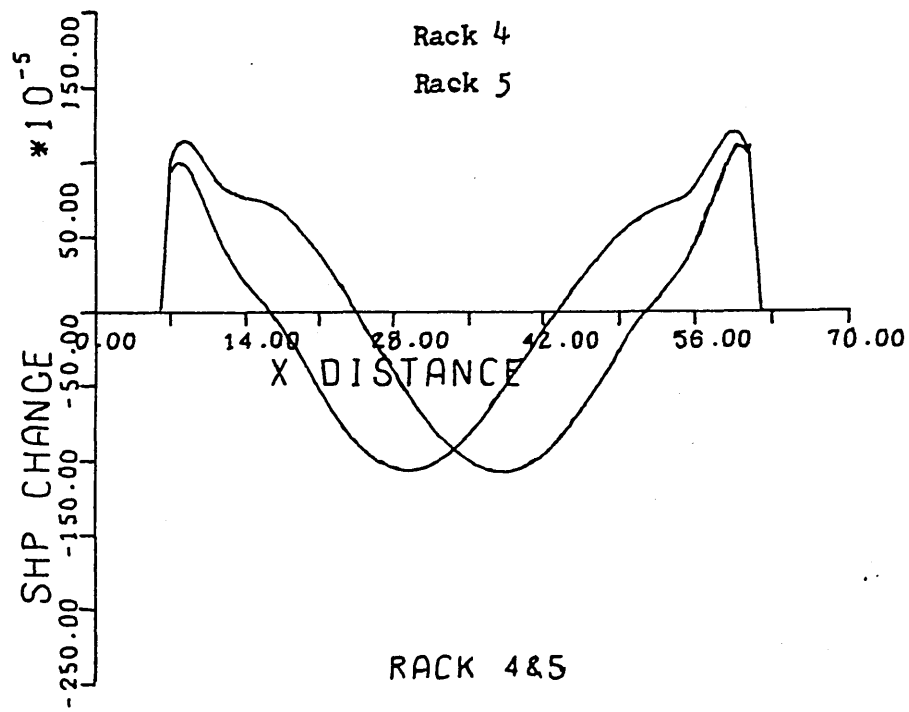
Fig. 6.12d.

Fig. 6.12. Shape profiles for RUN 11.
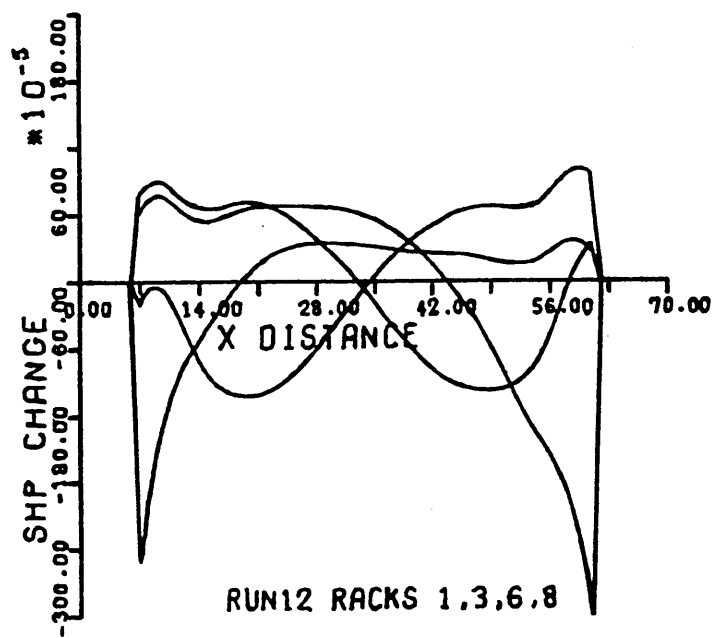
Fig. 6.13a.
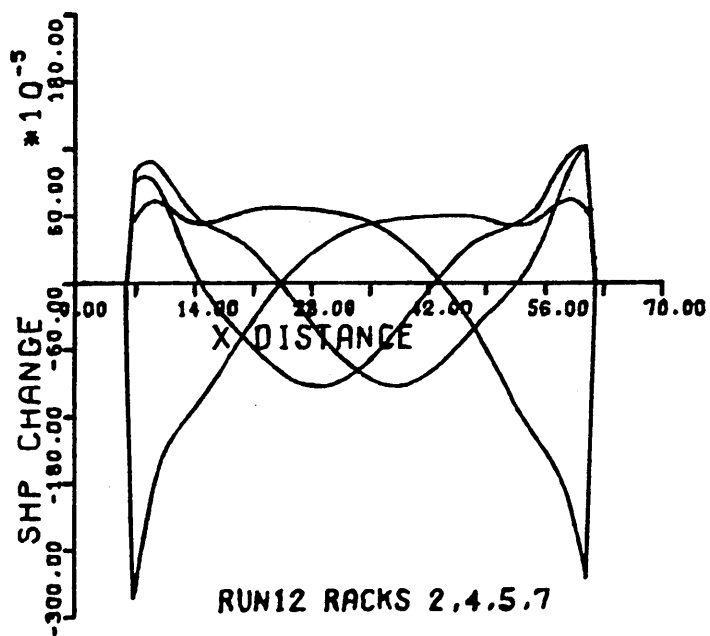
Fig. 6.13b.

Fig. 6.13. Shape profiles for RUN 12.

Fig. 6.14a.

RUN13 RACKS 2,4,5,7
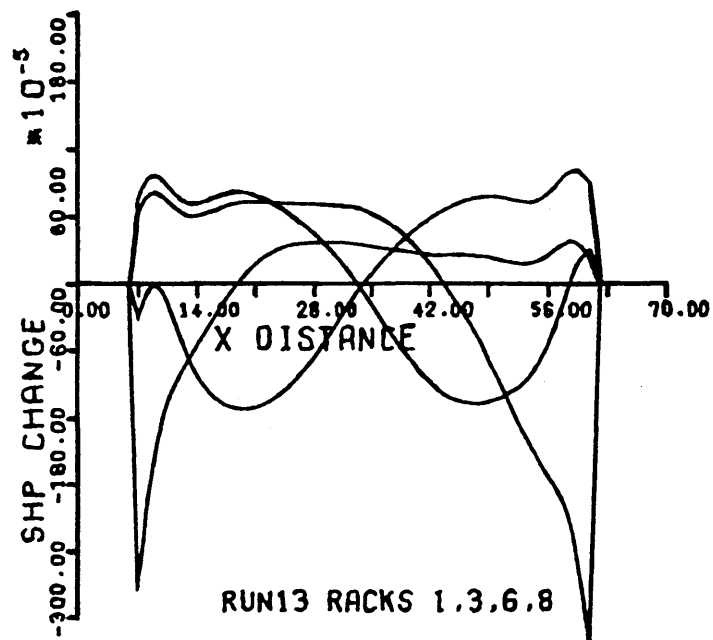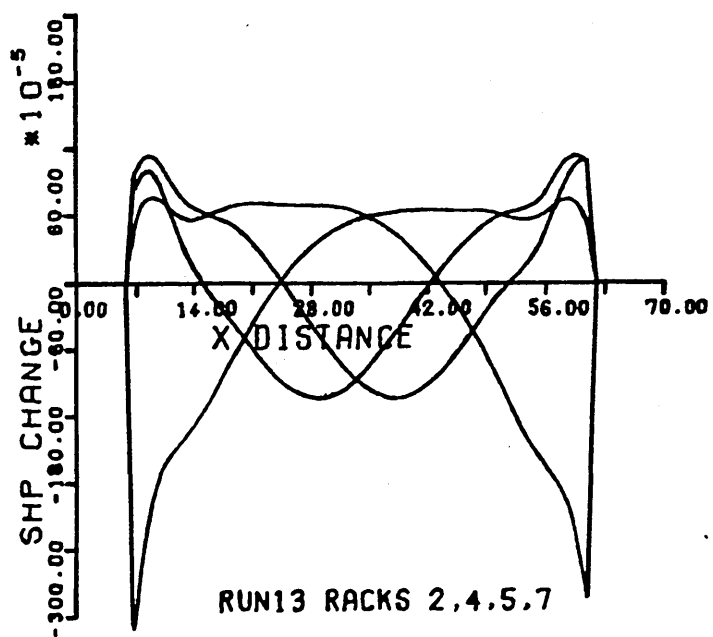
Fig. 6.14b.

Fig. 6.14.   Shape profiles   for   RUN 13.
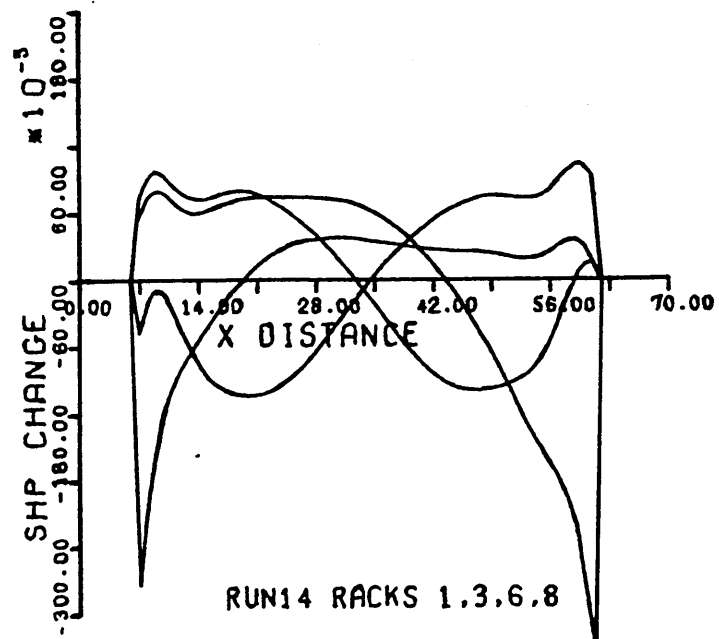
Fig. 6.15a.
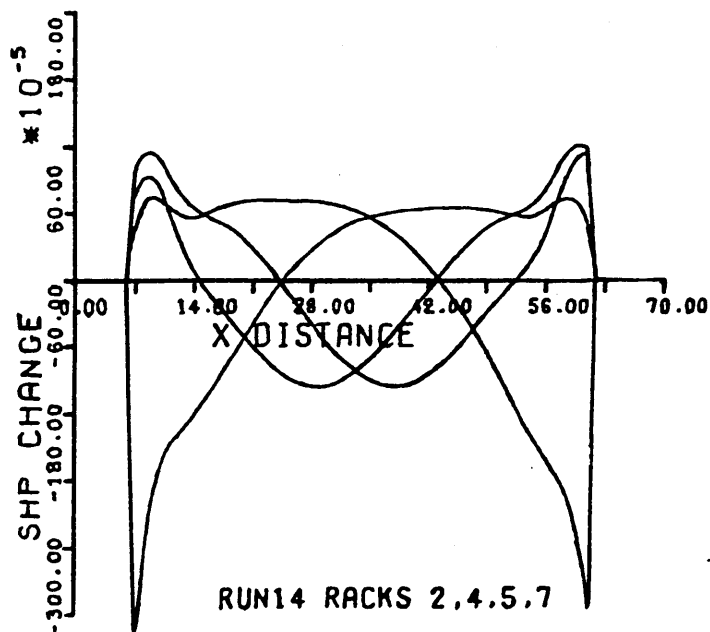
Fig. 6.15b.

Fig. 6.15. Shape profiles for RUN 14.
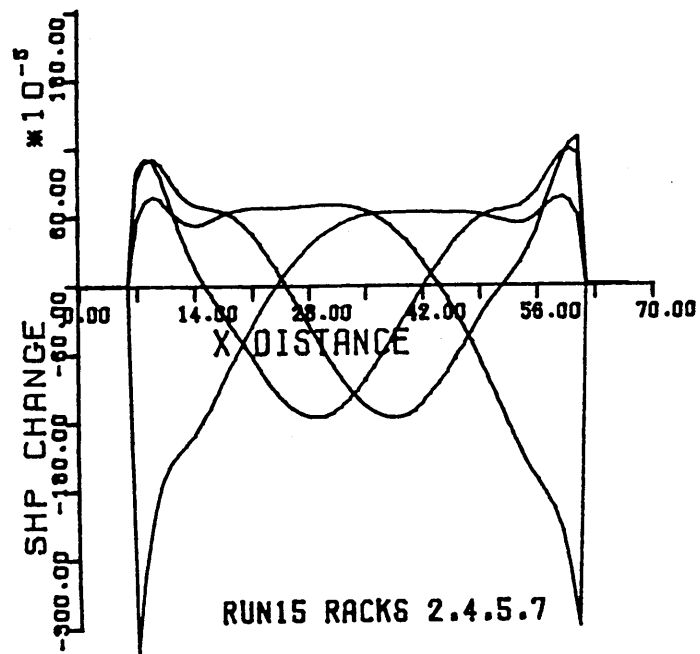
Fig. 6.16a.
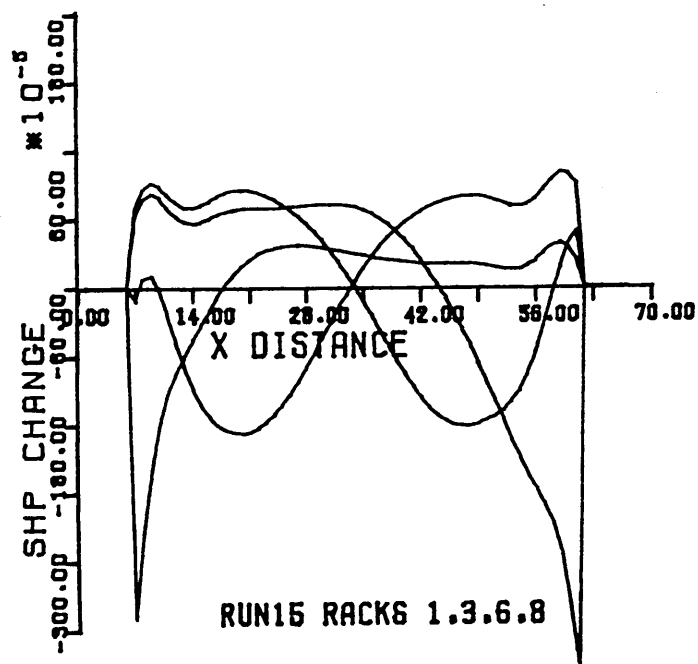
Fig. 6.16b.

Fig. 6.16. Shape profiles for RUN 15.
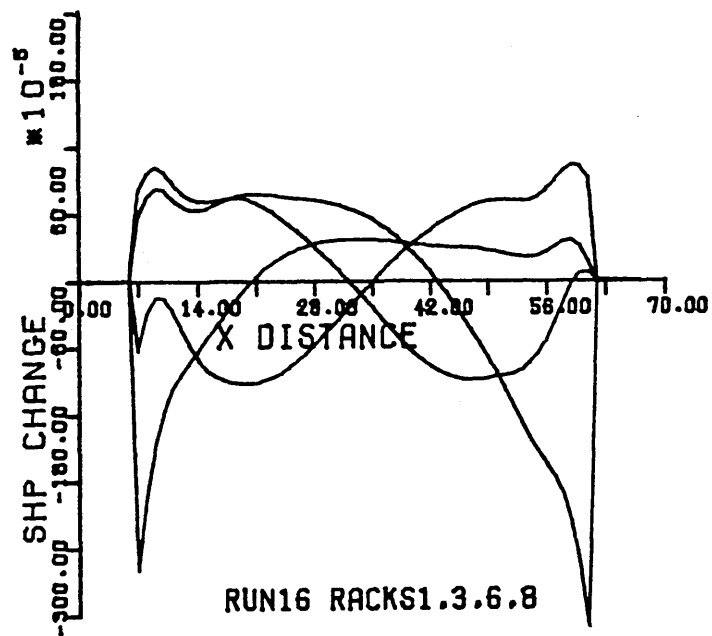
Fig. 6.17a.
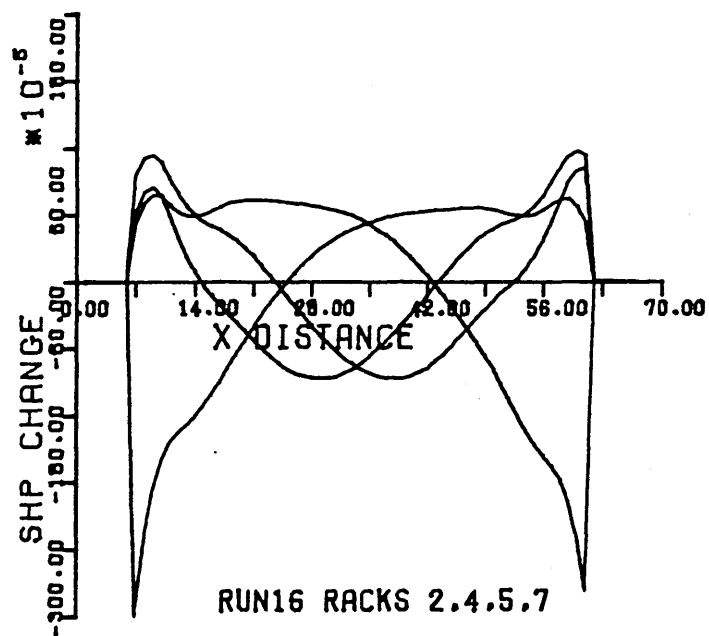
Fig. 6.17b.

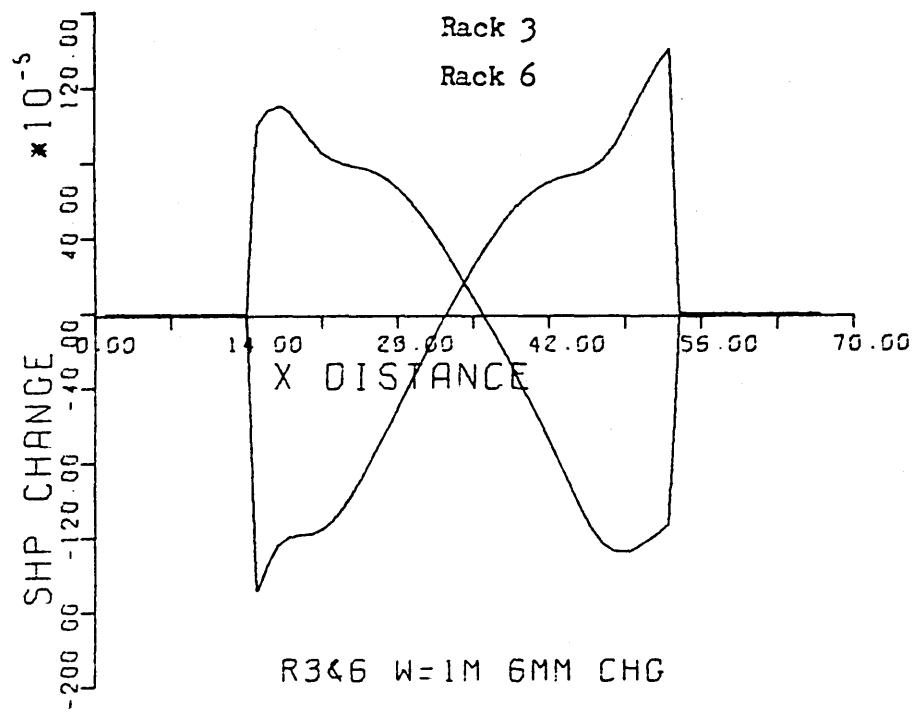Fig. 6.17. Shape profiles for RUN 16.

Fig. 6.18a.

Fig. 6.18b.

Rack 3
Rack 6

RACK 3&6

Fig. 6.18c.

Rack 4
Rack 5

RACK 4&5
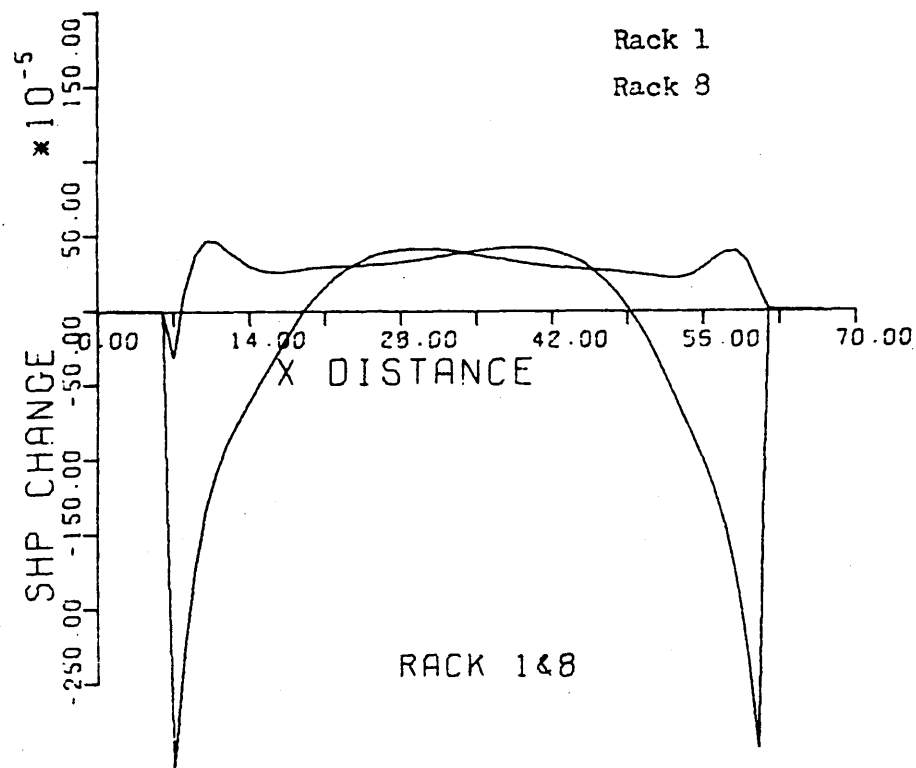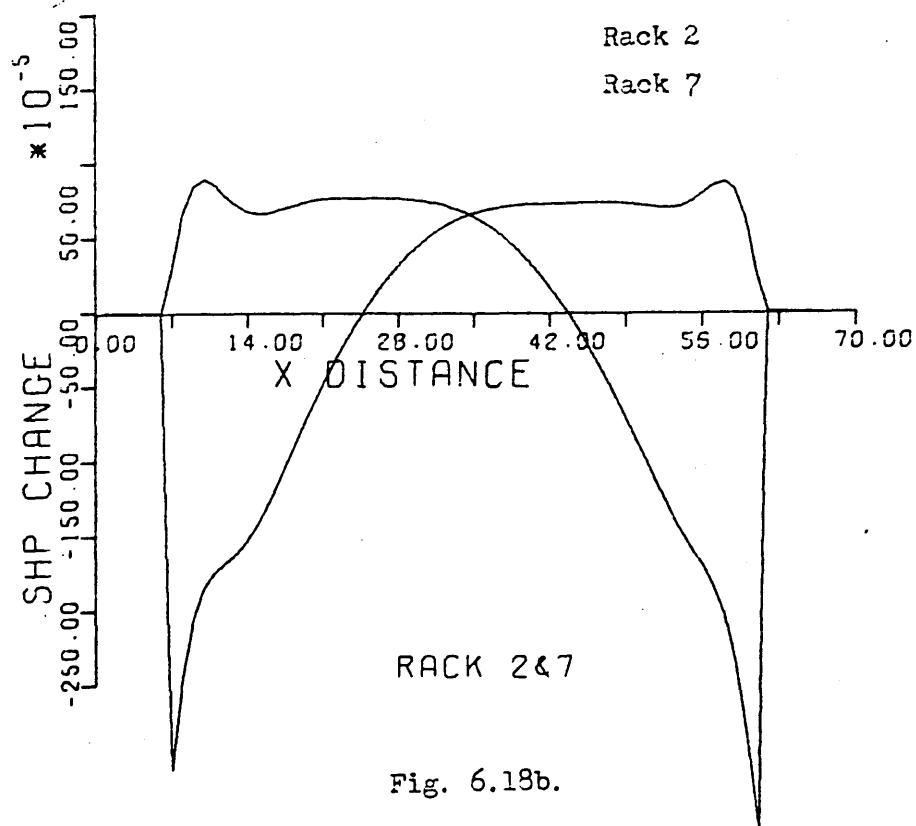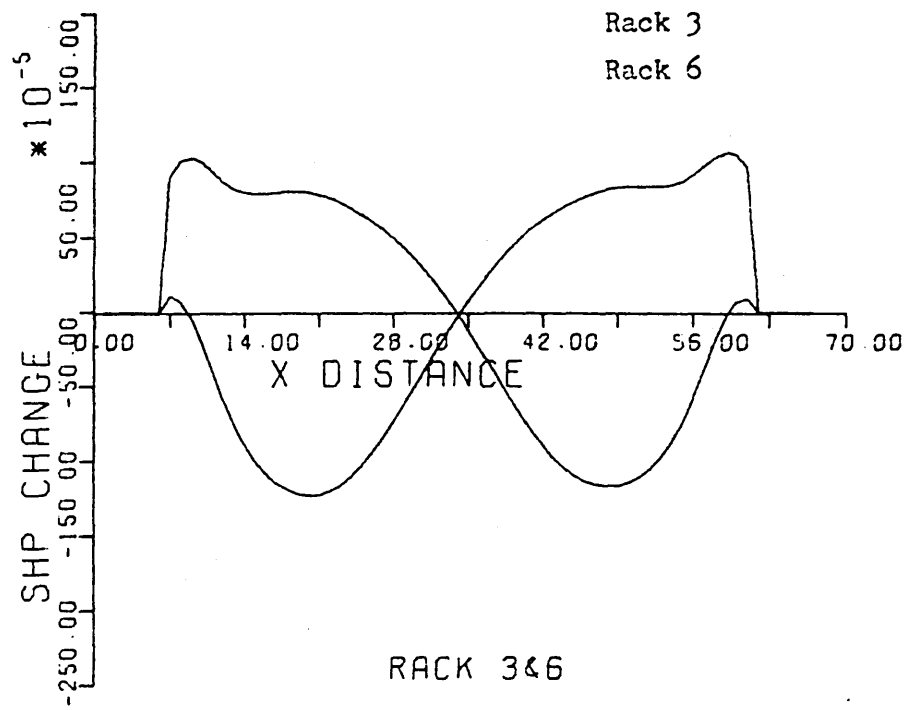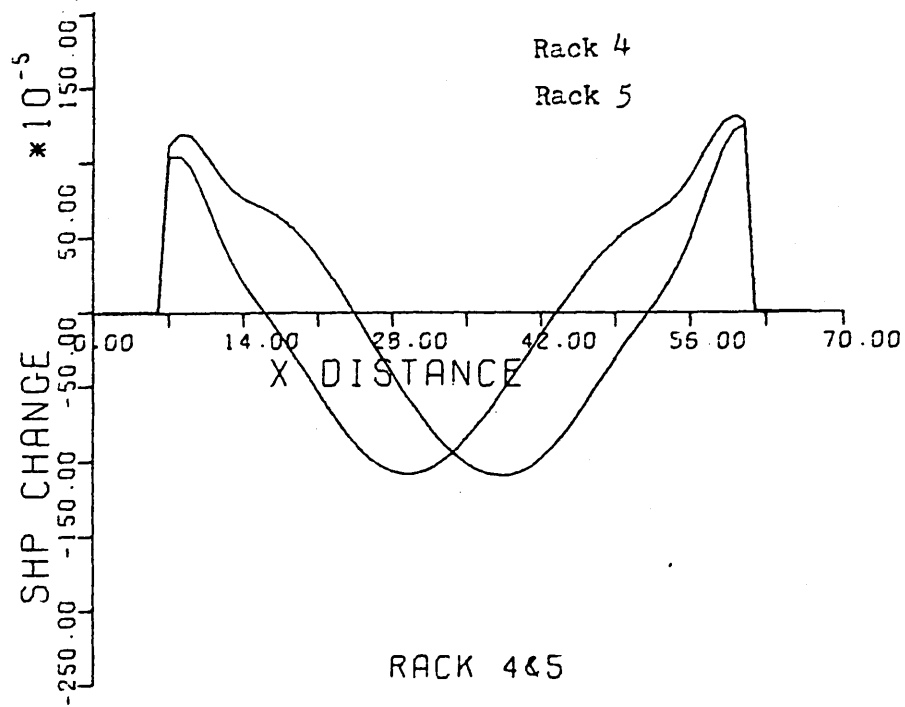
Fig. 6.18d.

Fig. 6.18. Shape profiles for RUN 17.

Fig. 6.19a.

Fig. 6.19b.

RACK 3&6

Fig. 6.19c.

RACK 4&5
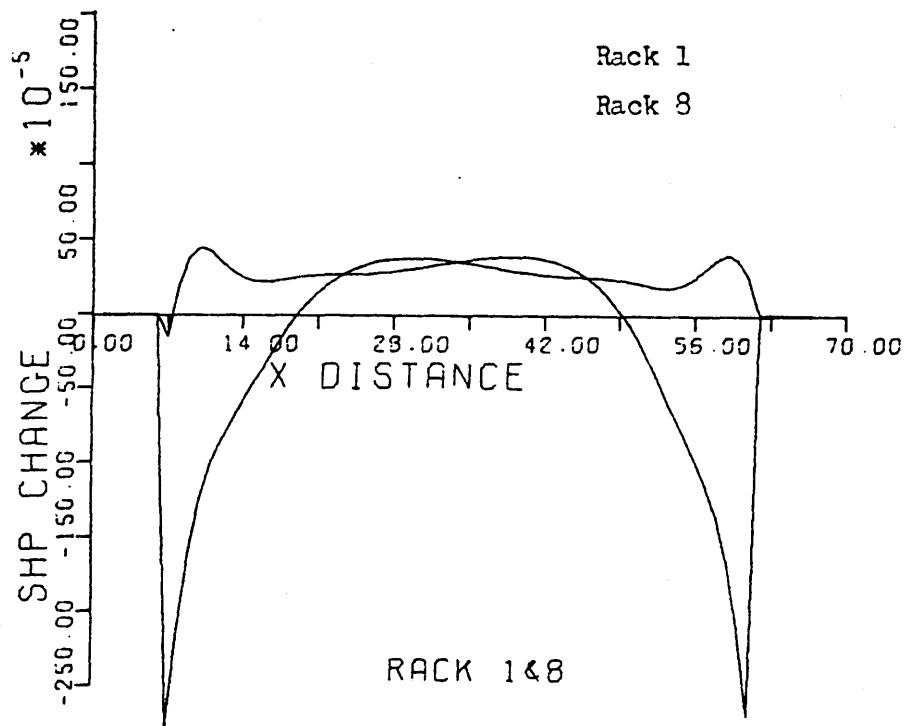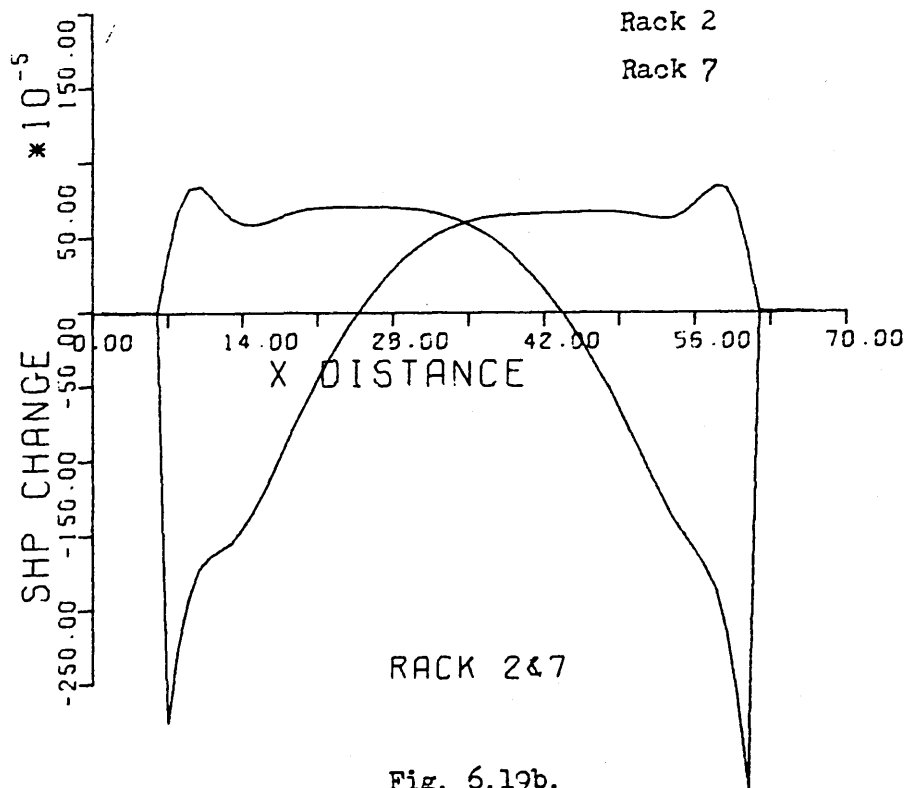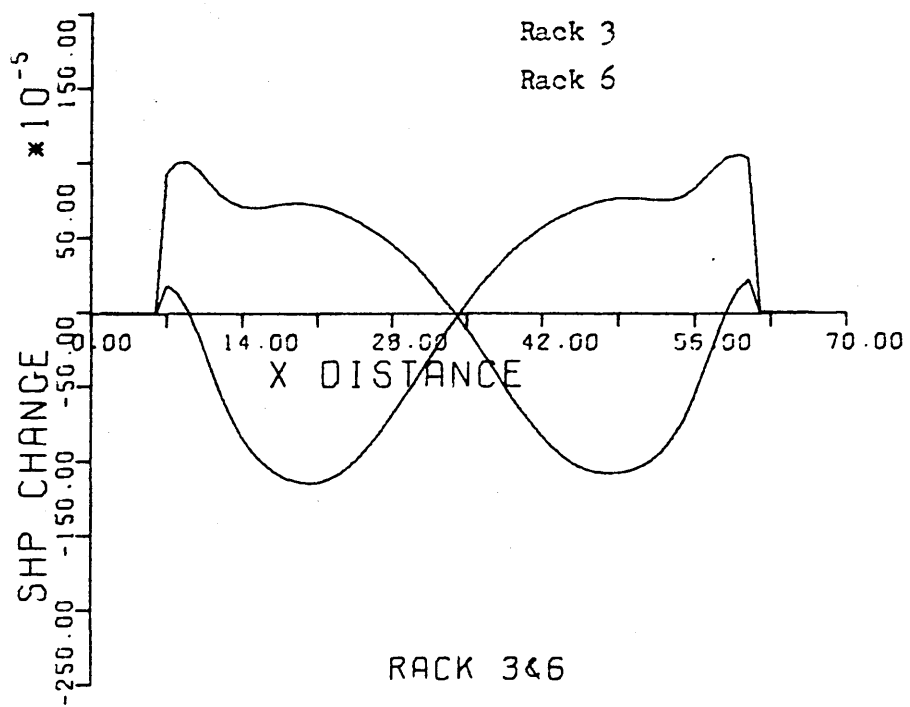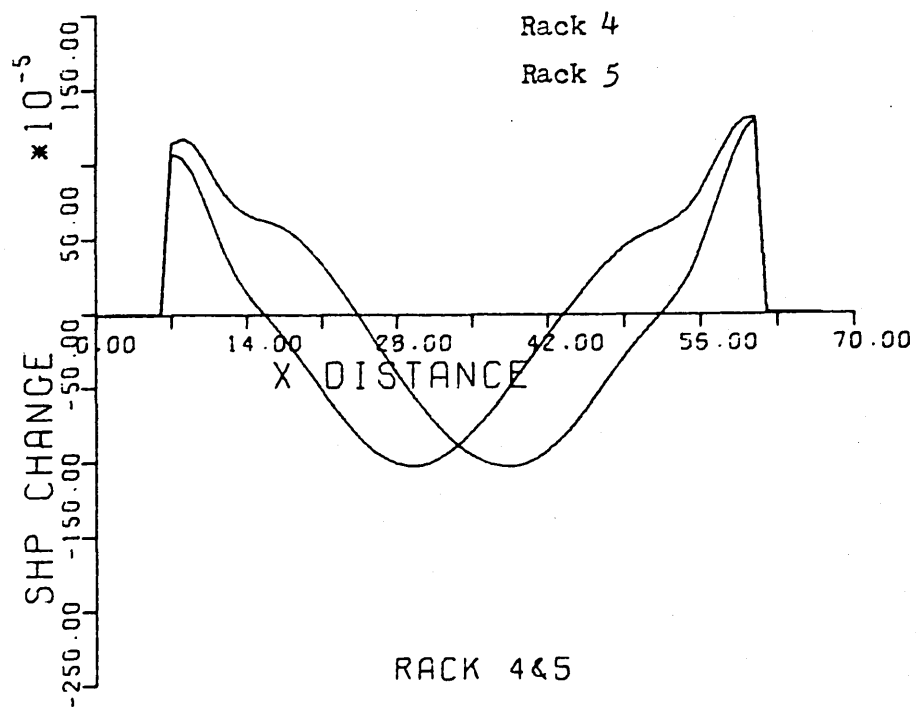
Fig. 6.19d.

Fig. 6.19. Shape profiles for RUN 18.
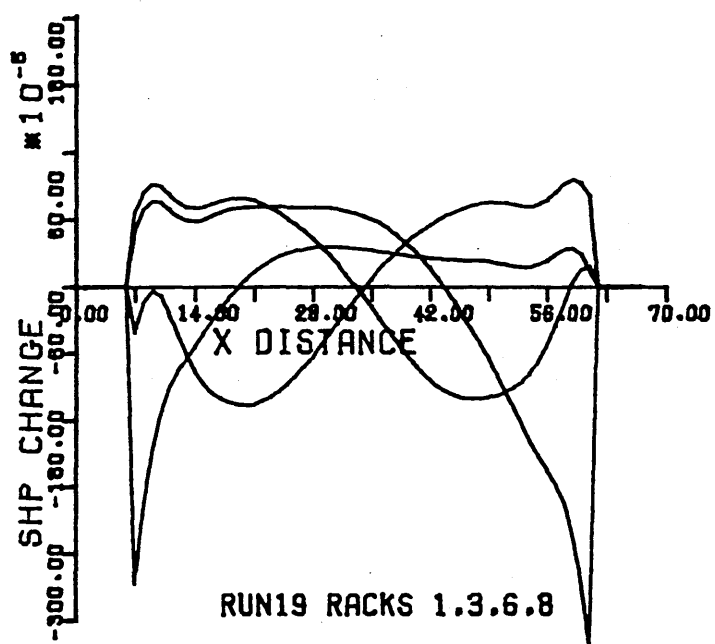
Fig. 6.20a.
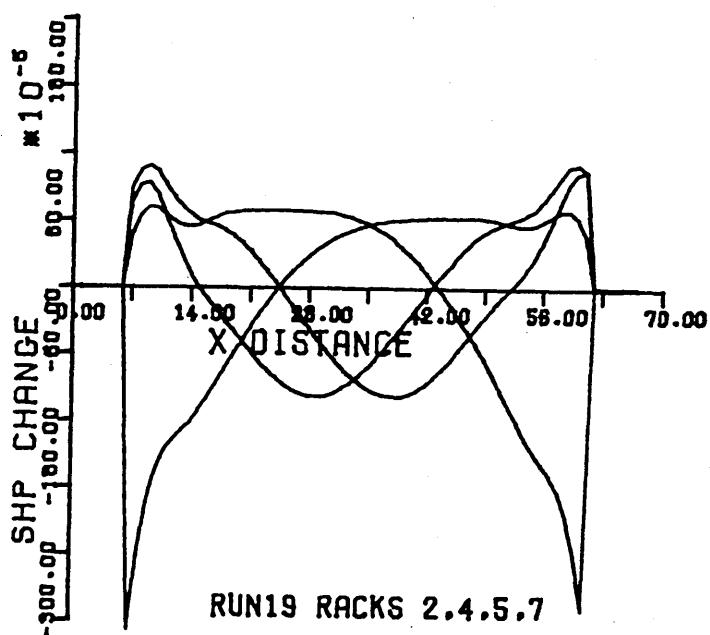
Fig. 6.20b.

Fig. 6.20. Shape profiles for RUN 19.
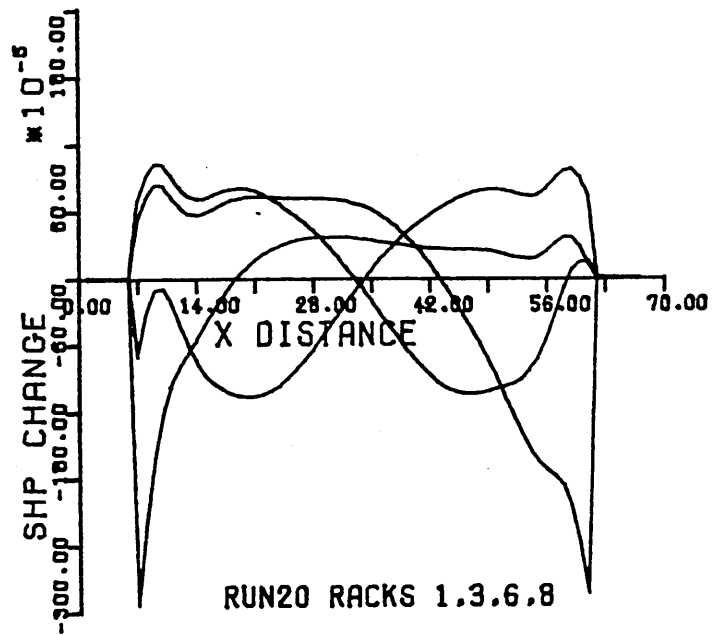
Fig. 6.21a.
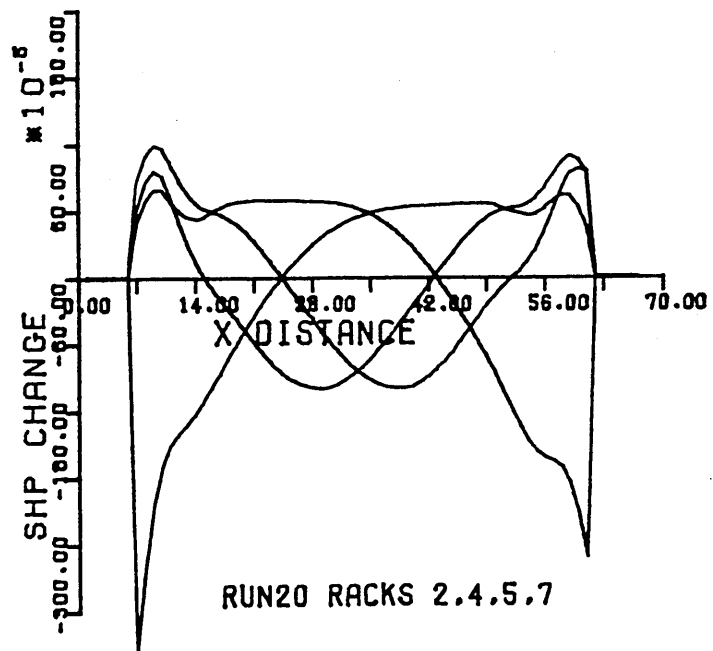
Fig. 6.21b.

Fig. 6.21. Shape profiles for RUN 20.
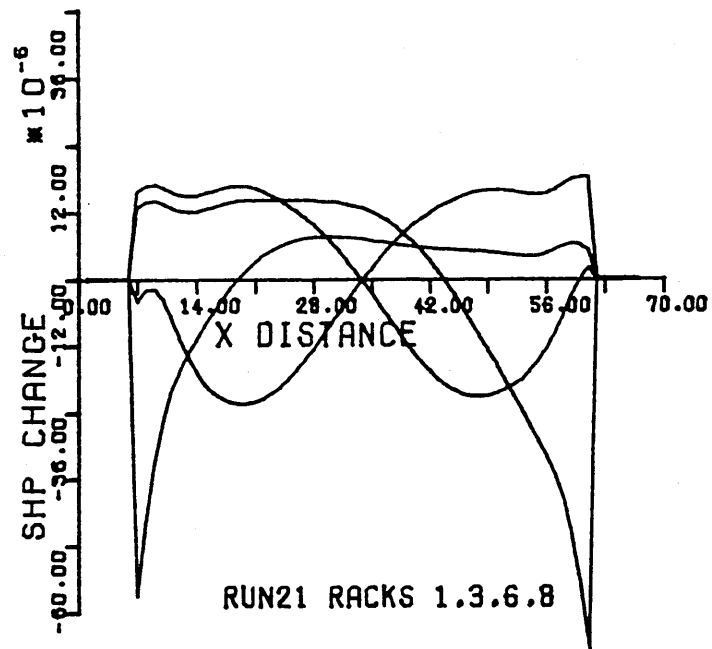
Fig. 6.22a.
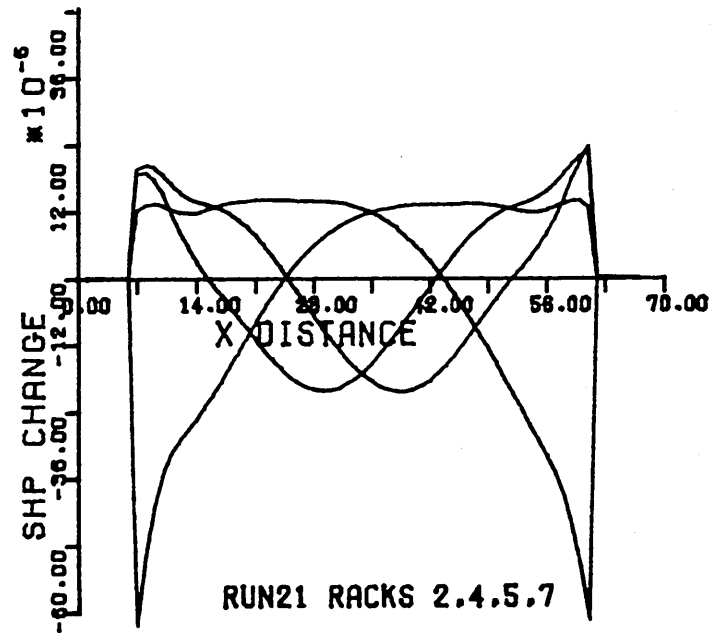
Fig. 6.22b.

Fig. 6.22. Shape profiles for RUN 21.
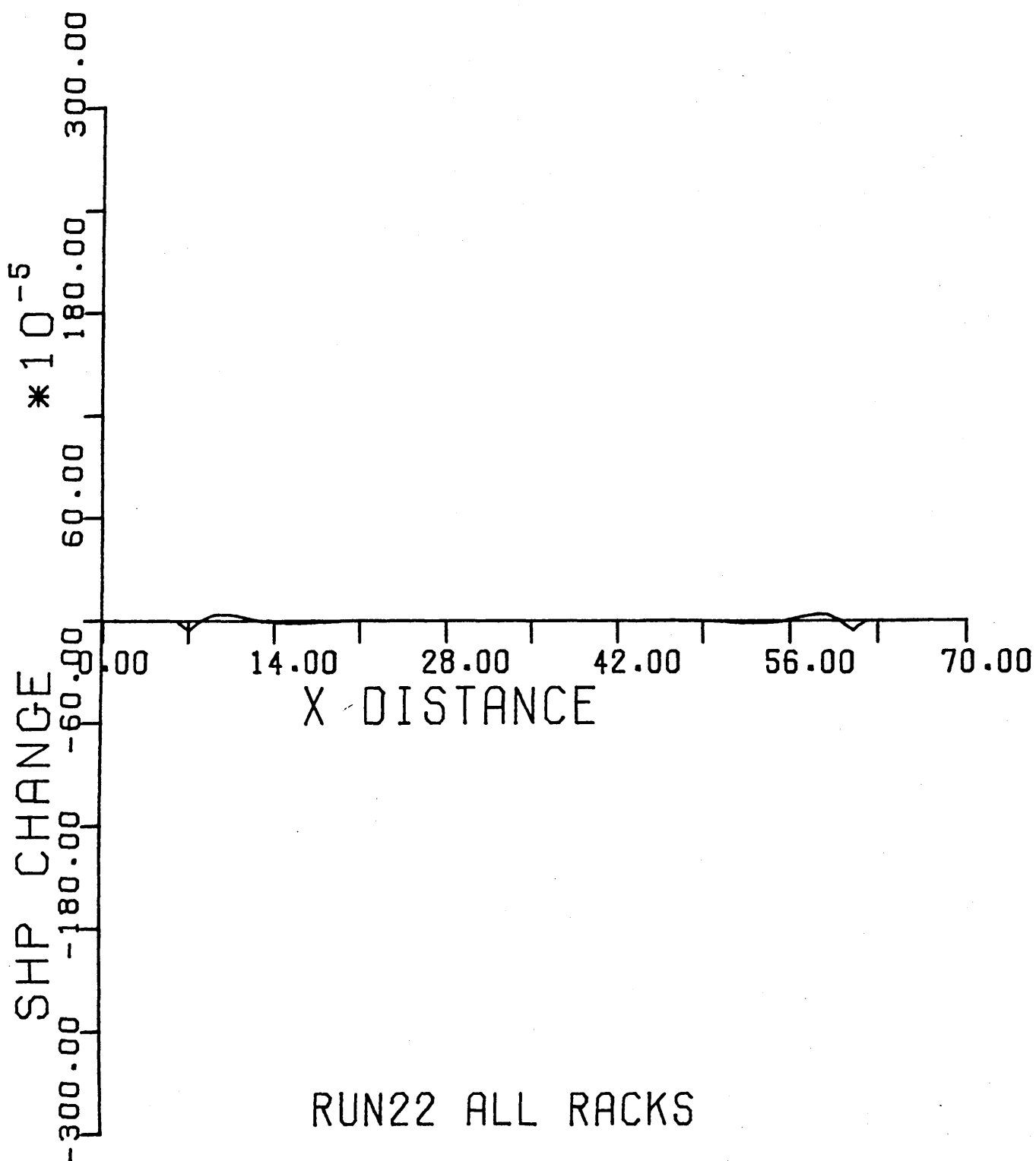
Fig. 6.23. Shape profile for RUN 22.
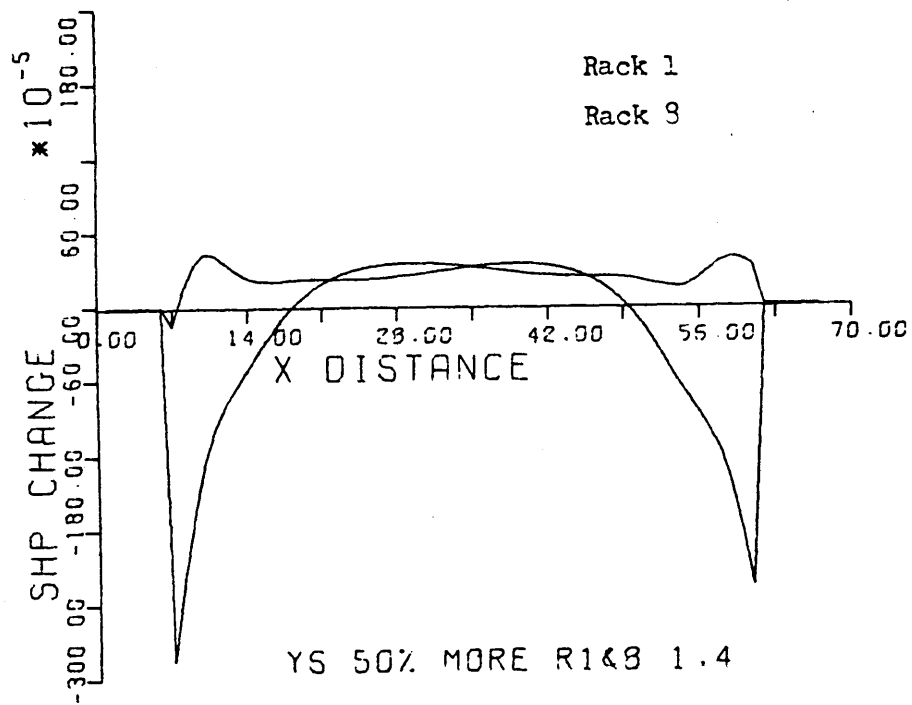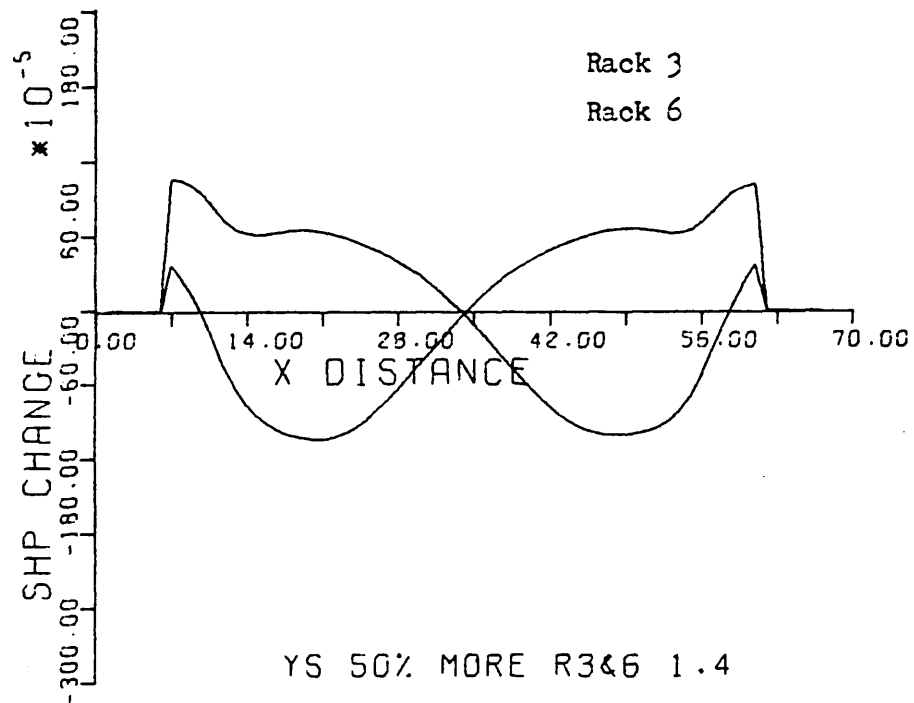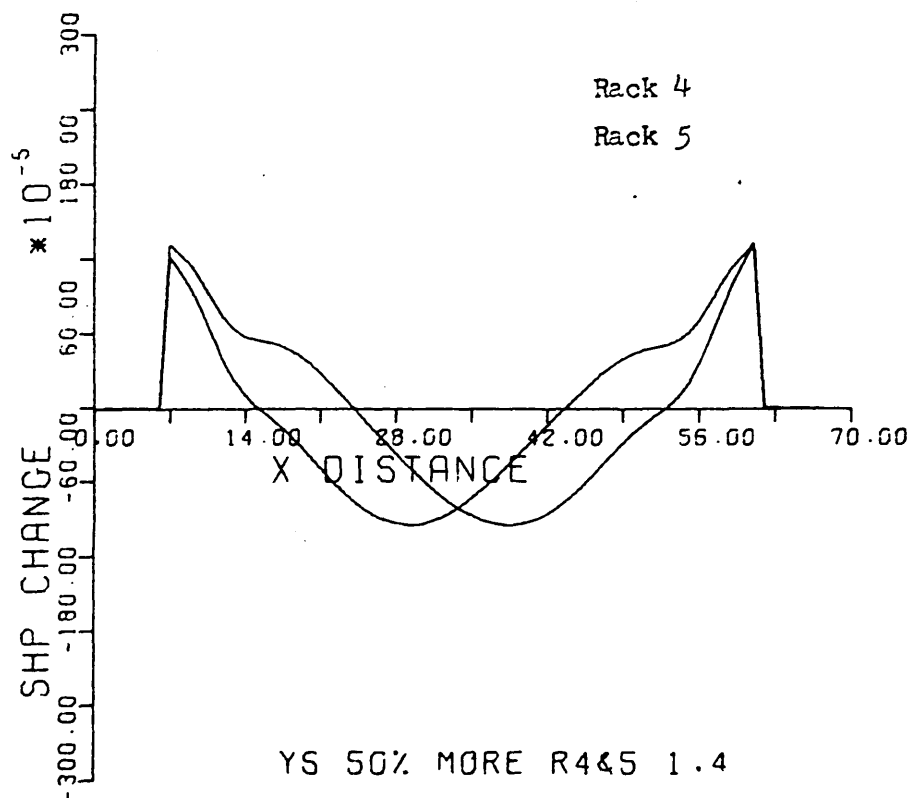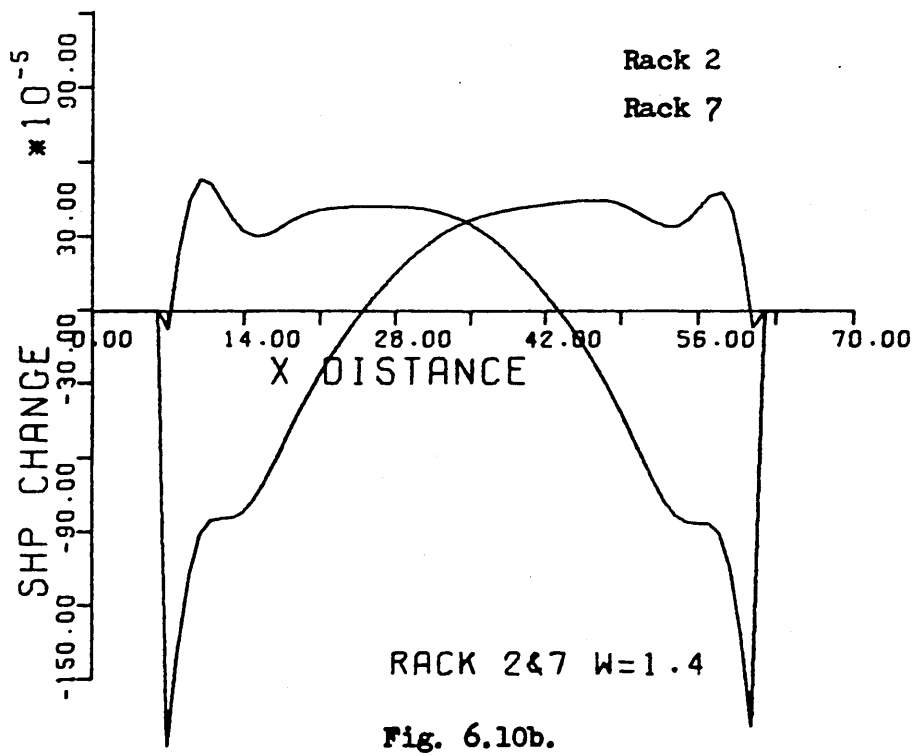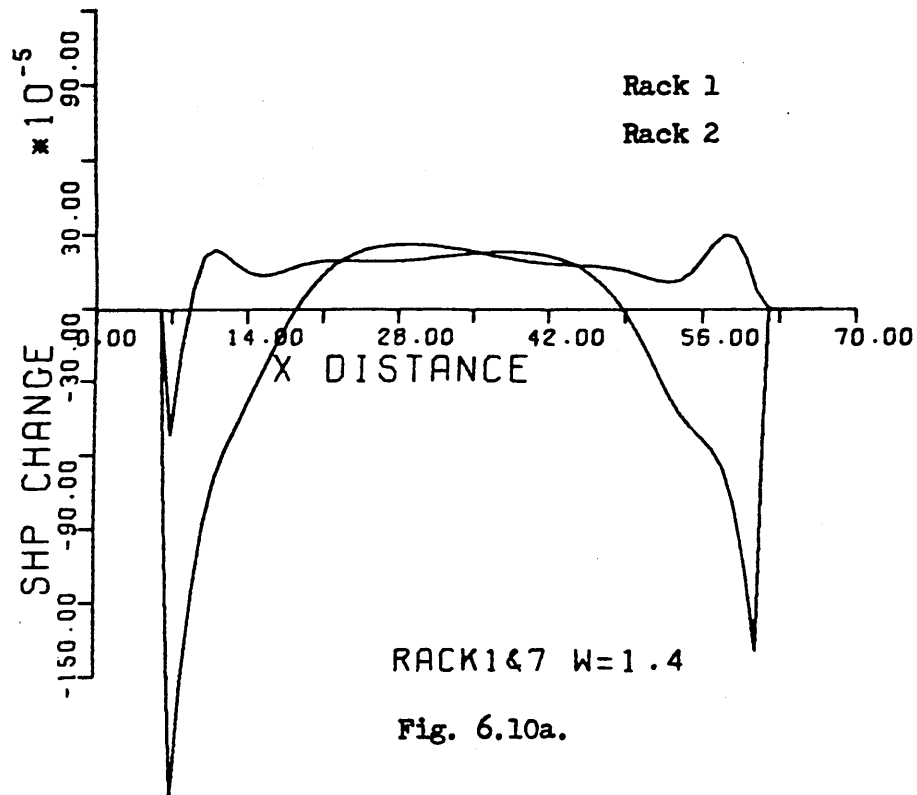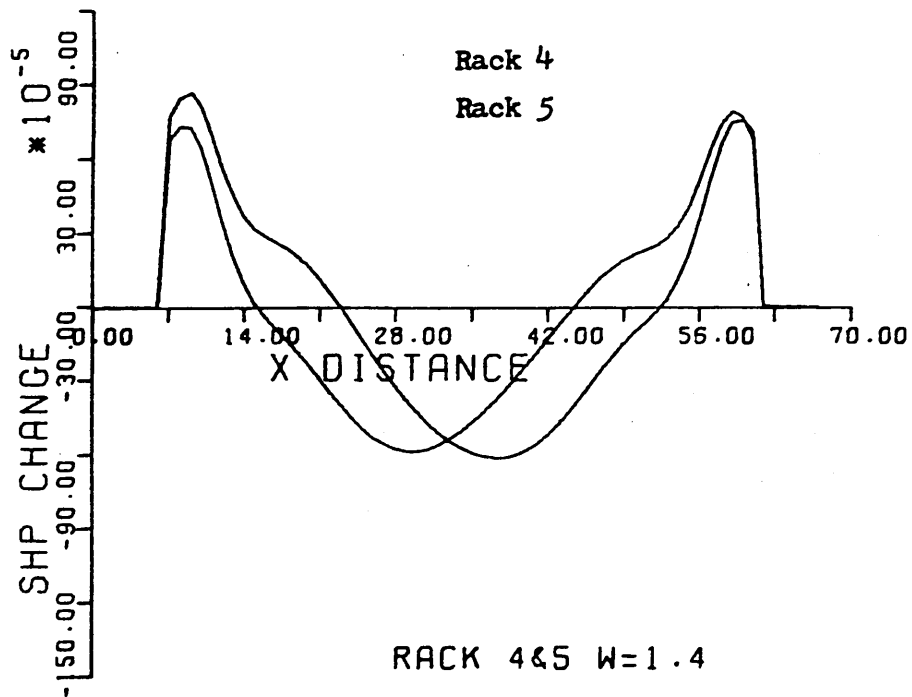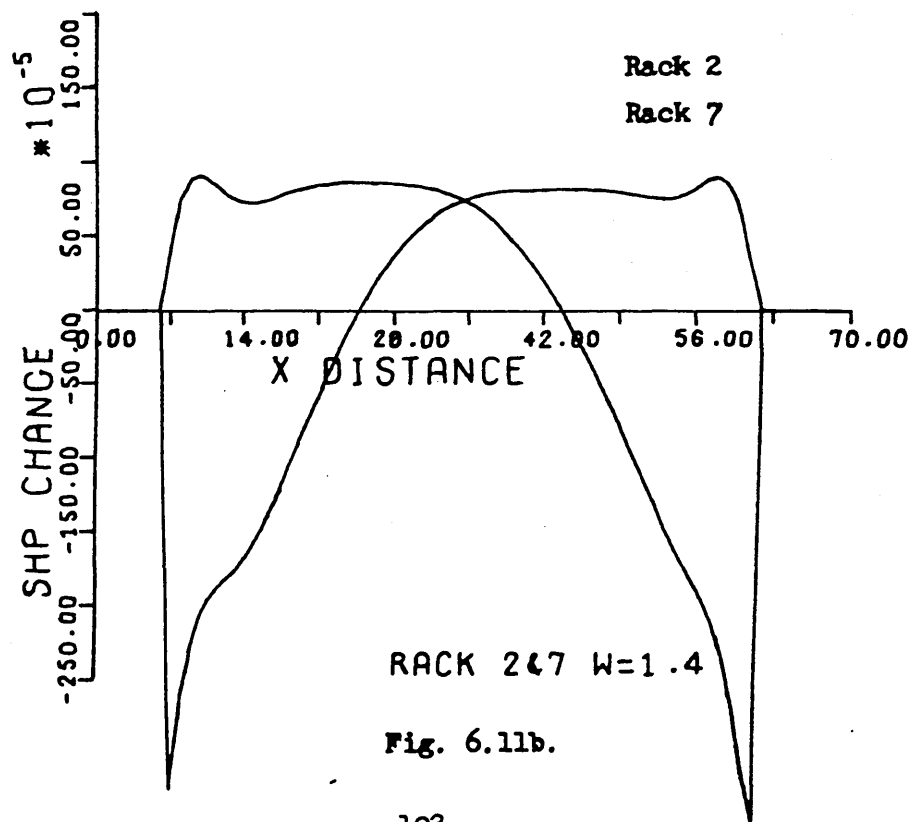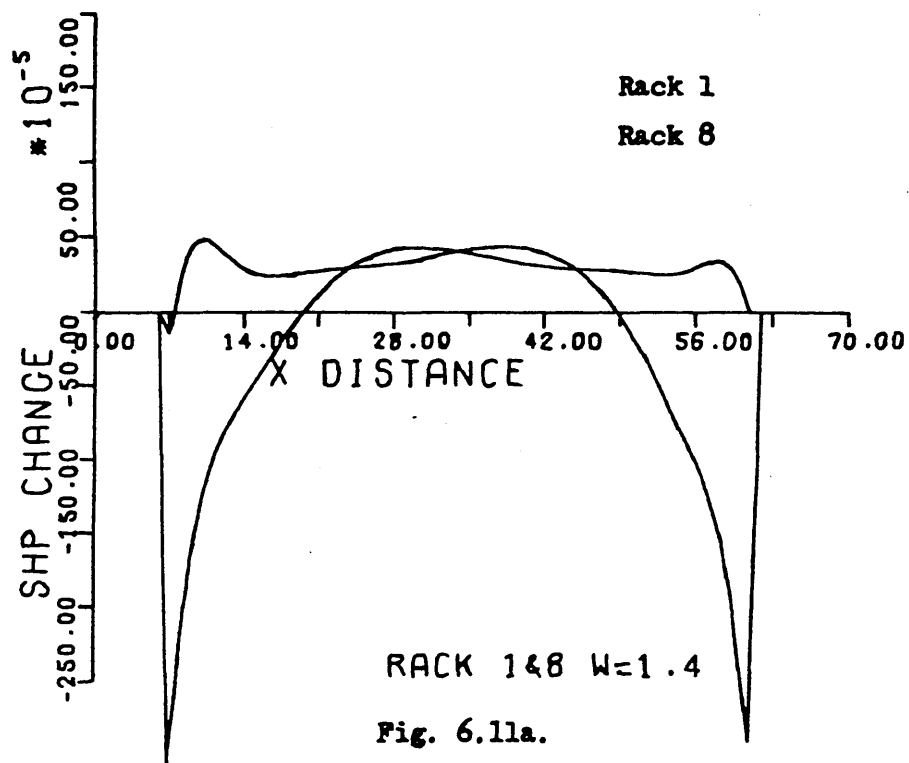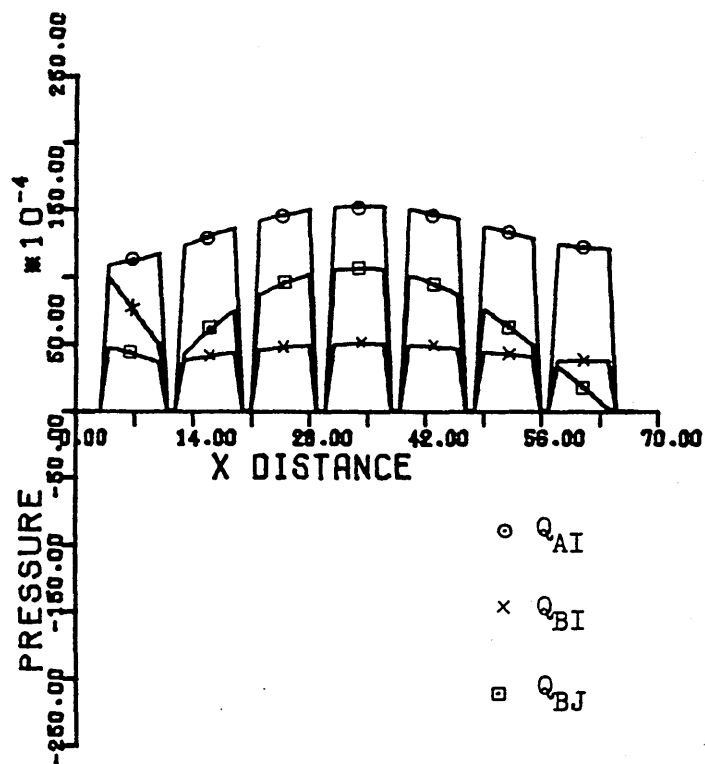
Fig. 6.24a.
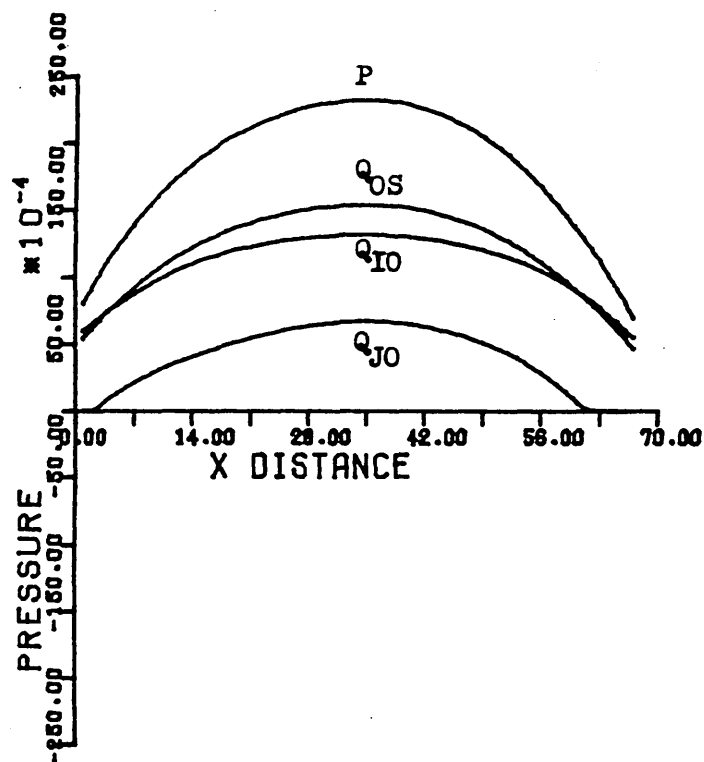
Fig. 6.24b.

Fig. 6.24. Inter-roll pressure profiles for RUN 1.
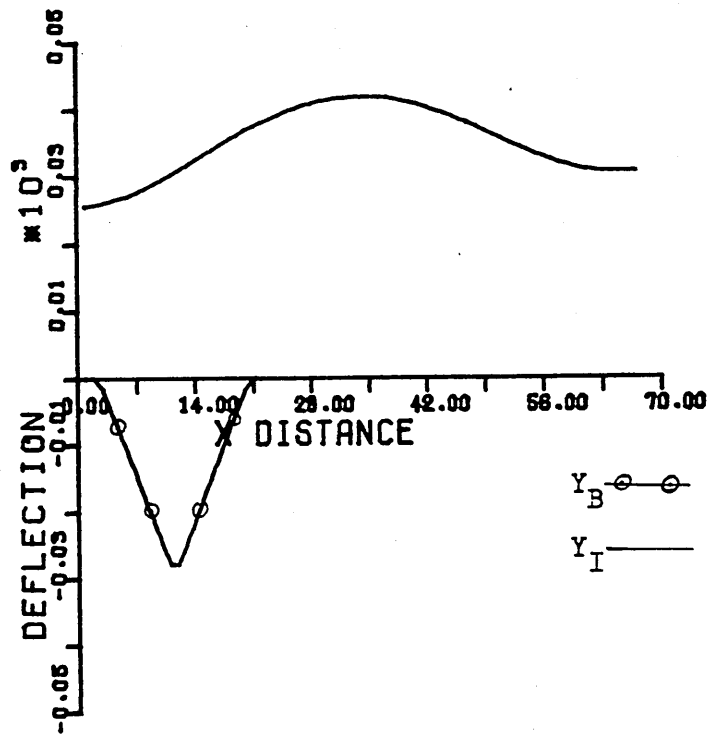
Fig. 6.25a.
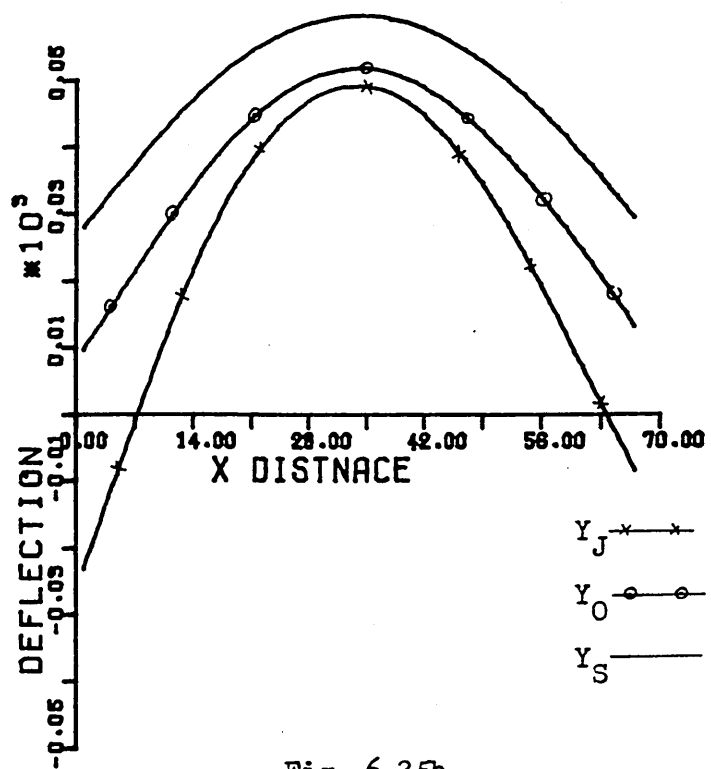
Fig. 6.25b.

Fig. 6.25. Roll deflections for RUN 1.
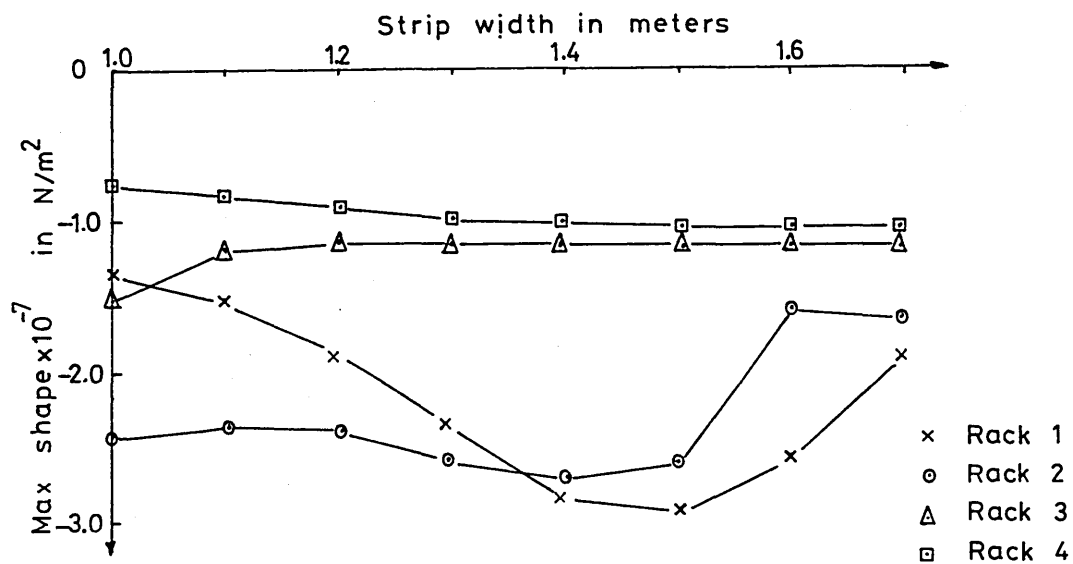
Fig. 6.26a.
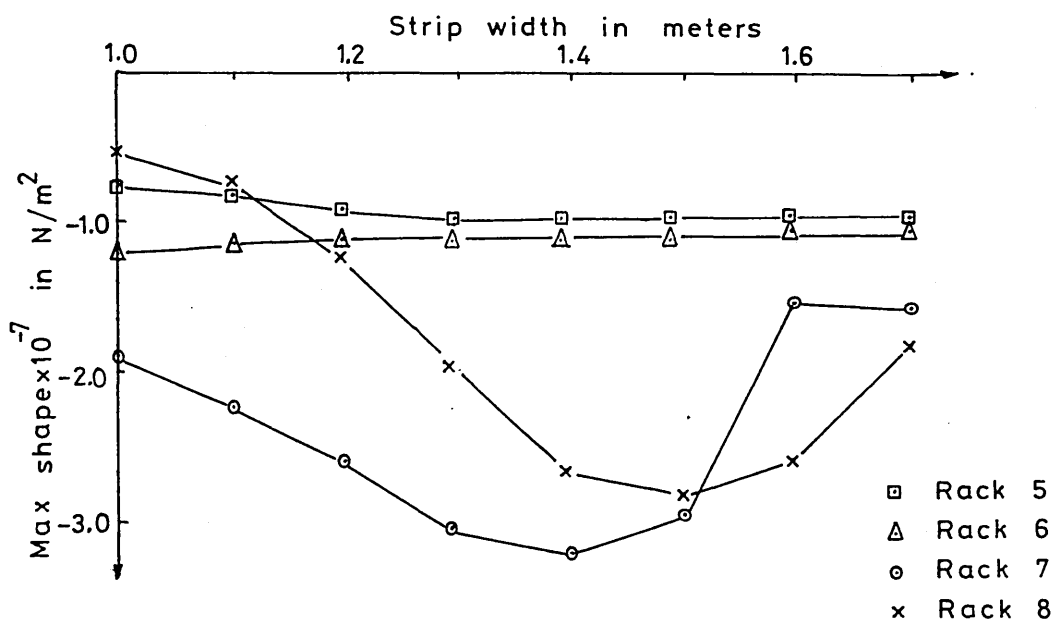
Fig. 6.26b.

Fig. 6.26. Variation in maximum shape with strip width.

Chapter 7.

CONCLUSIONS.

7.1. General conclusions.

In early days of rolling, mills were designed with the knowledge of how to obtain a desired result. In many cases the reasons were unknown and the practical knowledge was more advanced than the theory. The experience of success through failure stimulated the understanding of rolling. As technology advanced the demand for better products with uniform gauge and reasonable flatness increased. This needed the rolling mill research, which provides the knowledge and know how of rolling and shows ways of improvement.

The subject of this study is the 1-2-3-4 Sendzimir mill which has several advantages over conventional mills. The design of this mill permits a roll separating force to be transmitted through the mill cluster directly to the rigid mill housing and the support of the work rolls throughout their length. This allows the use of smaller work rolls. The first intermediate rolls are furnished with tapered ends which is an added advantage. Another feature is that the back-up roll has eight racks, which can be used to set any desired profile on the back-up roll.

In recent years, the gauge control problem has largely been solved. The major problem of current interest is the shape control problem or the control of internal stress. The main task of a shape control system is to produce a strip with very low or no transverse variations in stress at the mill exit. If it is a multistand mill, appreciable stress variations may be present between intermediate stands without affecting the primary aim, provided that buckling and edge tears do not develop. This is because the input stress has little influence on the output stress profile.

In general gauge and shape errors occur together. A gauge corrective action, such as a change in side screwdown settings, alters the roll force distribution across the roll gap and this influences the shape. Likewise a shape corrective action, such as a change in tension, changes the roll force which alters the mutual flattening between work roll and strip, and therefore gauge is affected. As a result separate control of shape and gauge is, in general, undesirable and it is advantageous to control both these quantities simultaneously in one integrated scheme. However, in most existing mills a gauge control system is already installed. Combined shape and gauge control schemes must be designed for new mills and the control system of existing mills must be redesigned by adding the shape control system. For a shape control

system to be successful the following requirements should be met:

1. The system should be non-interactive. This means corrective actions should not interfere with one another.

2. The steady state shape errors after a disturbance must be zero.

3. The overall system must be stable. This means that the system will settle to a steady state condition in a finite time interval after it is disturbed.

One of the main obstacles for automatic shape control system design was the availability of a reliable shape measuring device. There are two basic types of shape measuring instruments available, namely non-contact and contact instruments. The non-contact instruments or magnetic instruments use the properties of the strip itself and so have to be calibrated for each material and gauge. The contact instruments have the advantage of making a direct measurement and hence are independent of any intermediate material properties. The obvious difficulty is that of slip between strip and measuring roll, particularly during acceleration periods. This can be overcome to a large degree by using a high deflector or wrap angle. The Sendzimir mill in question uses a contact type instrument to measure the shape.

7.2. Shape profiles and static gains.

The study of any scheme for control of strip shape must be preceeded by an accurate analysis of the mill. The first requirement in the design of the shape control system for the Sendzimir mill is a mathematical model of the mill. Both static and dynamic models are required. The static model is a mechanical model which represents all force deformation relationships in the roll cluster and in the roll gap. The static model must allow for the bending and flattening of the rolls and for the plastic deformation of the strip in the roll gap. The model must provide mill gains and an understanding of the mechanisms involved. Such a model has been derived and presented in chapters 3 and 4. The model was developed in the form of a Fortran computer program. The model enabled the output shape profiles and hence the gains of the mill to be calculated and these were presented in chapter 6.

When the strip is placed at the centre of the mill, the shape profiles for racks 1 and 8 must be symmetrical about the vertical axis passing through the centre of the mill. (Similarly the profiles for racks 2 and 7, for racks 3 and 6 and for racks 4 and 5 should be symmetrical.) Inspection of all the shape profiles presented in chapter 6 verify this point.

Inspection of gain matrices presented in section 6.6 confirms the special property of symmetry discussed in section 6.2 if minor numerical errors are ignored. However, use of these symmetry properties may be made to reduce the effects of these numerical errors. Theoretically derived gain matrices must satisfy the properties described by eqs.(6.1) and (6.2). This means that G_m is not of full rank and therefore its inverse does not exist. It is seen, however, from section 6.6 that these matrices do not satisfy eqs.(6.1) and (6.2) and are of full rank. This is due to numerical problems and the sum of the column elements and the sum of the row elements will never be exactly zero.

The calculated gain matrices show that they are highly dependent on mill schedules. The strip width has a considerable effect on the shape and the variation of the gains is significantly large. The gains reduce with the strip width and the overall percentage change in gain show that the relationship is roughly linear. The hardness of the material being rolled has an effect on the shape and the results show that the gain becomes less when rolling harder materials. Softer materials are more likely to have worse shape defects.

The percentage reduction and the magnitude of mean thicknesses seem to affect the shape quite significantly. The results show that it is easier to

control strip shape when rolling thicker materials. It is a well known fact that shape defects increase as the strip thickness reduces in size, and there is a minimum thickness of the strip that can be rolled with good shape, for given rolling conditions.

The shape is affected by the roll diameters and the variations are discussed in section 6.4. For bigger rolls the mill has reduced gains, and results are consistent for the three cases considered (work roll, first and second intermediate rolls).

A slight change in the cluster angles will change the shape profile, as this will move the position of cluster rolls thus changing rolling pressures. For the case considered the gain has increased.

The output tensile force investigation shows that the shape defects increase with the reduction of tensile force. This is so as the buckling will increase with the reduction in tension.

The first intermediate rolls seem to have a greater effect on strip shape. The movement of the first intermediate rolls is available as a control input to the system. In normal practice the position of the tapered wedge is used to relieve the stress at the strip edge. Here the gain is increased when these rolls are pushed into the mill. This area must be investigated further.

- 217 -

The gain matrix is checked by increasing the
rack position by twice the distance, and obviously the
shape must be twice as before. It is seen that the gain
matrix remains almost the same, and the small variation
is due to numerical errors.

The derived model is based on theoretical
results and the accuracy of the model will depend upon
the assumptions made. One such assumption is that the
additional stresses at the strip edges due to roll
flattening are neglected. This will introduce errors into
the final results. When calculating the deflections of the
rolls the contribution due to shear is neglected This will
also introduce some minor errors.

The roll force model does not involve an
iterative procedure but uses an approximate explicit
solution. However, the iterative solution which employs
Hitchcock's formula is more accurate. These two methods of
solution of roll force were compared against different
input/output thicknesses, input/output tensions and input/output
yield stresses. The error of the approximate solution
was found to be less than 1 %.

7.3. Shape control design.

The design of closed loop shape control
systems is a relatively new problem. There is difficulty
in defining the dynamic model of the mill due to lack of

work in this area. For example, the best way to represent the strip transfer function is still debated. Identification methods can be helpful in choosing the most appropriate reperesentation of elements. However, the Sendzimir mill is used to roll stainless steel and therefore such tests can be expensive. A dynamic model is clearly necessary to test the controller design under various operating conditions.

Bad shape is often caused by the mismatch between the roll gap profile and the incoming strip thickness profile. It follows that in order to affect a change in shape of the rolled strip, one must alter either the cross sectional profile of the ingoing strip or the profile of the loaded roll gap. An idea for altering the input thickness has been patented[62] but so far this principle has not been tried. The latter method is used to regulate the shape of the mill in question.

The actuator movements affect the shape as seen from the static model results. There are eight actuators whose movements can be controlled. When the actuators are moved, a roll bending effect is introduced, which is transmitted through the cluster to the work roll, thus affecting the roll gap profile. From the static model it is seen that the output tension affects the strip shape. This is so as the tension alters the roll force, and so the degree of flattening of the rolls and hence the loaded roll gap profile. It is also concluded that

the position of the first intermediate rolls has an effect
on shape. Another method which can be used aims at
changing the thermal camber of the rolls by altering the
amount and/or distribution of coolants. However, thermal
effects are not considered for the present analysis.
Basically the shape control system must therefore consist
of feedback loops from the shapemeter to the back-up roll
actuators, tension controls and first intermediate roll
positions.

The mechanical construction of the mill
ensures that there are significant interactions between
actuator inputs and shape changes at each zone. This is
confirmed from the mill gains calculated from the static
model. These interactions are non-dynamic and the dynamic
elements of the mill system are non-interactive. The gain
matrix elements calculated have significant uncertainty due
to the complexity of the model. Due to the properties of
the gain matrix described by eqs.(6.1) and (6.2) the
inverse does not exist and therefore the control system
design cannot be based on G_m^{-1}. The design must be
relatively insensitive to errors in calculating G_m,
variations in G_m and changes in line speed. This allows a
minimum number of controller gains and time constants to
be used and stored. Thus, the objective of the
multivariable design must be to produce a design which is
robust to modelling errors. The steps in the design

procedure may be to calculate the transformation matrix, to calculate appropriate pre and post compensators U and V to diagonalise, and to calculate a cascade compensator using single loop techniques. The control design is not the main topic of this study and therefore will not be discussed any further.

7.4. Future work.

The derived model is based on theoretical analysis and must be tested against plant test results. This may be expensive as the mill in question is used to roll stainless steel.

One of the assumptions used in deriving the model is that the stresses at the edge of the strip may be neglected. The work roll flattening is modelled using the Hertzian expression for flattening between cylinders and flat plates. The Hertzian expression is true for cylinders having uniform pressure distributions. Over most of the strip width this method provides adequate results as the variations in the roll force profile are small. In the region of the strip edges the errors generated will be high as the roll force suddenly drops to zero. However, the model must be modified, to include the roll flattening at the strip edges, using the influence functions developed by Spooner and Bryant[13] The results from the improved model must be checked against the present results for accuracy.

When calculating the deflections of the rolls, the contribution due to shear is neglected. This will introduce some errors and these errors must be checked by including this effect.

Some results are obtained by varying the constant β which appears in the stress equation. This constant is varied between 0.2 and 1.0 and the results seem to be insensitive to these values of β. This must be confirmed by further investigation. The model produces reasonable results for strip shape, but this must be confirmed by detailed experimental investigations. Normal operating records can be used where possible to test the model.

References.

1. CHARLES G S , 'The inventions of Leonardo da Vinchi', Phaidon, Oxford, 1978.

2. 'A history of technology and inventions', edited by M. DAUMAS, translated by E. B. HENNESSY, pub. John Murray, London, 1969.

3. BURSTALL A F, 'A history of mechanical engineering', Faber and Faber, 1963.

4. EARNSHAW I, KEEFE J, SCHOFIELD P A, Review of hot mill developments, Metal Society Inter Conf on 'Flat rolling: a comparison of rolling mill types', Univ of Cardiff, Sept 1978.

5. MORRIS N, SCHOFIELD W H, FRANCIS P I T, Review of cold rolling mills, ibid.

6. EDWARDS J K, Automation of tandem mills, ibid.

7. UNDERWOOD L R, 'The rolling of metals theory and experiance', Vol 1, Chapman & Hall, London, 1950.

8. WARD H W, The continuing development of Sendzimir multi roll cold rolling mills in world wide strip production, Sheet Metal Industries, May 1969.

9. Publicity brochure, Sendzimir cold rolling mills, Poole, Leowy Robertson Eng Co Ltd, 1973.

10. BILL A J, SCRIVEN H, Sendzimir mills for cold rolling in BSC Stainless, Metal Society Inter Conf on 'Flat rolling: a comparison of rolling mill types, Univ of Cardiff, Sept 1978.

11. KIRKHAM R, Shape requirements and the problems of bad shape as experienced by uses of cold reduced wide strip and sheet steel, Metals Society, Shape Control Conf, Chester, Mar 1976.

12. SHEPPARD T, Shape in metal strip: the state of the art, ibid.

13. SPOONER P D, BRYANT G F, Analysis of shape and discussion of problems of scheduling set-up and shape control, ibid.

14. PEARSON W K J, Shape measurement and control, J of the Inst of Metals, vol 93, 1964 - 65.

15. SABATINI B, YEOMANS I C A, An algebra of strip shape and its application to mill scheduling, J of the Iron and Steel Inst, vol 206, Dec 1968.

16. HARAGUCHI S, KAJIWARA T, HATA K, Shape of strip steel in cold rolling process, Bulletin of JSME, vol 14, no 67, 1971.

17. O'CONNER H W, WEINSTEIN A S, Shape and flatness in thin strip rolling, Trans of the ASME J of Eng for Industry, Nov 1972.

18. JORTNER D, OSTERLE J F, ZOROWSKI C F, An analysis of cold strip rolling, Int J Mech Sci, vol 2, 1960.

19. GUNAWARDENE G W D M, GRIMBLE M J, Development of a static model for a Sendzimir cold rolling mill, presented at IMACS(AICA) symposium on Simulation of control systems, Tech Univ, Vienna, Austria, Sept 1978.

20. BUTTERFIELD M H, Set up by computer, and automatic gauge control of a 4 stand cold steel strip mill, Trans of the Society of Instrument Technology, Sept 1965.

21. GRIMBLE M J, Shape control for rolled strip, Inst Mech Eng, vol 92, Nov 1975.

22. DAVIES N, Measurement of strip shape, speed and length, Iron and Steel, Aug 1972.

23. BRAVINGTON C A, BARRY D C, McCLURE C H, Design and development of shape control system, Shape Control Conf, Metal Society, Chester, Mar 1976.

24. EDWARDS W J, SPOONER P D, Analysis of strip shape, from 'Automation of tandem mills', edited by G. F. BRYANT, pub by Iron and Steel Inst, 1973.

25. PAWELSKI O, SCHULER V, BERGER B, Development of a shape control system in cold strip rolling, Proc ICSTIS section 4, suppl Trans ISIJ, vol 11, 1971.

26. SHEPPARD T, ROBERTS J M, Shape control and correction in strip and sheet, Int Metallurgical Reviews, vol 18, 1973.

27. SANTO T, SAKAKI T, MATSUSHIMA T, SHIBATA H, EMORI T, ARIMIZU M, Automatic shape control, Proc of Int Conf on the Science and Technology of Iron and Steel, Tokyo, Sept 1970.

28. WISTREICH J G, Control of strip shape during rolling, J of the Iron and Steel Inst, Dec 1968.

29. SANSOME D H, Factors affecting the shape of strip emerging from a rolling mill, Metals Technology, Nov 1975.

30. SIVILOTTI O G, DAVIES W E, HENZE M, DAHLE O, ASEA-ALCAN AFC system for cold rolling flat strip, Iron and Steel Eng, Jun 1973.

31. KNOX T J, Operating experience with the Leowy Robertson Vidimon Shapemeter at Shotton works, Shape Control Conf, Metal Society, Chester, Mar 1976.

32. HENZE M, NILSSON A, Development of a new generation of STRESSOMETER shapemeter system, ibid.

33. WORTBERG H J, Operating experiences with the STRESSOMETER installed in cold mills at Alunorf GmbH, Federal Republic of Germany, ibid.

34. ASEA publicity pamphlet no AV83-102E, Jan 1971.

35. IWAWAKI A, SHIBATA H, EMORI T, Operating experience with the shapemeter for hot rolling mill, Shape Control Conf, Metal Society, Chester, Mar 1976.

36. URAYAMA S, TAKATOKU Y, NIWA Y, SAWADA Y, Experience in developing shape control for a Sendzimir mill, ibid.

37. STONE M D, GRAY R, Theory and practical aspects in crown control, Iron and Steel Eng, Aug 1965.

38. PAWELSKI O, SCHULER V, Time behaviour of thermal roll gap variation during cold rolling of strip, British Iron and Steel Translation Service, Sept 1972.

39. GUNAWARDENE G W D M, GRIMBLE M J, THOMSON A, Static model for Sendzimir cold rolling mill, Metals Technology, Jul 1981.

40. HETENYI M, 'Beams on elastic foundations', Univ of Michigan Press, 1946.

41. TIMOSHENKO S, GOODIER J N, 'Theory of elasticity', McGraw Hill, New York, 1951.

42. BLAND D R, A theoretical investigation of roll flattening, Proc Inst Mech Eng, vol 163, 1950.

43. ROARK R J, YOUNG W C, 'Formulas for stress and strain', 5th edition, McGraw Hill, 1975.

44. OROWAN E, The calculation of roll pressure in hot and cold flat rolling, Proc Inst Mech Eng, vol 150, 1943.

45. BLAND D R, FORD H, The calculation of roll force and torque in cold strip rolling with tensions, Proc Inst Mech Eng, vol 159, 1948.

46. GRIMBLE M J, FULLER M A, BRYANT G F, A non-circular arc roll force model for cold rolling, Int J for Numerical Methods in Eng, vol 12, 1978.

47. HITCHCOCK J H, Roll neck bearings, Report of ASME Research Commitee, 1935.

48. BRYANT G F, OSBORNE R, Derivation and assessment of roll force models, from 'Automation of tandem mills', edited by G. F. BRYANT, pub Iron and Steel Inst, London, 1973.

49. POLUKHIN V P, TUTYNIN V K, Calculation of inter roll pressures on multi roll mills, Izv Vuz Chern Met, 1973 (12), Translation BISITS 12222, Apr 1974.

50. KUO B C, 'Discrete data control systems', Prentice Hall Inc, 1970.

51. SAUCEDO R, SCHIRING E E, 'Introduction to continuous and digital control systems', Macmillan, 1968.

52. Research Report, edited by M. J. GRIMBLE, No EEE/36, Sheffield City Polytechnic, Mar 1979.

53. GRIMBLE M J, M.Sc. Thesis, Univ of Birmingham, 1971.

54. GRIMBLE M J, Catenary controls in metal strip processing lines, GEC J of Sci and Tech, vol 41, No 1, 1974.

55. GRIMBLE M J, Tension controls in strip processing lines, Metals Technology, Oct 1976.

56. DRAPER N R, SMITH H, 'Applied regression analysis', John Wiley, 1966.

57. MACFARLANE A G J, KOUVARITAKIS B, A design technique for linear multivariable feedback systems, Inst J Cont, vol 25, No 6, 1977.

58. ROSENBROCK H H, 'Computer aided control system design', Acadamic Press, 1974.

59. MACDUFFEE C C, 'The theory of matrices', Berlin: Springer, 1933.

60. KLEMA V C, LAUB A J, The singular value decomposition: its computation and some applications, IEEE Trans on Automatic Control, vol AC-25, No 2, Apr 1980.

61. GARBOW B S et al, Matrix eigensystem routines - EISPACK Guide Extension (Lect notes in computer science), vol 51, New York: Springer-Verlag, 1977.

62. Brit. Patent 1002936, 1964.

Bibliography.

1. BELLMAN R, 'Introduction to matrix algebra', McGraw Hill, 1970.

2. BERNSMANN G P, Lateral flow during cold rolling of strip, Iron and Steel Eng, Mar 1972.

3. CARLTON A J, EDWARDS W J, JOHNSTON P W, KUHN N, A sub-optimal approach to the scheduling of multistand cold rolling mills, The J of the Australian Inst of Metals, vol 18, no 1, 1973.

4. CARTER C E, GRIMBLE M J, Dynamic simulation and control of a Sendzimir cluster mill, Int Conf on Systems Eng, Lanchester polytechnic, Sept 1980.

5. CONTE S D, 'Elementary numerical analysis', McGraw Hill, New York, 1965.

6. CUMMING I G, SANDERS C, On line identification of tandem mills, from 'Automation of tandem mills', edited by G F BRYANT, pub by Iron and Steel Inst, 1973.

7. DAHM J R, On line sensor gages shape of strip steel, Instrumentation Technology, May 1970.

8. DOWSING R J, Rolling mill design matches modern flat rolling practice, Metals and Materials, Nov 1978.

9. EDWARDS W J, The influence of strip width on rolling mill stand deformation, Conf on Stress and Strain in Eng, Inst of Eng, Brisbane, Australia, Aug 1973.

10. FOTAKIS I E, Design of optimal control systems and industrial applications, Ph.D. Thesis, Sheffield City Polytechnic, 1981.

11. GRAYBILL F A, 'Introduction to matrices with application in statistics', Wadswath Publishing Co, Belmont, California, 1969.

12. GRIMBLE M J, A roll force model for tinplate rolling, GEC J of Science & Technology, vol 43, no 1, 1976.

13. GRIMBLE M J, Solution of the non-linear functional equations representing the roll gap relationships in a cold mill, J of Optimisation Theory and Applications, vol 26, no 3, Nov 1978.

14. GRIMBLE M J, Ph.D. Thesis, Univ of Birmingham, 1974.

15. GRIMBLE M J, FOTAKIS J, The design of strip shape control systems of Sendzimir mill, IEEE Trans on Automatic Control, vol AC27, no 3, Jun 1982.

16. HERMAN A S Jr, WRIGHT J, Determination of hot strip mill torque amplification factors, Iron & Steel Eng, Dec 1969.

17. HONJYO H, WATANABE H, Impact loading and vibration of the slabbing mill, Iron & Steel Eng, May 1975.

18. HUGGINS P J G, Roll indentation: Its relation to limiting thickness in cold rolling, J of Inst of Metals, 1966.

19. LARKE E C, 'The rolling of strip, sheet and plate', Chapman & Hall, 1957.

20. LOSS F J, WEINSTEIN A S, ZOROWSKI C F, Elastic behaviour in cold strip rolling at the onset of plasticity, J of the Inst of Metals, vol 92, 1963.

21. MORLEY A, 'Strength of materials', 11th edition, Longmans, 1954.

22. NOEL J H, MACDONALD A J, LATIMAR J V, Operating experience of the electric drives and control systems of an 84-inch cold rolling mill, IEEE Trans on Industry and General Applications, May/Jun, 1965.

23. OHAMA T, SASAKI S, SENDZIMIR M G, World's first Sendzimir tandem mill, Iron & Steel Eng, Apr 1973.

24. PAWELSKI O, SCHULER V, Experiments in controlling the flatness in cold strip rolling (BISI 9156) Stahl Eisen, 90 (22), 1970.

25. POLAKOWSKI N H, REDDY D M, SCHEISSING H N, Principles of self control of product flatness in strip rolling mills, Trans of the ASME J of Eng for Industry, Aug 1969.

26. RADZIMOVSKY E I, Stress distribution and strength condition of two rolling cylinders pressed together, Univ of Illinois Bulletin no 408, Feb 1953.

27. SABATINI B, WOODCOCK J W, YEOMANS K A, Shape regulation in flat rolling, J of the Iron & Steel Inst, Dec 1968.

28. SAXL K, Transverse gauge variation in strip and sheet rolling, Proc of the Inst of Mech Eng, vol 172, no 22, 1958.

29. SHIOZAKI H, The calculation of roll bending effects, IHI Eng Review, Special Issue, Jun 1970.

30. SHOHET K N, TOWNSEND N A, Roll bending methods of crown control in four high mills, J of the Iron & Steel Inst, Nov 1968.

31. SMITH J J, Torque monitoring for failure prevention on mill spindles and couplings, Iron & Steel Eng, Nov 1976.

32. SOROKIN V O, Design and operation of tensiometers, Iron & Steel Eng Year Book, 1961.

33. SPOONER P D, SMYTH R M, Diameter of back-up rolls in a 4-high rolling stand, Metals Technology, Nov 1975.

34. THOMAS H R, HOERSCH V A, Stresses due to pressure of one elastic solid upon another, Univ of Illinois Eng Experiment Station, Bulletin no 212, Jul 1930.

35. WILMOTTE S, MIGGON J, ECONOMOPOULOS M, A study of the cross profile of hot rolled strip, CRM no 30, Mar 1972.

36. YAMAZAWA K, Automation of the mill plant control system on the cold mill, IHI Eng review, Special Issue, Jun 1970.

37. YOKOTA T, ANBE Y, EZURE H, Hybrid simulation of tension control system for hot tandem mills, 'Simulation of Systems', ed by L DEKKAR, North Holland Publishing Co, 1976.

Appendix 1.

Forces in the Roll Gap.

By referring to fig.4.15 in which the width of the material is taken as unity, it will be seen that the normal force L acting on the elemental length AB due to a stress s is given by

$$L = sAB. \tag{A1.1}$$

The horizontal component is

$$L_h = sAB\sin\phi . \tag{A1.2}$$

Similarly the frictional force N acting on AB is

$$N = \mu sAB \tag{A1.3}$$

where μ is the coefficient of friction between strip and work roll.

From the plane of entry to the neutral plane the force N acts as a tensile pull on the material, while from the neutral plane to the plane of exit it acts as a compressive force. If compressive forces are taken as positive then over the full length of the arc of contact the horizontal component N_h can be written as

$$N_h = \mp \mu sAB\cos\phi . \tag{A1.4}$$

Here the negative sign refers to the entry zone. The total horizontal force is given by

$$L_h + N_h = sAB(\sin\phi \mp \mu\cos\phi) \tag{A1.5}$$

and by taking both rolls into account the force dF acting on the element dx is given by

$$dF = 2sAB(\sin\phi \mp \mu\cos\phi).$$ (A1.6)

Now

$$AB = Rd\phi$$

thus

$$\frac{dF}{d\phi} = 2Rs(\sin\phi \mp \mu\cos\phi).$$ (A1.7)

With the assumption of homogeneous plane deformation the stress f corresponding to a horizontal force F is given by

$$f = F/h$$ (A1.8)

which is taken as one of the three principal stresses. The other two principal stresses are q, the vertical component of the radial stress, and w which acts at right angles to both q and f. Then from Huber-von Mises equation we have

$$(q - f)^2 + (f - w)^2 + (w - q)^2 = 2K^2$$ (A1.9)

where K is the basic resistance to homogeneous compression.

If it is assumed that the width of the material suffers no strain then

$$\frac{1}{E}\left[w - v(q + f)\right] = 0 .$$ (A1.10)

The Poison's ratio v for plastic deformation is $\frac{1}{2}$ and

this gives

$$w = \tfrac{1}{2}(q + f).$$ (A1.11)

By substituting this value in eq.(A1.9) and simplifying we have

$$f = q - 1.555K$$

$$= q - k$$ (A1.12)

where k is the resistance to plane homogeneous deformation. This gives

$$F = h(q - k)$$ (A1.13)

and

$$\frac{dF}{d\phi} = \frac{d}{d\phi}\left[hk(\frac{q}{k} - 1)\right]$$

$$= hk \frac{d(q/k)}{d\phi} + (\frac{q}{k} - 1)\frac{d(hk)}{d\phi} .$$ (A1.14)

Bland and Ford assume the second term of eq.(A1.14) to be zero. It is also reasonable to assume the vertical pressure q is approximately equal to s. By eliminating $dF/d\phi$ from eqs(A1.7) and (A1.14) and rearranging we have

$$\frac{d(q/k)}{d\phi} \Big/ (q/k) = \frac{2R}{h}(\sin\phi \mp \mu\cos\phi).$$ (A1.15)

From fig.4.14

$$h = 2m + h_2$$ (A1.16)

and

$$\tan(\phi/2) = m/\ell .$$ (A1.17)

- 237 -

In cold rolling small angles are involved and therefore ϕ is very small. i.e,

$$\phi = 2m/\ell .\tag{A1.18}$$

But

$$\ell = R\phi \tag{A1.19}$$

and from eqs.(A1.16) to (A1.19) we have

$$h = h_2 + R\phi^2$$

and

$$\sin\phi \mp \mu\cos\phi \simeq \phi \mp \mu.\tag{A1.20}$$

Eq.(A1.15) becomes

$$\frac{d(q/k)}{d\phi} \bigg/ (q/k) = \frac{2R(\phi \mp \mu)}{h_2 + R\phi^2} .\tag{A1.21}$$

By integrating both sides of eq.(A1.21) we have

$$\log_e\left(\frac{q}{k}\right) = \log_e \frac{h_2 + R\phi^2}{R} \mp 2\mu\sqrt{\frac{R}{h_2}}\cdot\tan^{-1}\left(\sqrt{\frac{R}{h_2}}\phi\right) + \log_e A$$

$$= \log_e\left(\frac{h}{R}\right) \mp \mu H + \log_e A \tag{A1.22}$$

where

$$H = 2\sqrt{\frac{R}{h_2}}\cdot\tan\left(\sqrt{\frac{R}{h_2}}\phi\right).\tag{A1.23}$$

Eq.(A1.22) can be simplified as

$$q = A\cdot\frac{hk}{R}\,e^{\mp\mu H} .\tag{A1.24}$$

At the entry plane the angle $\phi = \theta$ and

$$H = H_1 = 2\sqrt{\frac{R}{h_2}} \cdot \tan^{-1}\left(\sqrt{\frac{R}{h_2}}\,\theta\right) \tag{A1.25}$$

and putting $k = k_1$ at this plane, from eq. (A1.24) we have

$$A = \frac{Rq}{h_1 k_1} e^{\mp \mu H_1} . \tag{A1.26}$$

If a decoiler tension σ_1 is applied at the entry side and since tensile forces are negative the value of f in eq. (A1.12) equals $-\sigma_1$ and

$$q = k_1 - \sigma_1 \tag{A1.27}$$

giving

$$A = \frac{R}{h_1} (1 - \sigma_1/k_1) e^{\mu H_1}. \tag{A1.28}$$

By substituting this in eq. (A1.24) for the entry zone we have

$$q = \frac{hk}{h_1} (1 - \sigma_1/k_1) e^{\mu(H_1 - H)} \qquad \text{(entry zone)}. \tag{A1.29}$$

At the exit plane the angle ϕ is zero and therefore H is also zero. By putting $k = k_2$ at this plane in eq. (A1.24) we have

$$A = \frac{Rq}{h_2 k_2} . \tag{A1.30}$$

With a coiler tension of σ_2 the magnitude of q at the

- 239 -

exit plane is, from eq.(A1.12)

$$q = k_2 - \sigma_2 \qquad\qquad (A1.31)$$

and

$$A = \frac{R}{h_2}(1 - \sigma_1/k_2). \qquad\qquad (A1.32)$$

By substituting this value of A in eq.(A1.24) for exit zone we have

$$q = \frac{hk}{h_2}(1 - \sigma_2/k_2)e^{\mu H} \qquad\text{(exit zone).}\qquad (A1.33)$$

By denoting the neutral plane by n the neutral angle θ_n can be obtained from eq.(A1.29) and (A1.33) since q_n has the same value in both of these equations. i.e.,

$$q_n = \frac{h_n k_n}{h_1}(1 - \sigma_1/k_1)e^{\mu(H_1 - H_n)} = \frac{h_n k_n}{h_2}(1 - \sigma_2/k_2)e^{\mu H_n}. \quad (A1.34)$$

By simplifying eq.(A1.34) we have

$$H_n = \frac{H_1}{2} - \frac{1}{2\mu}\log_e\left[\frac{h_1}{h_2} \cdot \frac{(1 - \sigma_2/k_2)}{(1 - \sigma_1/k_1)}\right]. \qquad (A1.35)$$

Substituting H_n for H in eq.(A1.23) and putting $\phi = \theta_n$, gives

$$\theta_n = \sqrt{\frac{h_2}{R}}\ \tan\left(\sqrt{\frac{h_2}{R}} \cdot \frac{H_n}{2}\right). \qquad (A1.36)$$

- 240 -

APPENDIX 2.

Theory on Elastic Foundations.

A2.1. The differential equation of the elastic foundation.

Consider a straight beam supported along its entire length by an elastic medium and subjected to vertical forces acting on the beam as shown in fig. A2.1. Because of the action of forces, the beam will bend, producing a continously distributed reaction force on the elastic foundation. These reaction forces are assumed to be proportional to the deflection of the beam as the supporting medium is elastic, i.e.

$$q = K \cdot y \qquad\qquad (A2.1)$$

where K is the constant of proportionality known as the elastic foundation constant.

Consider an infinitely small element whose length is taken at a distance x from the left hand corner. Consider also the forces acting on this element as shown in fig. A2.2. The upward acting shear force Q and the clockwise bending moment M to the left of the cross section are assumed to be positive. For equilibruim,

$$Q - (Q + dQ) + K \cdot y \cdot dx = 0 \qquad\qquad (A2.2)$$

$$\therefore \frac{dQ}{dx} = K \cdot y \ . \qquad\qquad (A2.3)$$

But

$$Q = \frac{dM}{dx} \qquad\qquad (A2.4)$$

$$\therefore \quad \frac{dQ}{dx} = \frac{d^2M}{dx^2} = K \cdot y \quad . \tag{A2.5}$$

Now the bending moment M is given by

$$M = - E \cdot I \cdot \frac{d^2y}{dx^2} \tag{A2.6}$$

Therefore from eqs. (A2.5) and (A2.6),

$$\frac{d^4y}{dx^4} + \frac{K}{E \cdot I} \cdot y = 0 \tag{A2.7}$$

Let

$$\lambda = \left(\frac{K}{4 \cdot E \cdot I} \right)^{\frac{1}{4}} \tag{A2.8}$$

$$\therefore \quad \frac{d^4y}{dx^4} + 4 \cdot \lambda^4 \cdot y = 0. \tag{A2.9}$$

A2.2. The general solution to the elastic foundations differential equation.

It is only sufficient to consider the general solution to eq. (A2.9), from which the complete solution can be obtained for the case where there is a point load, by adding the particular integral. The auxiliary equation for eq. (A2.9) is given by:

$$m^4 + 4 \cdot \lambda^4 = 0,$$

$$(m^2 - j \cdot 2 \cdot \lambda^2) \cdot (m^2 + j \cdot 2 \cdot \lambda^2) = 0,$$

$$\left[m^2 - \lambda^2 \cdot (1 + j \cdot 2 - 1) \right] \cdot \left[m^2 - \lambda^2 \cdot (1 - j \cdot 2 - 1) \right] = 0,$$

$$\left[m^2 - \lambda^2 \cdot (1 + j)^2 \right] \cdot \left[m^2 - \lambda^2 \cdot (- 1 + j)^2 \right] = 0,$$

$$\left[m - \lambda \cdot (1+j) \right] \cdot \left[m + \lambda \cdot (1+j) \right] \cdot \left[m - \lambda \cdot (-1+j) \right] \cdot \left[m + \lambda \cdot (-1+j) \right] = 0. \tag{A2.10}$$

The roots of the auxiliary equation can be wriiten as:

$$m_1 = -m_2 = \lambda(1 + j)$$

and

$$m_3 = -m_4 = \lambda(-1 + j). \tag{A2.11}$$

The general solution of eq. (A2.9) can therefore be written as:

$$y(x) = A_1 e^{m_1 x} + A_2 e^{m_2 x} + A_3 e^{m_3 x} + A_4 e^{m_4 x}$$

$$= A_1 e^{\lambda(1+j)x} + A_2 e^{-\lambda(1+j)x} + A_3 e^{\lambda(-1+j)x} + A_4 e^{-\lambda(-1+j)x}$$

$$= e^{\lambda x}(A_1 e^{j\lambda x} + A_4 e^{-j\lambda x}) + e^{-\lambda x}(A_2 e^{-j\lambda x} + A_3 e^{j\lambda x})$$

$$= e^{\lambda x}\left[(A_1 + A_4)\cos\lambda x + j(A_1 - A_4)\sin\lambda x\right]$$

$$+ e^{-\lambda x}\left[(A_2 + A_3)\cos\lambda x + j(A_3 - A_2)\sin\lambda x\right]$$

i.e.

$$y(x) = e^{\lambda x}(C_1 \cos\lambda x + C_2 \sin\lambda x) + e^{-\lambda x}(C_3 \cos\lambda x + C_4 \sin\lambda x). \tag{A2.12}$$

Eq. (A2.12) represents the general solution for the deflection of a straight bar supported on an elastic foundation with no loading. By differentiating eq. (A2.12) we obtain expressions for slope, bending moment and shear force which are given by

$$\frac{1}{\lambda} \cdot \frac{dy}{dx} = e^{\lambda x}\left[C_1(\cos\lambda x - \sin\lambda x) + C_2(\cos\lambda x + \sin\lambda x)\right]$$

$$- e^{-\lambda x}\left[C_3(\cos\lambda x + \sin\lambda x) - C_4(\cos\lambda x - \sin\lambda x)\right], \tag{A2.13}$$

$$\frac{1}{2\lambda^2} \cdot \frac{d^2 y}{dx^2} = - e^{\lambda x}(C_1 \sin\lambda x - C_2 \cos\lambda x) + e^{-\lambda x}(C_3 \sin\lambda x - C_4 \cos\lambda x), \tag{A2.14}$$

$$\frac{1}{2\lambda^3} \cdot \frac{d^3y}{dx^3} = e^{-\lambda x}\left[C_3(\cos\lambda x - \sin\lambda x) + C_4(\cos\lambda x + \sin\lambda x)\right]$$

$$- e^{\lambda x}\left[C_1(\cos\lambda x + \sin\lambda x) - C_2(\cos\lambda x - \sin\lambda x)\right], \quad (A2.15)$$

and

$$\tan\theta = \frac{dy}{dx}, \quad M = -E \cdot I \cdot \frac{d^2y}{dx^2}, \quad Q = -E \cdot I \cdot \frac{d^3y}{dx^3}.$$

A2.3. Interpretation of integration constants.

Conditions at left end point can be obtained by putting $x = 0$ in eqs.(A2.12) to (A2.15) giving,

$$y_o = C_1 + C_3, \tag{A2.16}$$

$$\theta_o = \lambda(C_1 + C_2 - C_3 + C_4), \tag{A2.17}$$

$$M_o = 2\lambda^2 E \cdot I(C_4 - C_2), \tag{A2.18}$$

$$Q_o = 2\lambda^3 E \cdot I(C_1 - C_2 - C_3 - C_4). \tag{A2.19}$$

By solving eqs.(A2.16) to (A2.19) for C_1, C_2, C_3 and C_4 in terms of y_o, θ_o, M_o and Q_o we have,

$$C_1 = \frac{1}{2} \cdot y_o + \frac{1}{4\lambda} \cdot \theta_o + \frac{1}{8\lambda^3 E \cdot I} \cdot Q_o, \tag{A2.20}$$

$$C_2 = \frac{1}{4\lambda} \cdot \theta_o - \frac{1}{4\lambda^2 E \cdot I} \cdot M_o - \frac{1}{8\lambda^3 E \cdot I} \cdot Q_o, \tag{A2.21}$$

$$C_3 = \frac{1}{2} \cdot y_o - \frac{1}{4\lambda} \cdot \theta_o - \frac{1}{8\lambda^3 E I} \cdot Q_o, \tag{A2.22}$$

$$C_4 = \frac{1}{4\lambda} \cdot \theta_o + \frac{1}{4\lambda^2 E \cdot I} \cdot M_o - \frac{1}{8\lambda^3 E \cdot I} \cdot Q_o. \tag{A2.23}$$

If these constants are substituted in eq.(A2.12) the expression

for $y(x)$ can be simplified as,

$$y(x) = y_0 f_1(\lambda x) + \frac{1}{\lambda} \theta_0 f_2(\lambda x) - \frac{1}{\lambda^2 E \cdot I} M_0 f_3(\lambda x)$$

$$- \frac{1}{\lambda^3 E \cdot I} \cdot Q_0 f_4(\lambda x) \qquad (A2.24)$$

where

$$f_1(\lambda x) = \cosh \lambda x \cdot \cos \lambda x, \qquad (A2.25)$$

$$f_2(\lambda x) = \frac{1}{2} (\cosh \lambda x \cdot \sin \lambda x + \sinh \lambda x \cdot \cos \lambda x), \qquad (A2.26)$$

$$f_3(\lambda x) = \frac{1}{2} \sinh \lambda x \cdot \sin \lambda x, \qquad (A2.27)$$

$$f_4(\lambda x) = \frac{1}{4} (\cosh \lambda x \cdot \sin \lambda x - \sinh \lambda x \cdot \cos \lambda x). \qquad (A2.28)$$

Eq.(A2.24) defines the deflection of a beam resting on an elastic foundation when there are no external forces applied, in terms of the conditions at the left end point. Now consider the case when there is a point load applied at a distance $x = a$, from left hand corner as shown in fig. 4.13. Assume that quantities y_0, θ_0, M_0 and Q_0 are known. The calculations are proceeded from the left end of the beam towards the right, along the unloaded portion AC until

the point where the point load is applied. This applied force F has an effect to the right of C ($x > a$), similar to that which the initial shear force Q_0 had on the portion AC ($0 > x > a$). From eq.(A2.24) it is seen that the factor associated with Q_0 is $(1/\lambda^3 EI) \cdot f_4(\lambda x)$, and it can be concluded that the force F has a modifying effect of $F \cdot (1/\lambda^3 EI) \cdot f_4 [\lambda(x - a)]$ on the elastic line to the right of C ($x > a$). Thus the deflection

curve on the portion CB can be obtained by adding this term to the expression given in eq. (A2.24). That is,

$$y(x) = y_0 f_1(\lambda x) + \frac{1}{\lambda} \cdot \theta_0 f_2(\lambda x) - \frac{1}{\lambda^2 E \cdot I} \cdot M_0 f_3(\lambda x)$$

$$- \frac{1}{\lambda^3 E \cdot I} \cdot Q_0 f_4(\lambda x) + \frac{1}{\lambda^3 E \cdot I} \cdot F \cdot f_4\left[\lambda(x - a)\right]. \tag{A2.29}$$

By differentiating eq. (A2.29) three times with respect to x expressions for θ_x, M_x and Q_x can be obtained. That is,

$$\theta_x = \frac{dy}{dx} = y_0 \cdot \frac{df_1}{dx} + \frac{Q_0}{\lambda} \cdot \frac{df_2}{dx} - \frac{M_0}{\lambda^2 E \cdot I} \cdot \frac{df_3}{dx} - \frac{Q_0}{\lambda^3 E \cdot I} \cdot \frac{df_4}{dx}$$

$$+ \frac{F}{\lambda^3 E \cdot I} \frac{df_4}{dx}\left[\lambda(x - a)\right]. \tag{A2.30}$$

Now

$$\frac{df_1}{dx} = \frac{d}{dx} (\cosh \lambda x \cdot \cos \lambda x)$$

$$= \lambda \sinh \lambda x \cdot \cos \lambda x - \lambda \cosh \lambda x \cdot \sin \lambda x$$

$$= - 4 \lambda f_4. \tag{A2.31}$$

Similarly it can be shown that,

$$\frac{df_2}{dx} = \lambda f_1, \quad \frac{df_3}{dx} = \lambda f_2 \quad \text{and} \quad \frac{df_4}{dx} = \lambda f_3. \tag{A2.32}$$

By substituting these in eq. (A2.30) and simplifying we obtain an expression for the slope given by,

$$\theta_x = \theta_0 f_1(\lambda x) - \frac{M_0}{\lambda E \cdot I} \cdot f_2(\lambda x) - \frac{Q_0}{\lambda^2 E \cdot I} \cdot f_3(\lambda x) - 4 \lambda y_0 f_4(\lambda x)$$

$$+ \frac{F}{\lambda^2 E \cdot I} \cdot f_3\left[\lambda(x - a)\right]. \tag{A2.33}$$

Similarly we can write expressions for M_x and Q_x as:

$$M_x = M_0 f_1(\lambda x) + \frac{Q_0}{\lambda} \cdot f_2(\lambda x) + 4E \cdot I \lambda^2 y_0 f_3(\lambda x)$$

$$+ 4E \cdot I \lambda^2 \theta_0 f_4(\lambda x) - \frac{F}{\lambda} \cdot f_2 \left[\lambda(x - a)\right], \tag{A2.34}$$

$$Q_x = Q_0 f_1(\lambda x) + 4E \cdot I \lambda^3 y_0 f_2(\lambda x) + 4E \cdot I \lambda^2 \theta_0 f_3(\lambda x)$$

$$- 4\lambda M_0 f_4(\lambda x) - F \cdot f_1 \left[\lambda(x - a)\right]. \tag{A2.35}$$

Now the conditions of the beam at the right end point can be obtained by putting $x = \ell$ in eqs. (A2.29), (A2.33), (A2.34) and (A2.35). In the mill cluster the rolls have both ends free. By applying conditions at the end points of a beam with free end points an equation for the deflection of rolls can be obtained for the use in the mill model.

The bending moment and shear force at the end points of a beam having free end points are zero. That is $M_0 = Q_0 = M = Q = 0$. By putting $x = \ell$ in eqs. (A2.34) and (A2.35) we have,

$$4E \cdot I \lambda^2 y_0 f_3(\lambda \ell) + 4E \cdot I \lambda \theta_0 f_4(\lambda \ell) - \frac{F}{\lambda} \cdot f_2 \left[\lambda(\ell - a)\right] = 0 \tag{A2.36}$$

and

$$4E \cdot I \lambda^3 y_0 f_2(\lambda \ell) + 4E \cdot I \lambda^2 \theta_0 f_3(\lambda \ell) - F \cdot f_1 \left[\lambda(\ell - a)\right] = 0 . \tag{A2.37}$$

Solving eqs. (A2.36) and (A2.37) for y_0 and 0_0 and expressing $4E\,I$ in terms of K from eq (A2.8) we have,

$$y_0 = \frac{F\lambda}{K} \cdot \frac{f_3(\lambda \ell) \, f_2\left[\lambda(\ell - a)\right] - f_4(\lambda \ell) \, f_1\left[\lambda(\ell - a)\right]}{f_3^2(\lambda \ell) - f_2(\lambda \ell) \, f_4(\lambda \ell)} \tag{A2.38}$$

and

$$\theta_o = \frac{F\lambda^2}{K} \cdot \frac{f_2(\lambda\ell) \cdot f_2\left[\lambda(\ell - a)\right] - f_3(\lambda\ell) \cdot f_1\left[\lambda(\ell - a)\right]}{f_2(\lambda\ell) \cdot f_4(\lambda\ell) - f_3^2(\lambda\ell)} . \qquad (A2.39)$$

Substituting these values for y_o, θ_o and $M_o = Q_o = 0$ in eq. (A2.29) and simplifying we can write an expression for $y(x)$ as:

$$y(x) = \frac{F\lambda}{K} \cdot \frac{1}{\sinh^2\lambda\ell - \sin^2\lambda\ell} \cdot 2 \cdot A \cdot \cosh\lambda x \cos\lambda x + B(C + D) \qquad (A2.40)$$

where

$A = \sinh\lambda\ell \cdot \cos\lambda a \cdot \cosh\lambda(\ell - a) - \sin\lambda\ell \cdot \cosh\lambda a \cdot \cos\lambda(\ell - a)$,

$B = \cosh\lambda x \cdot \sin\lambda x + \sinh\lambda x \cdot \cos\lambda x$,

$C = \sinh\lambda\ell \cdot \left[\sin\lambda a \cdot \cosh\lambda(\ell - a) - \cos\lambda a \cdot \sinh\lambda(\ell - a)\right]$,

$D = \sin\lambda\ell \cdot \left[\sinh\lambda a \cdot \cos\lambda(\ell - a) - \cosh\lambda a \cdot \sin\lambda(\ell - a)\right]$.
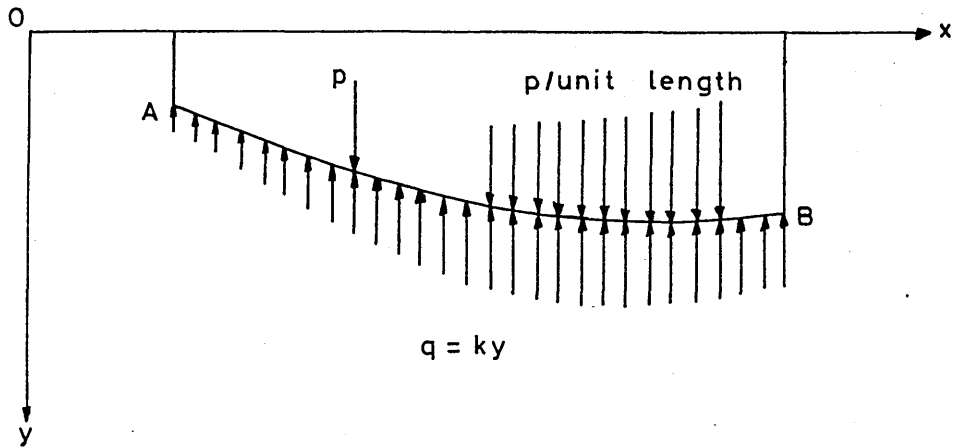
Fig. A 2.1. Forces acting on a beam.
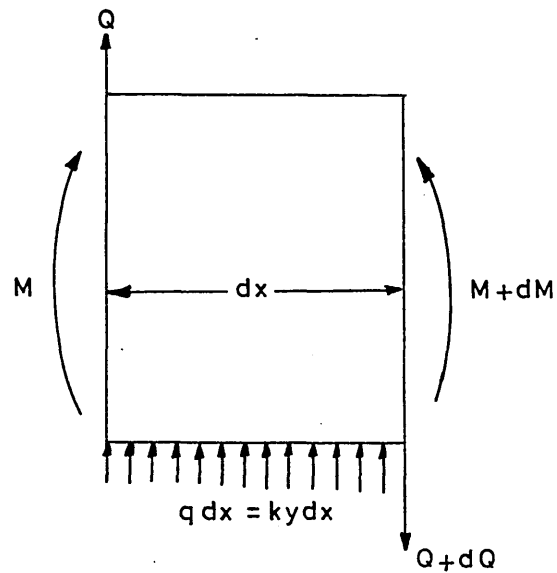
Fig. A 2.2. Forces acting on an element of the beam.

APPENDIX 3.

Actuator Transfer Function Gains.

A3.1. Actuator integral rate constant k_a.

An average value of rack response to a 10 V maximum demand is ± 1.5 divisions/sec. where the full scale deflection of the actuators is **roughly** ± 80 mm. corresponding to a ± 5 divisions. The input of this block is in volts and the output is in mm. If it is assumed that the actuator movement varies linearly with input voltage, then the integral rate constant k_a is given by

$$k_a = \frac{1.5 \frac{80}{5}}{10} \tag{A3.1}$$

$$= 2.4 \ mmV^{-1}s^{-1} .$$

A3.2. The feedback position transducer constant k_f.

A full scale movement of actuator is ± 80 mm for a full scale demand of ± 10 **V**. Therefore k_f is given by

$$k_f = \frac{10}{80} = 0.125 \ V/mm . \tag{A3.2}$$

A3.3. Calculation of forward gain k to give two equal roots.

The dead space time constant T_a is 0.1 sec. (supplied by BSC). The characteristic equation of the closed loop actuator transfer function from eq. (5.14) is

$$s(1 + s \cdot T_a) + k \cdot k_a k_f = 0 . \tag{A3.3}$$

i.e.

$$s^2 + \frac{1}{T_a} s + \frac{k \cdot k_a k_f}{T_a} = 0 . \tag{A3.4}$$

For equal roots,

$$\frac{1}{T_a^2} - \frac{4k \cdot k_a k_f}{T_a} = 0 \tag{A3.5}$$

which gives,

$$k = \frac{1}{4T_a k_a k_f} . \tag{A3.6}$$

i.e.

$$k = \frac{1}{4 \times 0.1 \times 2.4 \times 0.125} = 8.33 . \tag{A3.7}$$

Therefore the closed loop transfer function $g_a(s)$ becomes,

$$g_a(s) = \frac{8.33 \times 2.4}{0.1s^2 + s + 8.33 \times 2.4 \times 0.125} \tag{A3.8}$$

$$= \frac{200}{s^2 + 10s + 25}$$

$$= \frac{8}{(1 + 0.2s)^2} .$$

i.e. $K_A = 8$ and $T_A = 0.2$.

By substituting these values in eq. (5.17) we have,

$$A_a = \begin{bmatrix} 0 & 1 \\ -25 & -10 \end{bmatrix} , \quad B_a = \begin{bmatrix} 0 \\ 200 \end{bmatrix} \quad \text{and} \quad C_a = \begin{bmatrix} 1 & 0 \end{bmatrix} . \tag{A3.9}$$

APPENDIX 4.

Strip Dynamics.

A4.1. Derivation of the state space form of strip dynamics.

Let

$$A_d = \begin{bmatrix} 0 & 1 \\ -a & -b \end{bmatrix}, \quad B_d = \begin{bmatrix} -c \\ d \end{bmatrix} \quad \text{and} \quad C_d = \begin{bmatrix} 1 & 0 \end{bmatrix}. \quad (A4.1)$$

Therefore the strip transfer function can be written as

$$g_d(s) = C_d(sI - A_d)^{-1}B_d$$

$$= \begin{bmatrix} 1 & 0 \end{bmatrix} \cdot \frac{\begin{bmatrix} s + b & 1 \\ -a & s \end{bmatrix}}{s(s + b) + a} \cdot \begin{bmatrix} -c \\ d \end{bmatrix}$$

$$= \frac{-c(s + b) + d}{s^2 + bs + a}$$

$$= \frac{1 - \dfrac{c}{d - bc} \cdot s}{\dfrac{s^2}{d - bc} + \dfrac{b}{d - bc} \cdot s + \dfrac{a}{d - bc}}. \quad (A4.2)$$

From eq.(5.22) we can write $g_d(s)$ in terms of time constant T_d and time delay τ as:

$$g_d(s) = \frac{1 - \dfrac{\tau}{2}s}{\dfrac{\tau \cdot T_d}{2}s^2 + (\dfrac{\tau}{2} + T_d)s + 1}. \quad (A4.3)$$

Now equating coefficients of eqs.(A4.2) and (A4.3) we have

$$\frac{\tau}{2} = \frac{c}{d - bc}, \quad (A4.4)$$

$$\frac{\tau \cdot T_d}{2} = \frac{1}{d - bc} \quad , \tag{A4.5}$$

$$\frac{\tau}{2} + T_d = \frac{b}{d - bc} \quad , \tag{A4.6}$$

$$1 = \frac{a}{d - bc} \quad . \tag{A4.7}$$

By solving eqs. (A4.4) to (A4.7) for a,b,c and d we have

$$a = \frac{2}{\tau \cdot T_d} \quad , \quad b = \frac{\tau + 2 \cdot T_d}{\tau \cdot T_d} \quad , \quad c = \frac{1}{T_d} \quad \text{and} \quad d = \frac{4 \cdot T_d + \tau}{\tau \cdot T_d^2} \quad . \tag{A4.8}$$

A4.2. Strip time constant and time delay.

If a medium strip speed is considered, say 5 m/s, and the distance between the roll gap and the shapemeter is 1.75 m, then the time delay τ is given by,

$$\tau = \frac{1.75}{5.0} = 0.35 \text{ s} . \tag{A4.9}$$

The strip time constant may be derived as:

$$T_d = \frac{D}{V} = \frac{\text{Distance between coiler and roll gap}}{\text{Strip speed}}$$

$$= \frac{4.25}{5.0} = 0.85 \text{ s} . \tag{A4.10}$$

By substituting these in eq. (5.23) we have,

$$A_d = \begin{bmatrix} 0 & 1 \\ -6.7227 & -6.8908 \end{bmatrix} \quad , \quad B_d = \begin{bmatrix} -1.1765 \\ 14.8295 \end{bmatrix}$$

and

$$C_d = \begin{bmatrix} 1 & 0 \end{bmatrix} \quad , \tag{A4.11}$$

APPENDIX 5.

Shapemeter Time Constants.

A5.1. Shapemeter response time (ASEA manual).

Typical values of shapemeter dominant time constants for different speeds are given in the table below.

Strip speed (m/s)	Dominant time constant (sec)	0 - 90 % response time (sec)
0.3———➤1.0	4.35	10.0
1.0———➤2.0	1.43	3.3
2.0———➤5.0	0.74	1.7
5.0———➤15.0	0.30	0.7
15.0———➤50.0	0.11	0.25

Table A5.1.

Assuming a medium speed of 5 m/s T_{s1} is 0.74 sec., and the speed independent time constant T_{s2} is 0.01 sec. For the medium speed considered the matrices which describe the state space form of the shapemeter can be obtained by substituting the above values in eq. (5.27) as:

$$A_s = \begin{bmatrix} 0 & 1 \\ -135.135 & -101.351 \end{bmatrix} , \quad B_s = \begin{bmatrix} 0 \\ 135.135 \end{bmatrix} \text{ and } C_s = \begin{bmatrix} 1 & 0 \end{bmatrix}.$$

APPENDIX 6.

Mill Transfer Functions for Low, Medium and High Speeds.

The open loop mill transfer function has the form from eq. (5.45),

$$G(s) = \frac{N(s)}{D(s)} \cdot G_m .$$

For different speeds $G(s)$ has different functions since the time constants depend on the speed. Assuming three different speeds, low, medium and high, the numerator and denominator polynomials, $N(s)$ and $D(s)$, are calculated and given below. The low, medium and high speeds used are 2.0 m/s, 5.0 m/s and 15.0 m/s respectively.

For low speed,

$$N_\ell(s) = 8 (1 - 0.4375s),$$

$$D_\ell(s) = (1 + 0.2s)^2(1 + 0.4375s)(1 + 2.125s)(1 + 1.43s)(1 + 0.01s). \tag{A5.1}$$

For medium speed,

$$N_m(s) = 8 (1 - 0.175s),$$

$$D_m(s) = (1 + 0.2s)^2(1 + 0.175s)(1 + 0.85s)(1 + 0.74s)(1 + 0.01s). \tag{A5.2}$$

For high speed,

$$N_h(s) = 8 (1 - 0.0583s),$$

$$D_h(s) = (1 + 0.2s)^2(1 + 0.0583s)(1 + 0.283s)(1 + 0.3s)(1 + 0.01s). \tag{a5.3}$$

Appendix 7.

Yield Stress Curve for Stainless Steel Type 304.

Fig.A7.1 shows (supplied by the manufacturer) the yield stress of stainless steel type 304 plotted against the cold rolling percentage reduction. Data from this plot is used to calculate the yield stress at different reductions, which is used in the roll force model. This curve is modelled using a least square method for curve fitting, and a 6th order polynomial is derived and is given by

$$y(r) = 229.819 + 29.0302r - 0.114634r^2 - 0.0352014r^3$$
$$+ 0.00176116r^4 - 0.0000331418r^5$$
$$+ 0.000000215601r^6 \qquad (A7.1)$$

where $y(r)$ is the yield strength in N/mm^2 and r is the percentage reduction.

The numerical values from fig.A7.1 are tabulated in table A7.1 against the results obtained from eq.(A7.1) and the third column shows the percentage errors. The **relevent** percentage reductions lie between 8 % and 26 % and the percentage error in this region is less than 2 %.

% reduction	Yield stress from fig.A7.1 in N/mm^2	Yield stress from eq.(A7.1) in N/mm^2	% error
0.0	233.33	229.82	-1.5
2.0	293.33	287.16	-2.1
4.0	333.33	342.27	2.7
6.0	386.67	394.30	2.0
8.0	440.00	442.88	0.7
10.0	480.00	487.96	1.7
12.0	520.00	529.76	1.9
14.0	560.00	568.63	1.5
16.0	600.00	605.05	0.8
18.0	633.33	639.51	1.0
20.0	666.67	672.48	0.9
22.0	700.00	704.38	0.6
24.0	733.33	735.50	0.3
26.0	760.00	766.05	0.8
28.0	800.00	795.07	-0.5
30.0	820.00	825.48	0.7
32.0	850.67	854.07	0.4
34.0	877.33	881.52	0.5
36.0	900.00	907.41	0.8
38.0	922.67	931.28	0.9
40.0	940.00	952.67	1.3
42.0	960.00	971.16	1.2
44.0	973.33	986.46	1.3
46.0	986.67	998.48	1.2
48.0	993.33	1007.39	1.4
50.0	1006.33	1013.71	0.7
52.0	1013.33	1018.66	0.5
54.0	1020.00	1023.17	0.3
56.0	1033.33	1031.31	-0.2
58.0	1040.00	1044.69	0.5
60.0	1053.33	1068.10	1.4

Table A7.1.
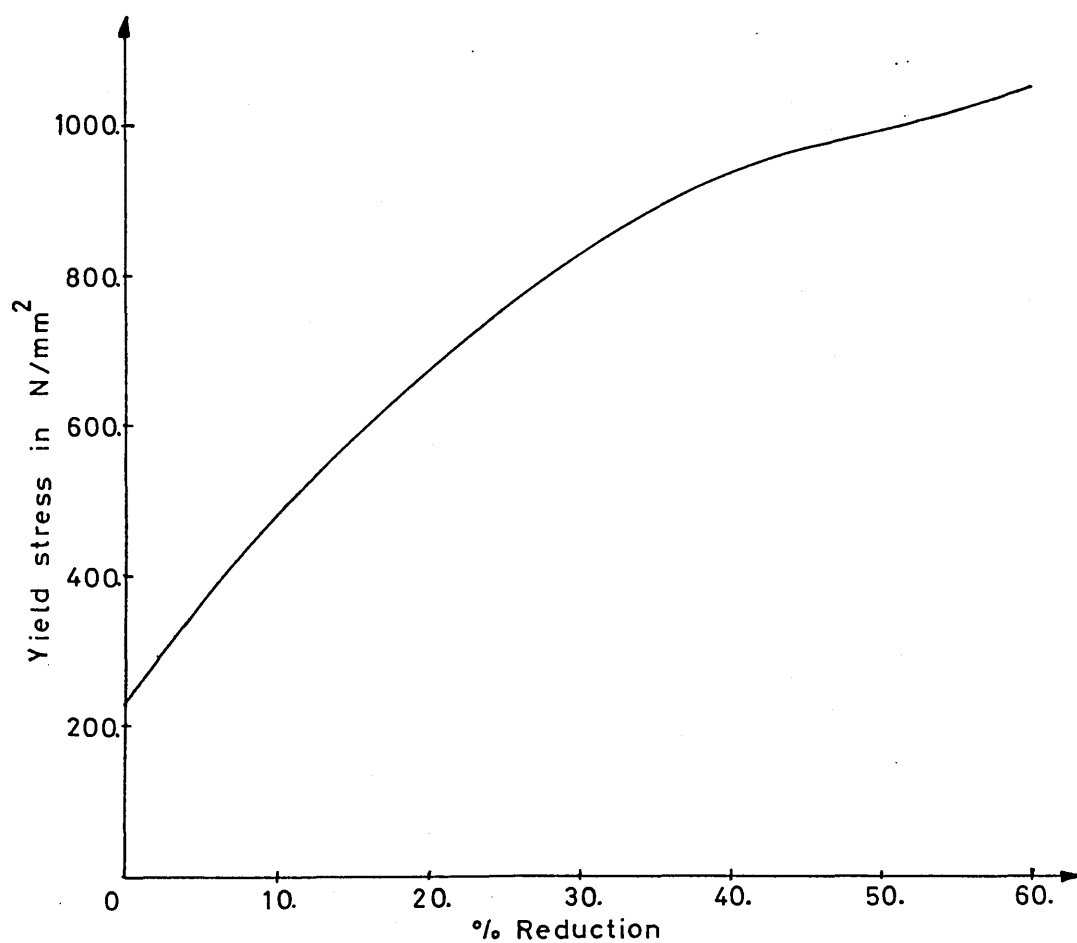
Fig.A7.1. Yield stress of stainless steel type 304.

Appendix 8.

The Transformation Matrix.

The transformation matrix may be derived using Chebychev polynomials given by $-w$, $-2w^2 + 1$, $-4w^3 + 3w$, $-8w^4 + 8w^2 - 1$ etc. The strip width is assumed to have a normalised value of 2 and is divided into eight sections. Each polynomial value is calculated at the mid-point of each section. The first column of X corresponds to the first order polynomial and the second column to the second order polynomial etc. The derived matrix X is given below.

$$
X = \begin{bmatrix}
0.875 & -0.531 & 0.055 & 0.435 \\
0.625 & 0.218 & -0.898 & 0.904 \\
0.375 & 0.718 & -0.914 & -0.033 \\
0.125 & 0.968 & -0.367 & -0.877 \\
-0.125 & 0.968 & 0.367 & -0.877 \\
-0.375 & 0.718 & 0.914 & -0.033 \\
-0.625 & 0.218 & 0.898 & 0.904 \\
-0.875 & -0.531 & -0.055 & 0.435
\end{bmatrix} .
$$

Development of a Static Model for A

Sendzimir Cold Rolling Mill

G W D M GUNAWARDENE   M J GRIMBLE
Department of Electrical and Electronic Engineering
Sheffield City Polytechnic
Pond Street
Sheffield

Presented at:

IMACS (AICA) SYMPOSIUM ON

SIMULATION OF CONTROL SYSTEMS

with Special Emphasis on

MODELLING AND REDUNDANCY

September, 27 - 29, 1978

Technical University
Vienna
Austria

DEVELOPMENT OF A STATIC MODEL FOR A SENDZIMIR COLD ROLLING MILL.

G. W. D. M. Gunawardene   M. J. Grimble

Department of Electrical & Electronic Engineering
Sheffield City Polytechnic
Pond Street, Sheffield S1 1WB
England

The development of a computer simulation for a single stand Sendzimir cold rolling mill is described. The model enables the output gauge profile to be calculated corresponding to given actuator forces. This type of model is required during the development of a shape control system. A shape control system controls internal stresses in the strip so that the rolled strip will have a given stress distribution and will therefore lie flat on a flat surface.

The computer program described involves an iterative procedure starting from given As-U-Roll actuator forces. Each interface between two sets of rolls and between the work rolls and the strip also involves the solution of non-linear equations by an iterative routine. The program calculates inter-roll pressure and roll profiles and the strip pressure and gauge profiles.

1. DEFINITION OF SYMBOLS USED

$(1-\nu^2)/\pi E$

Diameters of back up roll, 2nd intermediate roll, 1st intermediate roll and work roll

Young's modulus

Set of forces applied to back up roll

Input thickness profile of strip

Output thickness profile of strip

Predicted output thickness from work roll contours

$\pi d^4/64$ where d is the diameter

Modulus of the foundation

Length of one segment of the back up roll

Length of the roll

Rolling pressure on the strip

$_r(x)$ Inter roll pressure between back up roll and 2nd intermediate roll

$_r(x)$ Inter roll pressure between 2nd intermediate roll and 1st intermediate roll

$_w(x)$ Inter roll pressure between 1st intermediate roll and work roll

Work roll radius

Deformed work roll radius

(x)   Deflection of back up roll

(x)   Deflection of 2nd intermediate roll

(x)   Deflection of 1st intermediate roll

x)   Deflection of work roll

$_r(x)$ Interference between back up roll and 2nd intermediate roll

I Interference between 2nd intermediate roll and 1st intermediate roll

$_w$ Interference between 1st intermediate roll and work roll

(s)   Interference between work roll and strip

Poisson's ratio

Decoiler tension

Coiler tension

Distance from left hand corner of rolls

r Reduction ratio

ϕ_n Neutral angle

θ Rolling angle

2. INTRODUCTION

The design of shape control is an area of current interest in the steel industry. Previous problems in the design of control systems for steel mills have mostly been overcome, for example in the design of the gauge control loops. The next major problem is the design of shape control systems.

Bad shape is caused by differential elongation across the width of the strip which results from a variation of internal stresses within the strip. If the strip is to be flat after rolling, the reduction in thickness as it passes through the roll gap must be a constant across the strip width. Shape can be defined as the internal stress distribution due to a transverse variation of reduction of the strip thickness. Thus, shape control refers to the control of the internal stress distribution in steel strip exiting from a rolling mill. There are two types of bad shape, (a) latent shape where the strip may appear to have good shape as it remains flat but latent forces will be released causing deformation when slitting, (b) manifest shape where the strip will have bad shape in the form of waves or ripples extending along the length of the strip which are clearly visible.

It is only in the last ten years that reliable shape measuring devices have become available and have been applied in the steel industry. Most of the previous theoretical work was concerned with scheduling the mill to obtain good shape and not with the design of closed loop shape control systems, employing shape meters.
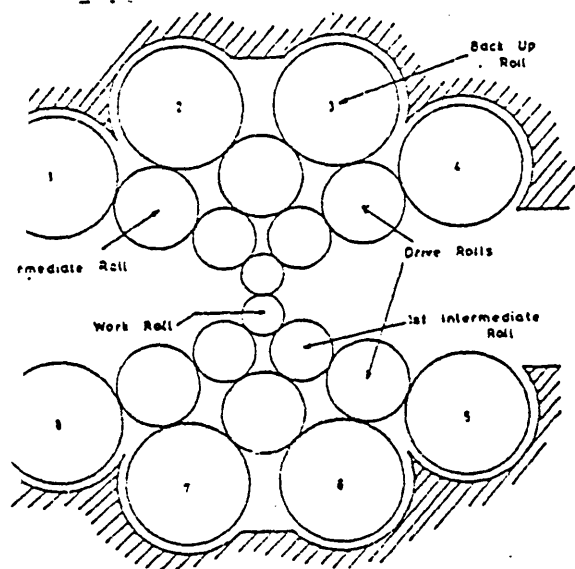
Figure 1

Sendzimir mill is a cluster mill (Fig 1)
e the work rolls rest between supporting
s which permit the roll separating force
e transmitted directly to the mill housing.
e are several types of Sendzimir mill but
he following the 1-2-3-4 mill will be
idered as shown in figure 1. In this type
ill there are eight backing shafts (numbered
. All bearing shafts are concentrically
ted on roller bearings and are located
.etrically on saddles. This type of mill
four drive rolls, to which power is
smitted through four large diameter
.dles. Both work rolls are driven by the
   drive rolls through friction contacts with
2nd intermediate rolls. By rotating the
ring shaft the position of the backing
ring, with respect to the housing, can be
nged to closely control the distance between
work rolls. This is the basic control
ement of a Sendzimir mill that permits
id parallel and extremely accurate
itioning of the rolls.

s type of mill has the As-U-Roll crown
ustment control motorised through small
raulic motors. This adjustment is provided
shafts 2 and 3 acting simultaneously through
ery small eccentric gear train. The
iustment can be made under load and therefore
. be changed while the mill is rolling.

e main objective of the project is to design
closed loop control system for the Sendzimir
ll, to control the shape of the strip.
wever a mathematical model must first be
veloped to represent the conditions within
e mill cluster. This paper is only concerned
th the development of this model. In the
llowing the static model is presented which

represents the Sendzimir mill cluster and the
conditions within the roll gap.

3. MODEL DESCRIPTION

The procedure for calculating the thickness
profile for a given set of forces applied to
the back up rolls is discussed in this section.
A flow chart showing the basic procedure is
given in figure 2. All the mathematical
formulae are given in the appendix. For the
present analysis the edge of the strip is
ignored and the strip width is assumed to be
the same as the length of the work rolls and
this will be improved in due course. A
simplified model was first developed which was
based on the mill configuration shown in
figure 3. This model can be modified to
represent the system shown in figure 1. However
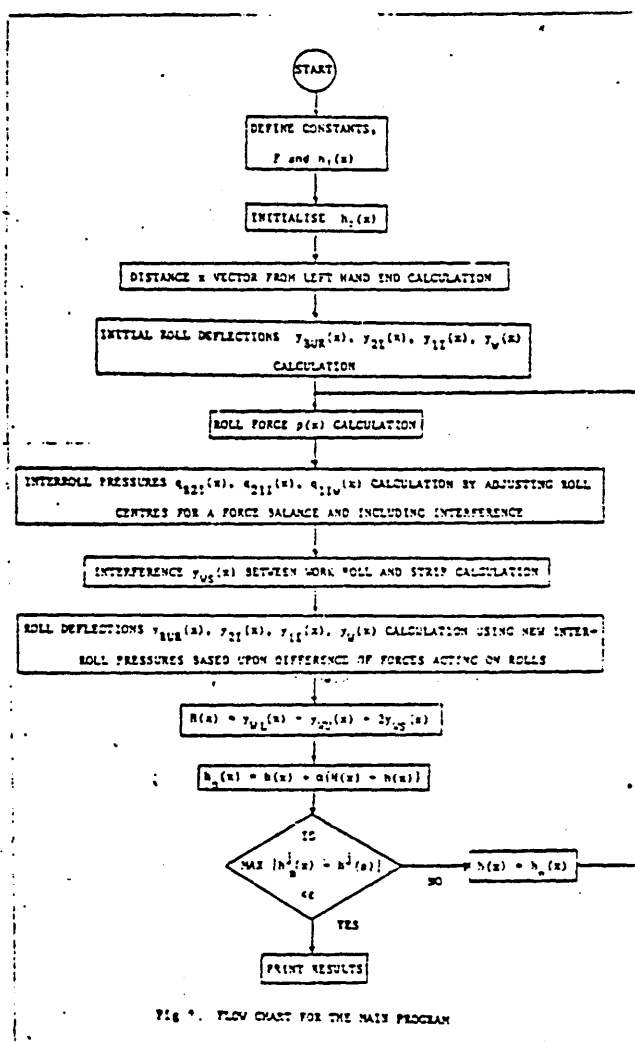for the present the simple configuration shown
in figure 3 will be discussed.

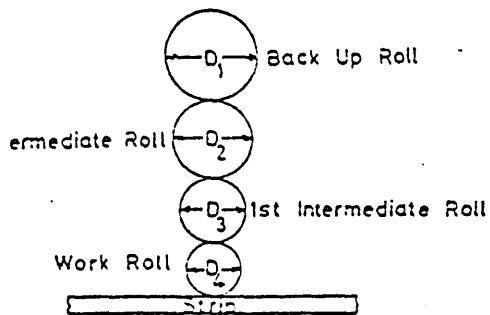Fig 2. FLOW CHART FOR THE MAIN PROGRAM

Figure 3

INITIAL ROLL DEFLECTION AND PRESSURE DISTRIBUTION CALCULATION

itial roll deflections $y_{BUR}(x)$, $y_{2I}(x)$,

and $y_w(x)$ due to a set of applied

are calculated using beam theory for
g. For the present analysis the
tions due to shear components are ignored.
s justified because the rolls with free
ave no shear bending and the span/depth
is very high. The left and right end
s of all the rolls are free and hence the
t and shear at these points are zero.

the deflection $y_{BUR}(x)$ of the back up

due to a set of forces F is calculated,
ing that it is resting on the 2nd inter-
te roll. As the back up roll is pressed
st the 2nd intermediate roll, by the
ed force, this results in a set of reaction
s between the back up roll and the 2nd
mediate roll. This pressure distribution
noted by $q_{B2I}(x)$ and is calculated using

quations (1), (5) and (6) in appendix 1.

forces acting at the point of contact of
back up roll and 2nd intermediate roll,
e a set of forces equal and opposite to
(x), acting on the 2nd intermediate roll.

set of forces can be considered as the
es acting on the 2nd intermediate roll.
deflection $y_{2I}(x)$, of the 2nd intermediate
, due to the pressure $q_{B2I}(x)$ is then
ulated (assuming the 2nd intermediate roll
esting on the 1st intermediate roll). This
ection will cause the 2nd intermediate roll
ress against the 1st intermediate roll,
rating another pressure profile, which is
ted $q_{2II}(x)$.

larly the pressure profile $q_{2II}(x)$ acts on
1st intermediate roll causing it to bend.
deflection of the 1st intermediate roll is
ted $y_{1I}(x)$. Clearly this deflection will
e the generation of another pressure profile

$q_{2II}(x)$ between the 1st intermediate roll and
the work roll. Finally the deflection $y_w(x)$
of the work roll, due to this pressure, is
calculated.

5. ROLLING PRESSURE CALCULATION

An extensive literature exists on the
calculation of the specific roll force as a
function of entry and exit thickness and
tensions. The rolling force is calculated by
dividing the strip into a number of sections
(in this analysis 10). Within each section all
the parameters are assumed to be constant. The
arc of contact is assumed to be circular for
this simple model.

When calculating rolling force a correction
must be made to allow for the affect of roll
flattening. This is achieved using Hitchcock's
formula together with an iterative solution
procedure. The solution is obtained when the
roll radius error $\left| \dfrac{R'_n - R'_{n-1}}{R'_n} \right|$ is less than a

given value, for example 1% (R' is the new roll
radius).

6. INTER ROLL PRESSURE DISTRIBUTION CALCULATION

The inter roll pressure distributions $q_{B2I}(x)$,
$q_{2II}(x)$ and $q_{1IW}(x)$ are calculated from the
degree of interferences between the back up roll
and 2nd intermediate roll, 2nd and 1st inter-
mediate rolls, and 1st intermediate roll and
work rolls respectively. These inter roll
pressures must satisfy the force equilibrium
criteria for all the rolls, that is

$$\int p(x)dx = \int q_{1IW}(x)\,dx \qquad (a)$$

$$\int q_{1IW}(x) = \int q_{2II}(x)dx \qquad (b)$$

$$\int q_{2II}(x)dx = \int q_{B2I}(x)dx \qquad (c) \qquad (1)$$

$$\int q_{B2I}(x)dx = \Sigma F \qquad (d)$$

If minor bending distortions are ignored the
roll surfaces can be assumed to be circular.
When two infinitely long elastic cylinders are
in contact the total interference between
cylinders y can be written as a function of the
load per unit length q.

$$\Delta = y = q(c_1+c_2)\log_e\left\{ \frac{{}^3\sqrt{e^2(D_1+D_2)}}{2q(c_1+c_2)} \right\} \qquad (2)$$

The interference between rolls can be calculated
from the roll contours y_1 and y_2 using the
relation (figure 4)

$$y_{12}(x) = y_2(x) - y_1(x) + y_{12}(0) \qquad (3)$$

The method of calculating q(x) is to sub-
stitute $y_{12}(x)$ calculated from equation (3) for
y in equation (2) and to adjust $y_{12}(0)$

tively until a solution to equations (1)
2) is obtained. This procedure has to be
ted three times to calculate the three
ure profiles by substituting the
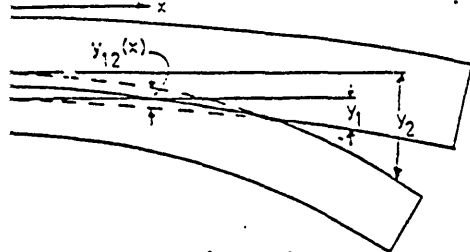priate variables.

Figure 4

CALCULATION OF NEW ROLL DEFLECTIONS
$y_{BUR}(x)$, $y_{2I}(x)$, $y_{1I}(x)$ and $y_W(x)$

ew deflections due to the inter roll
ure profiles are calculated in the
wing manner. Consider one particular roll.
are forces acting upwards and downwards
e roll. The deflection of the roll due
e downward forces and due to the upward
s are calculated in that order. The
erence between the two deflections is
lated to give the total deflection of the
. The deflection due to the downward
es is taken to be positive and that due
he upward forces is taken to be negative.

INTERFERENCE BETWEEN WORK ROLL AND STRIP

an elastic cylinder is resting on a flat
ace the interference y can be written as

$$y = 2pc_1 \log_e \{\frac{^3\sqrt{e^2 D_1}}{2c_1 p}\} \quad (4) \quad (ref 1)$$

e p is the pressure applied. When
ulating the interference between work roll
the strip, the work roll can be considered
cylinder resting on a flat surface. First
ll the pressure at the roll gap is
ulated using the roll gap model. Then the
sure $p(x)$ is substituted in equation (4)
ive the interference $y_{WS}(x)$ between the work

and the strip as a function of x.

PREDICTION OF THE NEW STRIP THICKNESS

variables given below are defined in
ure 5.

x)	= Input thickness
x)	= Output thickness
(s)	= Deflection of the upper work roll measured from the mill housing
(s)	= Deflection of the lower work roll measured from the mill housing
(x)	= Distance from the mill housing to the upper side of strip entering
(x)	= Distance from the mill housing to the lower side of strip entering
(x)	= Distance from the mill housing to the upper side of strip exiting

$h_{2L}(x)$ = Distance from the mill housing to the lower side of strip entering

$$h_1(x) = h_{1L}(x) - h_{1U}(x)$$

$$h_2(x) = h_{2L}(x) - h_{2U}(x)$$

$y_{WSU}(x)$ and $y_{WSL}(x)$ = Interference between the work roll and the strip due to flattening calculated from Hertzian expression referring to upper and and lower halves respectively.

$$h_{2U}(x) = y_{WU}(x) - y_{WSU}(x)$$

$$h_{2L}(x) = y_{WL}(x) + y_{WSL}(x)$$

$$h_2(x) = h_{2L}(x) - h_{2U}(x)$$

$$= y_{WL}(x) - y_{WU}(x) + y_{WSL}(x) + y_{WSU}(x)$$

If we assume that the system is symmetrical
about the centreline of the strip, then

$$y_{WSL}(x) = y_{WSU}(x) = y_{WS}(x)$$

Therefore the predicted thickness is given by
the affective work roll deflections plus the
flattening, thus

$$H(x) = y_{WL}(x) - y_{WU}(s) + 2y_{WS}(x)$$

Therefore the new estimate of strip thickness
is found by substituting this expression for
$H(x)$ in the equation given below.

$$h^k(x) = h^{k-1}(x) + \alpha[H(x) - h^{k-1}(x)]$$

where α is a convergence parameter selected to
obtain a stable solution.

_____ Entry thickness profile
_ _ _ _ . Exit thickness profile
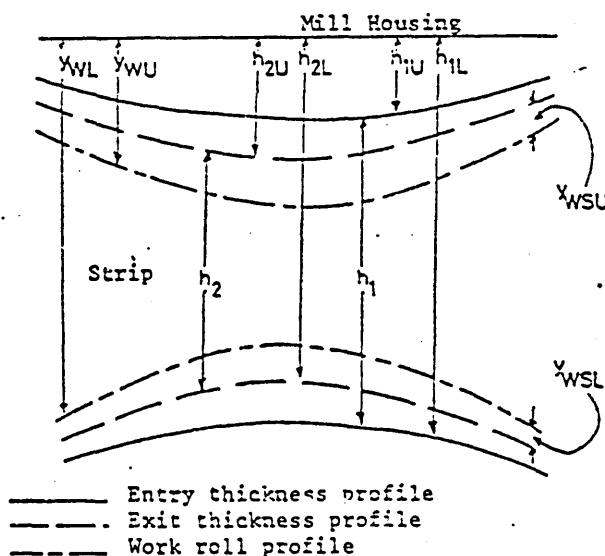_ _ _ _ Work roll profile

Figure 5

10. RESULTS AND CONCLUSIONS

tatic model has been derived to represent the
dzimir cold rolling mill for a shape control
tem. A typical computer output showing the
k roll profile for a given actuator force
shown in figure 7. This model should be
ted by detailed experimental investigation.
numerical values obtained for roll
lections due to bending seem to be feasible.
ip edge effects will be included in the
ure model. A simplified version of this
el can be used to develop the dynamic model
the mill which will be used in the closed
p control system design.

11. FUTURE WORK

re are many areas requiring further work.
e effects must be incorporated in the model
using influence functions to represent the
k roll deformation near the strip edges.
n a new method of modelling the roll gap
t be developed, which includes the inter-
ion between the strip shape changes and
roll force. A mathematical model to
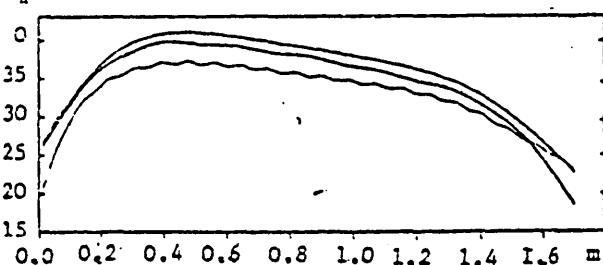resent the dynamics of the mill will also be
eloped.

Figure 7

APPENDIX

en a force P is applied to a beam on an
astic foundation the deflection y as a
nction of x can be written as: (Fig A1)

$$y(x) = \frac{P\lambda}{k} \cdot \frac{1}{A} \left[B(C-D) + E(F+G) \right] \qquad (1)$$

ere

$$\lambda = \left(\frac{k}{4EI} \right)^{\frac{1}{4}} \qquad \text{(reference 2)} \qquad (2)$$

$A = Sinh^2\lambda\ell - sin^2\lambda\ell$

$B = 2Cos\lambda x.cos\lambda x$

$C = Sinh\lambda\ell.cos\lambda a.Cosh\lambda b$

$D = sin\lambda\ell.Cosh\lambda a.cos\lambda b$

$E = Cosh\lambda x.sin\lambda x + Sinh\lambda x.cos\lambda x$

$F = Sinh\lambda\ell(sin\lambda a.Cosh\lambda b - cos\lambda a.Sinh\lambda b)$

$G = sin\lambda\ell(Sinh\lambda a.cos\lambda b - Cosh\lambda a.sin\lambda b)$

e above expression for y(x) is only for the
rtion AC. The same formulae can be used for
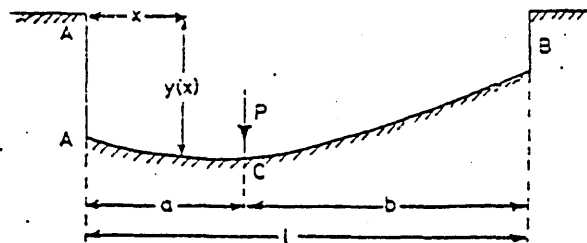
Figure A1

the section CB where x > a by measuring x from
B and replacing a by b and b by a.

The value of k is given by the expression

$$k = \frac{E\pi}{2(1-v^2)} \cdot \frac{1}{\left(\frac{2}{1} + \log_e \frac{2D_1}{d} + \log_e \frac{2D_2}{d} \right)} \qquad (3) \quad \text{(ref 3)}$$

where d = width of flattened contact area.
When two cylinders are pressed together the
expression for d can be written as

$$d = \sqrt{\frac{16(1-v^2)}{\pi} \cdot \frac{P'}{E} \cdot \frac{D_1 D_2}{D_1 + D_2}} \qquad (4) \quad \text{(ref 4)}$$

where P' = load per unit length.

By substituting the value of b in equation (3)
and using numerical values for E and v and
simplifying the expression for k can be
written as

$$k = \frac{3.5714 \times 10^{10}}{24.272 + \log_e (D_1 + D_2) - \log_e P'} \qquad (5)$$

$$q(x) = ky(x) \qquad (6)$$

The above expressions are only for a case where
there is only one point load acting on the beam.
The total deflection is calculated by adding
the deflections calculated separately for each
individual force.

REFERENCES

1. ROARK, R. J., YOUNG, W. C., "Formulas for
   stress and strain", 5th edition, McGraw-
   Hill, 1975.

2. HETENYI, M., "Beams on Elastic Foundations",
   University of Michigan Press, 1946.

3. STONE, M. D., GRAY, R., "Instant crown
   control in rolling mills", Iron and Steel
   Engineer, August 1965.

4. TIMOSHENKO, S. P., GOODIER, J. N., "Theory
   of Elasticity", 2nd edition, McGraw-Hill,
   New York, 1951.

GRIMBLE, M. J., "A roll force model for the cold rolling of thin sheet", Industrial Automation Group Report 4/74, Imperial College Science and Technology, April 1974.

GRIMBLE, M. J., "Shape control for rolled strip", Mech Eng, Nov 1975, pp 91-93.

GRIMBLE, M. J., "A roll force model for tin-plate rolling", GEC J of Science and Technology, Vol 23, No 1, 1976, pp. 5-12.

GRIMBLE, M. J., FULLER, M. A., BRYANT, G. F. "A non-circular arc roll force model for cold rolling", International J for Numerical Methods in Engineering, Vol 12, 1978, pp 643-663.

BRAVINGTON, C. A. BARRY, D. C., McCLURE C.H. "Design and development of a shape control system", Shape Control Confr, Metal Society, Chester, Mar 1976.

CONTE, S. D., "Elementary Numerical Analysis", McGraw-Hill, 1965.

EDWARDS, W. J., SPOONER, P. D., "Analysis of strip shape", in Automation of Tandem Mills edited by G. F. Bryant, pub Iron and Steel Inst, 1973, pp 177-212.

HARAGUCHI, S., KAJIWARA, T., HATA, K., "Shape of strip steel in cold rolling process", Bulletin of the ISME, No 67, Jan 1971, pp 104-112.

OROWAN, E., Proc IME, 1943, Vol 150.

SABATINI, B., YEOMANS, K. A., "An algebra of strip shape and its application to mill scheduling", J of the Iron and Steel Inst, Dec 1968, pp 1207-1217.

SAXL, K., "Transverse gauge variation in strip and sheet rolling", Proc of Inst of Mech Eng, Vol 172, No 22, 1958, pp 727-742.

SPOONER, P. D., BRYANT, G. F., "Analysis of shape and discussion of problems of scheduling set-up and shape control", Shape Control Conf Proc, Metal Society, Chester Mar 1976, pp 19-29.

7. UNDERWOOD, L. R., "The Rolling of Metals Theory and Experiment", Vol 1, Chapman & Hall Ltd, London 1950.

ACKNOWLEDGEMENTS

Reprinted from

METALS TECHNOLOGY

Static model for Sendzimir cold-rolling mill

The design of shape-control systems is an area of current interest in the steel industry. The object of shape control is to adjust the mill so that the rolled strip is free from internal stresses. Both static and dynamic mill models are required for this purpose. A static model enables shape profiles to be calculated for a given set of actuator positions, and is used to generate the steady-state mill gains. Such a model is presented in this paper. The method of calculation of shape profiles is discussed. These shape profiles are plotted against the distance across the strip. Linearized mill gains are calculated about a given shape-operating point and these relate the shape changes to the actuator changes. A mill gain matrix, obtained by measuring shape at eight points across the strip, is presented. MT/699

G. W. D. M. Gunawardene
M. J. Grimble
A. Thomson

© *1981 The Metals Society. Manuscript received 11 January 1980. G. W. D. M. Gunawardene is in the Department of Electrical and Electronic Engineering, Robert Gordon's Institute of Technology, Aberdeen, Dr Grimble is in the Department of Electrical and Electronic Engineering, Sheffield City Polytechnic, Sheffield, and Dr Thomson is with GEC Electrical Projects Ltd, Rugby.*

List of symbols

$C = (1 - v^2)/\pi E$ constant, $\mathrm{m^2 N}$

$d_1 =$ diameter of roll 1 when two rolls are pressed together, m

$d_2 =$ diameter of roll 2 when two rolls are pressed together, m

$E =$ Young's modulus of the material, $\mathrm{N\,m^{-2}}$

$F =$ total force applied, N

$G_m =$ gain matrix (shape change to rack change)

$h_1(x) =$ input-thickness profile, m

$h_2(x) =$ output-thickness profile, m

$\Delta h_2 =$ mean change in gauge profile, m

$\Delta h_2(x) =$ deviation of gauge profile from mean, m

$\Delta h_2'(x) =$ change in gauge profile, m

$I = \pi d^4/64$, $\mathrm{m^4}$

$K =$ elastic-foundation constant, $\mathrm{N\,m^{-2}}$

$\bar{k} =$ mean yield stress, $\mathrm{N\,m^{-2}}$

$k_1 =$ entry yield stress, $\mathrm{N\,m^{-2}}$

$k_2 =$ exit yield stress, $\mathrm{N\,m^{-2}}$

$N =$ no. of sections across mill width

$p(x) =$ specific rolling force, $\mathrm{N\,m^{-1}}$

$\bar{p} =$ mean rolling force, $\mathrm{N\,m^{-1}}$

$q(x) =$ inter-roll specific pressure between two rolls, $\mathrm{N\,m^{-1}}$

$R =$ work-roll radius, m

$R' =$ deformed roll radius, m

$w =$ work-roll width, m

$W =$ width of strip, m

$x =$ distance from left-hand corner of mill or roll, m

$y(x) =$ deflection of any roll, m

$y_s(x) =$ deflection of upper roll, m

$y_t(x) =$ deflection of lower work roll, m

$y_{wc}(x) =$ work-roll camber, m

$y_{ws}(x) =$ interference between work roll and strip, m

$\bar{y}_{ws}(x) =$ mean interference between work roll and strip, m

$y_1(x) =$ deflection of roll 1 when two rolls are pressed together, m

$y_2(x) =$ deflection of roll 2 when two rolls are pressed together, m

$y_{12}(x) =$ interference between two rolls pressed together, m

$\alpha =$ output stress-convergence parameter

$\beta =$ stress-equation constant

$\gamma =$ ratio of input–output deviation

$\delta = h_1(x) - h_2(x) =$ amount of reduction, m

$\mu =$ coefficient of friction

$v =$ Poisson's ratio

$\sigma_1(x) =$ input tensile stress, $\mathrm{N\,m^{-2}}$

$\sigma_2(x) =$ output tensile stress, $\mathrm{N\,m^{-2}}$

$\Delta\sigma_0(x) =$ input tensile stress deviation of first pass, $\mathrm{N/m^{-2}}$

$\Delta\sigma_2(x) =$ output tensile stress deviation from mean, $\mathrm{N/m^{-2}}$

$\phi_n =$ neutral angle

The design of shape-control systems is an area of current interest[1-4] in the steel industry. Previous problems in the design of control systems for steel mills have been overcome largely, for example, in the design of gauge-control loops. The next major problem involves the design of shape-control systems. Shape control refers to the control of the internal-stress distribution in steel strip leaving a rolling mill.[5,6] It is only in the last ten years that reliable shape-measuring devices have become available and have been applied in the steel industry.

To illustrate how bad strip shape might arise, consider strip having a uniform input thickness and a work roll which is deformed so that the output strip thickness is greater near the strip edges than in the central region. In the absence of lateral spread the strip must be larger in the central region than at the edges. Since the strip is one homogeneous mass, such differential elongations cannot occur and internal stresses result. Clearly, if the strip is to be flat after rolling the reduction in thickness, as it passes through the roll gap, must be constant across the strip width.

Shape may be defined as the internal-stress distribution owing to a transverse variation of reduction of the strip thickness. There are two types of bad shape: (a) a latent shape where the strip may appear to have good shape in the mill under tension, but where bad shape is evident during slitting operations, and (b) a manifest shape where the strip being rolled has bad shape in the form of waves and ripples, extending along the length of the strip, which are clearly visible, *see* Fig.1. The stress distributions associated with these basic defects are illustrated in Fig.2.
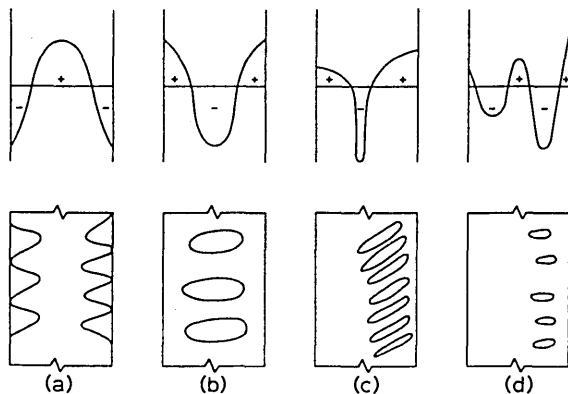
The first requirement in the analytical design of a shape-control system is for the development of a model of the
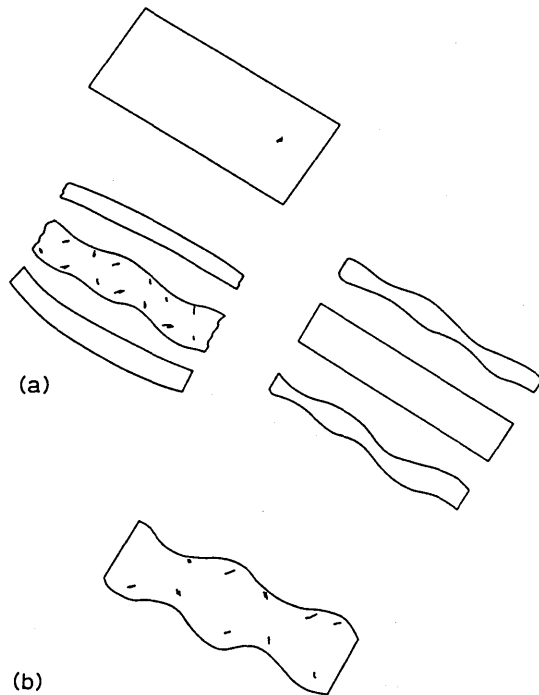
a latent shape on subsequent slitting along middle or long edge; *b* manifest shape with long edges
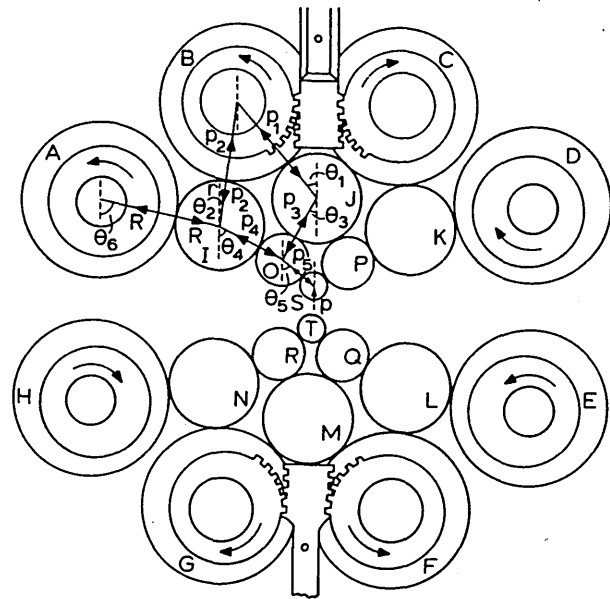
1 Various forms of shape defect

3 Sendzimir mill roll cluster

rolling mill. Both static and dynamic mill models are required. A static model enables shape profiles to be calculated for a given set of actuator positions and it is used to generate the steady-state mill gains. The dynamic model represents the dynamic performance of all the mill components, such as the actuators, and is based upon the equations of state for the system. The subject of this paper is the static model for a Sendzimir cold-rolling mill.[7,8] A Sendzimir mill is extremely complex mechanically, as may be seen from the roll configuration in Fig.3. There has been little published work on the development of such models for this type of mill.

Description of mill

GENERAL

The Sendzimir mill (Z mill) to be considered here is 1·7m wide and is a cluster mill where the work rolls rest between supporting rolls. The mill has eight backing shafts labelled *A–H*, six second intermediate rolls (*I–N*), four first intermediate rolls (*O–R*), and two work rolls (*S, T*), as shown in Fig.3. This type of mill is used for rolling hard materials such as stainless steel.

The motor drive is applied to the outer second intermediate rolls (*I, K, L, N*) and the transmission of the drive to the work rolls via the first intermediate rolls is due purely to inter-roll friction. Rolls labelled *I–T* have free ends and are free to float. The outer rolls (*A–H*) are split into seven roll segments, as shown in Fig.4. The shafts in which these rotate are supported by eight saddles per shaft, positioned between each pair of roll segments and at the shaft ends. The saddles are fixed rigidly to the mill housing, and contain eccentric rings. The outer circumferences of these rings are free to rotate in the circular saddle bores, while the inner circumferences are keyed to the shafts.

a long edge; *b* long middle; *c* herringbone; *d* quarter buckle

2 Stress distributions and manifest buckling forms
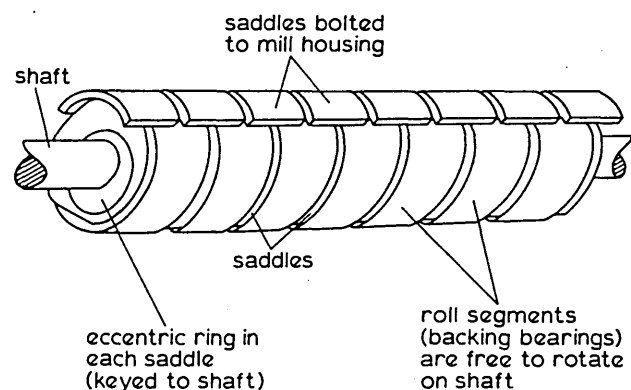
4 Backing shaft assembly, shafts *A* and *D–H*
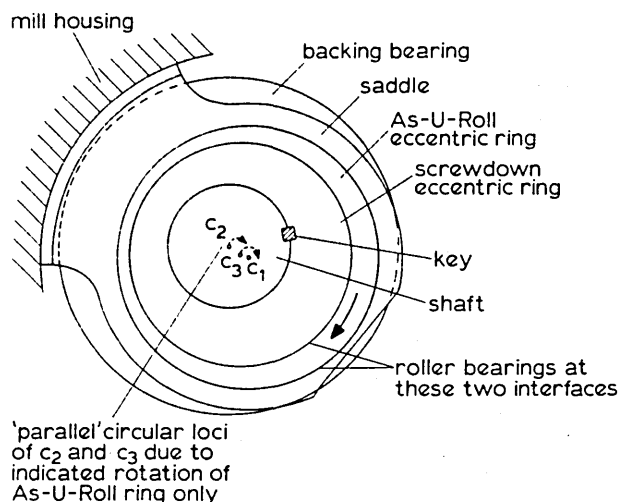
5 Saddle detail for shafts *B* and *C* (not to scale)

a racks before motion; *b* racks after motion
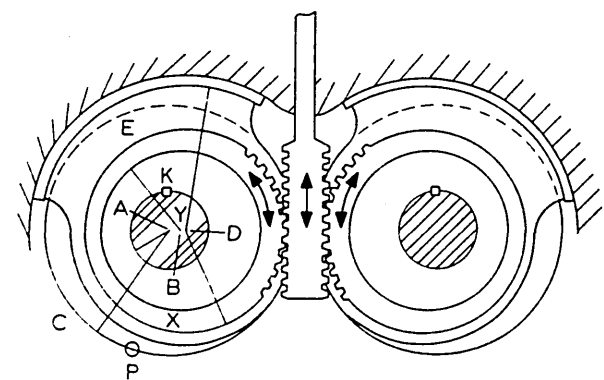
7 Example of As-U-Roll action

UPPER AND LOWER SCREWDOWN OPERATION

Operation of upper screwdown racks acts on assemblies *B* and *C*, and assemblies *F* and *G* are responsible for the lower screwup system. Each saddle of the assembly *B* and *C* is constructed as shown in Fig.5. The saddles on the *F* and *G* assembly are also constructed in the same way but without the 'As-U-Roll' eccentric rings.* When the shaft is rotated the eccentric screwdown ring also rotates in the saddle bore, since it is keyed to the shaft. This allows the centre c_2 of the shaft to rotate about the centre c_1 of the saddle bore, thus causing a net movement of the shaft towards or away from the mill housing. Since the shaft is keyed to the screwdown eccentric rings in all eight saddles the same motion will occur at each end and the shaft will remain parallel to the mill housing. Essentially, the screwdowns cause the movement of rolls *I, J, K, O, P,* and *S* up or down which enables the distance between the two work rolls to be adjusted finely during rolling. A similar operation, which is used principally for roll changing and mill threading, takes place at the lower assemblies *F* and *G*.

'AS-U-ROLL' OPERATION

In addition to the screwdown system, each of the saddles

*These are made by the Sendzimir Company; they allow roll bending to take place during rolling to adjust strip shape.

supporting the upper shaft assemblies *B* and *C* is fitted with an extra eccentric ring (Fig.5) situated between the saddle and the screwdown eccentric ring. This eccentric ring can be rotated independently of the shaft and screwdown eccentric ring, by moving a rack which operates on two annular cheeks fitted on each side of this extra ring, as shown in Fig.6. Such rotation will cause the centre c_3 of the inner bore of this ring to move in a circular locus about centre c_1. There are eight such As-U-Roll racks on saddles between segments. These racks are capable of individual adjustment, producing a different displacement between the shafts and the housing at each saddle position. This allows a profile to be forced on to the shaft, as shown in Fig.7, which will propagate to the work roll through the cluster. Although the As-U-Rolls and upper screwdowns act on the same common shaft they are essentially non-interactive.

6 As-U-Roll assembly
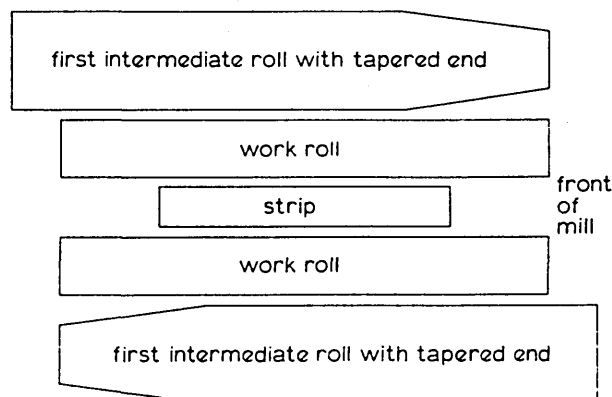
8 Tapered first intermediate rolls

FIRST INTERMEDIATE ROLL TAPERS

In addition to As-U-Roll control of strip shape there is another type of control on the Z-mill. The first intermediate rolls $O-R$ are furnished with tapered-off ends, *see* Fig.8. These rolls can be moved laterally in and out of the cluster. The top and bottom rolls may be moved independently, and it is thus possible to control the pressure at the edges of the strip within certain limits. These rolls are, therefore, used to control the stresses at the edge of the strip.

Static model for mill

A static model[7] for the single-stand cold-rolling mill, shown in Fig.3, may now be described. The static model is a mechanical model for the mill which represents all force–deformation relationships in the roll cluster and in the roll gap. It is important for control purposes to note that these relationships are very non-linear and schedule dependent.

The static model must allow for the bending and flattening of the rolls in the cluster and for the plastic deformation of the strip in the roll gap. The model must provide:

(i) linearized mill gains for use in the control system simulation (dynamic model) based upon a small perturbation analysis

(ii) an understanding of the way in which shape is affected by the mill actuators

(iii) details of the range of control which is available using the As-U-Roll or the first intermediate roll tapers.

The assumptions made in deriving the static model may be listed as:

(i) the mill is symmetrical about a line passing through the work-roll centres (this need not be the case if the side eccentrics are set differently)

(ii) strip edge effects may be ignored

(iii) deflections due to shear may be neglected

(iv) elastic recovery of the strip may be neglected

(v) horizontal deflections of rolls may be neglected

(vi) the centreline strip thickness is specified.

The model developed is in the form of a Fortran computer program. The model enables the output shape profile to be calculated corresponding to a given set of rack positions. The model is divided into three main sections, namely:

(i) roll bending: for calculating the roll-bending deflections due to a set of forces

(ii) roll flattening: for calculating the roll interference or roll flattening between two rolls forced together

(iii) roll force: for calculating the rolling force required to reduce the thickness of the strip by a given amount

(iv) gauge and shape: for calculating the output gauge and shape profiles corresponding to a given set of inter-roll pressure and deflection profiles.

The above topics are considered in the sections below.

Roll bending

It is well known that if a force is applied to a beam[9] supported at two ends, the reactions at the ends and the deflection of the beam can be calculated using simple bending theory. If the beam is resting upon an elastic foundation, where the whole length of the beam is in contact with the foundation, the deflection of the beam may be calculated by assuming that the deflection is proportional to the reaction

at that point.[10] In the mill all the rolls in the middle of the cluster are resting on one another and, since these rolls are elastic bodies, it can be assumed that each roll is resting on an elastic foundation. Thus, the actual bending deflections y can be calculated (*see* Appendix 1) as a function of the applied force F and the distance x from one end of the beam, i.e.

$$y = f(F,x) \dots \dots \dots \dots \dots \dots \dots \dots \dots \dots \dots \dots (1)$$

Roll flattening and inter-roll pressure distribution

The effect of roll flattening, [11],[12] and the resulting inter-roll pressure distribution, is considered in this section. Recall that when two elastic cylinders are rolled together under a load F, the roll axes are deflected. The roll surface of contact will also be flattened.

The amount of interference, or the flattening $y_{12}(x)$ between the rolls, can be calculated as a function of the inter-roll specific force $q(x)$. Alternatively, $q(x)$ can be calculated as a function of $y_{12}(x)$:

$$y_{12}(x) = f_1(q(x)) \dots \dots \dots \dots \dots \dots \dots \dots \dots \dots (2)$$

$$q(x) = f_2(y_{12}(x)) \dots \dots \dots \dots \dots \dots \dots \dots \dots \dots (3)$$

The interference can also be calculated using the roll contours due to bending. This is a function of the deflections $y_1(x)$ and $y_2(x)$ of the two rolls.

$$y_{12}(x) = f_3(y_1(x), y_2(x)) \dots \dots \dots \dots \dots \dots \dots \dots (4)$$

The full expressions are given in Appendix 2.

The deflections $y_1(x)$ and $y_2(x)$, clearly, will depend upon the pressure $q(x)$ and, hence, on $y_{12}(x)$. From equation (3) it may be seen that $q(x)$ depends on $y_{12}(x)$ and, hence, $q(x)$ and $y_{12}(x)$ must be calculated iteratively. The total pressure across the roll width must be equal to the applied force F for the system to be in equilibrium, i.e.

$$\int_0^w q(x) dx = F \dots \dots \dots \dots \dots \dots \dots \dots \dots \dots \dots (5)$$

The method of calculating $q(x)$ is to substitute for $y_{12}(x)$ in equation (3) from equation (4) and to solve equations (3) and (4) iteratively by changing the distance between the roll centres until equation (5) is satisfied to within a specified tolerance. The interference between the work roll and the strip is calculated in a similar manner (*see* Appendix 2).

Roll-force model

The amount of reduction in thickness of the strip is related to the total load in the mill or roll force.[13]–[15] Extensive literature exists on the calculation of specific rolling force $p(x)$ as a function of input–output thicknesses, input–output tensions, and work-roll radius.[16]

$$p(x) = f(h_1(x), h_2(x), \sigma_1(x), \sigma_2(x), R) \dots \dots \dots \dots \dots (6)$$

When rolling hard materials like stainless steel, very high forces must be applied. Since the work rolls are elastic bodies, they will be deformed and flattened at the roll gap.[17] In order to calculate the roll force, including the flattening effects, an iterative procedure must be adopted because the deformed roll radius is a function of the roll force. The deformed radius R' can be calculated using Hitchcock's formula, given as

$$\frac{R'}{R} = 1 + \frac{cp(x)}{\delta} \dots \dots \dots \dots \dots \dots \dots \dots \dots \dots \dots (7)$$

where c is a constant, R is the initial roll radius, and δ is the amount of reduction equal to $(h_1(x)-h_2(x))$. The roll force may be calculated by solving equations (6) and (7) iteratively.[18,19]

The disadvantage of the above approach for roll-force calculation is the time the algorithm takes to converge. For modelling purposes the width of the strip is split into N (typically 67) sections and the roll force must be calculated in each of these sections. The shape calculation is also iterative and, thus, all the roll-force calculations must be performed on each of the iterations of the shape algorithm. Thus, although the roll-force calculation does not require a very large computing time this is multiplied by the number of times it is performed. The above implicit roll-force relations are not, therefore, used in the present mill model.

Bryant and Osborn[15] developed an explicit roll-force formula which thus avoids iterative calculations. The formula is not as accurate as the above algorithm for this type of mill but is efficient in the use of computing time. The present mill model therefore uses this method of calculation. It may be necessary, however, to either modify or replace the formula in the light of plant-test results.

Output gauge and shape profile calculations

The output gauge profile may be calculated once a given set of inter-roll pressures and deflections is known. The shape profile then follows from the input and output gauge profile and the input shape profile. The equations governing these profiles are detailed below.

OUTPUT GAUGE PROFILE CALCULATION

The output gauge profile is determined by the combined effects of roll bending, thermal and ground roll cambers, and differential strip flattening. The change in the gauge profile due to these effects is given by

$$\Delta h_2'(x)=2(y_{ws}(x)-\bar{y}_{ws})+y_s(x)+y_t(x)+2y_{wc}(x) \quad \ldots \ldots (8)$$

where $y_{ws}(x)$ and $\bar{y}_{ws}$ represent interference and mean interference between the work roll and the strip, $y_s(x)$ and $y_t(x)$ represent the work roll S and T deflections, and $y_{wc}(x)$ represents the total work-roll camber. The mean deviation in the output gauge is given by

$$\Delta h_2=\frac{1}{W}\int_0^W \Delta h_2'(x)\mathrm{d}x \quad \ldots \ldots \ldots \ldots \ldots \ldots \ldots \ldots (9)$$

and, hence, the deviation from the mean is given by

$$\Delta h_2(x)=\Delta h_2'(s)-\Delta h_2 \quad \ldots \ldots \ldots \ldots \ldots \ldots \ldots \ldots (10)$$

The new output gauge deviation is calculated from the iterative formula

$$\Delta h_2^{k+1}(x)=\Delta h_2^k(x)-a[\Delta h_2^k(x)-\Delta h_2'(x)] \ldots \ldots \ldots (11)$$

where a is chosen to give a stable solution and the new gauge profile is calculated using
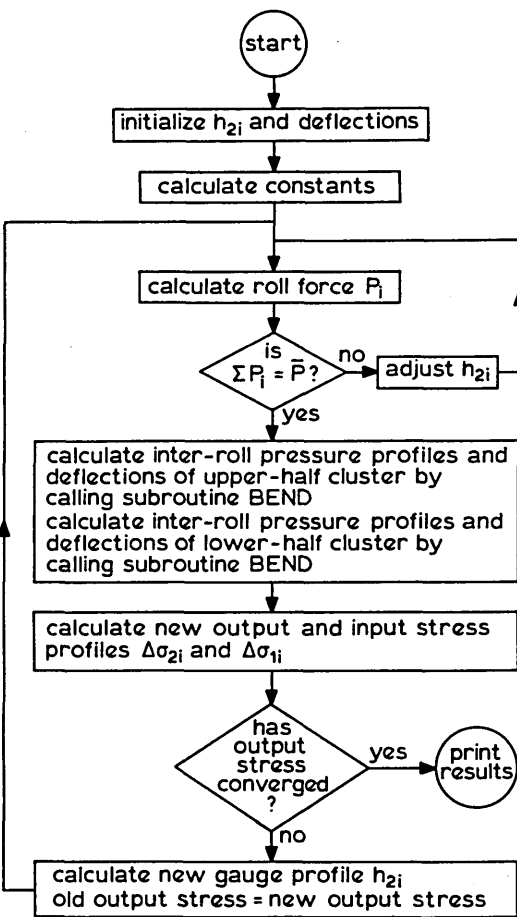
$$h_2(x)=\bar{h}_2+\Delta h_2^{k+1}(x) \ldots \ldots \ldots \ldots \ldots \ldots \ldots \ldots \ldots (12)$$

INPUT AND OUTPUT STRESS PROFILE CALCULATION

The new input and output stresses can be calculated using the new gauge profile, and the following results due to Edwards and Spooner[4]:

$$\Delta \sigma_2(x)=\beta E\left(\frac{h_2(x)}{h_1(x)}\cdot\frac{h_1}{h_2}-1\right)+\frac{\Delta\sigma_0(x)}{(1+\gamma)} \quad \ldots \ldots \ldots \ldots (13)$$

$$\Delta \sigma_1(x)=\gamma\Delta\sigma_2(x) \ldots \ldots \ldots \ldots \ldots \ldots \ldots \ldots \ldots \ldots (14)$$


9 Flow chart for main program

where γ is defined as $(\sigma_1(x)-\bar{\sigma}_1)/\sigma_2(x)-\bar{\sigma}_2)$, β is a constant $(\beta\approx0\cdot5)$, and E denotes Young's modulus of elasticity.

Static-model computer algorithm

The static-model program uses an iterative procedure, as shown in Fig.9. The model includes the calculations for the top half of the cluster as well as for the bottom half of the mill. It is assumed that the mill is symmetrical about the line passing through the work-roll centres. The model can be used for different values of strip width, but for the present analysis the roll-flattening equations ignore strip edge effects. The input data required by the program may be summarized as follows:

   (i) cluster angles (*see* Fig.3)
   (ii) roll diameters
   (iii) roll profiles (camber, wedge, etc.)
   (iv) As-U-Roll positions
   (v) first intermediate-roll positions
   (vi) entry gauge profile
   (vii) mean entry gauge
  (viii) mean exit gauge
   (ix) annealed gauge
   (x) yield stress curve
   (xi) entry tension
   (xii) exit tension
  (xiii) width of strip.
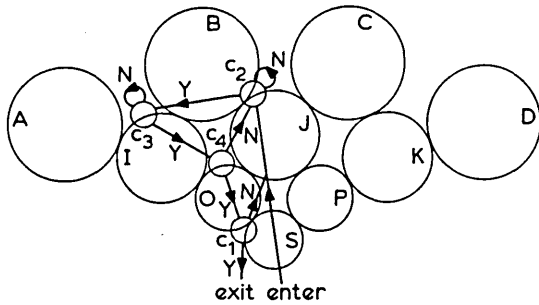
10 Path of calculation for subroutine BEND to calculate pressure profiles

The output data may be listed as:
(i) inter-roll pressure (12 profiles)
(ii) roll deflections (12 profiles)
(iii) exit shape (stress-distribution) profile
(iv) exit gauge profile
(v) roll-force profile.
The mill width is divided into a number of section multiples of 67 and the following assumptions are made (the number 67 is chosen to match the dimensions of the back-up roll and its segments):

(i) the pressure distribution in each section may be calculated using a point load applied at the centre of the section and the width of the section
(ii) the mean deflection of a roll over a section is taken to be equal to the deflection at the centre of the section.
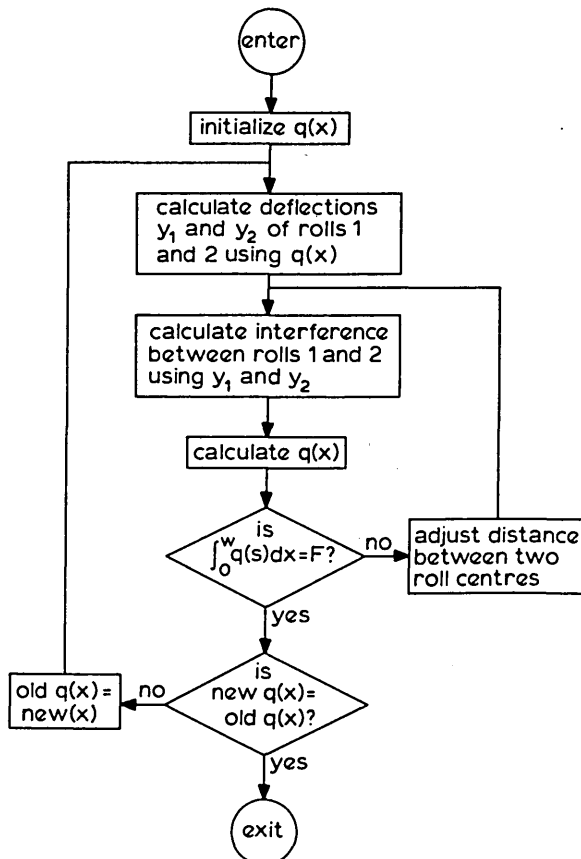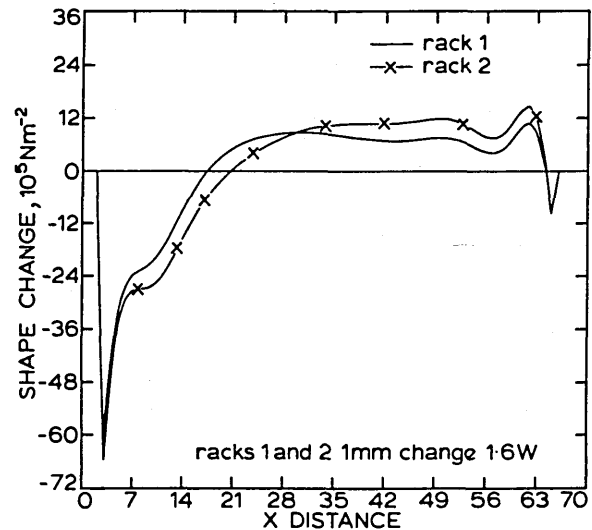
12 Shape profile for 1 mm change in racks 1 and 2

This principle also applies to the stress distribution, strip profile, roll-pressure profile, etc. The computer algorithm enables a change in the shape profile owing to a change in the rack position, and hence the gains of the mill, to be calculated. The flow chart for the main program is shown in Fig.9.

The program begins by initializing all the variables, and the roll force is then calculated using the roll-gap model. Symmetry about a line passing through the work-roll centres can be assumed so that calculations are necessary only for the left side of the cluster. The subroutine BEND calculates the pressure profiles and roll profiles of one half of either the top or bottom cluster. If symmetry is not assumed then the routine BEND has to be called four times to calculate all the pressure and roll profiles. At the end of each iteration a convergence test is carried out on the shape profile. The above calculations are repeated until the error between two successive shape profiles is less than a predetermined value.

The pressure and roll-profile calculation procedure is illustrated in Fig.10. Only the top-half cluster is shown in this figure and thick lines are drawn to show the path of calculation. The small circles labelled c_1, c_2, c_3, and c_4 represent an iterative process for a particular inter-roll pressure calculation. A satisfactory convergence in pressure is shown by Y and non-convergence is represented by N.

As the pressure profile between two rolls depends on the interference or flattening of the rolls, and the interference is itself dependent on the pressure, the process is iterative. Figure 11 shows the flow chart for one iterative calculation of inter-roll pressure. Here, y_1 and y_2 are the deflections of two rolls in contact, and $p(x)$ is the specific pressure profile between them.

11 Flow chart for calculating inter-roll pressure between two rolls

Results and discussion

The model provides the shape, gauge, and pressure profiles for a given rolling schedule. These are important when the control of a particular profile is of interest. Shape profiles for eight rack-position changes are shown in Figs.12–15 (e.g. in Fig.12 the curve represented by the continuous line
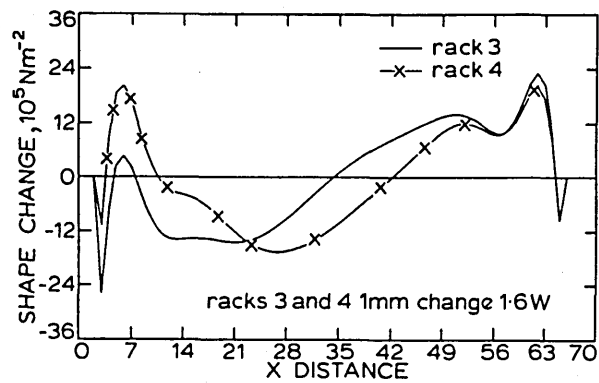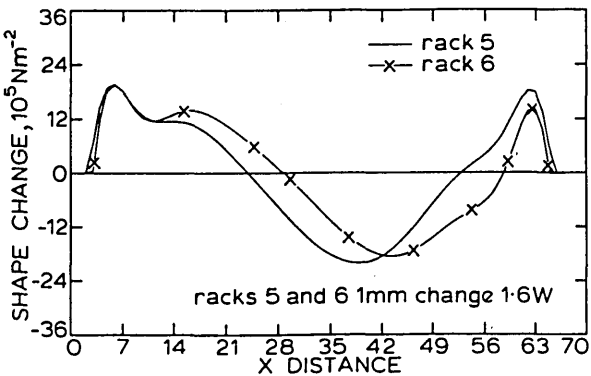
13 Shape profile for 1 mm change in racks 3 and 4

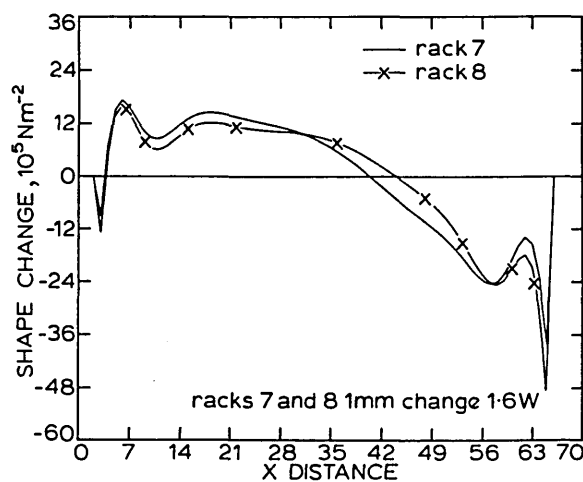**15 Shape profile for 1 mm change in racks 7 and 8**

is the shape profile when rack 1 is changed by 1 mm, keeping all other racks at the zero position. The curve marked by crosses is the shape profile due to a change of 1 mm in rack 2, keeping all other racks at the zero position, etc.). The largest shape change is found at a point across the strip width in the vicinity of a particular rack which has been changed.

The model discussed in the above sections ignores the strip edge effects. When the strip width is less than the mill width (or the length of the work rolls) there will be two portions from either end of the upper work roll with no support. The model is based on the assumption of zero shape directly under these two portions and, therefore, the shape changes from zero to a high value at the edge of the strip. This is shown in Figs.12–15 by the rapid change at the edges. The calculated shape near the edge is not the true shape. The model must be modified to include edge effects using work-roll influence functions as described by Spooner and Bryant.[20]

It is clear from Figs.12–15 that a rack change appears to affect widely separated sections of the strip. This can be explained by considering a localized change in the back-up rolls. This change in the back-up rolls will modify the inter-roll forces between the back-up and second intermediate rolls. Similarly, this change in the inter-roll force will change the effective profiles of both the back-up and second intermediate rolls. From the study of a point force acting on a roll it can be seen that the roll profile is changed, not just below the point of action of the force but over a region surrounding the point. The change is significant in the vicinity of the point of application of the force. Thus,

a localized change in the back-up roll profile is converted to a distributed change in the profile of the second intermediate roll.

Further interaction between the second intermediate rolls and the first intermediate roll, and between the first intermediate rolls and the work rolls, spreads the effect. Thus, in general, the largest shape change occurs under the actuator which is varied; however, care must be exercised in interpreting the curves since shape is defined in terms of deviations from the mean.

The shape profile for racks 1 and 8 should be symmetrized about a vertical axis passing through the mid point of the work roll. (Similarly, the profiles for racks 2 and 7, for racks 3 and 6, and for racks 4 and 5 should be symmetrical.) Figures 12–15 are symmetrical to an accuracy of about 10%. The profiles are not symmetrical at the edges and this is due to the fact that the edge effects are ignored in the model.

The model also provides mill gains. Linearized mill gains are calculated about a given shape-operating point, and these relate the shape changes to the rack changes. If the shape is measured at eight points across the strip the gain matrix has the form (units $= N\,mm^{-3}$):

$$
G_m = Y \begin{array}{c} X \\ \left[\begin{array}{cccc|cccc} 4{\cdot}09 & 2{\cdot}22 & 0{\cdot}65 & -0{\cdot}92 & -1{\cdot}48 & -1{\cdot}26 & -0{\cdot}75 & -0{\cdot}53 \\ 1{\cdot}67 & 4{\cdot}43 & 0{\cdot}95 & -0{\cdot}21 & -1{\cdot}31 & -1{\cdot}35 & -1{\cdot}12 & -0{\cdot}90 \\ -0{\cdot}32 & 0{\cdot}17 & 1{\cdot}41 & 1{\cdot}06 & -0{\cdot}63 & -1{\cdot}12 & -1{\cdot}38 & -1{\cdot}16 \\ -0{\cdot}85 & -0{\cdot}81 & 1{\cdot}76 & 1{\cdot}54 & 0{\cdot}93 & 0{\cdot}07 & -1{\cdot}05 & -0{\cdot}99 \\ \hline -0{\cdot}76 & -1{\cdot}06 & -0{\cdot}42 & 0{\cdot}60 & 1{\cdot}91 & 1{\cdot}44 & -0{\cdot}29 & -0{\cdot}59 \\ -0{\cdot}73 & -1{\cdot}14 & -1{\cdot}19 & -0{\cdot}69 & 1{\cdot}05 & 1{\cdot}60 & 0{\cdot}89 & -0{\cdot}36 \\ -0{\cdot}57 & -0{\cdot}94 & -1{\cdot}18 & -1{\cdot}15 & -0{\cdot}49 & 0{\cdot}46 & 2{\cdot}13 & 1{\cdot}99 \\ -0{\cdot}46 & -0{\cdot}73 & -1{\cdot}08 & -1{\cdot}13 & -1{\cdot}43 & -0{\cdot}96 & 2{\cdot}10 & 2{\cdot}73 \end{array} \right] \end{array} Y
$$
$$X$$

The eight rows of the gain matrix represent the eight points across the strip, and the eight columns correspond to eight racks, e.g. the elements in the second column give the shape at each point across the strip width when the second rack is moved by 1 mm. Thus, $g_{46} = 0{\cdot}07$ is the shape at point 4 when rack 6 is moved by 1 mm. The above matrix was obtained for a rectangular strip whose width was 1·6 m and whose mean input thickness was 2·42 mm, with 15% reduction. The gains include small errors due to numerical problems and the fact that the mill is non-linear. The gains show some dependence upon the strip width. It is noted that the above matrix is approximately symmetrical if the matrix is folded about the line XX and about the line YY. This will always be the case if the strip is centred in the mill.

14 Shape profile for 1 mm change in racks 5 and 6

Conclusions

The derived model is based on theoretical results and the accuracy of the model will depend upon the assumptions made. One such assumption is that the additional stresses at the strip edges due to roll flattening are neglected. This will introduce errors into the final results but the model will be modified to include the edge effects. The results from the improved model will be checked against the present results for accuracy.

When calculating the deflections of the rolls the contribution due to shear was neglected. This will also introduce some error which will be checked at a later stage.

The roll-force model does not involve an iterative procedure but uses an approximate explicit solution. However, the iterative solution which employs Hitchcock's formula is more accurate. These two methods of solution were compared and the error of the approximate solution was found to be less than 1 % for typical rolling schedules.

The effect on the final results of variations of the constant β which appears in the stress equation must also be determined. The model seems to produce reasonable results for strip shape, but this must be confirmed by detailed experimental investigation. Normal operating records will be used where possible to test the model, but two coils are also to be rolled for a specific set of shape experiments.

Acknowledgments

References

1. M. J. GRIMBLE: *Chart. Mech. Eng.*, 1975, 91–93.
2. N. DAVIES: *Iron Steel*, Aug. 1972, 391–395.
3. C. A. BRAVINGTON, D. C. BARRY, and C. H. MCCLURE: 'Shape control'. 82–88: 1976, London, The Metals Society.
4. W. J. EDWARDS and P. D. SPOONER: 'Automation of tandem mills', (ed. G. F. Bryant), 176; 1973, London, The Iron and Steel Institute.
5. W. K. J. PEARSON:*J. Inst. Met.*, 1964–65, 93, 169–178.
6. B. SABATINI and K. A. YEOMANS: *J. Iron Steel Inst.*, 1968, 206, 1207–1213.
7. G. W. D. M. GUNAWARDENE and M. J. GRIMBLE: 'Development of a static model for a Sendzimir cold rolling mill', presented at IMACS (AICA) symp. on simulation of control systems, Technische Universität, Vienna, Austria, Sept. 1978.
8. S. URAYAMA, Y. TAKATOKU, Y. NIWA, and Y. SAWADA: 'Shape control', 101–106; 1976, London, The Metals Society.
9. M. D. STONE and R. GRAY: *Iron Steel Eng.*, Aug. 1965.
10. M. HETENYI: 'Beams on elastic foundations'; 1946, University of Michigan Press.
11. S. TIMOSHENKO and J. N. GOODIER: 'Theory of elasticity', 380–433; 1951, New York, McGraw-Hill.
12. R. J. ROARK and W. C. YOUNG: 'Formulas for stress and strain', 5 ed.; 1975, New York, McGraw-Hill.
13. G. F. BRYANT and R. OSBORN: 'Automation of tandem mills', (ed. G. F. Bryant), 245–278; 1973, London, The Iron and Steel Institute.
14. M. J. GRIMBLE: PhD thesis, University of Birmingham, 1974.
15. G. F. BRYANT and R. OSBORN: 'Automation of tandem mills', (ed. G. F. Bryant), 279; 1973, London, The Iron and Steel Institute.
16. E. OROWAN: *Proc. Inst. Mech. Eng.*, 1943, 150, 140.
17. M. J. GRIMBLE, M. A. FULLER, and G. F. BRYANT: *Int. J. Numer. Methods Eng.*, 1978, 12, 643–663.
18. L. R. UNDERWOOD: 'The rolling of metals theory and experiment', Vol.1, 9–316; 1950, London, Chapman and Hall.
19. S. D. CONTE: 'Elementary numerical analysis'; 1965, New York, McGraw-Hill.
20. P. D. SPOONER and G. F. BRYANT: 'Shape control', 19–25; 1976, London, The Metals Society.

Appendix 1

Roll-bending equations and deflection

An expression is derived below for the roll deflection caused by a point load applied to a roll resting upon an elastic foundation. From simple bending theory the deflection y can be written as

$$EI\frac{d^4y}{dx^4}=F-ky \dots\dots\dots\dots\dots\dots\dots\dots(15)$$

where F is applied force and k is the elastic-foundation constant.[11] This equation is true only if the roll is in complete contact with its foundation, under no load. However, in the case when the roll is resting on an elastic foundation which is bent this is not the case (*see* Fig.16).

Let the gap between roll and foundation be Δy under no-load conditions. Then equation (15) becomes:

$$EI\frac{d^4y}{dx^4}=F-k(y-\Delta y)$$
$$=F-ky+k\Delta y$$

but
$$k\Delta y=\Delta F$$
and

$$EI\frac{d^4y}{dx^4}=(F+\Delta F)-ky \dots\dots\dots\dots\dots\dots(16)$$

The solution to equation (16) can be written as

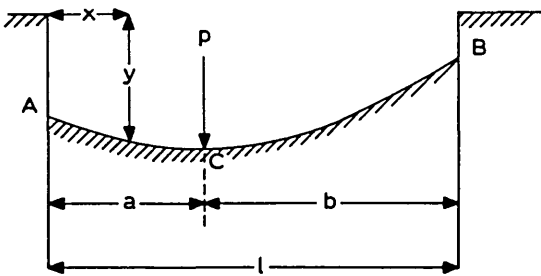$$y=\frac{F'\lambda}{k}\frac{1}{A}\Big[B(C-D)+E(F+G)\Big] \dots\dots\dots\dots(17)$$

where
$A=\sinh^2\lambda l-\sin^2\lambda l$
$B=2\cosh\lambda x.\cos\lambda x$
$C=\sinh\lambda l.\cos\lambda a.\cosh\lambda b$
$D=\sin\lambda l.\cosh\lambda a.\cos\lambda b$
$E=\cosh\lambda x.\sin\lambda x+\sinh\lambda x.\cos\lambda x$
$F=\sinh\lambda l(\sin\lambda a.\cosh\lambda b-\cos\lambda a.\sinh\lambda b)$
$F'=F+\Delta F$
$G=\sin\lambda l(\sinh\lambda a.\cos\lambda b-\cosh\lambda a.\sin\lambda b)$
$\lambda=\left(\dfrac{k}{4EI}\right)^{1/4}$

and constants a, b, and l are defined in Fig.17. Note also that equation (17) is true only for a concentrated force and when $0\leqslant x\leqslant a$. The method of calculating y when $a\leqslant x\leqslant b$ is to substitute a for b and b for a, and to measure x from the end B.

(a)   (b)

a no-load case; *b* loaded case
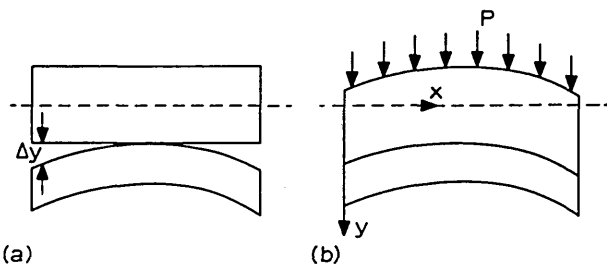
16 Example of loaded roll

oll resting on elastic foundation

pendix 2

-flattening equation

is section the local deformations due to flattening in
ntact regions between rolls in the cluster and between
rolls and strip are determined. The approach follows
of Timoshenko and Goodier[11] and, more recently,
rds and Spooner.[4]

en two infinitely long elastic cylinders are in contact
tal interference $y_{12}(x)$ can be written as a function of
ad per unit length $q(x)$ as

$$(x) = q(x)(c_1 + c_2) \ln \left[\frac{e^{2/3}(d_1 + d_2)}{2q(x)(c_1 + c_2)} \right] \dots \dots (18)$$

e d_1 and d_2 are the diameters of the cylinder and c_1 and
e two constants depending on the elastic properties.
loading is, of course, non-uniform but neglecting
d-order errors:

$$) = \frac{y_{12}(x)}{(c_1 + c_2) \ln \left[\frac{e^{2/3}(d_1 + d_2)}{2q(x)(c_1 + c_2)} \right]} \dots \dots (19)$$

w variable M is defined to eliminate $q(x)$ from the
-hand side of equation (19):

$$= \frac{q(x)}{F/w} \dots \dots (20)$$

e w is the length of the roll.

$$) = \frac{y_{12}(x)}{(c_1 + c_2) \left[\ln \left(\frac{e^{2/3}(d_1 + d_2)}{2(F/w)(c_1 + c_2)} \right) - \ln M \right]} \dots \dots (21)$$

$$M \ll \ln \left[\frac{e^{2/3}(d_1 + d_2)}{2(F/w)(c_1 + c_2)} \right]$$

$$) \approx F/w$$

ation (21) becomes:

$$) \approx \frac{y_{12}(x)}{(c_1 + c_2) \left\{ \ln \left[\frac{e^{2/3}}{2(c_1 + c_2)} \right] + \ln(d_1 + d_2) - \ln \left(\frac{F}{w} \right) \right\}} \quad (22)$$

above equation is true only for positive values of
). Therefore, it is assumed that when $y_{12}(x) \leqslant 0$,
$= 0$.

The interference $y_{12}(x)$ can also be calculated from roll
bending using the relation

$$y_{12}(x) = \tfrac{1}{2}(d_1 + d_2) - D_{12} + y_2(x) - y_1(x) + y_{wc}(x) \dots \dots (23)$$

where D_{12} is the distance between the two centres.

The model proposed by Edward and Spooner[4] is used to
calculate the work-roll flattening. The proposed model is

$$y_{ws}(x) = [b_1 + b_2 p(x)] y_H(x) \dots \dots (24)$$

where

$$y_H(x) = 2p(x) c \ln \left[\frac{e^{2/3} d}{2cp(x)} \right] \dots \dots (25)$$

is the Hertzian flattening which occurs between two in-
finitely long cylinders having the same diameter and the
same elastic properties. Equation (25) is obtained by
putting $d = d_1 = d_2$ and $c = c_1 = c_2$.

Constants b_1 and b_2 are estimated to be 0·5 and 0·325
mm t⁻¹ and p in equation (24) is the rolling pressure.

Appendix 3

Elastic-foundation constant K calculation

At various points in the roll cluster two rolls rest on one
roll. In order to use the bending equations it is convenient to
use a single equivalent value of the foundation constant K.
This is illustrated in Fig.18. This value of K is determined
below.

Let the deflection of roll A in the direction of P be y_A.
The deflection y_{AB} in the direction P_2 can be calculated as

$$y_{AB} = y_A \cos(\theta_2 - \theta)$$

and, similarly, the deflection y_{AC} in direction P_1 is given by

$$y_{AC} = y_A \cos(\theta_1 + \theta).$$

If K_1 and K_2 are the foundation constants between the
cylinders A and B and A and C, respectively, then

$$P_1 = K_1 y_{AC}$$

and

$$P_2 = K_2 y_{AB}$$

but

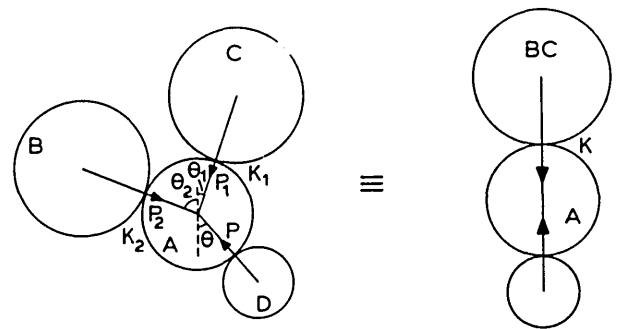$$P = P_1 \cos(\theta_1 + \theta) + P_2 \cos(\theta_2 - \theta)$$
$$= K_1 y_A \cos^2(\theta_1 + \theta) + K_2 y_A \cos^2(\theta_2 - \theta)$$

but

$$K = \frac{P}{y_A}$$

and we obtain

$$K = K_1 \cos^2(\theta_1 + \theta) + K_2 \cos^2(\theta_2 - \theta).$$

18 Equivalent loaded rolls

Appendix 4

Input and output stress profiles

From the geometry of Fig.19 it can be shown easily that

$$h_n \approx h_2 + R\phi_n{}^2 \quad\dotfill(26)$$

from continuity of mass flow

$$V_2 h_2 = V_n h_n \quad\dotfill(27)$$

By substituting h_n from equation (26) in (27) we get

$$V_2 = V_n\left(1 + \frac{R\phi_n{}^2}{h_2}\right) \quad\dotfill(28)$$

The per unit slip is defined as

$$s = \frac{V_2 - V_n}{V_n} \quad\dotfill(29)$$

From equations (28) and (29) the value of s is found to be

$$s = \frac{R\phi_n{}^2}{h_2} \quad\dotfill(30)$$

where

$$\phi_n = \sqrt{\frac{h_2}{R}}\tan\left(\frac{h_2}{R}\cdot\frac{H_n}{2}\right)$$

and

$$H_n = \frac{H_2}{2} - \frac{1}{2\mu}\ln\left[\frac{h_2}{h_1}\cdot\frac{1-\sigma_1/k_1}{1-\sigma_2/k_2}\right] \quad\dotfill(31)$$

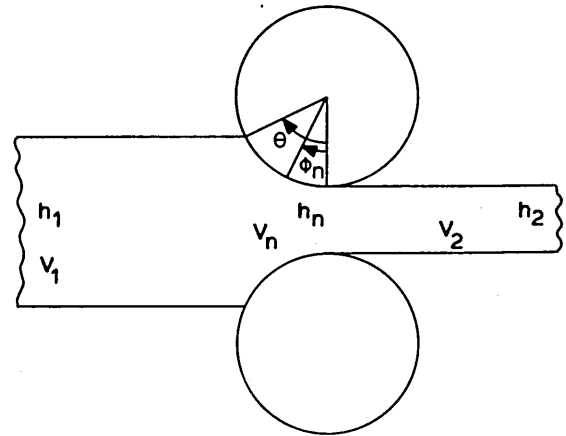Equation (31) can be derived by considering the roll-gap variables. by differentiating s with respect to σ_1:

$$\frac{ds}{d\sigma_1} = \frac{2R}{h_2}\phi_n\cdot\frac{d\phi_n}{d\sigma_1} \quad\dotfill(32)$$

$$= \frac{2R}{h_2}\cdot\phi_n\cdot\frac{d\phi_n}{dH_n}\cdot\frac{dH_n}{d\phi_n}$$

but

$$\frac{d\phi_n}{dH_n} = \frac{2h_2}{R}\left[1 + \tan^2\left(\sqrt{\frac{h_2}{R}\cdot\frac{H_n}{2}}\right)\right] \quad\dotfill(33)$$

and

$$\frac{dH_n}{d\sigma_1} = \frac{1}{2\mu}\cdot\frac{1}{k_1-\sigma_1} \quad\dotfill(34)$$

19 Roll-gap conditions

By substituting these values in equation (32) and simplifying we obtain

$$\frac{ds}{d\sigma_1} = \frac{a}{k_1-\sigma_1} \quad\dotfill(35)$$

where

$$a = \frac{2\phi_n}{\mu}\left[1 + \tan^2\left(\sqrt{\frac{h_2}{R}\cdot\frac{H_n}{2}}\right)\right] \quad\dotfill(36)$$

similarly,

$$\frac{ds}{d\sigma_2} = -\frac{a}{k_2-\sigma_2} \quad\dotfill(37)$$

but

$$\Delta s = \Delta\sigma_1\frac{ds}{d\sigma_1} + \Delta\sigma_2\frac{ds}{d\sigma_2} = 0 \quad\dotfill(38)$$

By substituting for $ds/d\sigma_1$ and $ds/d\sigma_2$ and simplifying we obtain

$$\Delta\sigma_1 = \gamma\Delta\sigma_2 \quad\dotfill(39)$$

where

$$\gamma = \frac{k_1-\sigma_1}{k_2-\sigma_2}$$

Edwards and Spooner[4] derive an equation to calculate the output stress which is given by

$$\Delta\sigma_2 = \beta E\frac{h_2}{h_1}\cdot\frac{h}{h_2} - 1 + \frac{\Delta\sigma_0}{1+\gamma} \quad\dotfill(40)$$